DEPARTMENT OF ELECTRONIC AND ELECTRICAL ENGINEERING

UCL

Modelling the Transport of Complex Modulation in Radio-over-Fibre Networks

Saad Sari

Doctor of philosophy (PhD) degree

Department of Electronic and Electrical Engineering

University College London

September 2007

ProQuest LLC
789 East Eisenhower Parkway
P.O. Box 1346
Ann Arbor, MI 48106-1346

Abstract

The proliferation of wireless LANs and other wireless devices coupled with increased demand for broadband services are putting pressure on wireless systems to increase capacity. This thesis is concerned with modelling Radio-over-Fibre (RoF) modulation techniques and investigating the performance of cost effective systems. The initial chapters outline optical communication techniques, benefits, applications, and limitations. The second part of the thesis is dedicated to the simulation of reported modulation techniques which are tolerance to optical fibre dispersion. Optical intensity modulation techniques of conventional Double Sideband (DSB), Single Sideband (SSB), and Double Sideband-Suppressed Carrier (DSB-SC) were considered in this work. Performance of the RoF modulation techniques were reported in terms of system linearity limitations and capability of transmitting complex signals. The last part of the thesis explores Orthogonal Frequency Division Multiplexing (OFDM) performance over fibre, considering dispersion tolerant modulation techniques, in terms of performance and limitations with various signal parameters.

Comparative assessments of dispersion tolerant Radio-over-Fibre modulation techniques based on Intensity Modulation-Direct Detection IM-DD, with particular attention to the Double Sideband-Suppressed Carrier (DSB-SC) modulation have been reported in this work. It has been found that each of the examined techniques has a unique advantages as well as weak points related to the performance or the system cost. The main advantage of the OSSB+C technique is that it can eliminate the power variation over the entire range of the modulation frequency and fibre length. Moreover, it has been demonstrated that the Double Sideband-Suppressed Carrier (DSB-SC) modulation can shift the dispersion effect to a higher frequency-length products. Finally, we have explored, for the first time, the performance of the RF up-converted OFDM signal over the RoF optical links. OFDM modulation signals based on BPSK, QPSK, 16-QAM and 64-QAM Gray coded mappings have been applied, and the effects of OFDM modulation parameters on the achievable signal transmission over the RoF link were assessed.

Acknowledgements

First, I would like to express my thanks to my supervisor Dr John E. Mitchell for his advice, guidance and support throughout the course of this research. Much of this work would not have been achieved without his support and encouragement during this period of time.

I would also like to thank Prof. Izzat Darwazeh for his valuable advice and helpful discussions on the work of this thesis. Also I want to thank al the present and past members of the Telecommunication Research Group who have offered valuable opinion and discussion, and who provide a friendly environment within the group. I would lake to mostly thank by name Dr Darren Shea, Bahman K. Sabet, and Kai li for the nice and friendly time we had together.

On the personal level, first I would like to mostly thank Mr. Y. Jameel for his invaluable support and tremendous encouragement from the day I have decided to start this work, and during the time period of the research.

I also would like to thank my family, my mother and my brothers Karam and Ahmad, for their support and patience through these years.

Last but not least I would like to wholeheartedly thank my wife, Lubna, for her unconditional support and commitment during this hectic time.

To the soul and memory of my father.

Table of Contents

List of Figures

List of Tables

Glossary of Abbreviations and Acronyms

ADSL	Asymmetric Digital Subscriber Line
AM	Amplitude Modulation
ASCII	American Standard Code for Information Interchange
ASK	Amplitude Shift Keying
AWG	Arrayed Waveguide Grating
AWGN	Additive White Gaussian Noise
BER	Bit Error Rate/Ratio
BS	Base Station
CJK	Chinese, Japanese, and Korean
CNR	Carrier to-Noise Ratio
CS	Central Stations
CU	Central Unit
CW	Continuous Wave
DAB	Digital Audio Broadcasting
DAS	Distributed Antenna System
DeMUX	De-multiplexer
DFB	Distributed Feedback
DFT	Discrete Fourier Transform
DIM	Direct Intensity Modulation
DIPP	Dispersion Induced Power Penalty
DM	Direct Modulation
DR	Dynamic Range
DSB	Double Sideband
DSB-SC	Double Sideband-Suppressed Carrier
DVB	Digital Video Broadcasting
DVB-H	Digital Video Broadcasting-Handheld
DVB-T	Digital Video Broadcasting-Terrestrial
EOM	Electro-Optical Modulation
FDM	Frequency Division Multiplexing

FEC	Forward Error Correction
FFT	Fast Fourier Transform
Flash-OFDM	Fast low-latency Access with Seamless Handoff OFDM
FLO	Forward Link Only
FM	Frequency Modulation
FSK	Frequency Shift Keying
FWA	Fixed Wireless Access
GHz	Giga Hertz
GSM	Global System for Mobile communications
GVD	Group Velocity Dispersion
HD	Hybrid Digital/analogue
HSOPA	High Speed OFDM Packed Access
ICI	Inter-Carrier Interference
IEEE	Institute of Electrical and Electronics Engineering
IF	Intermediate Frequency
IFFT	Inverse Fast Fourier Transform
IIP3	Third-order Input Intercept Point
IM3	Third-order Inter-Modulation
IMD	Inter-Modulation Distortion
IM-DD	Intensity Modulation-Direct Detection
IM-FDR	Inter-Modulation-Free Dynamic Range
ISDB	Integrated Services Digital Broadcasting
ISI	Inter-symbol Interference
ITU	International Telecommunication Union
LAN	Local Area Network
LD	Laser Diode
LO	Local Oscillator
MAN	Metropolitan Area Network
MB-OFDM	Multi-Band OFDM
MBS	Mobile Broadband System
MBWA	Mobile Broadband Wireless Access
MC-CDMA	Multi Carrier-Code Division Multiple Access
MHZ	Mega Hertz
MITB	Minimum Transmission Biasing

MoCA	Multimedia over Coax Alliance
MUX	Multiplexer
MVDS	Multipoint Video Distribution Services
MZI	Mach Zehnder Interferometer
MZM	Mach Zehnder Modulator
NF	Noise Figure
OFDM	Orthogonal Frequency Division Multiplexing
OFDMA	Orthogonal Frequency Division Multiple Access
OFLL	Optical Frequency-Locked Loop
OIL	Optical Injection Locking
OIPLL	Optical Injection Phase-Locked Loop
OOK	On-Off Keying
OPLL	Optical Phase-Locked Loop
OSSB	Optical Single Sideband
PAN	Personal Area Network
PAPR	Peak-to-Average-Power Ratio
PD	Photo Diode
PDA	Personal Digital Assistant
PIN	Positive-Intrinsic-Negative
PLC	Power Line Communication/Carrier
PM	Phase Modulation
POTS	Plain Old Telephone Service
PSK	Phase Shift Keying
PSM	Self-Phase Modulation
QAM	Quadrature Amplitude Modulation
QPSK	Quadrature Phase Shift Keying
RAU	Radio Antenna Unit
RF	Radio Frequency
RFI	Radio Frequency Interference
RHD	Remote Heterodyne Detection
RIN	Relative Intensity Noise
RoF	Radio over Fibre
RS	Remote Station
SC	Switching Centre

SCM	Sub-Carrier Multiplexing
SFDR	Spurious Free Dynamic Range
SM	Single Mode
SMF	Single Mode Fibre
SNR	Signal to-Noise Ratio
SSB+C	Single Sideband + Carrier
T-DMB	Terrestrial Digital Multimedia Broadcasting
THz	Tate Hertz
TSB	Terrestrial digital Sound Broadcasting
UMTS	Universal Mobile Telecommunications System
UWB	Ultra Wideband
VDSL	Very high speed Digital Subscriber Line
WDM	Wavelength Division Multiplexing
WiFi	Wireless Fidelity
WiMAX	World Interoperability for Microwave Access
WLAN	Wireless Local Area Network
XPM	Cross-Phase Modulation
3GPP	Third Generation Partnership Project

Chapter 1

Introduction

People have used light to transmit information for hundreds of years. However, it was not until the 1960s, with the invention of the laser, when widespread interest in optical (light) systems for data communications began. The invention of the laser prompted researchers to study the potential of fibre optics for data communications, sensing, and other applications. Laser systems could send a much larger amount of data than telephone, microwave, and other electrical systems. The first experiment with the laser involved letting the laser beam transmit freely through the air. Researchers also conducted experiments letting the laser beam transmit through different types of waveguides. Glass fibres, gas-filled pipes, and tubes with focusing lenses are examples of optical waveguides. Glass fibres soon became the preferred medium for fibre optic research.

Fibre optic systems have many attractive features that are superior to electrical systems. These include improved system performance, immunity to electrical noise, signal security, and improved safety and electrical isolation. Other advantages include reduced size and weight, environmental protection. Moreover, the impressive results from early researches show many advantages offered by fibre optic systems which permitted the introduction of fibre optics into present applications. These applications were grown to include cable television, computer networks, video systems, and data links. Therefore, current researches will be focusing on increases system performance and provide solutions to existing problems in conventional applications.

For a multifunctional RoF system, the required electrical signal at the input of the RoF system depends on the RoF technology, the functionality desired, and the radio link being transported. Subsequently, the converted back electrical signal from the photo detector must meet the specifications required by the wireless link. Optically fed wireless systems have been investigated for many applications. The principal advantage of the transmission of high frequency signals over fibre is low attenuation and cost when compared to the conventional coaxial cable or radio transmission.

Since RoF involves analogue modulation, and detection of light, it is fundamentally an analogue transmission system. Therefore, signal impairments such as noise and distortion, which are important in analogue communication systems, are also important in RoF systems. These impairments tend to limit the Noise Figure (NF) and Dynamic Range (DR) of the RoF links. The noise sources in analogue optical fibre links are arise from optical devices and also include the fibres dispersion. In Single Mode Fibre (SMF) based RoF systems, chromatic dispersion may limit the fibre link lengths and may also cause phase de-correlation leading to increased RF carrier phase noise.

Although the RoF transmission system itself is analogue, the radio system being distributed need not be analogue, but it may be digital using comprehensive multi-level signal modulation formats such as M-QAM, or Orthogonal Frequency Division Multiplexing (OFDM). Research of the RoF systems applications for delivering mm-wave signals based on complex digital modulation schemes are not widely investigated. Moreover, performance evaluation of modulation standards such as OFDM signals still need to be examined over RoF systems when applied at RF frequency bands.

1.1 Thesis Organisation

Following this introductory chapter, a common structure is used throughout this thesis. Each chapter opens with an introduction detailing the aims and contents of the chapter, and is concluded with a summary of the main results and contributions. The organisation of this thesis is as follows;

Chapter 2 reviews the optical communications technology influencing the work in this thesis, specifically wireless communications based on Radio-over-Fibre (RoF). Particular applications of interest, such as wireless LANs and Fixed Wireless Access (FWA) systems are discussed in details. We present the concept of optical modulation as well as introducing the characteristics of the modulation techniques used for generating and distributing microwave signals with extensive mathematical analysis of the optical fibre waveguides properties.

Chapter 3 assesses the performance of a number of reported RoF systems that use dispersion tolerant modulation techniques based on Intensity Modulation-Direct Detection (IM-DD). We provide a comparison with conventional dispersive IM-DD optical RoF links. The optical modulation characteristics, advantages, and disadvantages of Optical Single Sideband (OSSB), and Optical Double Sideband-Suppressed Carrier (DSB-SC) modulation, are demonstrated as dispersion elimination techniques for directly modulated lasers and external modulators. We provide a mathematical analysis of RoF links performance with respect to fibre dispersion.

Chapter 4 demonstrates with simulation models the performance evaluation of the RoF techniques detailed in chapter 3 applying digital signals of QPSK, 16-QAM and 64-QAM modulation. The systems investigated were the conventional Intensity Modulation-Direct Detection (IM-DD) as well as reported dispersion tolerant modulation techniques for delivering microwave frequencies over fibre. Moreover, the chapter explores a comparison of the performance, advantages and disadvantages of each individual technique used to eliminate chromatic dispersion.

Chapter 5 investigates a class of RoF systems that have good immunity to fibre dispersion, and explore their performance with respect to system Inter-Modulation-Free Dynamic Range (IM-FDR). We apply a two tone test as an Inter-Modulation Distortion (IMD) measurement, with experimental justification of simulation models and devices influencing the performance of the modelled systems. More advanced systems with transmitting capability of multi-wavelength and multi-channel signals based on DSB-SC technique are presented and their performances were evaluated.

Chapter 6 studies the performance of the RF modulated OFDM signal over optical systems. The concept of Orthogonal Frequency Division Multiplexing (OFDM) is introduced. Simulation based performance analysis of OFDM over the DSB-SC optical system is developed and presented with mathematical analysis based on RF OFDM with BPSK, QPSK, 16-QAM and 64-QAM mappings.

Chapter 7 concludes the thesis, summarising the main contributions and suggesting further lines of research. While appendix A includes the detailed devices settings of the constructed models in chapters 4 and 5 in addition to the Matlab codes used to convert the generated Matlab coded signals to ASCII code and vice versa in order to playback the signals using the optical model.

1.2 Contributions

The main contributions made by this research may be summarised as follows:

- Evaluation through rigorous analysis of the Inter-Modulation Distortion (IMD) of a set of dispersion-tolerant Radio-over-Fibre techniques. Optimisation of the systems, based on this parameter, is then achieved.

- Demonstration for the first time of the impact of chromatic dispersion on radio frequency OFDM signals transmitted over a DSB-SC RoF system.

- Novel exploration of the influence of OFDM modulation characteristics on the signal performance over fibre considering fibre dispersion and modulation technique limitations.

- Comparative assessments of dispersion tolerant RoF modulation techniques based on Intensity Modulation-Direct Detection IM-DD, with particular attention to the Double Sideband-Suppressed Carrier (DSB-SC) modulation based on directly modulated lasers and second order optical up-conversion.

- Investigating the performance of the multi-wavelength DSB-SC system to monitor the impact of the multi-wavelength upconversion on the RoF system performance.

- Demonstration of novel mathematical performance analysis of DSB-SC modulation with detailed performance comparison to the Conventional Double Sideband (DSB) modulation and Optical Single Sideband (OSSB+C) modulation.

- Development of simulation models of RF up-converted Orthogonal Frequency Division Multiplexing (OFDM) modulation systems based on BPSK, QPSK, 16-QAM and 64-QAM digital modulation mappings.

1.3 Publications

- Saad M. H. Sari, J. E. Mitchell, "Performance of M-QAM signals using Radio-over-Fibre optical link", *EPSRC, IEEE, IEE, Postgraduate Research Conference in Electronics, Photonics, Communications and Networks, and Computing Science (PREP 2005)*, University of Lancaster, Lancaster UK, March 2005.

- Sari S., Mitchell J. E. "Comparison of modulation techniques in radio-over-fibre links to limit the effect of fibre chromatic dispersion", *10th European Conference on Networks and Optical Communications NOC*, 313-319, July 2005.

- S. Sari and J.E. Mitchell, "RF OFDM Performance over RoF links", *International Union of Radio Science URSI, UK National URSI Symposium*, University of Portsmouth, Portsmouth, UK, July 2007.

- S. Sari, B. Kalantari Sabet, J. C. Attard, J. E. Mitchell, "Radio Over Fibre Networks"(Invited), Second International Conference on Access Networks (AccessNets'07), Ottawa, Canada, August 2007.

- Sari S., Mitchell J. E. "Performance Analysis of Multi-Wavelength Radio-over-Fibre system applying Double Sideband-Suppressed Carrier DSB-SC modulation", *London Communications Symposium LCS 2007*, University College London, London, UK, September 2007.

- Sari S., "Dispersion tolerant modulation techniques in Radio-over-Fibre links applying complex signal modulation", the International Journal of Business Data Communication and Networking (Submitted).

- S. Sari, J. E. Mitchell, "Performance Analysis of Radio-over-Fiber system with Optical Double Sideband Suppressed Carrier DSB-SC modulation", The Iranian Journal of Engineering Sciences (Submitted).

Chapter 2

Optical Communications

This chapter reviews the current technology of optical communications influencing the work in this thesis. Following to this paragraph, an introduction to wireless communications is presented defining and listing applications of the Radio-over-Fibre (RoF) technology. Moreover, Direct Intensity Modulation (DIM) and Remote Heterodyne Detection (RHD) techniques used for generating and distributing microwave signals are presented in this chapter, whereas requirements of wireless access systems based on RoF technology are also listed and discussed. Particular applications of interest, such as wireless LANs and Fixed Wireless Access (FWA) systems, are also discussed with more details presenting the conception of the optical modulation and the techniques used in current systems. Finally, an extensive study with mathematical analysis of optical fibre waveguides characteristics and modes are also presented. A summary of the contributions were given in the last section of this chapter.

2.1 Wireless Communications

Wireless Communication is becoming an integral part of today's society. The proliferation of mobile and other wireless devices coupled with increased demand for broadband services are putting pressure on wireless systems to increase capacity. To achieve this, wireless systems must have increased feeder network capacity, operate at higher carrier frequencies, and cope with increased user population densities. However, raising the carrier frequency and thus reducing the radio cell size leads to costly radio systems while the high

installation and maintenance costs associated with high-bandwidth silica fibre render it economically impractical for in-home and office environments.

RoF technology has emerged as a cost effective approach for reducing radio system costs because it simplifies the remote antenna sites and enhances the sharing of expensive radio equipment located at appropriately sited (e.g. centrally located) Switching Centres (SC) or otherwise known as Central Stations (CS).

2.2 What is Radio-over-Fibre Technology?

Radio-over-Fibre (RoF) technology is a technology by which electrical signals are converted to optical domain and distributed by means of optical components and techniques. A RoF system consists of a Central Unit (CU) and a Remote Antenna Unit (RAU) connected by an optical fibre link or network. A Radio-over-Fibre system distributes wireless Radio Frequency (RF) signals after conversion to optical domain over optical fibre and currently installed systems are based on analogue intensity modulation of the semiconductor laser source and its demodulation through the direct detection performed by a PIN photodiode [1]. Therefore, RoF is fundamentally an analogue transmission system because it distributes the radio waveform, directly at the radio carrier frequency, from a CU to RAU. Although this transmission system is analogue, the radio system itself may be digital. For the down link, the received RF signals at each remote antenna are transmitted over an analogue optical fibre link to the central site /station where all the signal processing is done. In this way, each remote antenna site simply consists of a linear analogue optical transmitter, an amplifier, and antenna [1].

The integration of wireless and optical networks is a potential solution for increasing capacity and mobility as well as decreasing costs in the access network. By using Radio-over-Fibre (RoF), the capacity of optical networks can be combined with the flexibility and mobility of wireless access networks. The concept of Radio-over-Fibre means to transport information over optical fibre by modulating the light with the radio signal. This technique can be used in the backbone of a wireless access network.

The frequencies of the radio signals distributed by RoF systems span a wide range (usually in the GHz region) and depend on the nature of the applications. For a multifunctional RoF system, the required electrical signal at the input of the RoF system depends on the RoF technology, the functionality desired, and the radio link being transported. The electrical signal may be baseband data, modulated IF, or the actual modulated RF signal to be distributed. The electrical signal is used to modulate the optical source. The resulting optical signal is then carried over the optical fibre link to the remote station. Here, the data is converted back into electrical form by the photodetector. The generated electrical signal must meet the specifications required by the wireless link.

By delivering the radio signals directly, the optical fibre link avoids the necessity to generate high frequency radio carriers at the antenna site. Since antenna sites are usually remote from easy access, there is a lot to gain from such an arrangement. However, the main advantage of RoF systems is the ability to concentrate most of the expensive, high frequency equipment at a centralized location, thereby making it possible to use simpler remote sites (Radio Antenna Unit RAU). Furthermore, RoF technology enables the centralising of mobility functions such as macro-diversity for seamless handover. The benefits of having simple remote sites are many. They are discussed in the following section.

2.3 Benefits of Radio-over-Fibre Systems

Advantages and benefits of the RoF technology include the following:

2.3.1 Low Attenuation Loss

Electrical distribution of high frequency RF signals either in free space or through transmission lines is problematic and suffers from high loss. In free space, losses due to absorption and reflection increase with frequency. In transmission lines, impedance rises with frequency as well. Therefore, distributing high frequency radio signals electrically over long distances requires expensive regenerating equipment. As for mm-waves, their distribution via the use of transmission lines is not feasible for useful distances due to the high loss

for such high frequency bands. The alternative solution to this problem is to distribute baseband signals or low intermediate frequencies (IF) from the Switching Centre (SC) to the Base Stations (BS) [1]. The baseband or IF signals are then up converted to the required microwave or mm-wave frequency at each base station, amplified and then radiated. Such a system places stringent requirements (such as linearity) on repeater amplifiers and equalisers. In addition, high performance local oscillators would be required for up conversion at each base station. This arrangement leads to complex base stations with tight performance requirements. An alternative solution is to use optical fibres, which offer much lower losses.

Commercially available standard Single Mode Fibres (SMFs) made from glass (silica) have attenuation loss around 0.2 dB/km at 1550 nm. This loss is much lower than those encountered in free space propagation and copper wire transmission of high frequency microwaves. Therefore, by transmitting microwaves in the optical form, transmission distances are increased several fold and the required transmission power is reduced greatly.

2.3.2 Large Bandwidth

Optical fibres offer enormous bandwidth. There are three main transmission windows, which offer low attenuation, at 850*nm*, 1310*nm* and 1550*nm*. For a single SMF optical fibre, the combined bandwidth of the three windows is in the excess of 50 THz. However, today's state-of-the-art commercial systems utilize only a fraction of this capacity. But developments to exploit more optical capacity per single fibre are still continuing.

The enormous bandwidth offered by optical fibres has other benefits apart from the high capacity for transmitting microwave signals. The high optical bandwidth enables high speed signal processing that may be more difficult or impossible to do in electronic systems. In other words, some of the demanding microwave functions such as filtering, mixing, up- and down-conversion, can be implemented in the optical domain. For instance, mm-wave filtering can be achieved by first converting the electrical signal to be filtered into an optical

signal, then performing the filtering by using optical components such as the Mach Zehnder Interferometer MZI or (Bragg gratings), and then converting the filtered signal back into an electrical signal [2]. Furthermore, processing in the optical domain makes it possible to use cheaper low bandwidth optical components such as Laser Diodes (LD) and modulators, and still be able to handle high bandwidth signals [3-6].

The utilization of the enormous bandwidth offered by optical fibres is severely hampered by the limitation in bandwidth of electronic systems, which are the primary sources and end users of transmission data. This problem is referred to as the *"electronic bottleneck"*. The solution around the electronic bottleneck lies in effective multiplexing. In analogue optical systems including RoF technology, Sub-Carrier Multiplexing (SCM) is used to increase optical fibre bandwidth utilization. In SCM, several microwave sub-carriers, which are modulated with digital or analogue data, are combined and used to modulate the optical signal, which is then carried on a single fibre. This makes the RoF system cost effective.

2.3.3 Immunity to Radio Frequency Interference

Immunity to electromagnetic interference is a very attractive property of optical fibre communications, especially for microwave transmission. This is so because signals are transmitted in the form of light through the fibre. Because of this immunity, fibre cables are preferred even for short connections at mm-waves. Related to RFI immunity is the immunity to eavesdropping, which is an important characteristic of optical fibre communications, as it provides privacy and security.

2.3.4 Easy Installation and Maintenance

In RoF systems, complex and expensive equipment is kept at the SCs, thereby making remote base stations simpler. For instance, most RoF techniques eliminate the need for a local oscillator and related equipment at the Remote Station (RS). In such cases a photodetector, an RF amplifier, and an antenna

make up the RS equipment. Modulation and switching equipment are kept in the SC and shared by several RS. This arrangement results in smaller and lighter RS, which effectively reducing system installation and maintenance costs. Easy installation and low maintenance costs of RS are very important requirements for mm-wave systems, because of the large numbers of the required antenna sites. Having expensive RS would render the system costs prohibitive. The numerous antennas are needed to offset the small size of radio cells (micro- and pico-cells), which is a consequence of limited propagation distances of mm-wave microwaves. In applications where RSs are not easily accessible, the reduction in maintenance requirements has many positive implications. In addition, the simplicity of installing, and the maintenance of the optical fibres compared to the conventional RF systems using the coaxial cables, which have a large size and significant weight when compared with the very small and light fibre cables.

2.3.5 Reduced Power Consumption

Reduced power consumption is a consequence of having simple RSs with reduced equipment. Most of the complex equipment is kept at the central SC. In some applications, the antenna sites are operated in passive mode. For instance, some 5 GHz Fibre-Radio systems employing pico-cells (small radio cells) can have the RSs (BSs) operate in passive mode [1]. Reduced power consumption at the RSs is significant considering that RSs are sometimes placed in remote locations not fed by the power grid.

2.3.6 Operational Flexibility

RoF does offer operational benefits in terms of operational flexibility. Firstly, depending on the microwave generation technique, a RoF distribution system can made signal format transparent. For instance the Intensity Modulation and Direct Detection (IM-DD) technique can be made to operate as a linear system and therefore as a transparent system. This can be achieved by using single-mode fibre (SMF), with effective dispersion-limited modulation techniques, in combination with pre-modulated RF sub-carriers (SCM). When this happens,

then, the same RoF network can be used to distribute multi-operator and multi-service traffic, potentially resulting in huge economic savings.

2.3.7 Ability to Effectively Transport mm-Waves

Millimetre waves offer several benefits. However, as discussed previously, mm-waves cannot easily be distributed electrically due to high RF propagation losses. In addition, generating mm-wave frequencies using electrical devices is challenging. These issues describe the *electronic bottleneck* already discussed above. The most promising solution to the problem is to use optical techniques. Low attenuation and large bandwidth make the distribution of mm-waves using optical fibre cost effective. Furthermore, some optical based techniques have the ability to generate very high frequencies. Advantages and disadvantages of mm-waves are listed below.

2.3.7.1 Advantages of mm-waves

They provide high bandwidth due to the high frequency carriers. Secondly, due to high RF propagation losses in free space, the propagation distances of mm-waves are severely limited. This allows for well-defined small radio cell sizes (micro- and pico-cells), where considerable frequency re-use becomes possible so that services can be delivered simultaneously to a larger number of subscribers.

2.3.7.2 Disadvantages of mm-waves

The negative side of mm-waves is the need for numerous BSs, which is a consequence of high RF propagation losses. Unless the BSs are simple enough, installing and maintaining the mm-wave system can be economically prohibitive owing to the numerous required BSs.

2.3.8 Radio System Functionalities

As stated earlier, RoF technology is not only used for distributing RF signals but for radio system functionalities as well. Among these, modulation and

frequency conversion have been mentioned above. However, application of RoF technology for radio system functionalities goes beyond modulation and frequency conversion to encompass signal processing at very high frequencies. These functions include filtering, attenuation control and signal processing in high frequency antenna systems. These functions are also referred to as microwave functions. Many of these functions are difficult to achieve in the electrical domain due to limited bandwidth and other electromagnetic wave propagation limitations. However, if the processing is done in the optical domain, enormous signal processing bandwidth becomes available. As a result, many microwave functions can be performed by optical components without the need to electro/optical (E/O) conversion for processing by microwave components and vice versa [2].

2.4 Limitations of Radio-over-Fibre Technology

Since RoF involves analogue modulation, and detection of light, it is fundamentally an analogue transmission system. Therefore, signal impairments such as noise and distortion, which are important in analogue communication systems, are important in RoF systems as well. These impairments tend to limit the Noise Figure (NF) and Dynamic Range (DR) of the RoF links [7]. DR is a very important parameter for mobile (cellular) communication systems [8]. The noise sources in analogue optical fibre links include the laser's Relative Intensity Noise (RIN), the laser's phase noise, the photodiode's shot noise, the amplifier's thermal noise, and the fibre's dispersion. In Single Mode Fibre (SMF) based RoF, systems, chromatic dispersion may limit the fibre link lengths and may also cause phase de-correlation leading to increase RF carrier phase noise [6]. It must be stated that although the RoF transmission system itself is analogue, the radio system being distributed need not be analogue as well, but it may be digital (e.g. WLAN), using comprehensive multi-level signal modulation formats such as M-QAM, or Orthogonal Frequency Division Multiplexing (OFDM).

2.5 Applications of Radio-over-Fibre Technology

The applications of RoF technology include satellite communications, mobile radio communications, broadband access radio, Multipoint Video Distribution Services (MVDS), Mobile Broadband System (MBS), vehicle communications and control, and wireless LANs over optical networks. RoF technology is generally unsuitable for system applications, where high Spurious Free Dynamic Range (SFDR is the maximum output signal power for which the power of the third-order intermodulation product is equal to the noise floor) is required, because of the limited DR due to devices nonlinearity. This is especially true of wide coverage mobile systems such as GSM, where SFDR of > 70 dB (outdoor) are required. However, most indoor applications do not require high SFDR. For instance, the required (uplink) SFDR for GSM reduces from >70 dB to about 50 dB for indoor applications [7]. Therefore, RoF distribution systems can readily be used for in-building (indoor) distribution of wireless signals of both mobile and data communication (e.g. WLAN) systems. In this case the RoF system becomes a Distributed Antenna System (DAS).

The RoF systems are also attractive for other present and future applications where high SFDR is not required. For instance, UMTS users are required to control their transmitter power so that equal power levels are received at the BS. Thus, UMTS does not need the high SFDR required in GSM, so that RoF distribution systems may be used for both indoor and outdoor UMTS signal distribution [8]. Another application area is in Fixed Wireless Access (FWA) systems, such as WiMAX, where RoF technology may be used to optically transport signals over long distances bringing the significantly simplified RAUs closer to the end user, from where wireless links help to achieve broadband first/last mile access, in a cost effective way. The main application area of interest is briefly discussed below.

2.5.1 Wireless LANs

As portable devices and computers become more and more powerful as well as widespread, the demand for mobile broadband access to LANs will also be on the increase. This will lead once again, to higher carrier frequencies in the bid to meet the demand for capacity. For instance most current wireless LANs operate at the 2.4 GHz bands and offer the maximum capacity of 11 Mbps per carrier (IEEE 802.11b) [9]. Second generation broadband wireless LANs are offering up to 54 Mbps per carrier, and require higher carrier frequencies in the 5 GHz band (IEEE 802.11a) [8].

2.5.2 WiMAX

A promising wireless data technology IEEE 802.16 standard [10] referred to as WiMAX (World Interoperability for Microwave Access) that covers ranges up to 50 km instead of a few hundreds of meters for data rates many times higher than for Wi-Fi 802.11b technology [9] and even higher than for the newer 802.11a and 802.11g. Security features are included to protect the sensitive data, low latency and guaranteed quality of service lacking in Wi-Fi for uninterrupted transmission of time-critical voice and video data. WiMAX would allow access by hundreds or even thousands of wireless users, unlike Wi-Fi which can connect only tens of users [11]. Many companies are examining WiMAX for "last mile" connectivity at high data rates [12].

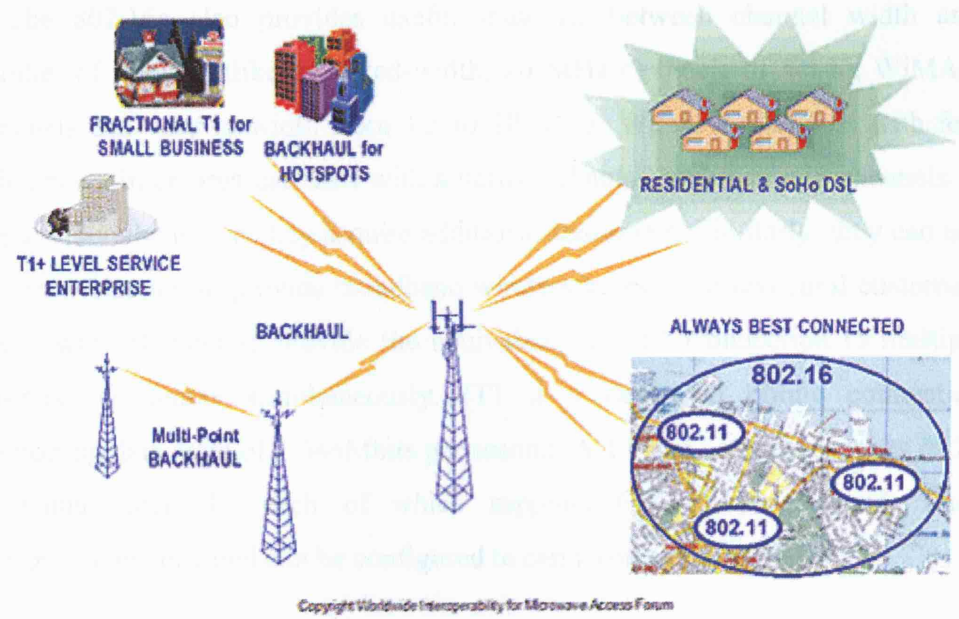

Figure 2.1: 802.16 and 802.16a used for broadband wireless access and 802.11 backhaul [11].

The 802.16a standard will soon make possible "last mile" broadband wireless access in areas that are too remote or too difficult or too expensive to reach with wire or fibre. It will also serve as Wi-Fi backhaul, enabling quick and easy connection of Wi-Fi hot spots to the internet when there's no convenient access to a wire line. As shown in figure (2.1), eventually, it will enable notebook computers and PDAs to connect directly to metropolitan-area networks (MANs) that provide geographically continuous wireless coverage.

The flexibilities that come from trading off range and throughput, the 802.16a operates at a range of up to 30 miles and provides a data rate of up to 70 Mbps, Table (2.5.1), but not at the same time. A wireless subscriber unit near a base station and receiving a strong signal can use an efficient modulation scheme, such as 64-QAM, and get the highest possible data rate. A unit further away, however, might require a more noise robust scheme like 16-QAM, which, being less efficient, will provide a lower rate, but at least keep the unit connected. Furthermore, the modulation method can change in real time, from user to user and even from packet to packet for a single user. An 802.16a system thus can continually provide the highest data rates for the conditions that exist.

The 802.16a also provides useful tradeoffs between channel width and number of users. Unlike the fixed-width, 20 MHz channels of Wi-Fi, WiMAX channels can vary in width from 1.5 to 20 MHz. Wireless operators with few subscribers in an area can start with a narrow channel and then add channels or use a wider channel as they acquire additional customers. Similarly, they can use a narrow channel to provide broadband wireless access to a few rural customers and a wide channel to provide the equivalent of a T1 Connection to multiple business customers simultaneously. (T1 is a dedicated phone connection supporting data rates of 1.544Mbits per second. A T1 line actually consists of 24 individual channels, each of which supports 64Kbits per second. Each 64Kbit/second channel can be configured to carry voice or data traffic)

	802.16	802.16a	802.16e
Completed	December 2001	January 2003	Mid '04
Spectrum	10-66 GHz	<11 GHz	<6 GHz
Channel Conditions	Line of sight only	Non line of sight	Non line of sight
Bit Rate	32-134 Mbps in 28 MHz channel bandwidth	Up to 75 Mbps in 20 MHz channel bandwidth	Up to 15 Mbps in 5 MHz channel bandwidth
Modulation	QPSK, 16QAM, 64QAM	OFDM 256 subcarriers, QPSK, 16QAM, 64QAM	Same as 802.16a
Mobility	Fixed	Fixed, portable	Nomadic portability
Channel Bandwidths	20, 25, 28 MHz	Scalable 1.5 to 20 MHz	Same as 802.16a with uplink subchannels
Typical Cell Radius	2-5 km	7-10 km max. range 50 km	2-5 km

Table 2.5.1: IEEE 802.16 standard. Source: Worldwide Interoperability for Microwave Access Forum (WiMAX).

2.6 Optical Modulation

In order to transmit information via an optical fibre communication system, the information must first be encoded to modulate the property of the light with the information signal. The modulated light property might be intensity, frequency, phase or polarization with either digital or analogue signals. Analogue techniques include amplitude modulation (AM), frequency modulation (FM), and phase modulation (PM). Digital techniques include amplitude shift keying (ASK), frequency shift keying (FSK), and phase shift keying (PSK). The choices are indicated by the characteristics of the optical fibre, the available optical sources detectors, and considerations of the overall system.

Binary ASK, also known as on-off keying (OOK), is a preferred method of digital modulation because of its simplicity. With this method, the signal is switched between two power levels. The lower power level represents a "0" bit, while the higher power level represents a "1" bit. In systems employing OOK, modulation of the signal can be achieved by simply turning the laser on and off (direct modulation). In general, however, this can lead to chirp, or variations in the laser's amplitude and frequency, when the laser is turned on. A preferred approach for high bit rates is to have an external modulator that modulates the light coming out of the laser. The external MZ modulator blocks or passes light depending on the current applied to it. A drive voltage is applied to one of two waveguides, creating an electric field that causes the signals in the two waveguides to be either in phase or 180 out of phase, resulting in the light from the laser's being either passed through the device or blocked.

External optical modulators are active devices which tend to be used primarily to modulate the frequency or phase of the light, but may also be used for time division multiplexing and switching of optical signals. In addition, MZ amplitude modulators can offers wide bandwidths [13]. One of the advantages of using integrated-optics devices such as the MZ interferometer is that the laser and modulator can be integrated on a single structure, which may potentially be cost effective. Also, integrating the laser with the modulator eliminates the need for polarization control and results in low chirp.

Considering the recent interest in integrated optical devices it is likely that external optical modulators utilized more in order to achieve grater bandwidths and allow the use of nonsemiconductor sources which cannot be directly modulated at high frequency.

2.7 Optical Techniques for Distributing and Generating Microwave Signals

Several techniques for distributing and generating microwave signals via optical fibre exist. The techniques may be classified into two main categories namely Intensity Modulation-Direct Detection (IM-DD) and Remote Heterodyne Detection (RHD) techniques [14]. The electrical signal at the BS of the optical link may be one of three kinds namely, baseband, modulated IF, or the modulated RF signal itself. Whatever the case, the aim is to produce appropriate RF signals at the remote station, which meet the specifications of the wireless application. This means that apart from signal purity, robustness against noise, and power issues, the generated RF signals must also contain data in the appropriate modulation format. If only baseband data is available at the BS, the RoF system must also perform the modulation function in addition to transportation and frequency up-conversion of the data. Therefore, a RoF system may have to perform radio-system functions as well as signal transportation. Apart from functionality, there are other factors such as performance, complexity and power issues to consider when selecting a suitable RoF system to employ. Overall, the RoF system must be cost-effective for the application concerned.

2.7.1 RF Generation by Direct Intensity Modulation (DIM)

The simplest method for optically distributing RF signals is simply to directly modulate the intensity of the light source with the RF signal itself and then to use direct detection at the photodetector to recover the RF signal. This method falls under the Intensity Modulation-Direct Detection (IM-DD) technique. There are

two ways of modulating the light source. The laser diode can itself be modulated directly by using the appropriate RF signal to drive the laser bias current, this modulation is limited due to the laser diodes limitation [15;16]. The second option is to operate the laser in continuous wave (CW) mode and then use an external modulator such as the Mach-Zehnder Modulator (MZM), to modulate the intensity of the light. The two options are shown in Figure (2.2). In both cases, the modulating signal is the actual RF signal to be distributed. The RF signal must be appropriately pre-modulated with data.

After transmission through the fibre and direct detection (on a PIN photodiode or electro-absorption transceiver) the photocurrent will be a replica of the modulating RF signal applied either directly to the laser or to the external modulator at the transmitter. The photocurrent undergoes trans-impedance amplification to yield a voltage that is in turn used to excite the antenna. If the RF signal used to modulate the transmitter is itself modulated with data, then the generated RF signal will be carrying the same data. The modulation format of the data is preserved.

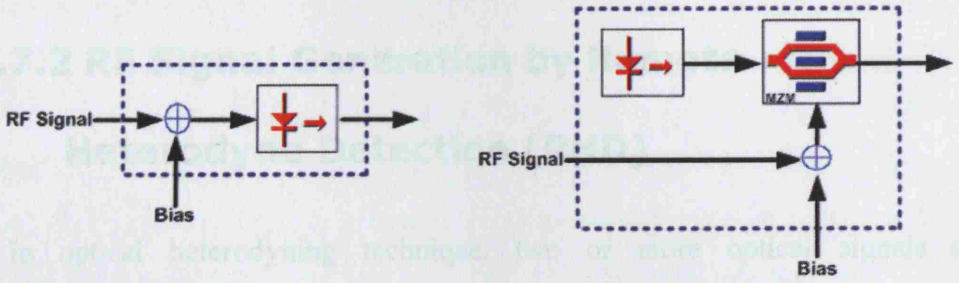

Figure 2.2: Generating RF Signals by Direct Intensity Modulation (a) of the Laser, (b) using an external modulator.

2.7.1.1 Advantages

The advantage of this method is that it is simple. Secondly, if low dispersion fibre is used together with effective dispersion-limited modulation techniques, the system can be efficiently linear. Consequently, the optical link acts only as an amplifier or attenuator and is therefore transparent to the modulation format of the RF signal [17]. That is to say that both Amplitude Modulation (AM) based schemes and constant envelop based modulation schemes such as Phase

Modulation (PM / QPSK) can be used. Such a system needs little or no upgrade whenever changes in the modulation format of the RF signal occur. Sub-Carrier Multiplexing (SCM) can also be used on such a system. Furthermore, unlike direct laser bias modulation, external modulators such as the Mach Zehnder Modulator (MZM) can be modulated with mm-wave signals approaching 100 GHz [18].

2.7.1.2 Disadvantages

The disadvantage of this method lays in the fact that only low RF frequency signals can be generated (distributed). This is because to generate higher frequency signals, the modulating signal must also be at the same high frequency. For direct laser modulation, this is not possible due to lack of bandwidth, and laser non-linearity, which leads to inter-modulation product terms that cause distortions. On the other hand, external modulators such as the MZM can support high frequency RF signals. Further disadvantages have to do with fibre chromatic dispersion, and the fact that analogue applications are more sensitive to system non-linearity.

2.7.2 RF Signal Generation by Remote Heterodyne Detection (RHD)

In optical heterodyning technique, two or more optical signals are simultaneously transmitted and are heterodyned in the receiver. One or more of the heterodyning products is the required RF signal [14]. Heterodyning can be realized by the Photo Diode (PD) itself or the optical signals can be detected separately and then converted in an electrical RF mixer. There are several ways of generating the two optical carriers for coherent heterodyning. One approach is to use an optical phase modulator to generate several optical sidebands, and then selecting the required components [19]. Another approach is to use two separate laser sources. The two laser diodes are made to emit light at frequencies (wavelengths) separated by the required microwave frequency [20].

Because phase noise is a key problem in digital mm-wave transmission, care must be taken to maintain a small phase noise by the heterodyned signals. This can be achieved if the two (or more) optical signals are phase coherent, this can be realized if the different frequency optical signals are deduced from a common source [21], or they are phase-locked to one master source [22;23]. There are several Techniques to maintain the required frequency offset and phase noise performance between the two lasers. These techniques include:

1. Optical Frequency-Locked Loop (OFLL)
2. Optical Phase-Locked Loop (OPLL)
3. Optical Injection Locking (OIL) and
4. Optical Injection Phase-Locked Loop (OIPLL)

2.7.2.1 Advantages of Optical Heterodyning

Benefits of using optical heterodyning are, it offers flexibility in frequency since very high frequencies can be generated, limited only by the photodetector bandwidth. Furthermore, heterodyning yields high-detected power (higher link gain) and higher carrier-to-noise ratio (CNR). That is due to the optical powers of the both optical fields contribute to the power of the generated microwave signal. Moreover, If only one of the two optical carriers is modulated with data, system sensitivity to chromatic dispersion can be reduced greatly [24]. This is not possible in direct intensity modulation conventional method, where the two optical sidebands end up both being modulated with data. Another advantage of optical heterodyning detection (RHD) is the capability of photonic signal processing and radio system functions such as phase control, filtering, and frequency conversion [14].

2.7.2.2 Disadvantages of Optical Heterodyning

The major drawback of RHD is the strong influence of laser phase noise and optical frequency variations on the purity and stability of the generated RF carriers. Since semiconductor lasers have large spectral widths, extra measures to reduce the linewidth of the generated RF signals have to be taken. These

measures often lead to more complex systems. Techniques including Optical Phase Locked Loops (OPLL) and Optical Injection Locking (OIL) used to reduce phase noise sensitivity.

2.8 RoF-Based Wireless Access System Requirements

In general, the RoF system to be designed must be able to distribute the Fixed Wireless Access (FWA) signals efficiently and in conformity with all aspects of the appropriate standard, such as signal purity and power levels. The system must also be easy to upgrade for operation with future systems. If we consider that future wireless LANs will consist of a high density of small radio cells, this makes the issue of system cost a major challenge [25]. Therefore, it is essential to have simple, and easy to maintain base stations (BS). The complexity of the BS's is linked to the radio-over-fiber (RoF) techniques employed [26]. Therefore, the choice of the microwave generation method is significant. Furthermore, the kind of distribution network infrastructure deployed is another fundamental issue [27]. The required RoF system must not only meet the present demand for capacity, but it must also be suitable to meet anticipated future bandwidth demands [28]. The requirement for broadband wireless services translates into the requirement for increased capacity in the distribution network. Optical fibre is the best candidate for this, where the standard single mode fibre can offers the enormous bandwidth.

Moreover, the RoF system to be used must be capable of generating microwave signals with appropriate data modulation. This functionality depends on the choice of the RoF technique used [29;30]. Consequently, the RoF system to be used must be capable of distributing Phase Shift Keying (PSK), Quadrature Amplitude Modulation (QAM) and Orthogonal Frequency Division Multiplexing (OFDM) signals. Therefore, the main issues and parameters that are likely to influence the design of such a system are:

2.8.1 System Cost

The fact that future wireless LANs will consist of a high density of small radio cells makes the issue of system cost a major one. It is imperative to have simple and easy to maintain base stations (BS). The complexity of the base station is related to the RoF techniques employed. Therefore, the choice of the microwave generation method is important.

2.8.2 Bandwidth Requirements and Link Lengths

The required RoF system must not only meet the present demand for capacity, but it must also be suited to meet anticipated future bandwidth demands. The requirement for broadband wireless services translates into the requirement for increased capacity in the distribution and feeder networks. As stated above, optical fibre is the best candidate for this.

2.9 Optical Fibre Waveguides

In this section we will discuss the optical fibre types and characteristics for better understanding of the applications and the limitations of the fibre.

2.9.1 Transmission Characteristics of Optical Fibres

The transmission characteristics of most interest are those of attenuation and bandwidth. A plane electromagnetic wave, such a beam of light, travels in vacuum at the speed $c = 3 \cdot 10^8$ m/s. different light frequencies correspond to different colours. The two most important frequencies for optical fibre communications are in the infrared region: f = 231 THz, corresponding to the vacuum wavelength of $\lambda = c/f = 1.3\mu m$, and f = 194 THz, corresponding to the vacuum wavelength of $\lambda = c/f = 1.55\mu m$. The first frequency correspond to the minimum dispersion in regular single-mode fibre, the second one corresponds to

the minimum attenuation. The attenuation is due to absorption in the glass, fibres have been fabricated with losses lower than 0.2 dB/km at 1550 nm [31].

The other characteristic of primary importance is the bandwidth of the fibre. This is limited by the signal dispersion within the fibre, which determines the number of bits of information transmitted in a given time period [31]. The ratio of the speed of light in vacuum, c, to the speed of light in medium, v, called refractive index [32]

$$n = c/v \qquad \ldots (2.1)$$

The refractive index may (and generally does) depend on light frequency. This phenomenon is known as *chromatic dispersion* and is fundamental limitation of optical fibre communication systems.

The wavelength is, by definition, the distance travelled by light during one light period. Hence, the relationships between the vacuum wavelength, λ, the medium wavelength, λ_m, and the light frequency and velocity look as follows:

$$\lambda = c/f \qquad \ldots (2.2)$$

$$\lambda_m = v/f \qquad \ldots (2.3)$$

$$\lambda_m = \lambda / n \qquad \ldots (2.4)$$

Therefore, once the attenuation was reduced to acceptable levels attention was directed towards the dispersive properties of fibres. Again, this has led to substantial improvements, giving wideband bandwidths of many tens of gigahertz over a number of kilometres.

2.9.2 Multi-Modes and Single-Mode Fibres

If a waveguide can support more than one mode, it is called multimode. If it can support only one mode, it is called single mode. With respect to dispersion, single-mode fibres can carry much more information than multimode fibres. Hence, it is important to develop a waveguide that can support only one mode. The advantage of the propagation of a single mode within an optical fibre is that the signal dispersion caused by the delay differences between different modes in a multimode fibre may be avoided. Multimode step index fibres do not lend themselves to the propagation of a single mode due to the difficulties of maintaining single-mode operation within the fibre when mode conversion (i.e. coupling) to other guided modes takes place at both input mismatches and fibre imperfections. Hence, for transmission of a single-mode the fibre must be designed to allow propagation of only one mode, whilst all other modes are attenuated by leakage or absorption [31].

Since single-mode fibres emerged as a viable optical communication medium they have quickly become the dominant and the most widely used fibre type within long distance telecommunications. Major reasons for this situation are as follows:

1. They currently exhibit the greatest transmission bandwidths and the lowest losses of the fibre transmission media.

2. They have a superior transmission quality over other fibre types because of the absence of modal noise.

3. They offer a substantial upgrade capacity (i.e. future proofing) for future wide bandwidth services using either faster optical transmitters and receivers or advanced transmission techniques.

4. Points above (1 to 3) provide a confidence that the installation of single-mode fibre will provide a transmission medium which will have adequate performance such that it will not require replacement over its twenty-plus-year anticipated lifetime.

2.9.3 Optical Fibre Mathematical Analysis

To understand the characteristics of the light propagation in medium such as optical fibre, we have to study and analyze the light propagation controlling properties and factors in vacuum and waveguides.

2.9.3.1 Phase Velocity

A monochromatic wave travelling in the Z-direction, such as a mode in fibre or in a waveguide, it is given by

$$E(t, z) = A \exp[j(\omega t - \beta z)] \quad \ldots (2.5)$$

where ω is the wave frequency in radians per second, and β is the propagation constant in inverse meters. The phase velocity is defined as the velocity an observer must maintain to observe the field with a constant phase [32]. In other words, to find the value of the phase velocity, one must trace a point of constant phase:

$$\omega t - \beta z = const \quad \ldots (2.6)$$

The phase velocity, v, must give $z = vt$ that (2.6) holds true. Substituting $z = vt$ into (2.6), we obtain

$$\omega t - \beta v t = const \text{ for } \forall t \quad \ldots (2.7)$$

Equation (2.7) can be valid only if

$$v = \omega / \beta \quad \ldots (2.8)$$

Equation (2.8) specifies the relationship between the phase velocity, frequency, and propagation constant of an electromagnetic wave. The ratio of the speed of light to the phase velocity is known as the refractive index (or as the phase refractive index):

$$n \equiv c/v \qquad \ldots (2.9)$$

Equation (2.9) is similar to (2.1) but is in more precise we specify now that the velocity in question is the phase velocity.

In free space (but not in waveguide), $v = c$ and $n = 1$ if the wave propagates along the z-axis. If the wave does not propagate along the z-axis, the phase velocity can be larger than the speed of light, *c*. figure (2.3) illustrates such a case: a plane wave propagates at an angle α with respect to the z-axis. Its "natural" (i.e., measured along the direction of propagation) wavelength is λ. However, its wavelength along the z-axis is larger than λ and is equal to

$$\lambda' = \lambda/\cos\alpha > \lambda \qquad \ldots (2.10)$$

The field along the z-axis is given by A.exp [$j(\omega t - \beta z)$], with β being given by:

$$\beta = \frac{2\pi}{\lambda'} = \frac{2\pi}{\lambda}\cdot\cos\alpha < k \qquad \ldots (2.11)$$

Thus, the propagation constant along the z-axis in figure (2.3) is smaller than the vacuum propagation constant. It follows from (2.8) and (2.11) that the phase velocity along the z-axis is

$$v = \frac{\omega}{\beta} = \frac{\omega\lambda}{2\pi\cos\alpha} = \lambda f \cdot \frac{1}{\cos\alpha} = \frac{c}{\cos\alpha} > c \qquad \ldots (2.12)$$

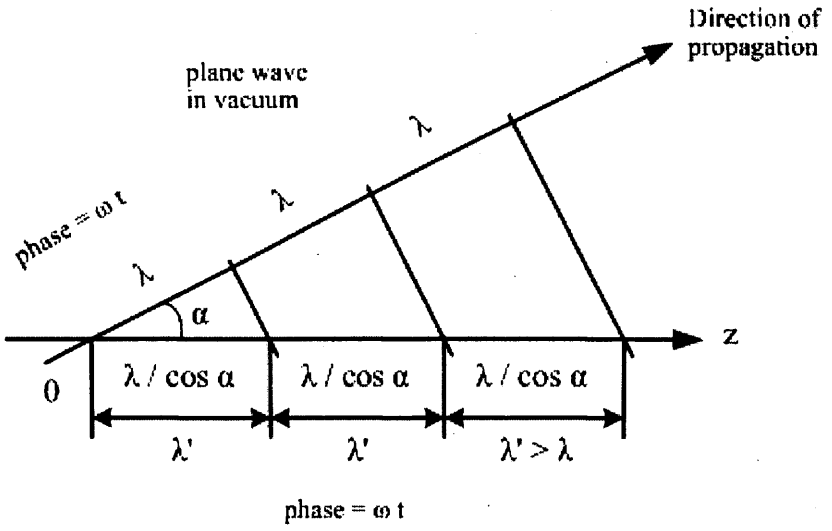

Figure 2.3: plane wave propagating at an angle α with respect to the z-axis. Its wavelength along the z-axis is λ', and λ' is larger than λ.

Thus, the phase velocity can be larger than the speed of light. This result does not contradict Einstein's relativity theory and does not mean that information can travel faster than the speed of light, since the phase velocity characterize only the rate of phase change in space, not the rate of power or envelope propagation (the latter is characterized by the group velocity).

If k_1 and k_2 are the propagation constants, it can be shown that in the waveguide aligned with the z-axis,

$$k_2 < \beta < k_1 \qquad \ldots (2.13)$$

It follows from (2.8) and (2.13) that the phase velocity, v, of a made in the waveguide/fibre is bounded by the speeds of light in the cladding:

$$v_1 < v < v_2 < c \qquad \ldots (2.14)$$

In conclusion, the relationships between the mode wavelength, λ_{mode}, the mode propagation constant, β, and the mode (phase) refractive index, n:

$$\lambda_{mode} = \frac{2\pi}{\beta} \qquad \ldots (2.15)$$

$$\beta = \frac{2\pi}{\lambda_{mode}} \quad \ldots (2.16)$$

$$\lambda_{mode} = \frac{\lambda}{n} \quad \ldots (2.17)$$

Both the mode wavelength, λ_{mode}, and the mode phase velocity, v, depend, in general, on the light frequency (ω), on the mode type (TE or TM), and on the mode number.

2.9.3.2 Group Velocity

A modulated lightwave is, strictly speaking, not monochromatic: Fourier theory indicates that it must contain several frequency components. Different frequency components travel through the fibre with generally different phase velocities and, therefore, accumulate generally different phase shifts. In other words, fibre may introduce *a phase distortion.*

In many practical cases, the relative bandwidth of the optical signal is small:

$$\frac{B}{f} << 1 \quad \ldots (2.18)$$

where B is the optical signal bandwidth and f is the optical frequency. In such cases, the impact of the fibre-induced phase distortion can characterized by the *group velocity* and by the group velocity dispersion.

The group velocity is, by definition, the velocity of the envelope (amplitude modulation) of the optical signal and is, in general, different from the phase velocity. The easiest way to derive an expression for the group velocity and understand the difference between the group velocity and the phase velocity is to consider a simple test signal and investigate its propagation through a fibre. Thus, let us consider an amplitude-modulated (AM) optical signal:

$$e_{AM}(t, z = 0) = E(1 + m\cos\omega_1 t)\cos\omega_c t \quad \ldots (2.19)$$

where $z = 0$ means that the wave at the entrance to a fibre, E is the field amplitude, m is the modulation depth, ω_1 is the modulation frequency (cosine modulation wave), and ω_c is the light frequency. In most cases, $\omega_1 << \omega$. The cosine modulation of the field assumed in (2.19) does not correspond to the cosine modulation of the power or intensity since the light power is proportional to the field squared.

Using trigonometry and Euler's formula, we can rewrite (2.19) as follow:

$$e_{AM}(t, z = 0) = E\mathrm{Re}\left\{\exp(j\omega_c t) + \frac{m}{2}\exp[j(\omega_c - \omega_1)t + \frac{m}{2}\exp[j(\omega_c + \omega_1)t]\right\} \quad \ldots (2.20)$$

Equation (2.20) indicates that our signal, $e_{AM}(t, z = 0)$, contains three different frequency components having the frequencies of $\omega_c, \omega_c - \omega_1$, and $\omega_c + \omega_1$. Each of these components will travel at its own phase velocity and accumulate its own phase shift [32].

In general, we must know β for each value of ω to find the output field. It is convenient to expand β into a Taylor power series:

$$\beta(\omega) = \beta_c + \dot{\beta}\Delta\omega + \frac{1}{2}\ddot{\beta}(\Delta\omega)^2 + \frac{1}{6}\dddot{\beta}(\Delta\omega)^3 + \ldots \quad \ldots (2.21)$$

Where β_c is the value of β at the "carrier" frequency, ω_c, $\Delta\omega$ is the difference between ω and ω_c, and $\dot{\beta}, \ddot{\beta}$ *and* $\dddot{\beta}$ are the derivatives of β with respect to ω evaluated at $\omega = \omega_c$:

$$\Delta\omega \equiv \omega - \omega_c \quad \ldots (2.22)$$

$$\dot{\beta} = \left.\frac{\partial \beta}{\partial \omega}\right|_{\omega=\omega_c} \quad \ldots (2.23)$$

$$\ddot{\beta} = \left.\frac{\partial^2 \beta}{\partial \omega^2}\right|_{\omega=\omega_c} \quad \ldots (2.24)$$

$$\dddot{\beta} = \left.\frac{\partial^3 \beta}{\partial \omega^3}\right|_{\omega=\omega_c} \quad \ldots (2.25)$$

As we will see later, $\dot{\beta}$ does not lead to envelope distortion, while $\ddot{\beta}$ and higher-order terms do. For that reason, $\ddot{\beta}$ is known as the first-order dispersion coefficient, $\dddot{\beta}$ is known as the second-order dispersion coefficient, and so on.

If we neglect the dispersion (come to it next), hence, (2.21) yields

$$\beta(\omega) \cong \beta_c + \dot{\beta}\,\Delta\omega \quad \ldots (2.26)$$

Thus, the propagation constants of the three frequency components of the AM signal (2.20) are given by:

$$\text{at } \omega_c - \omega_1 : \beta = \beta_c - \Delta\beta \quad \ldots (2.27)$$

$$\omega_c : \beta = \beta_c \quad \ldots (2.28)$$

$$\text{at } \omega_c + \omega_1 : \beta = \beta_c + \Delta\beta \quad \ldots (2.29)$$

where

$$\Delta\beta \equiv \dot{\beta}\,\omega_1 \quad \ldots (2.30)$$

Because the propagation constants of the three frequency components are now known, we can write the expression for the field at the output of a z-meters-long fibre (with neglecting the attenuation)

$$e_{AM}(t,z) = E\,\mathrm{Re}\{\exp[j(\omega_c t - \beta_c z)]\} + \frac{m}{2}\exp\{j[(\omega_c - \omega_1)t - (\beta_c - \Delta\beta)z]\} + \frac{m}{2}\exp\{j[(\omega_c + \omega_1)t - (\beta_c + \Delta\beta)z]\} \quad \ldots (2.31)$$

This equation is obtained be adding an appropriate phase shift, $\beta(\omega)\cdot z$, to each of the three components of (2.20).

We can manipulate equation (2.31) into the following form:

$$e_{AM}(t,z) = E[1 + m\cos(\omega_1 t - \Delta\beta z)]\cos(\omega_c t - \beta_c z) \quad \ldots (2.32)$$

Equation (2.32) shows that the phase shift accumulated by the carrier (i.e., Light) is equal to $\beta_c z$ while the phase shift accumulated be the modulation is equal to $\Delta\beta z$.

The group velocity, V_g, is defined as the velocity one must maintain to observe a constant phase of *the envelope*. In other words, when $z = v_g t$, $\omega_1 t - \Delta\beta z$ must be constant:

$$\omega_1 t - \Delta\beta z = const \text{ for } \forall t \quad \ldots (2.33)$$

substituting $z = v_g t$ and (2.30) into (2.33), we obtain

$$\omega_1 t - \dot{\beta}_1 v_g t = const \text{ for } \forall t \quad \ldots (2.34)$$

Equation (2.34) has a solution if and only if $const = 0$, in which case

$$v_g = \frac{1}{\dot{\beta}} = \frac{\partial \omega}{\partial \beta} \qquad \ldots (2.35)$$

Comparison of (2.35) with (2.8) indicate that while both the phase velocity, v, and the group velocity, V_g, are determined by the shape of the β-versus-ω curve, they are, in general, different. Even though ω is an independent variable and β depends on ω, it is customary to illustrate the difference between v and v_g on the ω-versus-β plane, as shown in figure 2.4.

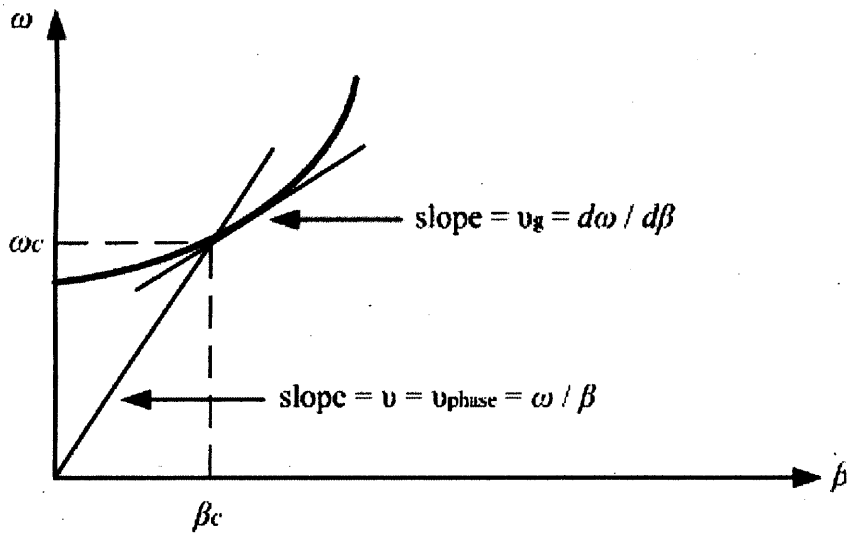

Figure 2.4: The shape of the ω-versus-β curve determines the group velocity, vg, and the phase velocity, v. in general, $v \neq$ vg.

What happens if the optical signals in (2.19) and (2.32) are detected by two separate photodiodes? Since photodiodes respond to optical signal power only (and not to signal phase), the photocurrents produced in both cases are *identical*, except for a phase difference of $\Delta\beta z$. Thus, the term $\dot{\beta}$ in (2.21) does not lead to the detected signal distortion, even though the optical signal is distorted [compare (2.19) with (2.32)].

We conclude by writing (2.32) once more to emphasize the difference between the phase velocity and group velocity:

$$e_{AM}(t,z) = e = E\left[1 + m \cdot \cos\omega_1\left(t - \frac{z}{v_g}\right)\right] \cdot \cos\omega_c\left(t - \frac{z}{v}\right) \quad \ldots (2.36)$$

2.10 Fibre Dispersion

Different light components (different modes and/or different frequencies, or colours) travel through the fibre at generally different velocities. This phenomenon is known as *dispersion.* Dispersion is the widening of pulse duration as it travels through fibre. As a pulse widens, it can broaden enough to interfere with neighbouring pulses (bits) on the fibre, leading to inter-symbol interference. Dispersion thus limits the bit spacing and the maximum transmission rate on a fibre-optic channel. When a composite optical signal travels through the fibre, it can be distorted due to fibre dispersion.

Fibre dispersion of the transmitted optical signal causes distortion for both digital and analogue transmission along optical fibres. If fibre supports several modes, the dominant dispersion mechanism is the *modal* or *intermodal* dispersion (i.e., different modes travelling with different velocities). Intermodal dispersion does not occur in a single-mode fibre. If a fibre supports only one mode, the dominant dispersion mechanism is the material or *chromatic* dispersion. In a dispersive medium, the index of refraction is a function of the wavelength. Thus, if the transmitted signal consists of more than one wavelength, certain wavelengths will propagate faster than other wavelengths (i.e., different light frequencies travelling with different velocities). Since no laser can create a signal consisting of an exact single wavelength, chromatic dispersion will occur in most systems [33].

When considering the major implementation of optical fibre transmission which involves some form of digital modulation, then dispersion mechanisms within the fibre cause broadening of the transmitted light pulses as they travel

along the channel. The phenomenon is illustrated in figure 2.5, where it may be observed that each pulse broadens and overlaps with its neighbours, eventually becoming indistinguishable at the receiver input. The effect is known as Inter-Symbol Interference (ISI). Thus an increasing number of errors may be encountered on the digital optical channel as the ISI becomes more pronounced. The error rate is also a function of the signal attenuation on the link and subsequent signal to noise ratio (SNR) at the receiver. However, signal dispersion alone limits the maximum possible bandwidth attainable with a particular optical fibre to the point where individual symbols can no longer be distinguished.

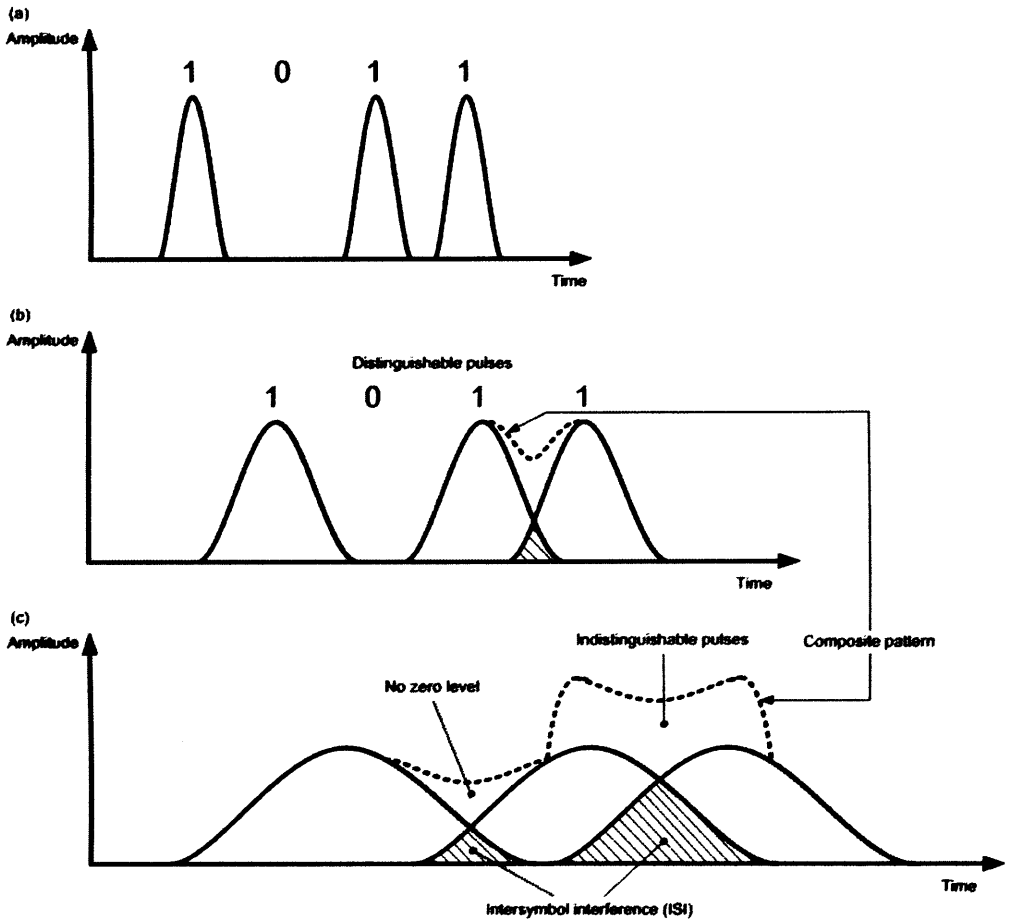

Figure 2.5: An illustration using the digital bit pattern 1011 of the broadening of light pulses as they are transmitted along a fibre: (a) fibre input; (b) fibre output at a distance $L1$; (c) fibre output at a distance $L2 > L1$.

In particular, pulses used in optical systems may become longer due to fibre dispersion by a certain amount we will denote by $\Delta\tau$. Obviously, it is desirable

to keep $\Delta\tau$ within a reasonably small fraction of the pulse duration, T. For no overlapping of light pulses down on an optical fibre link the digital bit rate BT must be less than reciprocal of the broadened (through dispersion) pulse duration $(3\Delta\tau)$. Hence:

$$\Delta\tau \leq \frac{1}{3}T \qquad \ldots (2.37)$$

$$B_T \leq \frac{1}{3\Delta\tau} \qquad \ldots (2.38)$$

where $B_T \equiv 1/T$ is the information transmission rate in bits per second.

This assumes that the pulse broadening due to dispersion on the channel is $\Delta\tau$ which dictates the input pulse duration which is T. Hence equation (2.38) gives a conservative estimate of the maximum bit rate that may be obtained on an optical fibre link as $1/3\Delta\tau$.

Another more accurate estimate of the maximum bit rate for an optical channel with dispersion may be obtained by considering the light pulses at the output to have Gaussian shape with an rms width of σ. Unlike the relationship given in equation (2.38), this analysis allows for the existence of a certain amount of signal overlap on the channel, while avoiding any SNR penalty which occurs when intersymbol interference becomes pronounced. The maximum bit rate is given approximately by:

$$B_T(\max) \approx 0.33/\sigma \text{ bit/s} \qquad \ldots (2.39)$$

It must be noted that certain sources [34;35] give the constant term in the numerator of equation (2.39) as 0.25. However, we take the slightly more conservative estimate given, following Olshansky [36] and Gambling *et al.* [37]. Equation (2.39) gives a reasonably good approximation for other pulse shapes which may occur on the channel resulting from various dispersive mechanisms

within the fibre. Also, σ may be assumed to represent the rms impulse response for the channel.

The conversion of bit rate to bandwidth in hertz depends on the digital coding format used. For metallic conductors when a nonreturn to zero code is employed, the binary one level is held for the whole bit period T. in this case there are two bit periods in one wavelength (i.e. two bits per second per hertz). Hence the maximum bandwidth B is one half the maximum data rate or

$$B_T(\max) = 2B \qquad \ldots (2.40)$$

Hence, when the limitations in the bandwidth of a fibre due to dispersion are stated (i.e. optical bandwidth B_{opt}), it is usually with regard to a return to zero code where the bandwidth in hertz is considered equal to the digital bit rate. The single-mode fibre gives the minimum pulse broadening and thus is capable of the greatest transmission bandwidths which are currently in gigahertz range, whereas transmission via multimode step index fibre is usually limited to bandwidths of a few tens of megahertz. However, the amount of pulse broadening is dependent upon the distance the pulse travels within the fibre, and hence for a given optical fibre link the restriction on usable bandwidth is dictated by the distance between regenerative repeaters (i.e. the distance the light pulse travels before it is reconstituted). Thus the measurement of the dispersive properties of a particular fibre is usually stated as the pulse broadening in time over a unit length of the fibre (i.e. ns/km).

Hence, the number of optical signal pulses which may be transmitted in a given period, and therefore the information-carrying capacity of the fibre, is restricted by the amount of pulse dispersion per unit length. In the absence of mode coupling or filtering, the pulse broadening increases linearly with fibre length and thus the bandwidth is inversely proportional to distance. This leads to the adoption of a more useful parameter for the information-carrying capacity of an optical fibre which is known as the bandwidth-length product (B_{opt} x L).

In order to appreciate the reasons for the different amounts of pulse broadening within the various types of optical fibre, it is necessary to consider the dispersive mechanisms involved. These include material dispersion, waveguide dispersion, and intermodal dispersion. Since, we are dealing with the single-mode fibre the considered dispersion will be just the intramodal dispersion or *Chromatic dispersion.*

2.10.1 Chromatic Dispersion in Optical Fibres

The chromatic dispersion is a linear phenomenon. Mathematically, the chromatic dispersion can be characterized either by $\ddot{\beta}$, the second derivative of the β-versus-ω characteristic (2.21) or by the so-called *group velocity dispersion* (**GVD**) coefficient normally denoted be D. Of course, the two coefficients, $\ddot{\beta}$ and D, are related since they describe the same physical phenomenon. To understand their relationship, let us first find the pulse spread due to chromatic dispersion in terms of $\ddot{\beta}[\sec^2/(m \cdot rad^2)]$.

Let τ be the propagation delay at particular value of ω:

$$\tau = \frac{L}{v_g} \qquad \ldots (2.41)$$

where L is the fibre length, and v_g is the group velocity corresponding to ω. Since v_g is general frequency-dependent, it follows from (2.41) and (2.35) that

$$\frac{\partial \tau}{\partial \omega} = L\frac{\partial}{\partial \omega}\frac{1}{v_g} = L\frac{\partial^2 \beta}{\partial \omega^2} = L\ddot{\beta} \qquad \ldots (2.42)$$

If a signal has a frequency spectral width of $\Delta\omega$ [32], then the difference in propagation time of parts of the signal at the opposite extremes of the spectrum will be

$$\Delta\tau = \left|\frac{\partial\tau}{\partial\omega}\right|\Delta\omega = \left|\frac{\partial^2\beta}{\partial\omega^2}\right| \cdot L \cdot \Delta\omega = \left|\ddot{\beta}\right| L\Delta\omega \qquad \ldots (2.43)$$

Thus, the pulse spread is proportional to $\ddot{\beta}$, fibre length L, and signal spectrum width $\Delta\omega$.

Now, let us evaluate the pulse spread in terms of **GVD** coefficient D (ps/nm.km), defined as

$$D = \frac{1}{L}\frac{\partial\tau}{\partial\lambda} \qquad \ldots (2.44)$$

It follows from (2.44) that

$$D = \frac{1}{L}\frac{\partial\tau}{\partial\lambda} = \frac{1}{L}\frac{\partial\tau}{\partial\omega}\cdot\frac{\partial\omega}{\partial\lambda} \qquad \ldots (2.45)$$

It follows from (2.45) that

$$\frac{\partial\omega}{\partial\lambda} = \frac{\partial}{\partial\lambda}\left(\frac{2\pi}{\lambda}\right) = -\frac{2\pi c}{\lambda^2} \qquad \ldots (2.46)$$

Substituting (2.43) and (2.46) into (2.45), we obtain

$$D = \frac{1}{L}\cdot L\cdot\ddot{\beta}\cdot\left(-\frac{2\pi c}{\lambda^2}\right) = -\frac{2\pi c}{\lambda^2}\ddot{\beta} \qquad \ldots (2.47)$$

Equation (2.47) specifies the relationship between the two dispersion coefficients, $\ddot{\beta}$ and D. Note that the nominal units of $\ddot{\beta}$ are $\sec^2/(m\cdot rad^2)$, while the nominal units of D are $\sec m^2$. Typically, D is expressed in ps/nm.km.

The expression for the pulse spread in terms of D can be obtained either by direct integration of (2.45) or by substituting (2.47) into (2.43), the result is, of course, the same in both cases:

$$\Delta\tau = |D| \cdot \Delta\lambda \cdot L \qquad \ldots (2.48)$$

where $\Delta\lambda$ is the optical signal spectral width with expressed on wavelength units (typically, nm). The values of $\ddot{\beta}$ and **GVD** coefficient D depend on two chromatic dispersion phenomena:

1. Material dispersion. The silica dielectric constant, ε, and, therefore, the refractive index, n, depend on the light frequency, ω.

2. Waveguide dispersion. The propagation constant, β, depends on the light frequency, ω, in a nonlinear fashion even if ε were independent of ω.

Figure 2.6 shows the material dispersion, waveguide dispersion, and the total dispersion, D, versus wavelength for two fibre designs: conventional single-mode fibre and dispersion-shifted fibre.

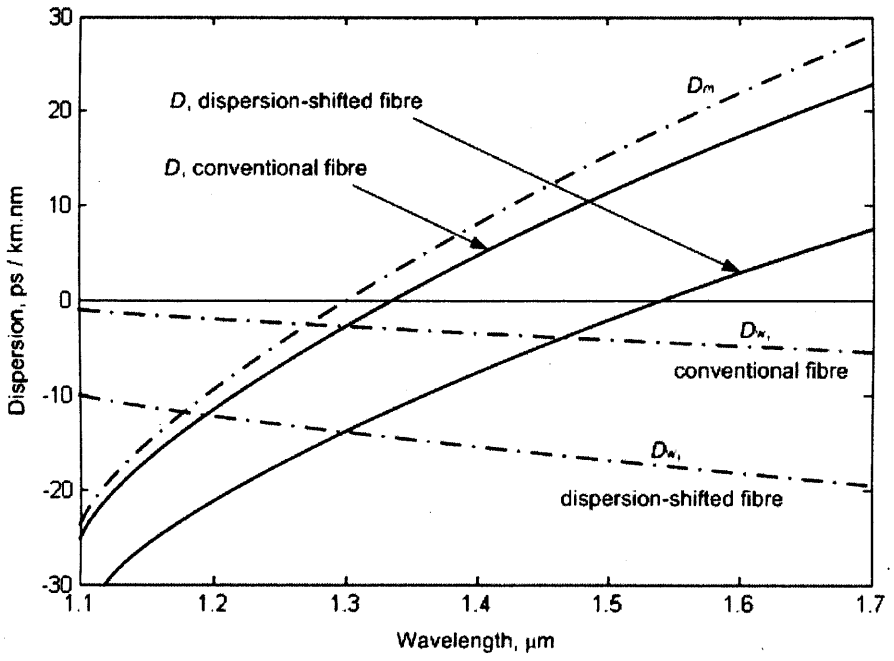

Figure 2.6: Total dispersion, D, and contributions of material dispersion, Dm, and waveguide dispersion, Dw, for conventional single-mode fibres and dispersion-shifted fibres. The zero dispersion wavelength shifts to a higher value because of the waveguide contribution. (Source: [32;38]. © 1986 IEEE.)

The inspection of figure 2.6 reveals interesting conclusions:

1. For $\lambda > 1.3\mu m$, the material dispersion is positive $(D_m > 0)$, while the waveguide dispersion is negative $(D_w < 0)$.

2. At a certain wavelength, the wave guide dispersion cancels the material dispersion, giving the total dispersion of zero: $D_m + D_w = 0$, that wavelength is known as the zero-dispersion wavelength, λ_{ZD}.

The zero-dispersion wavelength depend on fibre type, it is approximately equal to $1.3\mu m$ for conventional single-mode fibres and $1.55\mu m$ for dispersion-shifted fibres.

2.10.2 Chromatic Dispersion in Single-Mode Fibres

Single-mode fibres support only one mode, thus avoiding metal dispersion. Therefore, dispersion is due to *chromatic dispersion* and can be quantitatively ascribed to one of two parameters: D (defined as group velocity dispersion coefficient) or $\ddot{\beta}$, the second derivative of the propagation constant β with respect to the angular light frequency ω in radians per second [32]. They are related through (2.47). At the wavelengths used for optical communications, D and $\ddot{\beta}$ assume values of the same order of magnitude and opposite signs. Assuming that the fibre is linear, the dispersion effects on the propagating pulse depend only on the magnitude of $\ddot{\beta}$ (or D) for zero chirp. When chirp is not zero, the sign of product $c \cdot \ddot{\beta}$, where c is the chirp parameter, also influences the dispersion effects.

Nonlinear phenomena in the fibre, on the other hand, produce different effects depending on the sign of dispersion. A typical example is provided by modulation instability. For that reason, it is important to distinguish between

systems that use fibres with positive or negative dispersion. It is common practice to say that a negative value of D (or, equivalently, a positive value of $\ddot{\beta}$) and in the anomalous dispersion regime when D is positive (or $\ddot{\beta}$ is negative).

Imposing the rule-of-thumb $\Delta\tau \leq (T/3)$ leads to the following inequality:

$$B_T \leq \frac{1}{3|D|\Delta\lambda} \cdot \frac{1}{L} \qquad \ldots (2.49)$$

where $\Delta\lambda$ is the signal bandwidth expressed in terms of the occupied wavelength interval.

For systems that employ lasers with several longitudinal modes, $\Delta\lambda$ is essentially determined by the laser spectral width. On the other hand, for single-longitudinal-mode lasers with small bandwidth, $\Delta\lambda$ depends on the modulation bandwidth and, consequently, on the information rate through

$$\Delta\lambda \cong \frac{\lambda^2}{c} B_T \qquad \ldots (2.50)$$

where λ is the central light wavelength, expression (2.50) assumes that the chirp is negligible. Substituting (2.50) into (2.49) yields

$$B_T^2 \leq \frac{c}{3|D|\lambda^2} \cdot \frac{1}{L} \qquad \ldots (2.51)$$

notice that in (2.51) B_T^2 is proportional to $1/L$, instead of B_T being proportional to $1/L$, as encountered as far.

In the case of a system operating in the 1550nm range, with D = 16 ps/nm.km and a single-longitudinal-mode laser. Using (2.51), we obtain:

$$B_T^2 \leq \frac{2.6x10^3}{L} \quad \ldots (2.52)$$

where B_T is expressed in gigabits per second and L in kilometres. As an example, for L = 1 km we have a bit rate of $B_T \leq 50.99$ Gbps.

2.11 Fibre Nonlinearities

Nonlinear effects in fibre may potentially have a significant impact on the performance of wavelength division multiplexing (WDM) optical communications systems. Nonlinearities in fibre may lead to attenuation, distortion, and cross-channel interference. In a WDM system, these effects place constraints on the spacing between adjacent wavelength channels, limit the maximum power on any channel, and may also limit the maximum bit rate.

In optical fibre, the index of refraction depends on the optical intensity of signals propagating through the fibre [39]. Thus, the phase of the light at the receiver will depend on the phase of the light sent by the transmitter, the length of the fibre, and the optical intensity. Two types of nonlinear effects caused by nonlinear refraction phenomenon, which are Self-Phase Modulation (SPM) and Cross Phase Modulation (XPM). SPM is caused by variations in the power of an optical signal and results in variations in the phase of the signal. The amount of phase shift introduced by

$$\theta_{NL} = n_2 k_o L|E|^2 \quad \ldots (2.53)$$

where n_2 is the nonlinear coefficient for the index of refraction, $k_o = 2\pi/\lambda$, L is fibre length, and $|E|^2$ is the optical intensity.

In Phase-Shift-Keying (PSK) systems, SPM may lead to a degradation of the system performance since the receiver relies on the phase information. SPM also leads to the spectral broadening of pulses. Moreover, Instantaneous variations in

a signal's phase caused by changes in the signal's intensity will result in instantaneous variations of frequency around the signal's central frequency. For very short pulses, the additional frequency components generated by SPM combined with the effects of material dispersion will also lead to spreading or compression of the pulse in the time domain, affecting the maximum bit rate and the BER. On the other hand, XPM is a shift in the phase of a signal caused by the change in intensity of a signal propagating at a different wavelength.

The XPM can lead to asymmetric spectral broadening, and combined with SPM and dispersion may also affect the pulse shape in the time domain. Although XPM may limit the performance of fibre-optic systems, it may also have advantageous applications. XPM can be used to modulate a pump signal at one wavelength from a modulated signal on a different wavelength. Such techniques can be used in wavelength conversion devices. Consequently, fibre nonlinearities are a major limiting factor in the available number channels in a WDM system, however, especially those operating over distances greater than 30 km [39]. The existence of these nonlinearities suggests that WDM protocols that limit the number of nodes to the number of channels do not scale well [17].

2.12 Summary

In this chapter we have presented an extensive review of optical communications particularly Radio-over-Fibre (RoF) technology as a wide bandwidth and cost effective solution for millimetre-wave distribution for wireless networks. This review included a study of the benefits of the RoF systems together with the applications and the ability of these systems to effectively transport mm-waves. Moreover, this chapter presented a review of the optical modulation techniques used for generating and distributing microwave and mm-wave signals.

Optical communication systems can offers many advantages over electrical communication systems by working in the optical domain including high bandwidth and flexibility, while it suffers from restrictions created within the optical medium such as noise and distortion. The characteristics of the optical fibre as a transmission waveguide have been presented in this chapter and were supported by comprehensive mathematical analysis. The study was takes into account fibre nonlinearity as well as fibre dispersion as a destructive parameter when applying RF signals over single and multi mode fibres.

Chapter 3

Dispersion Tolerant Modulation Techniques of IM-DD RoF Systems

This chapter is concerned with investigating RoF optical systems which are applying dispersion tolerant modulation techniques, and based on Intensity Modulation-Direct Detection (IM-DD). After this introductory paragraph, a review of analogue dispersive IM-DD optical RoF links with their applications and limitations are presented. A literature review of the reported optical modulation techniques to overcome fibre chromatic dispersion in RoF links, including Optical Single Sideband (OSSB) and Optical Double Sideband-Suppressed Carrier (DSB-SC) modulation, are reviewed and discussed with details throughout this chapter. Moreover, performance mathematical analysis of RoF links over fibre with respect to fibre chromatic dispersion is extensively demonstrated. Finally a consequential comparison of reported modulation techniques and chapter contributions summary are given in the end sections of this chapter.

3.1 Analogue Dispersive IM-DD Optical RoF Links

Radio over Fibre (RoF) technology gained a significant interest in the last decades due to several benefits and perspective applications [40]. The simplest method for optically distributing RF signals is the Intensity Modulation-Direct Detection (IM-DD) techniques, which is mainly directly modulating the intensity of light source with RF signal and then directly detect the signal with a photodetector to recover the RF signal. However, the conventional modulation techniques are limited by fibre dispersion. With conventional intensity modulation systems of a single mode fibre (SMF), chromatic fibre dispersion, especially at 1550nm, can cause severe signal power penalties at certain distances and frequencies, which limits the bandwidth-length product. Figure (3.1) illustrate the two modulation schemes of a conventional IM-DD modulation with directly modulated laser, figure (3.1 a), and externally modulated laser using MZ modulator, figure (3.1 b).

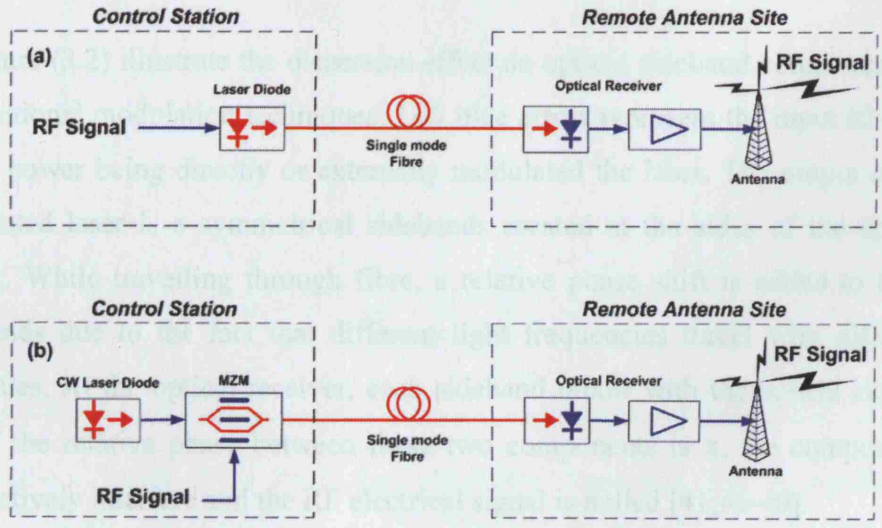

Figure 3.1: Schematic diagram of the conventional RoF systems with (a) direct modulation, and (b) external modulation scheme.

The basic phenomenon of fibre dispersion penalty in optical transmission of millimetre-wave signals were reported by early 90's [41;42], then it has been first demonstrated experimentally by H. Schmuck [43]. Dispersion effect is

independent of modulation format of RF signal. Accordingly, it is valid for any type of RF signal frequency and modulation. It has been found that the detected RF signal power variation caused by fibre dispersion is proportional to [43-45]:

$$P = \cos^2\left(\pi\lambda^2 DLf_c^2 / c\right) \quad \ldots (3.1)$$

where D is the dispersion parameter, L is fibre length, f_c is the modulation carrier frequency, λ is the laser light wavelength, and c is the speed of light in vacuum.

In order to be able to identify fibre dispersion effect with conventional RoF schemes, it would be useful to discuss in further details. With conventional intensity modulation of a single mode fibre (SMF) at 1550nm, symmetrical sidebands are created on the optical carrier. Thus, a composite optical signal travels through the optical fibre, it can be distorted due to fibre dispersion, and as the fibre supports only one mode, SMF, the dominant dispersion mechanism is the chromatic dispersion, where a relative phase shift is added to those sidebands, which depends on optical wavelength, modulation frequency and fibre length.

Figure (3.2) illustrate the dispersion effect on optical sideband components of conventional modulation techniques. Left blue arrow represent the input RF data signal power being directly or externally modulated the laser. The output of the modulated laser is a symmetrical sidebands created at the sides of the optical carrier. While travelling through fibre, a relative phase shift is added to those sidebands due to the fact that different light frequencies travel with different velocities. At the optical receiver, each sideband mixes with the optical carrier, and if the relative phase between these two components is π, the components destructively interfere and the RF electrical signal is nulled [41;46-49].

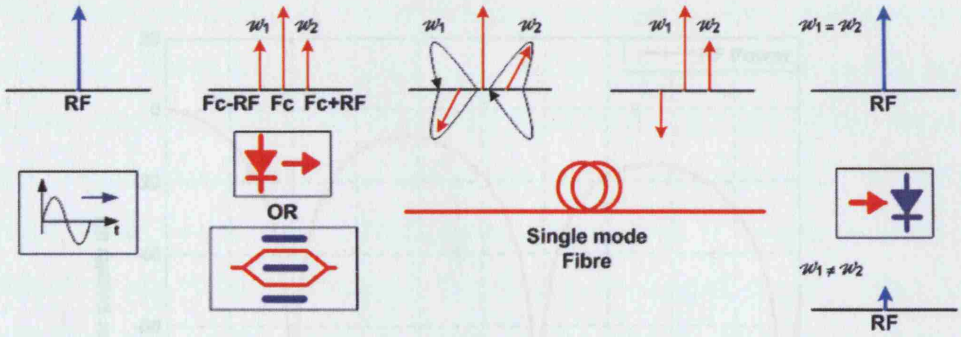

Figure 3.2: Schematic diagram of conventional RoF link illustrating fibre dispersion effect.

Figure (3.3) show an example of normalized power penalty induced corresponded to RF frequencies being transmitted over 15 km of single mode fibre. It can be seen that received signal power is attenuated sharply at specific frequencies due to fibre dispersion.

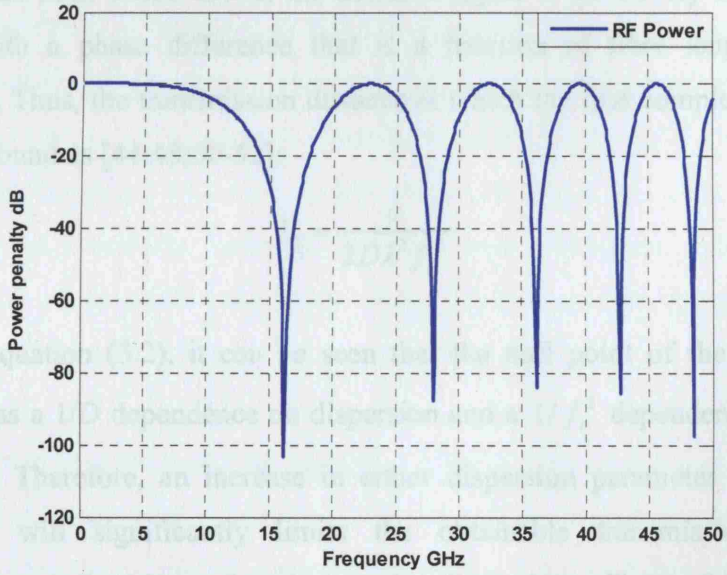

Figure 3.3: Fibre dispersion power penalty versus input RF frequency in IM-DD RoF links.

Therefore, figure (3.3) state that chromatic dispersion has a significant influence on the obtainable transmission distance in intensity modulated direct detection IM-DD RoF links where the RF signal is above 10 GHz Range. Moreover, figure (3.4) show an example of induced power penalty of received RF frequency of 20 GHz transmitted over conventional modulation RoF system with varying fibre lengths. It can be seen that the first power null occur at 10 km of fibre, and it becomes more frequent at higher fibre lengths and frequencies.

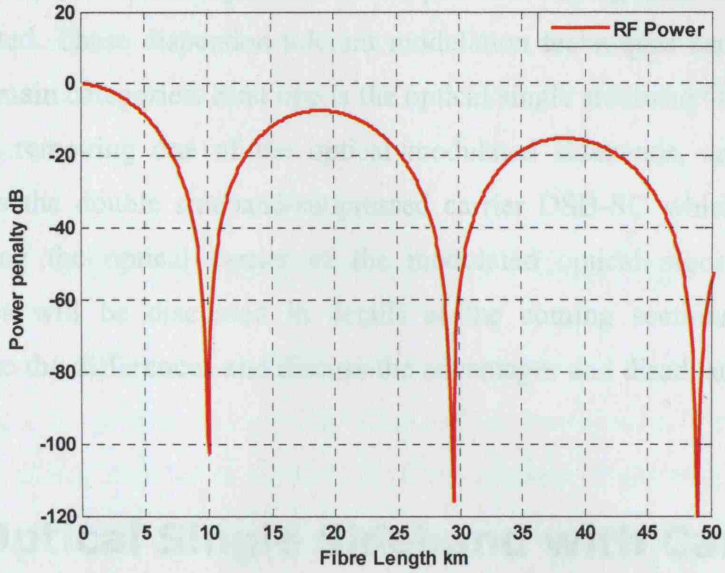

Figure 3.4: Fibre dispersion power penalty versus Fibre length in IM-DD RoF links.

As it has been stated above, the detected signal is effectively a sum of two signals with a phase difference that is a function of fibre length, and RF frequency. Thus, the transmission distance at which the first complete extinction occurs is found as [44;48;50-52]:

$$L_1 = \frac{c}{2D\lambda^2 f_c^2} \qquad \ldots (3.2)$$

From equation (3.2), it can be seen that the null point of the fibre length distance has a $1/D$ dependence on dispersion and a $1/f_c^2$ dependence on carrier frequency. Therefore, an increase in either dispersion parameter D or carrier frequency will significantly limits the obtainable transmission distance. Furthermore, it has been found that the dispersion effect exhibit a cyclic behaviour. The period length is found as [50]:

$$\Delta L = \frac{c}{D\lambda^2 f_c^2} \qquad \ldots (3.3)$$

In order to eliminate, or at least shift, fibre dispersion penalty to useful frequencies and distances product, several modulation techniques have been developed to limit the fibre dispersion penalties of the single-mode fibre links on

RoF systems [43-45;50-56]. These techniques are varying from simple to more complicated. These dispersion tolerant modulation techniques can be classified into two main categories. First one is the optical single sideband OSSB, which is based on removing one of the optical modulated sidebands, and the second method is the double sideband-suppressed carrier DSB-SC which is based on suppressing the optical carrier of the modulated optical signal. These two techniques will be discussed in details at the coming sections in order to investigate the differences and discuss the advantages and disadvantages of each technique.

3.2 Optical Single Sideband with Carrier (SSB+C)

This technique is based on removing one of the optical carrier sidebands of the modulated optical signal to produce single-sideband optical modulation. In this form, it would be possible to eliminate the RF signal power variation over modulation frequency and fibre length, therefore, dispersion only adds a phase shift with no amplitude variation. Two different techniques were reported to remove one of the carrier sidebands of the optical spectrum to produce single-sideband optical modulation.

The first technique based on adding an optical filter to the conventional RoF system of external MZ modulator. This technique is first demonstrated with baseband high-speed digital transmission using a Mach-Zehnder type optical filter [52]. Following, it has been first reported and demonstrated on conventional external optical intensity modulation at millimetre-waves using a fibre Bragg grating filter in 1997 by J. Park et al [51]. The second technique of generating single sideband modulation is by using external dual arm MZ to modulate the CW laser. This technique is first proposed and demonstrated by G.H Smith et al [55;56]. Recently more sophisticated approaches were proposed to enhance the performance of this modulation technique [53;57-59]. Each of these techniques has advantages and disadvantages. The main drawback of all these OSSB modulation techniques is that they rely on filtering or dual arms

modulators. Hence, their deployment could lead to tuning limitations and complicity or equipment high cost. We would like to discuss the key rule of these techniques with further details in order to compare with other dispersion-tolerant modulation schemes.

3.2.1 SSB+C Generation by Filtering

By simply adding an optical filter to conventional RF intensity modulation RoF system, to produce single-sideband optical modulation, the problem of dispersion power penalty is eliminated. Consequently, dispersion only adds a phase shift to the received RF signal with no amplitude change. Either upper or lower sidebands can be removed to produce the required single-sideband optical modulation. Moreover, the filter can be placed at the transmitter side (output of the modulator) or at the receiver side (fibre far end) to give same results. Figure (3.5) illustrate a single sideband modulation system model with using optical filter after the modulator to remove one of the modulated sideband. It can be seen that this model is identical to conventional system except having optical filter following the modulator.

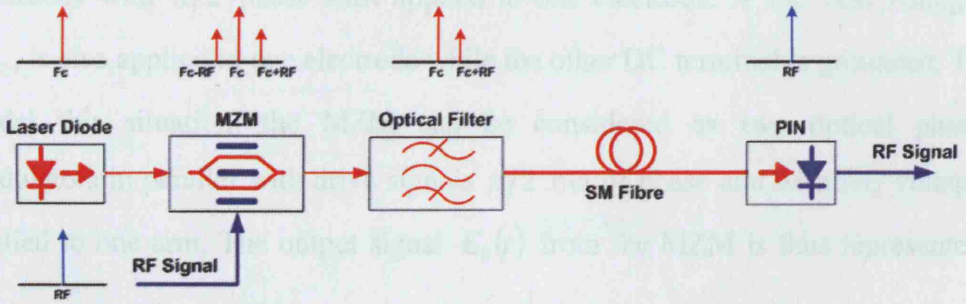

Figure 3.5: Schematic diagram of optical SSB+C RoF system by Filtering.

3.2.1.1 Advantages

Adding an optical filter to the conventional system is easy to apply. Figure (3.5) show the schematic model for a RoF system with an optical filter placed at the output of the modulator. The filter requirements would relaxed as the RF modulation frequency is increased due to the increasing in the separation between the sidebands and the optical carrier wavelength.

3.2.1.2 Disadvantages

The main disadvantage of this technique is the need for filtering out one of the sidebands. For that reason, temperature control is very important in order to keep the filter aligned with the optical sideband to be filtered. Therefore, this method is limited by the filter characteristics and can be too complicated to implement. Moreover, by removing one of the optical sidebands, half of the optical sideband power is removed (3dB) which results in a (6dB) electrical loss relative to the maximum electrical signal power when no filter is used. An additional loss would be added due to the filter insertion loss. However, these losses can be compensated with amplifiers.

3.2.2 SSB+C Generation by Dual Arm MZM

Generating an optical carrier with single-sideband modulation can be achieved by using a dual arm Mach-Zehnder modulator. A CW laser signal with amplitude A and frequency f_c is externally modulated by an RF signal with amplitude V_{ac} and frequency f_{RF} using the dual arm MZM. The RF signal is applied to both electrodes with $\pi/2$ phase shift applied to one electrode. A DC bias voltage, V_{DC}, is also applied to one electrode while the other DC terminal is grounded. To model this situation, the MZM can be considered as two optical phase modulators in parallel with drive signals $\pi/2$ out of phase and with DC voltage applied to one arm. The output signal $E_0(t)$ from the MZM is thus represented by:

$$E_{MZM}^{out} = \frac{A}{2}\left[\cos\left(\omega_c t + \beta\pi + \alpha\pi\cos\omega_{RF}t\right) + \cos\left(\omega_c t + \beta\pi + \alpha\pi\sin\omega_{RF}t\right)\right] \quad \ldots (3.4)$$

where $\omega_c = 2\pi f_c$, $\omega_{RF} = 2\pi f_{RF}$, $\beta = V_{DC}/V_\pi$, where V_π is the MZM switching voltage, and $\alpha = V_{AC}/V_\pi$.

If the MZM is biased so that $\beta = 1/2$ (i.e. at quadrature) and is driven such that $\alpha < 1/\pi$, equation (3.4) can be expanded using Bessel function to:

$$E_{MZM}^{out} = \frac{A}{2}\left[J_0(\alpha\pi)\cos\omega_c t - J_0(\alpha\pi)\sin\omega_c t - 2J_1(\alpha\pi)\cos(\omega_c - \omega_{RF})\ t\right] \ldots (3.5)$$

The Fourier transform of the autocorrelation of $E_0(t)$ will give a power spectral density $S_E(\omega)$:

$$S_E(\omega) = \frac{A^2}{4}J_0^2(\alpha\pi)\ \pi\delta(\omega+\omega_c) + \frac{A^2}{4}J_1^2(\alpha\pi)\ \pi\delta(\omega+(\omega_c-\omega_{RF})) \ldots (3.6)$$

The first term is the optical carrier at wavelength $\lambda_c = 2\pi c/\omega_c$, while the second term represents the lower sideband at the optical frequency $\omega_c - \omega_{RF}$ (seen as an upper sideband in the optical wavelength spectrum).

Mathematical analysis of this system was first reported in [55]. Producing a single sideband modulation with this approach will eliminate the dispersion power penalty induced in conventional RoF systems. Figure (3.6) illustrate the schematic diagram of this system.

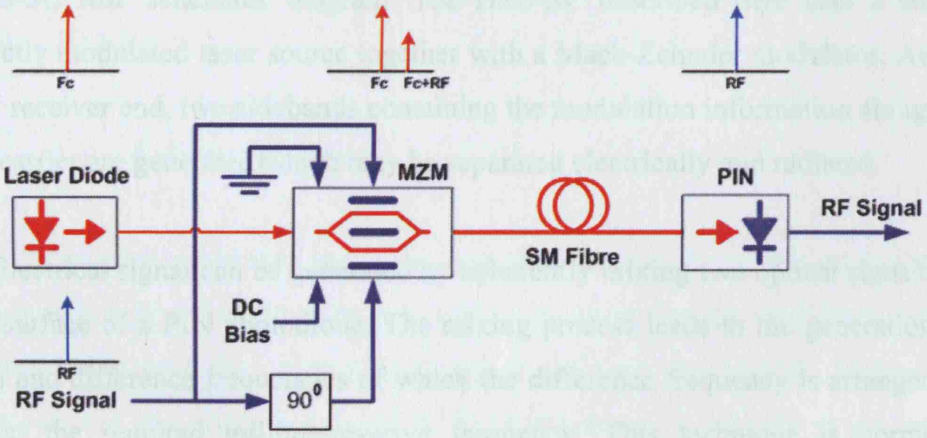

Figure 3.6: Schematic diagram of optical SSB+C RoF system using dual arm MZ modulator.

3.2.2.1 Advantages

This technique is robust as no optical filtering is required and uses only one dual arm MZ modulator to generate optical single sideband [56]. This technique avoids the need to filter out one of the modulated sideband as well as eliminating controlling difficulties introduced with using optical filter.

3.2.2.2 Disadvantages

Using a dual arm MZ modulator could be a costly solution, as it will need to incorporate extra parts within the transmitter in order to perform as required. In addition losses are still introduced due to the removal of one of the optical sidebands, as the case with the optical single sideband by filtering.

3.3 Optical Double Sideband-Suppressed Carrier (DSB-SC) Modulation

Optical DSB-SC system is essentially a combine of two modulation techniques. First forming technique is the laser directly modulation, which is directly modulating the intensity of the laser light by driving the laser bias current with Intermediate Frequency (IF) data signal. The second technique is the use of external modulator to modulate the output intensity of the directly modulated laser light with RF electrical carrier to up-convert the optical signal by applying nonlinear biasing of the external MZ modulator. Figure (3.7) illustrate a DSB-SC RoF schematic diagram. The DSB-SC described here uses a single directly modulated laser source together with a Mach-Zehnder modulator. At the PIN receiver end, two sidebands containing the modulation information along the RF carrier are generated which may be separated electrically and radiated.

Electrical signal can be generated by coherently mixing two optical signals on the surface of a PIN photodiode. The mixing process leads to the generation of sum and difference frequencies of which the difference frequency is arranged to be at the required millimetre-wave frequency. This technique is normally implemented by frequency locking two lasers to the required separation. This method has been extensively described in the remote heterodyning detection RHD literatures [60-62]. Optical modulation technique based on the mixing of two optical carriers on PIN photodiode, whose frequencies differ by the required millimetre-wave frequency, generated from single CW laser, was first proposed and demonstrated in 1992 by J. O'Reilly et al [21].

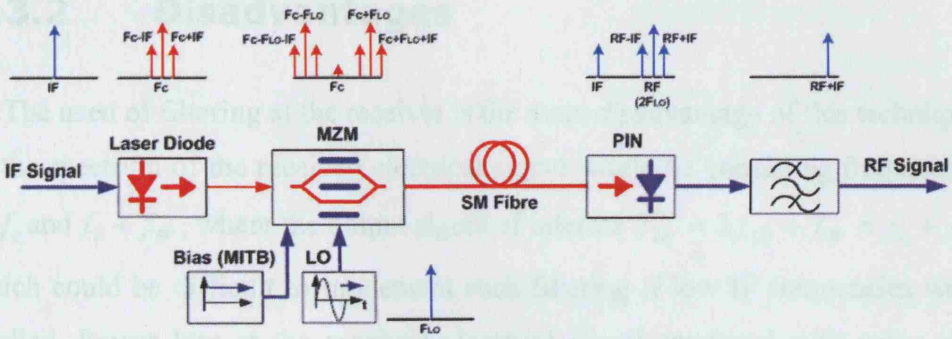

Figure 3.7: Schematic diagram of optical DSB-SC RoF system.

The externally modulation using Mach-Zehnder modulator biased at a nonlinear biasing point reported as electro-optical up-converting scheme at the transmitter. This technique was first proposed in 1997 by J.M. Fuster et al [63-65]. The chromatic dispersion effects occurring in up-converting fibre optic links with electro-optical modulation (EOM) has been reported and demonstrated by [65]. Moreover, dispersion induced with different biasing points of MZ modulator using this technique have been demonstrated by [66-68]. It have been found that this method provides sharp reduction of the induced frequency-length product of fibre chromatic dispersion power penalty at the fibre optic links when the second order harmonic up-conversion of the LO source is performed at the MITB point [67].

3.3.1 Advantages

This method is simple and potentially low-cost method for the remote delivery and generation of millimetre-waves as well as by using directly modulated laser, it removes the need for complex circuitry to maintain the required frequency offset between two lasers with using RHD techniques as it use only single laser source. In addition, this technique uses an IF band input signal to modulate the laser rather than RF frequencies. This could be useful in RoF systems as it will be possible to generate a high frequency signals using components working at lower frequencies, this could be very useful and cost effective factor with regard to the applications and requirements of such systems.

3.3.2 Disadvantages

The need of filtering at the receiver is the main disadvantage of this technique, as the spectrum of the received electrical signal would be consisting frequencies of f_c and $f_c + f_{IF}$, where the output signal of interest $f_{RF} = 2f_{LO} + f_{IF} = f_c + f_{IF}$ which could be difficult to implement such filtering if low IF frequencies were applied. Power loss at the received electrical signal produced with using this technique due to suppressing the optical carrier is other disadvantage of this technique.

3.4 RoF Links Performance with Respect to Fibre Dispersion

In order to clarify the characteristics of optical transmission techniques through fibre optic links, we need to explore characteristics of modulation techniques to compare with the conventional scheme. Furthermore, we need to investigate the performance of those techniques over fibre optic link with respect to fibre dispersion, as well as exploring the system principle and perform a system mathematical analysis of input and output signals with the existence of the optical fibre link. To achieve this, we have developed here for the first time a mathematical model of the DSB-SC technique based on the second order optical upconversion modulation.

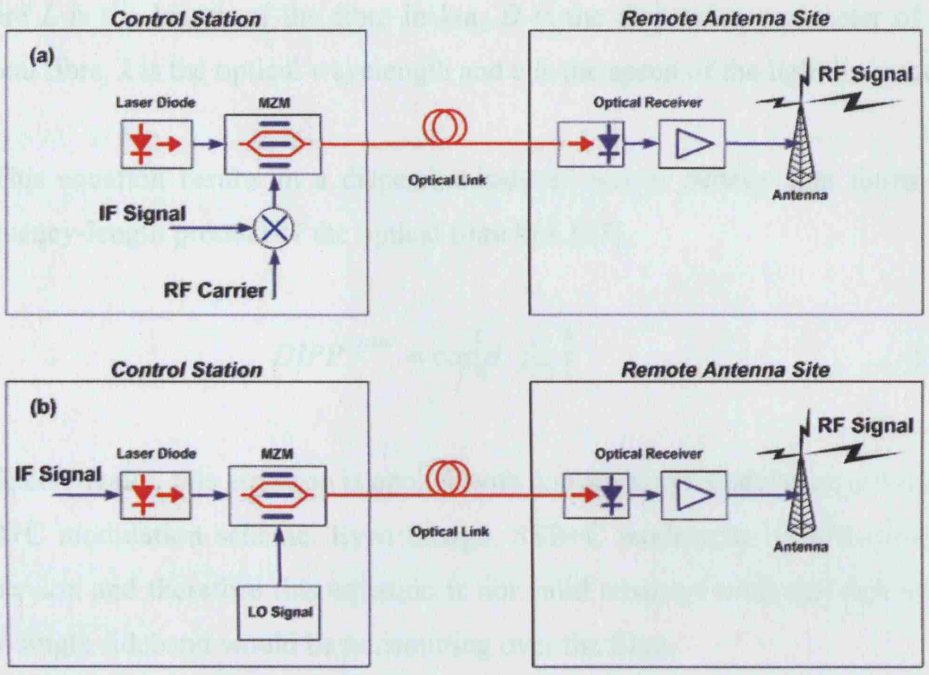

Figure 3.8: Schematic diagram of the RoF (a) conventional, and (b) the up-conversion scheme.

In the conventional scheme, the RF signal to be radiated on the antenna is externally modulated onto the optical carrier. Alternatively, in the up-converting system, an intermediate frequency IF signal directly modulates the optical source, and optical up-conversion is achieved through the LO signal driving the external modulator figure (3.8 a and b). In either case, the modulated or up-converted RF signal is launched into the optical fibre and may be optically amplified if necessary. At the receiving end, the detected RF signal at the output of the photodetector is amplified by an RF power amplifier prior to be radiated.

In the conventional link (Figure 3.8 a), fibre chromatic dispersion affects the transmission frequency-length product of the millimetre-wave signals, the detected RF current at the output of the photodetector is proportional to:

$$i_{phot} \propto \cos\left(\beta f_{RF}^2\right) \qquad \ldots (3.7)$$

where β is:

$$\beta = \frac{\pi D \lambda^2 L}{c} \qquad \ldots (3.8)$$

where L is the length of the fibre in km, D is the dispersion parameter of the optical fibre, λ is the optical wavelength and c is the speed of the light in vacuum.

This equation results in a dispersion-induced power penalty that limits the frequency-length product of the optical fibre link [67].

$$DIPP^{CONV} = \cos\left[\beta\ f_{RF}^2\right] \quad \ldots (3.9)$$

Theoretically, this equation is applies with conventional modulation as well as SSB+C modulation scheme. Even though, SSB+C modulation eliminates fibre dispersion and therefore this equation is not valid anymore with this scheme as only single sideband would be transmitting over the fibre.

When harmonic up-conversion is performed Figure (3.8 b), the impact of the fibre chromatic dispersion depends on the biasing point of the MZM. If the modulator biased at the minimum transmission biasing (MITB) point (the null point), results of up-converted signals of frequency

$$f_{RF} = 2kf_{LO} + f_{IF} \quad \ldots (3.10)$$

with k = 0, 1, 2, ...

Mathematical analysis of electro-optical up-converting modulation, figure (3.7), would be useful to illustrate the modulation technique performance with respect to fibre dispersion, and to compare with conventional modulation. Starting from the directly modulated DM laser input, the output filed of the un-modulated laser can be described by:

$$E^{CW} = E_{laser}e^{j\omega_0 t} \quad \ldots (3.11)$$

Also a sinusoidal modulating voltage applied to the DM laser can be described by:

$$V(t)_{laser} = m_i \cos(\omega_{IF} t) \quad \ldots (3.12)$$

where m_i is the laser modulation index, ω_{IF} is the input signal frequency, while the directly modulated laser output field can be described by

$$E_{laser}^{DM} = E_{laser} e^{j\omega_0 t} + E_{laser} m_i \cos(\omega_{IF} t)\ e^{j\omega_0 t} \quad \ldots (3.13)$$

$$= E_{laser}\left[1 + m_i \cos(\omega_{IF} t)\right]\ e^{j\omega_0 t} \quad \ldots (3.14)$$

Moreover, a sinusoidal modulating voltage applied to the MZ modulator can be described by:

$$V(t)_{MZM} = V_\pi (1+\varepsilon) + \alpha_{LO} V_\pi \cos(\omega_{LO} t) \quad \ldots (3.15)$$

where ε is the normalized bias point of the modulator, ω_{LO} is the LO frequency, and α_{LO} is the normalized amplitude of the drive voltage given by:

$$\alpha_{LO} = \frac{\pi}{2} \frac{V_{LO}}{V_{\pi(f_{LO})}} \quad \ldots (3.16)$$

where V_{LO} is the voltages of the LO signal and $V_{\pi(f_{LO})}$ is the half-wave voltage at the LO frequency.

Also it can be shown that the transfer function of the balanced modulator can be described by:

$$\frac{E_{MZM}^{out}}{E_{MZM}^{in}} = \cos\left[\frac{\pi}{2}\frac{V}{V_\pi}\right] \quad \ldots (3.17)$$

Therefore,

$$E_{MZM}^{out} = \cos\left[\frac{\pi}{2}\frac{V}{V_\pi}\right] \times E_{MZM}^{in} \quad \ldots (3.18)$$

where V is the applied voltage to the MZM.

Therefore, applying the output field of the DM laser as an input field to the MZM and $V(t)_{MZM}$ as an input modulating signal, the output field from the modulator can be described by:

$$E_{MZM}^{out} = E_{laser}[1+m_i\cos(\omega_{IF}t)]\times\cos\left[\frac{\pi}{2}[(1+\varepsilon)+\alpha_{LO}\cos(\omega_{LO}t)]\right] e^{j\omega_0 t} \quad \ldots (3.19)$$

$$= E_{laser}[1+m_i\cos(\omega_{IF}t)]\left[\cos\left(\frac{\pi}{2}(1+\varepsilon)\right)\cos(\alpha_{LO}\cos(\omega_{LO}t)) - \sin\left(\frac{\pi}{2}(1+\varepsilon)\right)\sin(\alpha_{LO}\cos(\omega_{LO}t))\right] e^{j\omega_0 t} \quad \ldots (3.20)$$

If the modulator is biased at the nonlinear minimum transmission bias (MITB) point V_π (i.e. $\varepsilon = 0$) then the term ($\cos\frac{\pi}{2}(1+\varepsilon) = \cos\frac{\pi}{2} = 0$) therefore,

$$E_{MZM}^{out} = E_{laser}[1+m_i\cos(\omega_{IF}t)]\,[-(1)\sin(\alpha_{LO}\cos(\omega_{LO}t))]\, e^{j\omega_0 t} \quad \ldots (3.21)$$

Expanding the output with Bessel function would leads to describe the output field by:

$$E_{MZM}^{out} = E_{laser}[1+m_i\cos(\omega_{IF}t)]\left[\ \ldots - (1)\left[2\sum_{k=0}^{\infty}(-1)^k J_{2k+1}(\alpha_{LO})\cos((2k+1)\omega_{LO}t)\right]\right] e^{j\omega_0 t} \quad \ldots (3.22)$$

Submitting values of k = 0, 1, 2, ...

$$E_{MZM}^{out} = -2J_1(\alpha_{LO})E_{laser}\left[1+m_i\cos(\omega_{IF}t)\right]\left[\cos(\omega_{LO}t)\right]\ e^{j\omega_0 t}$$
$$+2J_3(\alpha_{LO})E_{laser}\left[1+m_i\cos(\omega_{IF}t)\right]\left[\cos(3\omega_{LO}t)\right]\ e^{j\omega_0 t}$$
$$-2J_5(\alpha_{LO})E_{laser}\left[1+m_i\cos(\omega_{IF}t)\right]\left[\cos(5\omega_{LO}t)\right]\ e^{j\omega_0 t}+\ldots \qquad \ldots (3.23)$$

where $J_k(\cdot)$ stands for the k-th-order Bessel function of the first kind.

It shows that the frequency terms of the MZM output field would be as below:

$$=(\omega_0 \pm \omega_{LO})+(\omega_0+\omega_{LO})\pm\omega_{IF}+(\omega_0-\omega_{LO})\pm\omega_{IF}$$
$$+(\omega_0 \pm 3\omega_{LO})+(\omega_0+3\omega_{LO})\pm\omega_{IF}+(\omega_0-3\omega_{LO})\pm\omega_{IF} \qquad \ldots (3.24)$$

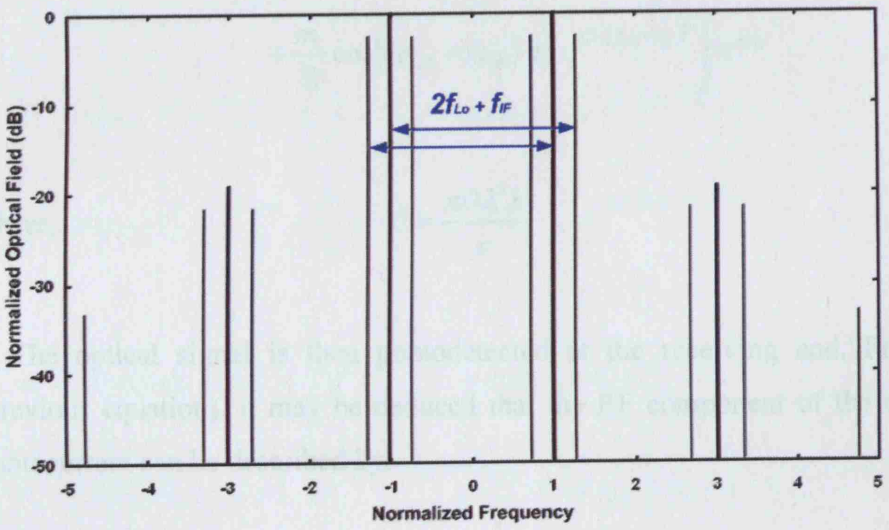

Figure 3.9: Optical spectrum of the second harmonic up-converted DSB-SC

Just the first term will be considered at this stage as the higher terms values will be significantly small and therefore can be neglected.

Exploring the first term of the above equation will give:

$$E_{MZM}^{out} = -2J_1(\alpha_{LO})E_{laser}\left[\cos(\omega_{LO}t)+\frac{m_i}{2}\cos(\omega_{LO}+\omega_{IF})\ t+\frac{m_i}{2}\cos(\omega_{LO}-\omega_{IF})\ t\right]\ e^{j\omega_0 t}$$

$$\ldots (3.25)$$

Moreover, it can be shown that the equivalent transfer function of the dispersive fibre can be described by:

$$\frac{E_{fibre}^{out}}{E_{fibre}^{in}} = e^{j\beta(f)^2} \qquad \ldots (3.26)$$

Therefore, after propagation through the optical fibre, the electrical field E_{Fibre}^{MITB} can be described by:

$$E_{fibre}^{MITB} = -2J_1(\alpha_{LO})\ E_{laser}\Big[\cos(\omega_{LO}\ t)\ e^{j\beta\ (f_{LO})^2} + \frac{m_i}{2}\cos((\omega_{LO}+\omega_{IF})\ t)\ e^{j\beta\ (f_{LO}+f_{IF})^2} + \frac{m_i}{2}\cos((\omega_{LO}-\omega_{IF})\ t)\ e^{j\beta\ (f_{LO}-f_{IF})^2}\Big]\ e^{j\omega_0 t} \qquad \ldots (3.27)$$

where, $$\beta = \frac{\pi D \lambda^2 L}{c}$$

The optical signal is then photodetected at the receiving end. From the (previous equation), it may be deduced that the RF component of the detected photocurrent can be described by:

$$i_{photo} = \left|E_{fibre}^{MITB}\right|^2 \qquad \ldots (3.28)$$

$$= E_{fibre}^{MITB} .^* E_{fibre}^{MITB} \qquad \ldots (3.29)$$

Therefore,

$$i_{photo} = 4J_1{}^2(\alpha_{LO})\ E^2{}_{laser}\Big[\cos(\omega_{LO}\ t)\ e^{j\beta\ (f_{LO})^2} + \frac{m_i}{2}\cos((\omega_{LO}+\omega_{IF})\ t)\ e^{j\beta\ (f_{LO}+f_{IF})^2}$$

$$+\frac{m_i}{2}\cos\left(\left(\omega_{LO}-\omega_{IF}\right)t\right)e^{j\beta\,(f_{LO}-f_{IF})^2}\Big]\Big[\cos\left(\omega_{LO}\,t\right)e^{-j\beta\,(f_{LO})^2}$$

$$+\frac{m_i}{2}\cos\left(\left(\omega_{LO}+\omega_{IF}\right)t\right)e^{-j\beta\,(f_{LO}+f_{IF})^2}$$

$$+\frac{m_i}{2}\cos\left(\left(\omega_{LO}-\omega_{IF}\right)t\right)e^{-j\beta\,(f_{LO}-f_{IF})^2}\Big]\,e^{j\omega_0 t}e^{-j\omega_0 t} \quad \ldots (3.30)$$

Expanding the equation by multiplying each term of the first part of the equation by the conjugate of the equation will give us:

$$i_{photo}=4J_1^{\,2}(\alpha_{LO})\;E^2{}_{laser}\Big\{$$

$$\left(\cos\left(\omega_{LO}\,t\right)e^{j\beta\,(f_{LO})^2}\times\cos\left(\omega_{LO}\,t\right)e^{-j\beta\,(f_{LO})^2}\right)$$

$$+\left(\cos\left(\omega_{LO}\,t\right)e^{j\beta\,(f_{LO})^2}\times\frac{m_i}{2}\cos\left(\left(\omega_{LO}+\omega_{IF}\right)t\right)e^{-j\beta\,(f_{LO}+f_{IF})^2}\right)$$

$$+\left(\cos\left(\omega_{LO}\,t\right)e^{j\beta\,(f_{LO})^2}\times\frac{m_i}{2}\cos\left(\left(\omega_{LO}-\omega_{IF}\right)t\right)e^{-j\beta\,(f_{LO}-f_{IF})^2}\right)$$

$$+\left(\frac{m_i}{2}\cos\left(\left(\omega_{LO}+\omega_{IF}\right)t\right)e^{j\beta\,(f_{LO}+f_{IF})^2}\times\cos\left(\omega_{LO}\,t\right)e^{-j\beta\,(f_{LO})^2}\right)$$

$$+\left(\frac{m_i}{2}\cos\left(\left(\omega_{LO}+\omega_{IF}\right)t\right)e^{j\beta\,(f_{LO}+f_{IF})^2}\times\frac{m_i}{2}\cos\left(\left(\omega_{LO}+\omega_{IF}\right)t\right)e^{-j\beta\,(f_{LO}+f_{IF})^2}\right)$$

$$+\left(\frac{m_i}{2}\cos\left(\left(\omega_{LO}+\omega_{IF}\right)t\right)e^{j\beta\,(f_{LO}+f_{IF})^2}\times\frac{m_i}{2}\cos\left(\left(\omega_{LO}-\omega_{IF}\right)t\right)e^{-j\beta\,(f_{LO}-f_{IF})^2}\right)$$

$$+\left(\frac{m_i}{2}\cos\left(\left(\omega_{LO}-\omega_{IF}\right)t\right)e^{j\beta\,(f_{LO}-f_{IF})^2}\times\cos\left(\omega_{LO}\,t\right)e^{-j\beta\,(f_{LO})^2}\right)$$

$$+\left(\frac{m_i}{2}\cos\left(\left(\omega_{LO}-\omega_{IF}\right)t\right)e^{j\beta\,(f_{LO}-f_{IF})^2}\times\frac{m_i}{2}\cos\left(\left(\omega_{LO}+\omega_{IF}\right)t\right)e^{-j\beta\,(f_{LO}+f_{IF})^2}\right)$$

$$+\left(\frac{m_i}{2}\cos\left(\left(\omega_{LO}-\omega_{IF}\right)t\right)e^{j\beta\,(f_{LO}-f_{IF})^2}\times\frac{m_i}{2}\cos\left(\left(\omega_{LO}-\omega_{IF}\right)t\right)e^{-j\beta\,(f_{LO}-f_{IF})^2}\right)\Big\}$$

$$\ldots (3.31)$$

$$= 4J_1^2(\alpha_{LO})\, E^2_{laser}\Bigg\{$$

$$\frac{1}{2}\Big(1+\cos(2\omega_{LO}\, t)\Big)$$

$$+\frac{m_i}{4}\Big(\cos(2\omega_{LO}+\omega_{IF})\, t+\cos(-\omega_{IF})\, t\Big)\, e^{j\left(\beta\,(f_{LO})^2-\beta\,(f_{LO}+f_{IF})^2\right)}$$

$$+\frac{m_i}{4}\Big(\cos(2\omega_{LO}-\omega_{IF})\, t+\cos(+\omega_{IF})\, t\Big)\, e^{j\left(\beta\,(f_{LO})^2-\beta\,(f_{LO}-f_{IF})^2\right)}$$

$$+\frac{m_i}{4}\Big(\cos(2\omega_{LO}+\omega_{IF})\, t+\cos(+\omega_{IF})\, t\Big)\, e^{j\left(\beta\,(f_{LO}+f_{IF})^2-\beta\,(f_{LO})^2\right)}$$

$$+\frac{m_i^2}{8}\Big(1+\cos 2(\omega_{LO}+\omega_{IF})\, t\Big)$$

$$+\frac{m_i^2}{8}\Big(\cos(2\omega_{LO})\, t+\cos(+2\omega_{IF})\, t\Big)\, e^{j\left(\beta\,(f_{LO}+f_{IF})^2-\beta\,(f_{LO}-f_{IF})^2\right)}$$

$$+\frac{m_i}{4}\Big(\cos(2\omega_{LO}-\omega_{IF})\, t+\cos(-\omega_{IF})\, t\Big)\, e^{j\left(\beta\,(f_{LO}-f_{IF})^2-\beta\,(f_{LO})^2\right)}$$

$$+\frac{m_i^2}{8}\Big(\cos(2\omega_{LO})\, t+\cos(-2\omega_{IF})\, t\Big)\, e^{j\left(\beta\,(f_{LO}-f_{IF})^2-\beta\,(f_{LO}+f_{IF})^2\right)}$$

$$+\frac{m_i^2}{8}\Big(1+\cos 2(\omega_{LO}-\omega_{IF})\, t\Big)\Bigg\} \qquad \ldots (3.32)$$

Now, adding the similar terms together and take the common factors we will get:

Term 2 with 4

Term 3 with 7

Term 6 with 8

And the terms 1, 5 and 9 as follows:

$$i_{photo} = 4J_1^2(\alpha_{LO})\ E^2{}_{laser}\Bigg\{$$

$$\frac{m_i}{4}\left(\cos(2\omega_{LO}+\omega_{IF})\ t+\cos(-\omega_{IF})\ t\right) e^{j\left(\beta\ (f_{LO})^2-\beta\ (f_{LO}+f_{IF})^2\right)}$$

$$+\frac{m_i}{4}\left(\cos(2\omega_{LO}+\omega_{IF})\ t+\cos(+\omega_{IF})\ t\right) e^{j\left(\beta\ (f_{LO}+f_{IF})^2-\beta\ (f_{LO})^2\right)}$$

$$+\frac{m_i}{4}\left(\cos(2\omega_{LO}-\omega_{IF})\ t+\cos(+\omega_{IF})\ t\right) e^{j\left(\beta\ (f_{LO})^2-\beta\ (f_{LO}-f_{IF})^2\right)}$$

$$+\frac{m_i}{4}\left(\cos(2\omega_{LO}-\omega_{IF})\ t+\cos(-\omega_{IF})\ t\right) e^{j\left(\beta\ (f_{LO}-f_{IF})^2-\beta\ (f_{LO})^2\right)}$$

$$+\frac{m_i^2}{8}\left(\cos(2\omega_{LO})\ t+\cos(+2\omega_{IF})\ t\right) e^{j\left(\beta\ (f_{LO}+f_{IF})^2-\beta\ (f_{LO}-f_{IF})^2\right)}$$

$$+\frac{m_i^2}{8}\left(\cos(2\omega_{LO})\ t+\cos(-2\omega_{IF})\ t\right) e^{j\left(\beta\ (f_{LO}-f_{IF})^2-\beta\ (f_{LO}+f_{IF})^2\right)}$$

$$+\frac{1}{2}\left(1+\cos(2\omega_{LO}\ t)\right)$$

$$+\frac{m_i^2}{8}\left(1+\cos 2(\omega_{LO}+\omega_{IF})\ t\right)$$

$$+\frac{m_i^2}{8}\left(1+\cos 2(\omega_{LO}-\omega_{IF})\ t\right)$$

$$\Bigg\} \qquad \ldots (3.33)$$

Reforming the mathematical expression of the exponential terms $\frac{e^{jX}+e^{-jX}}{2}=\cos X$, therefore,

$$i_{photo} = 4J_1^{\,2}(\alpha_{LO})\; E^2{}_{laser}\Bigg\{$$

$$\frac{m_i}{2}\times\cos(2\omega_{LO}+\omega_{IF})\;t\times\cos\left(\beta\;(f_{LO}+f_{IF})^2-\beta\;(f_{LO})^2\right)$$

$$+\frac{m_i}{2}\times\cos(\omega_{IF})\;t\times\cos\left(\beta\;(f_{LO}+f_{IF})^2-\beta\;(f_{LO})^2\right)$$

$$+\frac{m_i}{2}\times\cos(2\omega_{LO}-\omega_{IF})\;t\times\cos\left(\beta\;(f_{LO}-f_{IF})^2-\beta\;(f_{LO})^2\right)$$

$$+\frac{m_i}{2}\times\cos(\omega_{IF})\;t\times\cos\left(\beta\;(f_{LO}-f_{IF})^2-\beta\;(f_{LO})^2\right)$$

$$+\frac{m_i^2}{4}\times\cos(2\omega_{LO})\;t\times\cos\left(\beta\;(f_{LO}+f_{IF})^2-\beta\;(f_{LO}-f_{IF})^2\right)$$

$$+\frac{m_i^2}{4}\times\cos(2\omega_{IF})\;t\times\cos\left(\beta\;(f_{LO}+f_{IF})^2-\beta\;(f_{LO}-f_{IF})^2\right)$$

$$+\frac{1}{2}+\frac{1}{2}\times\cos\left(2\omega_{LO}\;t\right)$$

$$+\frac{m_i^2}{8}+\frac{m_i^2}{8}\times\cos 2(\omega_{LO}+\omega_{IF})\;t$$

$$+\frac{m_i^2}{8}+\frac{m_i^2}{8}\times\cos 2(\omega_{LO}-\omega_{IF})\;t$$

$$\Bigg\} \quad \ldots (3.34)$$

As the frequency of interest is $f_{RF} = 2f_{LO} + f_{IF}$, therefore the first term of the equation is representing this frequency component. Simplifying that term will lead us to:

$$= 2m_i J_1^2(\alpha_{LO})\; E^2{}_{laser}\left\{\cos(2\omega_{LO}+\omega_{IF})\;t\times\cos(\beta f_{IF}(2f_{LO}+f_{IF}))\right\} \quad \ldots (3.35)$$

$$= 2m_i J_1^2(\alpha_{LO})\, E^2{}_{laser}\left\{ \cos(2\omega_{LO} + \omega_{IF})\, t \times \cos(\beta f_{IF} f_{RF}) \right\} \quad \ldots (3.36)$$

Equation (3.36) above resulting in dispersion induced power penalty DIPP factor of the second harmonic modulation of

$$DIPP_2^{MITB} = \cos[\beta f_{IF} f_{RF}] \quad \ldots (3.37)$$

Figure (3.10) shows theoretical power penalty curves of the received RF signal when using the conventional DSB modulation compared to the second harmonic up-converted DSB-SC. Figure shows a power penalty of 6 dB after 100 km of fibre when DSB-SC used, while four nulled power penalty points are produced at the first 100 km of fibre with conventional DSB modulation. Therefore, Optical up-conversion modulation scheme is a modulation technique where fibre dispersion effect is shifted to higher frequency ranges in order to increase the frequency-length product of RoF systems.

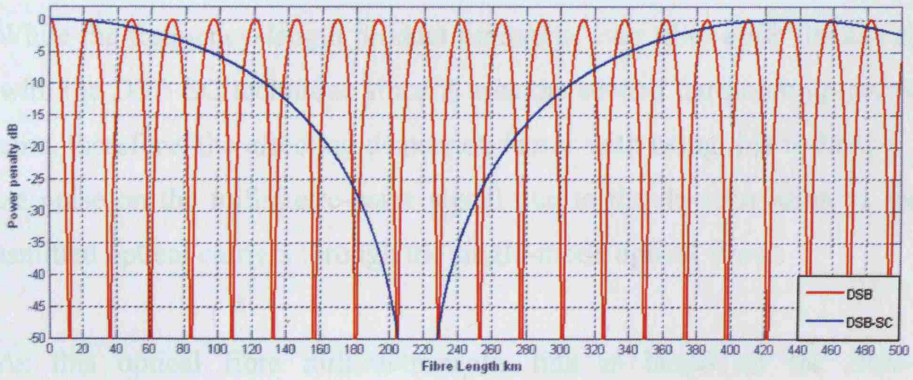

Figure 3.10: Theoretical dispersion-induced power penalty DIPP curves against fibre length of 18 GHz conventional DSB Vs second harmonic up-converted DSB-SC.

3.5 Modulation Effects of Fibre Dispersion

Since with this modulation technique two phase correlated optical carriers are generated at the output of the MZ modulator, therefore, the fibre optic links dispersion characteristics of this technique are lies under the dispersion characteristics of the remote heterodyne detection RHD links.

In this link, two phase correlated optical carriers are generated, in an external MZ modulator, with a frequency offset f_c equal to the desired millimetre-wave carrier frequency. Furthermore, both of the two optical carriers are modulated by the information to be contained in the millimetre-wave signal. Both optical signals are then transmitted through the optical fibre, and the millimetre-wave signal is generated by heterodyning of the two optical signals in a photodiode. In this approach, the fibre chromatic dispersion becomes a limiting factor for the transmission distance as it results in a CNR penalty as well as an increase of phase noise on the millimetre-wave signal, both due to decorrelation of the two transmitted optical carriers.

While the frequency-length product limitation over fibre optic links is shifted up with the DSB-SC technique since it uses the second harmonic up-converting scheme, therefore, the effecting dispersion factor with using this technique is the phase noise on the millimetre-wave signal due to the de-correlation of the two transmitted optical carriers through the single-mode optical fibre.

As this optical fibre millimetre-wave link is based on the fibre-optic transmission of two phase-correlated optical signals, at frequencies f_1 and f_2, that are offset the desired millimetre-wave carrier frequency f_c. With this transmitter concept, both of phase-correlated optical signals are phase-equal with the signal from the master laser. For a perfect transmission without influence of the fibre or other optical devices, the two optical signals are also phase-correlated at the remote photodiode detector where the heterodyning takes place. Consequently, the resulting beat signal is highly pure millimetre-wave carrier at f_c.

However, due to the fibre chromatic dispersion, the two optical signals experience a differential propagation delay, $\Delta\tau_{disp}$ as they travel through the fibre [50]. Furthermore, if the two optical signals, before they are injected into the same fibre, propagate separate paths that are not perfectly balanced, they also experience a differential propagation delay, $\Delta\tau_{path}$. The sum differential propagation delay, given by:

$$\Delta\tau = \left|\Delta\tau_{disp} + \Delta\tau_{path}\right| \quad \ldots (3.38)$$

Since with the used technique only single optical laser is generating the two optical carriers, therefore, no path delay introduced with this technique $\left(\Delta\tau_{path} = 0\right)$.

Therefore,

$$\Delta\tau = \left|\Delta\tau_{disp}\right| \quad \ldots (3.39)$$

Results in a state of partial phase decorrelation. The amount of decorrelation, and thus the increase in phase noise on the remotely generated millimetre-wave carrier depends on the introduced amount of differential delay as illustrated in figure (3.11). Assuming that the master laser, from which the two phase correlated optical signals are derived, has a Lorentzian shaped power spectrum, then the power spectral density of the f_c signal at the output of the photodetector of figure (3.11) can be described by [50]:

As shown in figure (3.11), for a small differential delay $\left(\Delta\tau \approx 0\right)$, the two optical signals remain correlated and the resulting beat spectrum is a delta function. At the other extreme, for a very large differential delay, the two optical signals get completely decorrelated and the beat spectrum then becomes Lorentzian shaped with a linewidth of $2 \cdot \Delta V_m$. At intermediate values of $\Delta\tau$, the beat spectrum is a combination of a delta function and a sinc shaped spectrum with spectral zeros spaced by $1/\Delta\tau$.

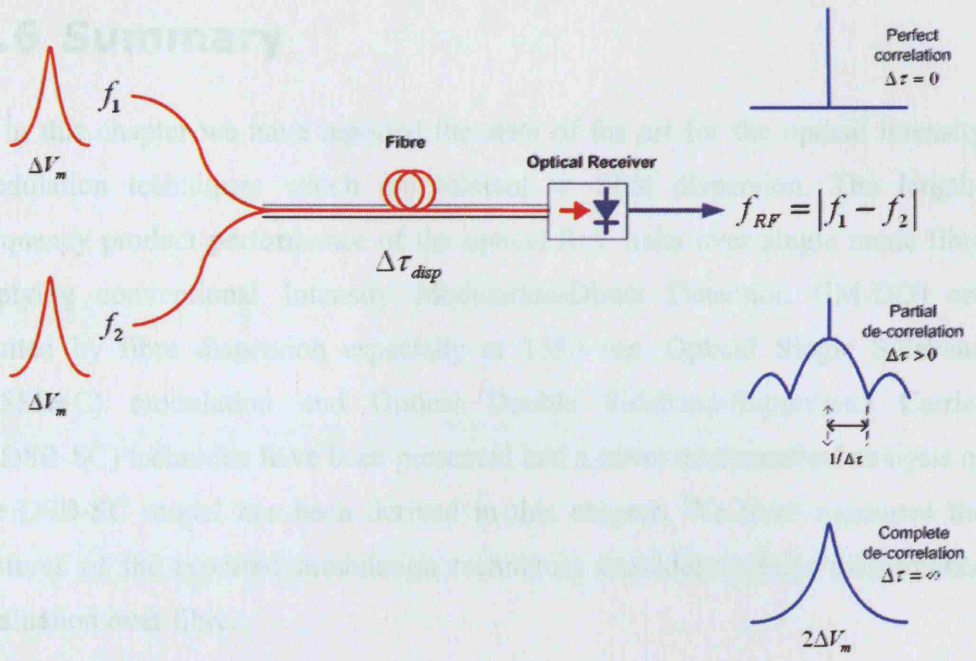

Figure 3.11: Phase de-correlation effect of fibre dispersion at mw links.

The decorrelation results in both a decrease of the Carrier to Noise Ratio (CNR) and an increase of the phase noise. These two effects are closely related as the decrease in signal power is due to the increase of the phase noise power at all offset frequencies. Both effects must be considered and treated separately as they may result in limitations of obtainable frequency-distance product.

with the used modulation technique, the differential delay is only due to fibre chromatic dispersion and depends on the transmission distance, L, the wavelength λ, the frequency offset, $f_c = 2f_{LO}$ (millimetre-wave carrier frequency), between the two optical signals and the fibre dispersion parameter, D. this part constitutes the delay reference and is therefore always taken as positive. It is seen that the delay induced rms phase error increases as the differential delay increases. It is given by:

$$\Delta\tau_{disp} = D \cdot L \cdot \frac{\lambda^2}{c} \cdot f_c \qquad \ldots (3.40)$$

3.6 Summary

In this chapter we have reported the state of the art for the optical intensity modulation techniques which are tolerant to fibre dispersion. The length-frequency product performance of the optical RoF links over single mode fibre applying conventional Intensity Modulation-Direct Detection (IM-DD) are limited by fibre dispersion especially at 1550 nm. Optical Single Sideband (OSSB+C) modulation and Optical Double Sideband-Suppressed Carrier (ODSB-SC) technique have been presented and a novel mathematical analysis of the DSB-SC model has been derived in this chapter. We have examined the features of the reported modulation techniques considering their performance evaluation over fibre.

We have shown through analytical derivations that the Optical Single Sideband (OSSB+C) modulation, regardless the method of implementing, is a technique which can totally eliminate the effect of chromatic dispersion over the entire length of the fibre link. Moreover, it has been shown that the second order up conversion Optical Double Sideband-Suppressed Carrier (ODSB-SC) modulation is a technique where it can shift the fibre dispersion power penalty nulls to a higher length-frequency products. Other dispersion effects associated with the modulated laser phase correlation were identified and described mathematically.

Chapter 4

Performance of Modulation Techniques with Respect to Chromatic Dispersion (Theory and Simulation Results)

This chapter demonstrates, using simulation models, the performance evaluation of modulation techniques reported in chapter 3 for delivering microwave frequencies over optic fibre in terms of fibre chromatic dispersion. In chapter 3 conventional Intensity Modulation-Direct Detection (IM-DD) modulation were discussed as well as modulation techniques which can overcome fibre chromatic dispersion effects. Theoretical analysis of modulation techniques showed a great potential, with differences between each individual technique, to eliminate chromatic dispersion effects in RoF optical links. After this introductory section, the optical fibre systems, structure, elements and parameters are discussed in this chapter. The work objectives of this chapter are then explained along with the methodology of using the simulation platforms to construct and investigate the performance of the systems. Thereafter, the performance evaluation of the constructed electrical models and the measurements of the optical system models were carried out. The conclusion and important results are summarised at the end of this chapter.

4.1 Optical fibre systems

The transfer of information in the form of light propagating within an optical fibre requires the successful implementation of an optical fibre communication system. This system, in common with all systems, is composed of a number of discrete components which are connected together in manner that enables them to perform a desired task. Hence, to achieve reliable and secure communication using optical fibres it is essential that all the components within the transmission system are compatible so that their individual performances, as far as possible, enhance rather than degrade the overall system performance.

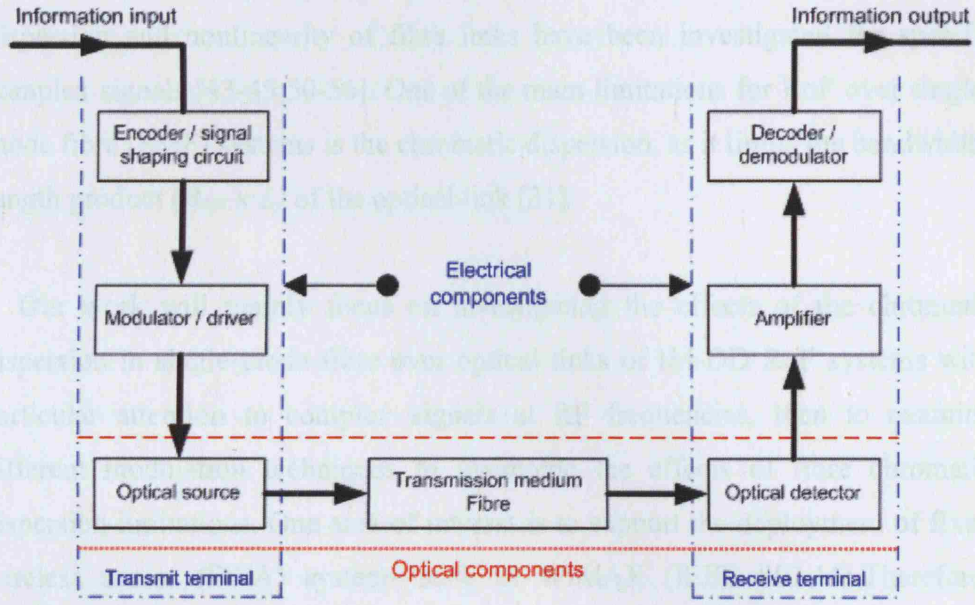

Figure 4.1: The principal components of an optical fibre communication system.

The principal components of a general optical fibre communication system for either digital or analogue transmission are shown in system block schematic of figure (4.1). The transmitter terminal equipment consists of an information encoder or signal shaping circuit preceding a modulation or electronic driver stage which operates the optical source. Light emitted from the source is launched into an optical fibre incorporated within a cable which constitutes the transmission medium. The light emerging from the far end of the transmission medium is converted back into an electrical signal by an optical detector positioned at the input of the receiver terminal equipment. This electrical signal

is then amplified prior to decoding or demodulation in order to obtain the information originally transmitted.

4.2 Work Objectives

Radio over fibre as a research area still an interesting and active area for researchers. Analyzing the work done so far and recent research, it can be seen that different signals and modulation techniques have been used to reach the optimum performance of RoF systems as it discussed it chapter 3. Signals and frequencies of interest of radio access communication systems are studied to monitor the performance and to find the appropriate methods and modulation techniques to propagate those signals. Factors such as distortion, attenuation, dispersion and nonlinearity of fibre links have been investigated for specific complex signals [43-45;50-56]. One of the main limitations for RoF over single-mode fibre (SMF) systems is the chromatic dispersion, as it limits the bandwidth-length product (B_{opt} x L) of the optical link [31].

Our work will mainly focus on investigating the effects of the chromatic dispersion in single-mode fibre over optical links of IM-DD RoF systems with particular attention to complex signals at RF frequencies, then to examine different modulation techniques to overcome the effects of fibre chromatic dispersion limitations. One area of interest is to support the deployment of fixed wireless access (FWA) systems such as WiMAX (IEEE 802.16).Therefore; complex signals such as QPSK, M-QAM and OFDM are the main signals of interest.

A number of different spectral bands are possible; of particular interest are the 10, 20 and 28 GHz bands as proposed for use with fixed wireless access services using external modulation techniques with RF signals to modulate the optical carrier. These RoF systems with such characteristics have not been investigated before. Our aim is to examine and explore techniques to optimize the optical links performance of such systems.

4.3 Work scenario

Signals and frequencies have to be verified and chosen according to the area of interest. Three main signals have been chosen to work with, QPSK, 16QAM and 64QAM in addition to the OFDM in a form used in the 802.11 and 802.16 standards [10;69] which will be discussed in a separate chapter (Chapter 6). The methodology used is to generate the signals in Matlab (electrical system, transmitters and receivers) then transport it to OptSim (optical systems), and back to Matlab to be demodulated and for comparison of the recovered signals with the transmitted one. Signals of interest details are as below:

1. Gray coded 50Mbps QPSK at 10, 20 and 28 GHz.
2. Gray coded 50Mbps 16QAM at 10, 20 and 28 GHz.
3. Gray coded 50Mbps 64QAM at 10, 20 and 28 GHz.

4.3.1 MatLab Modelling

The systems to generate the required signals are constructed using the Matlab Simulink library blocks, in particular, the communication blockset have been used to build the transmitters and receivers for the 4-QAM (QPSK), 16-QAM and 64-QAM systems.

In order to investigate if the system's performance complies with theoretical values for BER, an Additive White Gaussian Noise (AWGN) channel has been added to the systems to ensure systems are performing within the standards before going through any optical link. Results show a good match between simulated and theoretical Es/No vs. BER curves. Simulations are performed for all signals within the bands of interest using the constructed systems. Curves are introduced for the simulated systems.

To get accurate measurements of systems performance, a large number of bits have to be generated and transmitted. Low numbers of simulated bits will result in inaccurate measurements, while an excess of simulated bits will result in a long simulation time [70]. Therefore, careful calculations have to be done to

control the parameters such as number of transmitted bits, signal power and the sampling time of signals transmitted over the systems.

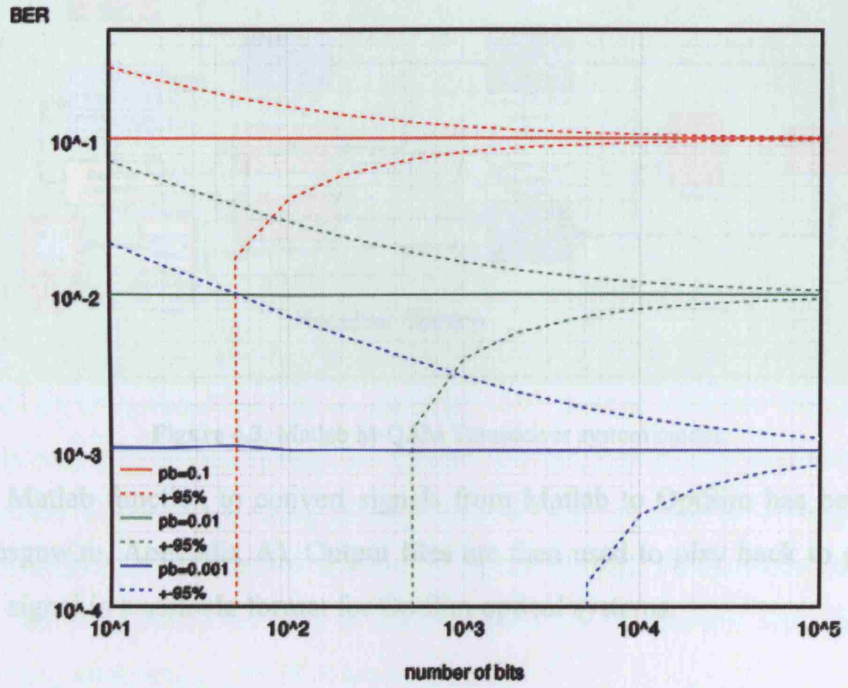

Figure 4.2: Diagram of how many Bits should be transmitted for a single point of a BER curve.

4.3.1.1 The Constructed M-QAM Systems with Matlab:

A group of systems were constructed to examine signal performance without an optical link, and to certify matching the theoretical performance. These systems are:

1. 10, 20 and 28 GHz QPSK transceiver system with AWGN channel and bit error rate (BER) calculator.

2. 10, 20 and 28 GHz 16QAM transceiver system with AWGN channel and bit error rate (BER).

3. 10, 20 and 28 GHz 64QAM transceiver system with AWGN channel and bit error rate (BER).

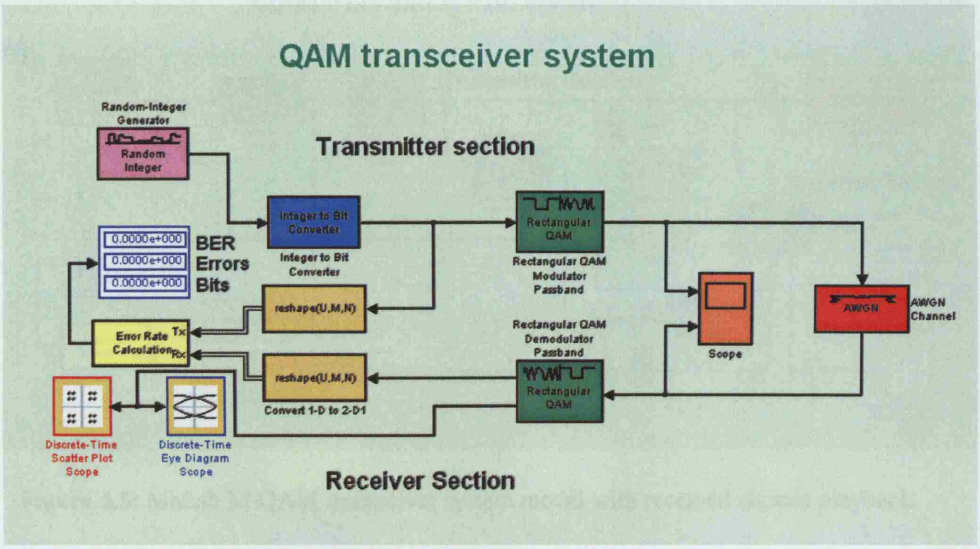

Figure 4.3: Matlab M-QAM Transceiver system model.

A Matlab function to convert signals from Matlab to OptSim has been used (op_esgnw.m, Appendix A). Output files are then used to play back to give the input signal in a suitable format for OptSim optical systems.

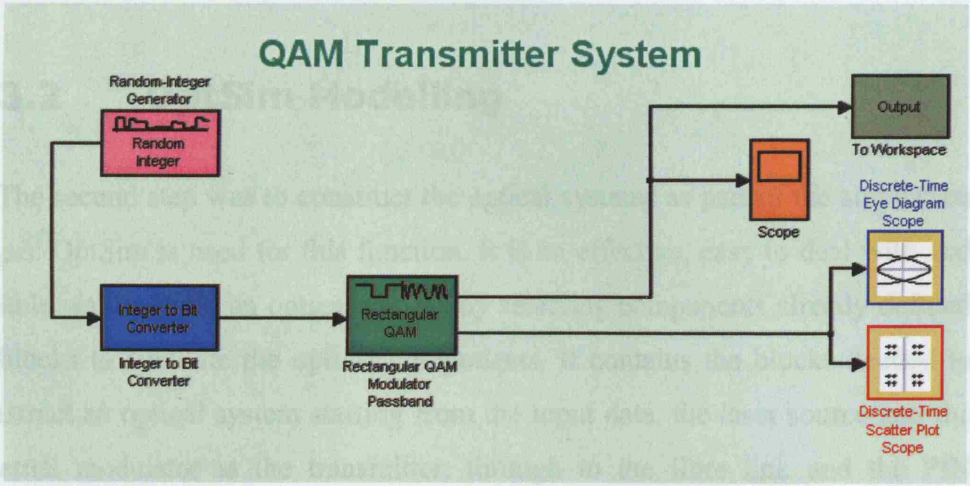

Figure 4.4: Matlab M-QAM Transmitter model.

The last part of the Matlab systems are the full systems of the Transceivers with an extra part to recover the output of optical systems after changing it back to Matlab files format using a Matlab function to convert signals from OptSim output to Matlab form (op_esgnr.m, Appendix A).

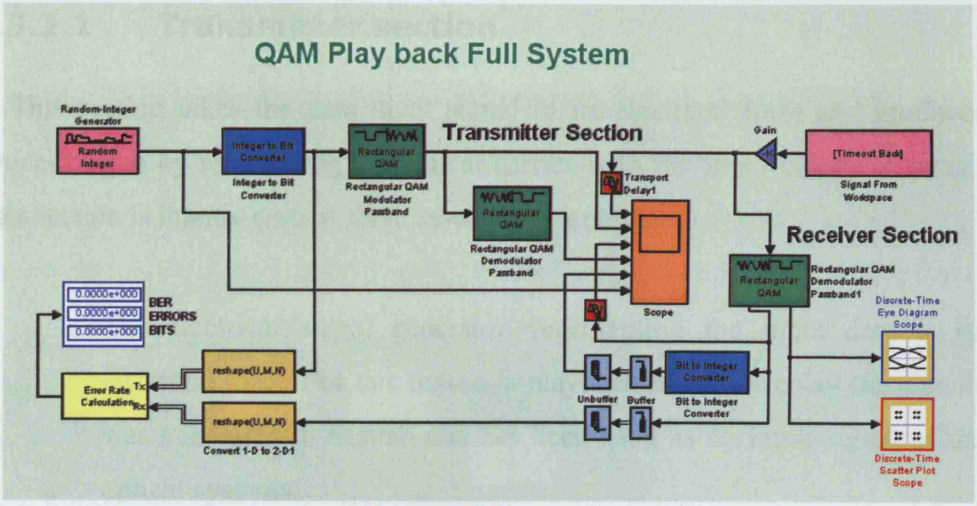

Figure 4.5: Matlab M-QAM transceiver system model with received signals playback.

This set of systems has been constructed to be used to compare the recovered signals once propagated through the optical systems, and signals generated at the transmitter side without being through optical link, in order to investigate the characteristics and changes that occur to signals through the constructed optical links, and to monitor the optical link performance. Parameters such as power distortion, attenuation, and BER are monitored.

4.3.2 OptSim Modelling

The second step was to construct the optical systems as part of the simulation stages. OptSim is used for this function. It is an effective, easy to deal with and reliable way to build an optical system by selecting components already defined as blocks to simulate the optical components. It contains the blocks needed to construct an optical system starting from the input data, the laser source and the external modulator at the transmitter, through to the fibre link and the PIN photodiode at the receiver. Signals generated in Matlab had been converted to a compatible form to be used as input data to the optical system in OptSim. Simulations with different fibre lengths and modulation techniques have been performed with OptSim to monitor the chromatic dispersion effect on signals of interest.

The optical systems were constructed from three main sections:

4.3.2.1 Transmitter section

This section takes the data input signal in its electrical form and produces optical output by modulating the optical carrier with the input electrical signal. This section is mainly consist three essential components

1. The electrical signal generator, representing the input data in its electrical form. For this reason, a playback block to replay the signals was generated in Matlab and has been used as an input signal of the optical systems.

2. The laser source (laser diode) representing the optical carrier source to be modulated with input data.

3. The external modulator (Mach-Zehnder Modulator MZM) which it represent the external modulation device at the transmitter section of the optical system to externally modulate the light, from laser diode, with electrical input data or RF electrical carrier to form the modulated output optical signal.

Other components and devices in the transmitter section, as biasing source, electrical and optical filters, have been used for supporting the function of the three main parts. Settings and parameters for these components of the transmitter are illustrated with system's details and figures.

4.3.2.2 Optical link section

This part of the system is mainly represented by the optical fibre link. The optical fibre is the propagating medium been used to send out signals in the optical systems. Standard single-mode fibre (SMF) has been used, in the constructed optical systems, with different lengths in order to inspect the effect of the chromatic dispersion and other fibre's parameters. Fibre parameters for this part of the systems are illustrated with the system's figures.

4.3.2.3 Receiver section

The main part of this section is the PIN photodiode, which converts the received optical signal back to its electrical form. PIN photodiodes represent a simple and efficient way of implementing the direct detection technique to recover the optical received signals to their original electrical form. Other components are required to perform the function of the receiver section, such as filters (optical and electrical), optical attenuator and electrical amplifier. All components settings and parameters are illustrated with the system's figures.

Supporting components such as scopes, spectrum analyzers, power and frequency meters are added to the system to monitor the system's performance in each section, to ensure that each component is correctly participate to form the overall required system task. The output terminal side of the constructed optical system consists of signal recorder block to record the output signals after being transmitted through the optical system. The output of OptSim had to be converted back to a format compatible with Matlab platform, in order to perform the required performance measurements.

The RoF systems with different modulation techniques constructed and simulated using OptSim, are listed below with their diagrams.

4.3.3 Conventional IM-DD DSB RoF System

Figure (4.6) is an OptSim model of the conventional IM-DD RoF system. As illustrated in the previous section, this system is constructed from three parts.

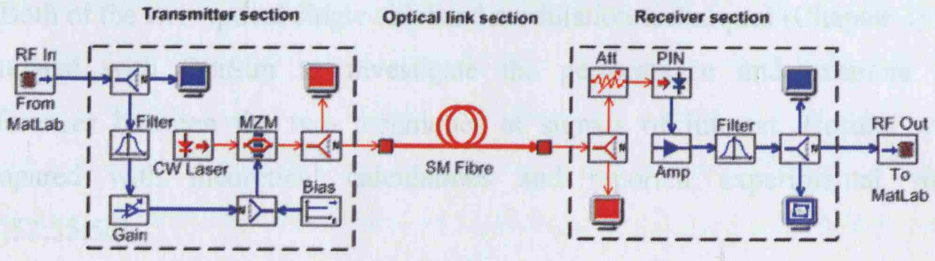

Figure 4.6: OptSim conventional IM-DD DSB RoF system model.

The first part of the system is the transmitter section, which contains the laser source (CW Laser) and the external MZ modulator with a DC biasing source. The transmitter section has other components such as the electrical filter, amplification, and the electrical and optical spectrum analysers. The RF input signal is firstly applied to the input of the electrical filter to remove any harmonics outside the required signal frequency band.

The second part is the optical link section, standard single-mode fibre with dispersion parameter of 16 ps/nm.km, and attenuation of 0.2 dB/km has been used for the simulations with different lengths according to the required measurements.

The third part of the system is the receiver section which is constructed from a PIN diode, which is the main receiver's device, the electrical amplifier and filter to amplify and filtering the recovered RF signal. Other components such as optical attenuator have been used to control the optical received signal power.

Simulations have been done for the complex signals and frequencies of interest with different parameters and fibre lengths to examine the system performance and to compare with the theoretical calculations and reference practical performed experiments. All components with their parameters and characteristics for this system are listed and explained in (Appendix A).

4.3.4 Optical Single Sideband (SSB+C) RoF system

Both of the two optical single sideband modulation techniques (Chapter 3) are simulated with OptSim to investigate the performance and examine the differences between the two techniques at signals of interest. Results were compared with theoretical calculations and reported experimental work [51;52;55;56].

4.3.4.1 Optical single sideband SSB+C (by Filtering)

This method is based on adding an optical filter to remove one of the optical sidebands, either upper or lower, to eliminate the effects of fibre chromatic dispersion. Figure (4.7) shows the constructed OptSim system model of single sideband modulation by filtering technique.

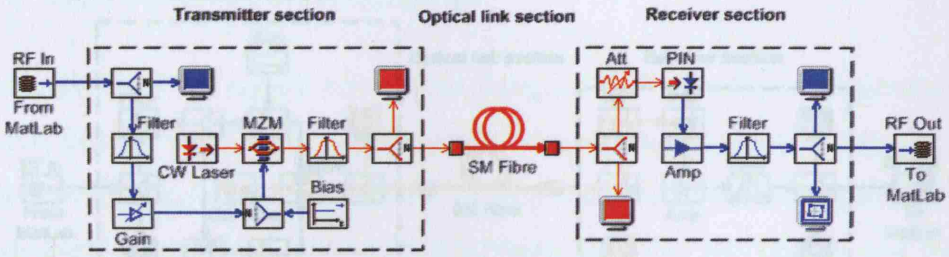

Figure 4.7: OptSim IM-DD OSSB+C (by filtering) RoF system model.

It can be seen that there is no changes in the optical link or the receiver section with compare to the conventional IM-DD DSB technique. This technique is simply applied by adding an optical filter to the transmitter section at the output of the modulator, to remove one of the modulated optical sidebands, to form an optical single sideband modulation scheme. All other components and parameters are still same as with DSB system, figure (4.6). It is useful to know that the optical filter can be added at the far end of the fibre link just before the PIN diode at the receiver instead of the transmitter side to give same results.

4.3.4.2 Optical Single Sideband SSB+C (using Dual arm MZM)

The generation of the single sideband modulation scheme can be achieved with using an external dual arm MZM and phase shifter at the transmitter section, (Chapter 3, section 3.2.2). Therefore, the transmitter section of this technique will be reasonably different from the conventional DSB and SSB by filtering transmitters. To simulate this system in OptSim, external dual arms MZM with two DC biasing, signal splitter, and phase shifter blocks, have been used. Figure (4.8) shows the OptSim system model of the OSSB applying this technique.

Optical and electrical spectrum analyzers added to the system to investigate the performance in each single section. The optical link and the receiver section of this system were remaining with no changes compared to the conventional DSB and filtering SSB systems. All components with their parameters and characteristics for this system are listed and explained in (Appendix A).

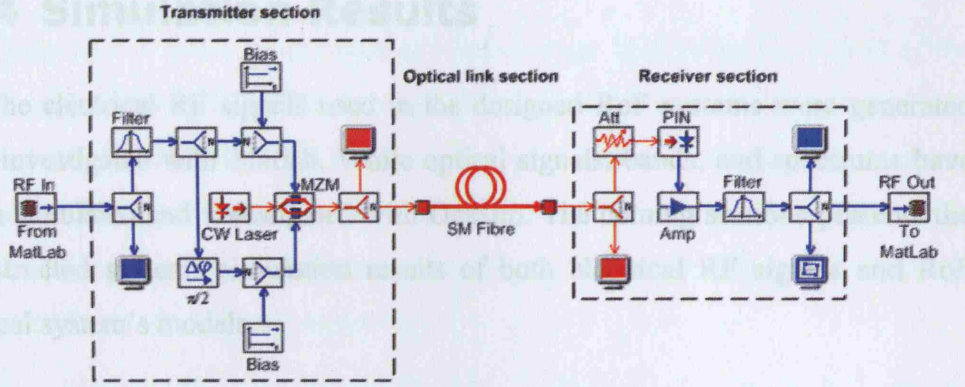

Figure 4.8: OptSim IM-DD OSSB (using dual arm MZM) RoF system model.

4.3.5 Double Sideband-Suppressed Carrier (DSB-SC) RoF System

To construct this modulation technique, an IF signal is directly modulates the laser light. Then the modulated laser forms the input of the MZ modulator, where the modulation frequency of *fc*/2 is used to up-convert the modulated laser output light. Figure (4.9) shows the constructed OptSim model of the double side band-suppressed carrier DSB-SC system.

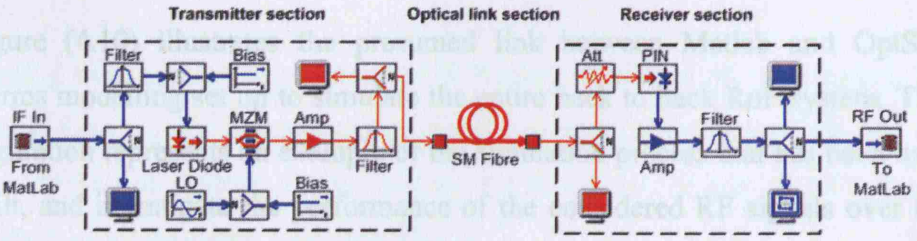

Figure 4.9: OptSim IM-DD DSB-SC RoF system model.

As it can be seen from the figure, a single arm MZM with direct laser modulation has been used at the transmitter section of this system. Other sections of the system were remaining same as for the previous techniques. All components with their parameters and characteristics for this system are listed and explained in (Appendix A).

4.4 Simulation Results

The electrical RF signals used in the designed RoF systems were generated and investigated with Matlab. While optical signals, bands, and spectrums have been simulated and investigated with OptSim. The coming sections presents the constructed systems simulation results of both electrical RF signals and RoF optical system's models.

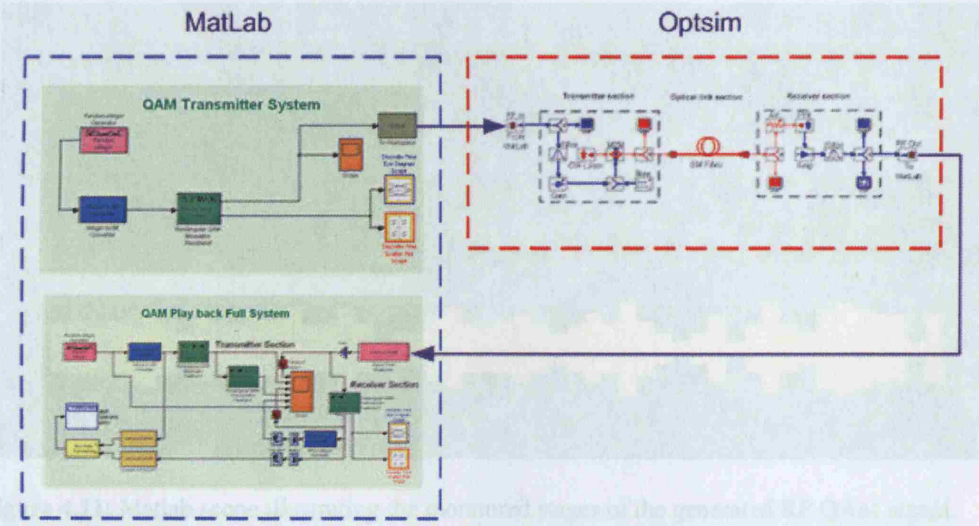

Figure 4.10: Simulation platforms configuration of the implemented systems.

Figure (4.10) illustrates the presumed link between Matlab and OptSim platforms modelling set up to simulate the entire back to back RoF system. This configuration represents an example of the simulation process that has been used to built, and investigate the performance of the considered RF signals over the constructed RoF systems.

4.5 Matlab results

The MatLab systems constructed to generate the RF QAM signals were shown in section 4.3.1 and figure (4.10) above. The output of these systems were monitored and investigated for the modulation schemes and frequencies of interest.

Figure (4.11) shows an example of Matlab scope illustrating the output of the QAM transmitter system. The first row showing the random 64 integer levels to generate the base band 64-QAM signal, while the second row is the bit stream of the generated signal. Each colour is representing a bit in the 6 bits 64-QAM symbols. The third row is showing the output RF 20GHz 50 Mbps 64-QAM signal of the QAM Matlab transmitter.

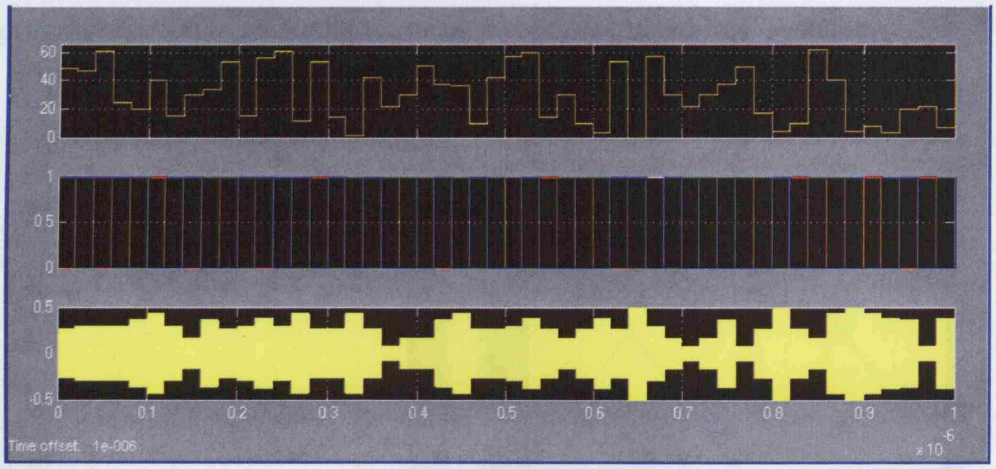

Figure 4.11: Matlab scope illustrating the monitored stages of the generated RF QAM signal.

4.5.1 QPSK signal Generation

Starting with a Quadrature Phase Shift Keying (QPSK or 4QAM) signal, the following figures show samples of the signal generated at the transmitter and the transceiver Matlab systems at frequencies of interest, 10, 20 and 28 GHz to use as an input of the designed RoF systems.

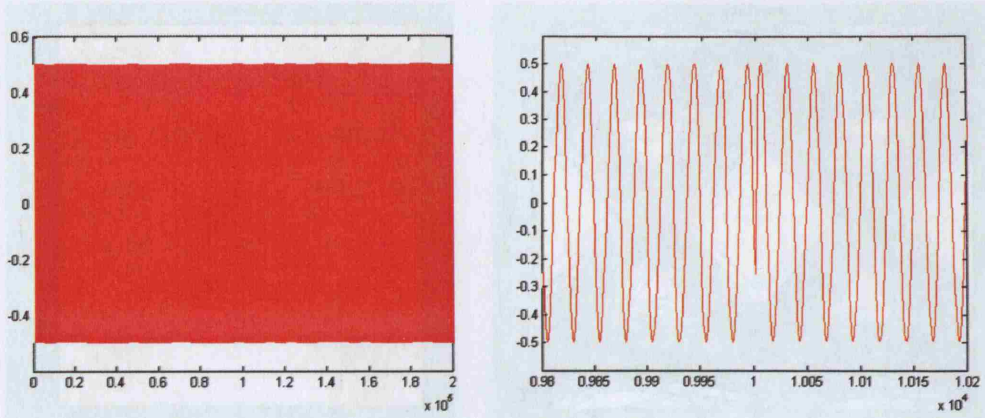

Figure 4.12: RF QPSK bit stream illustrating the amplitude and phase levels.

Figures (4.13) and (4.14) shows the constellation and eye diagrams of the pure and noised QPSK signal transmitted through Matlab transceiver system at figure (4.3). The system performance were examined by plotting the BER curve of simulated system and compared with theoretical performance of the QPSK signal. Results justified the constructed Matlab transmitter output as an appropriate QPSK input signal to use with the constructed RoF systems.

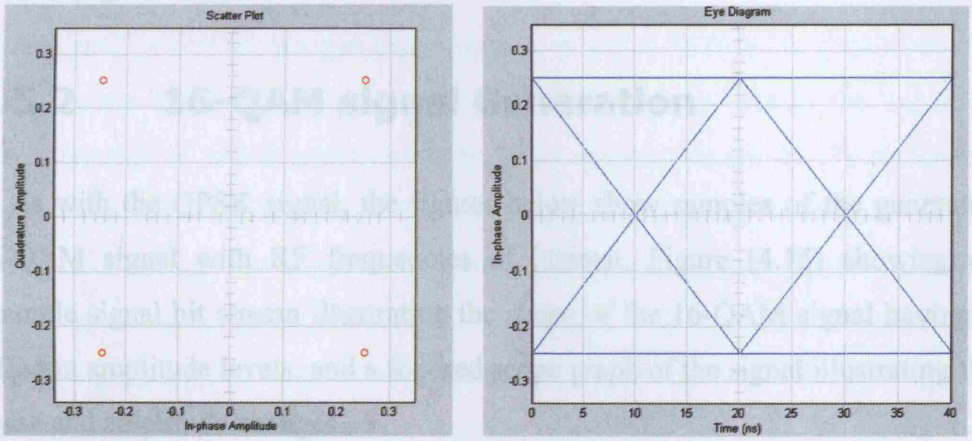

Figure 4.13: Constellation and eye diagram of pure transmitted RF QPSK signal.

The constellation and the eye diagrams obtained show no differences with the three frequencies of interest. Therefore, the obtained results states that the modulation electrical RF systems performance does not depend on the frequency of the carrier signal as far as the sampling requirements are maintained.

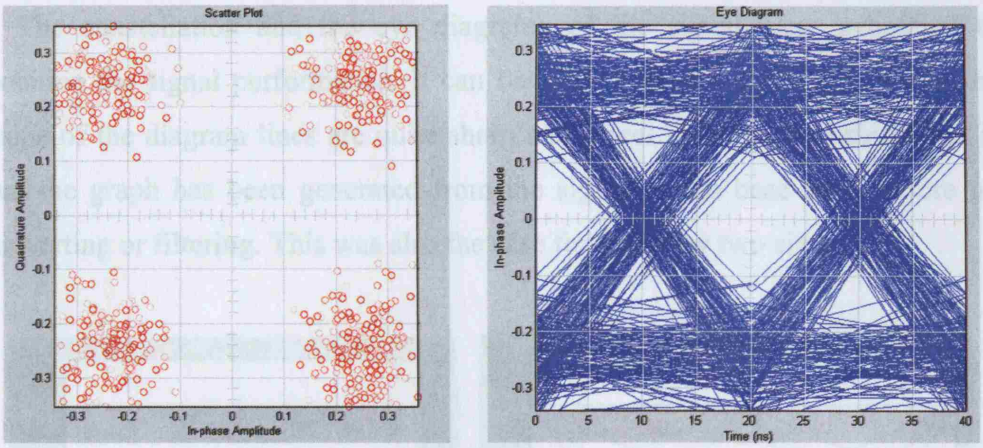

Figure 4.14: Constellation and eye diagram of recovered RF QPSK signal after transmission through an AWGN channel.

The peak signal power for the generated signal was set to 128mW to give a peak to peak voltage of 1 Volt (Vpp = 1V) to ensure working within the specified characteristics of the MZM. The BER performance curves of the simulated and theoretical QPSK signal, with other signals of interest, are illustrated in the BER against the Symbol over Noise Energy ratio (Es/No) graph at the end of this section (figure 4.22).

4.5.2 16-QAM signal Generation

As with the QPSK signal, the figures below show samples of the generated 16-QAM signal with RF frequencies of interest. Figure (4.15) showing an example signal bit stream illustrating the shape of the 16-QAM signal having 3 different amplitude levels, and a focused scope graph of the signal illustrating the phase and amplitude changes.

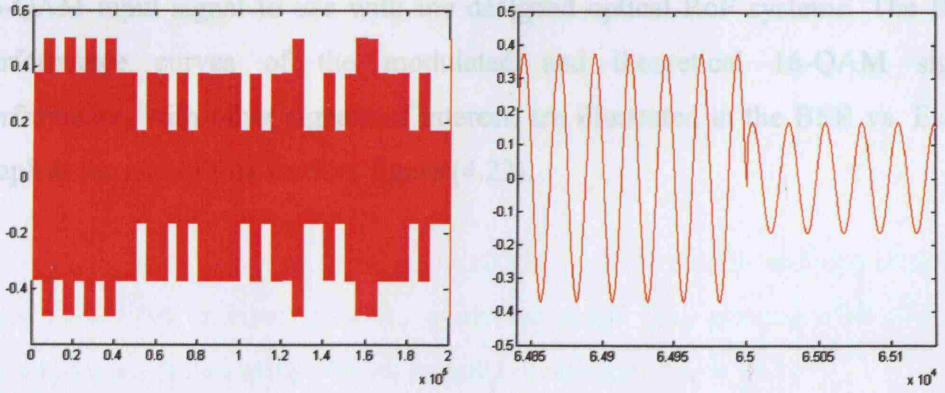

Figure 4.15: RF 16-QAM bit stream illustrating the amplitude and phase levels.

The constellation and the eye diagrams of the signal were generated to examine the signal performance. It can be seen from the eye diagram that the shape of the diagram lines are quite sharp and direct. The reason behind that is that the graph has been generated from the signal at the base band before up converting or filtering. This was also the case for the other two signals.

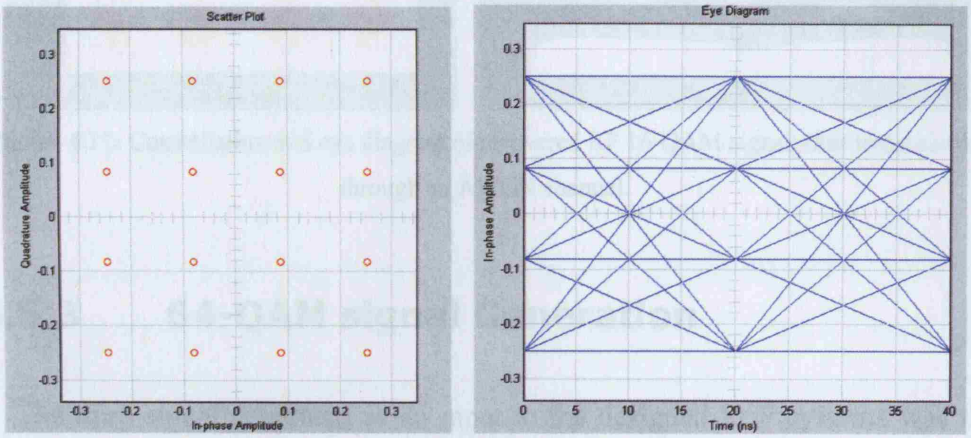

Figure 4.16: Constellation and eye diagrams of pure transmitted RF 16QAM signal.

The peak power for the generated signal was set to 128mW to give a peak to peak voltage of 1 Volt (Vpp = 1V) to ensure working within the specified characteristics of MZM constructing the RoF system. Figure (4.17) shows the constellation and eye diagrams of the generated 16-QAM with noise signal transmitted through the constructed Matlab transceiver system, figure (4.3). The system performance is examined by plotting the BER curve of the simulated system and compared with theoretical performance curve of 16-QAM signal. Results obtained have justified the Matlab transmitter output as an appropriate 16-QAM input signal to use with the designed optical RoF systems. The BER performance curves of the modulated and theoretical 16-QAM signal performance, with other signals of interest, are illustrated in the BER vs. Es/No graph at the end of this section, figure (4.22).

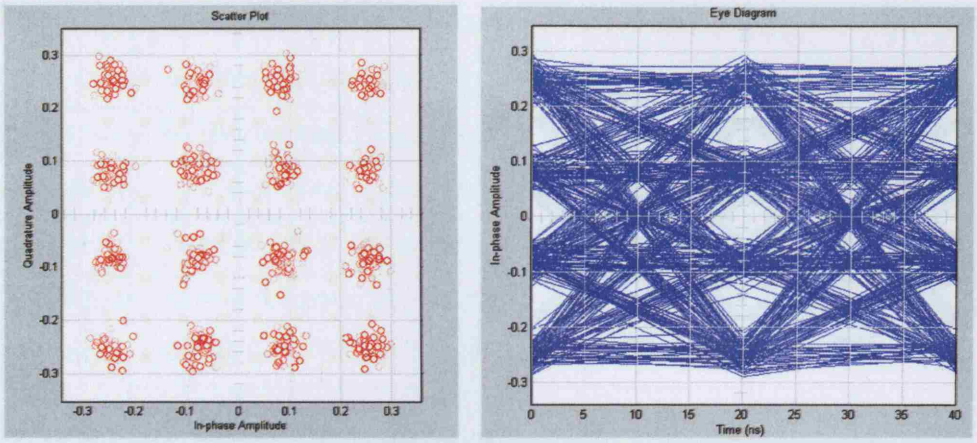

Figure 4.17: Constellation and eye diagram of recovered RF 16-QAM signal after transmission through an AWGN channel.

4.5.3 64-QAM signal Generation

The third signal generated as an input to the designed RoF systems was the 64-QAM signal. A sample bit stream of the generated RF 64-QAM signal is shown in figure (4.18), it can be seen that the signal has 7 different amplitude levels; figure illustrates an example of phase and amplitude change between two adjacent bits.

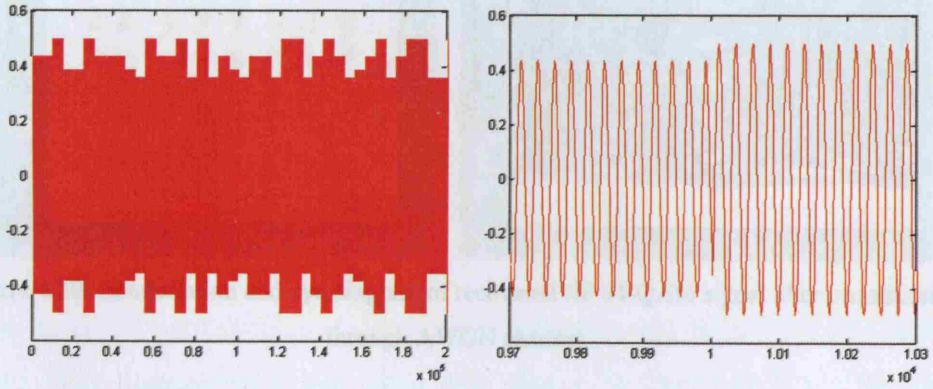

Figure 4.18: RF 64-QAM bit stream illustrating the amplitude and phase levels.

As is the case with the previous signals, the constellation and eye diagrams were monitored to investigate the generated signal performance with different signal to noise ratios using Matlab transceiver system, figure (4.3).

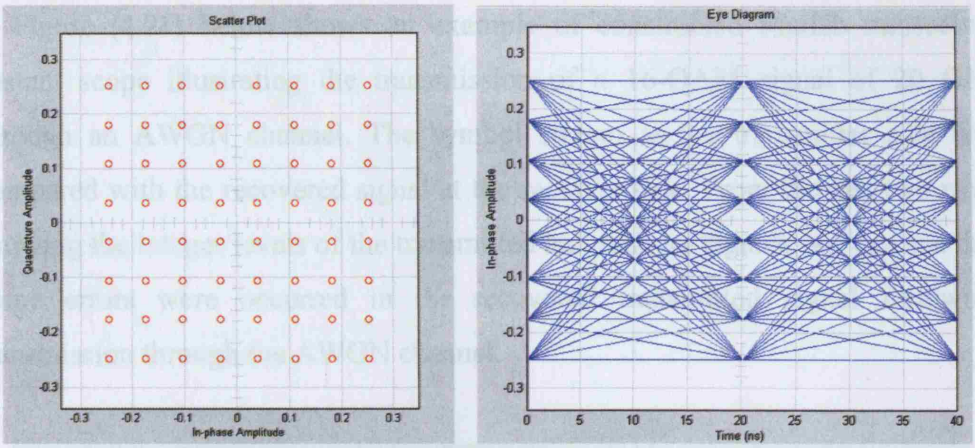

Figure 4.19: Constellation and eye diagram of pure transmitted RF 64-QAM signal.

Figures (4.19) and (4.20) show constellation and eye diagrams of the pure and with noise 64-QAM signals. To ensure that the generated RF signals satisfy the theoretical performance, signals have been transmitted through the transceiver system with different signal to noise ratios using AWGN channel to model a noisy transmission medium to provide BER curves.

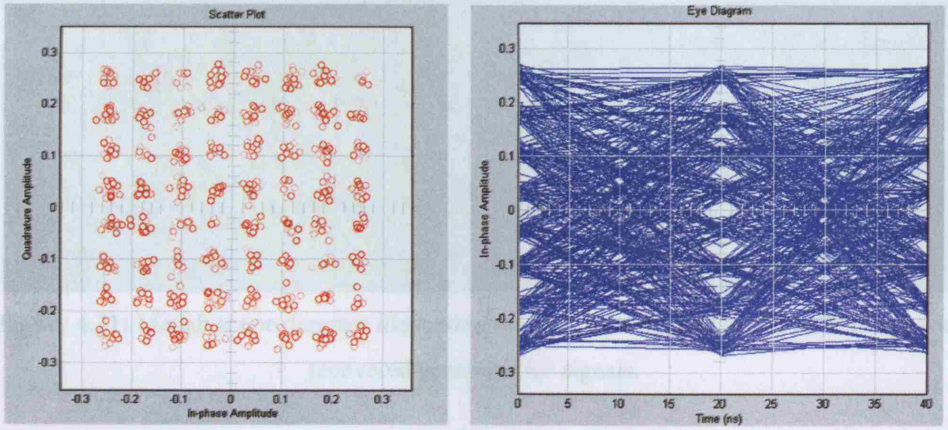

Figure 4.20: Constellation and eye diagram of recovered RF 64-QAM signal after transmission through AWGN channel.

The signal peak power for the generated signal was set to 128mW to give a peak to peak voltage of 1 Volt (Vpp = 1V) to ensure working within the specified characteristics of the RoF system MZM. The BER performances of the generated and theory 64-QAM signal curves with other signals of interest are illustrated in the BER vs. Es/No graph at the end of this section, figure (4.22).

Figure (4.21) below shows an example of constructed Matlab transceiver system scope illustrating the transmission of a 16-QAM signal of 20 GHz through an AWGN channel. The symbol stream at the transmitter side was compared with the recovered signal at the receiver side. From the last two rows showing the integer levels of the transmitted and recover signals, we can see that some errors were occurred in the recovered transmitted signal following transmission through the AWGN channel.

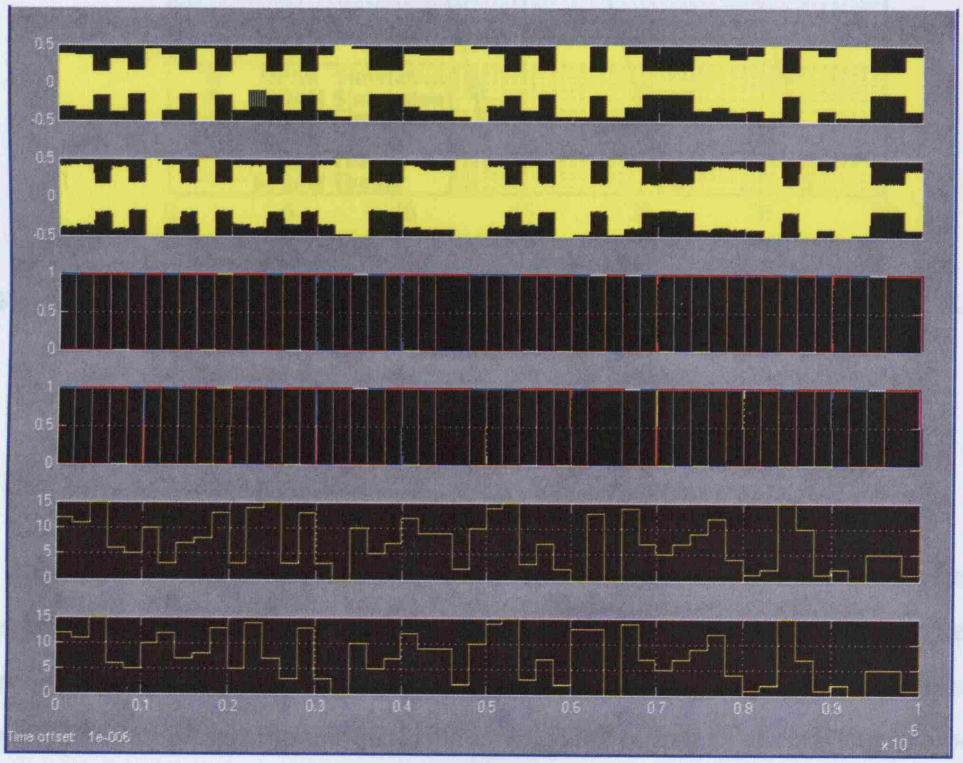

Figure 4.21: Matlab scope diagram illustrating the comparison between the transmitted and recovered generated RF signals.

To summarise the work and results in this section, the BER vs. Es/No curves of the three signals were generated and plotted in figure (4.22). The figure illustrates the theoretical and simulation curves of QPSK, 16-QAM and 64-QAM RF signals generated with Matlab. The curves are valid for the three RF bands of interest. It is clear from the figure that the constructed systems satisfy the theoretical performance of these signals, and therefore are qualified for use as an input to the RoF systems models to be investigated.

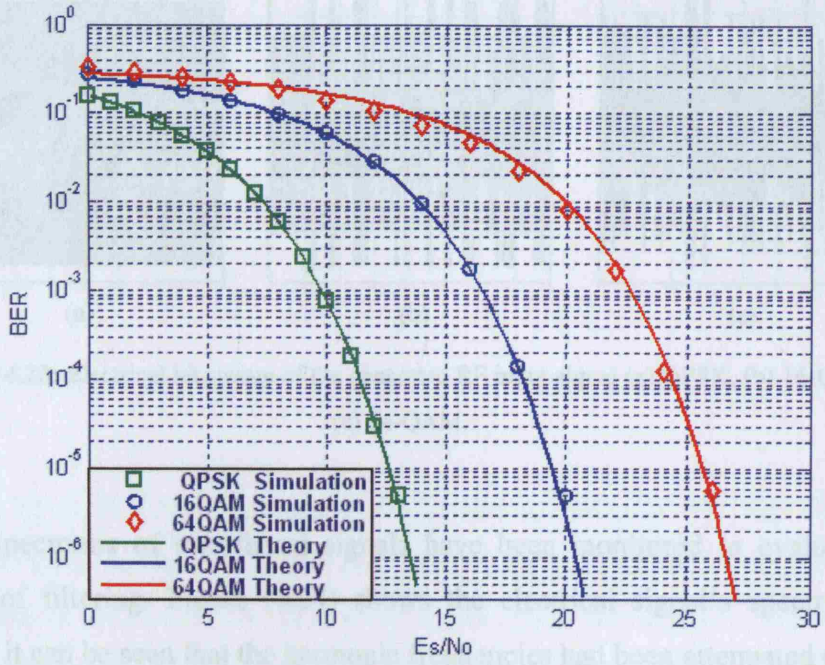

Figure 4.22: Theory and simulation BER versus Es/No curves of gray coded mapping RF M-QAM signals.

4.6 OptSim Results

After confirming the accuracy of constructed systems with Matlab to generate the complex RF signals to use as an input of RoF systems, simulations were carried out with the optical systems using OptSim platform. First, the transferred signals had to be investigated and monitored at the output of the playback block of the constructed RF systems, in order to make sure that signals retain the required signal's characteristics and quality as was on Matlab. Hence, the signal's sampling time had to be specified to match the sampling time used in Matlab; otherwise the performance of the signal will degraded due to the incorrect sampling process. Secondly, the signals were filtered to remove the harmonic frequencies. Moreover, the amplitude of the signal is important, and it must be kept within the modulator's operation limits, to optimise the efficiency of the modulation process. Therefore, signal's amplitude were controlled and monitored to achieve that. Figure (4.23) shows samples of the three signals after filtering, and prior biasing.

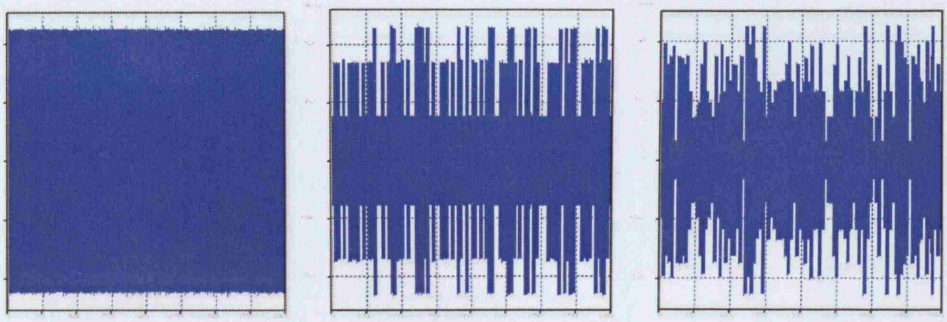

(a) (b) (c)

Figure 4.23: Electrical bit stream of the generated RF input signal (a) QPSK, (b) 16-QAM, (c) 64-QAM.

The spectrums of transferred signals have been monitored to evaluate the process of filtering. Figure (4.24) shows the electrical signal's spectrums in OptSim, it can be seen that the harmonic frequencies had been attenuated prior to biasing and modulation.

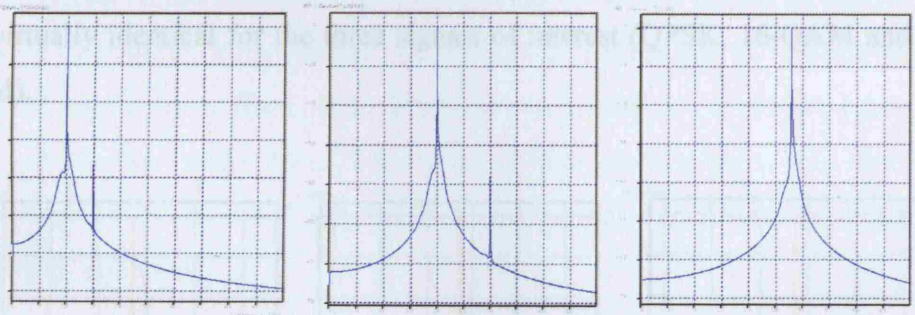

(a) (b) (c)

Figure 4.24: Electrical spectra of RF M-QAM input signals of RoF systems at (a) 10GHz, (b) 20GHz, and (c) 28GHz.

4.6.1 Conventional DSB RoF system results

The next group of figures shows the instantaneous output power at the output of the MZM of the conventional IM-DD RoF system (figure 4.6) of the three RF signals of interest. Input electrical RF data was QPSK, 16-QAM, and 64-QAM respectively. Signal amplitude and power were monitored to give an accurate representation for the three signal schemes.

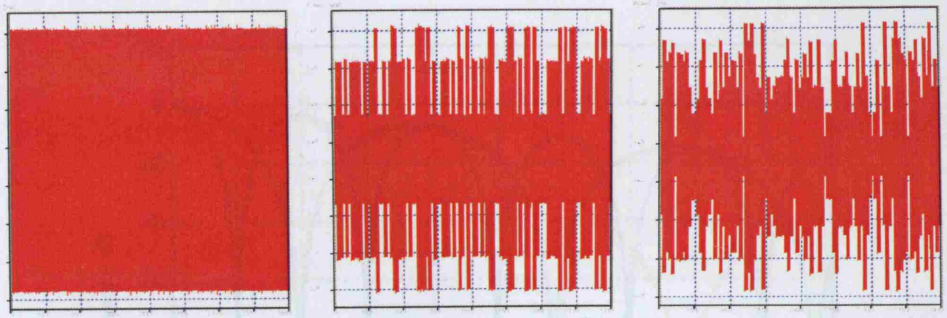

(a) (b) (c)

Figure 4.25: Optical instantaneous power of RoF system (a) QPSK, (b) 16-QAM, (c) 64-QAM.

It can be seen, figure (4.25), that the Continues Wave (CW) laser light had been externally modulated to produce an instantaneous optical output power which follows the modulation scheme of the RF input data signals. Furthermore, figure (4.26) below shows the optical spectra at the output of the MZM for the same system. The figure demonstrates the optical carrier at 194 THz (1550 nm) and the sidebands of the DSB modulation at 10, 20, and 28 GHz. The spectrums are virtually identical for the three signals of interest (QPSK, 16-QAM and 64-QAM).

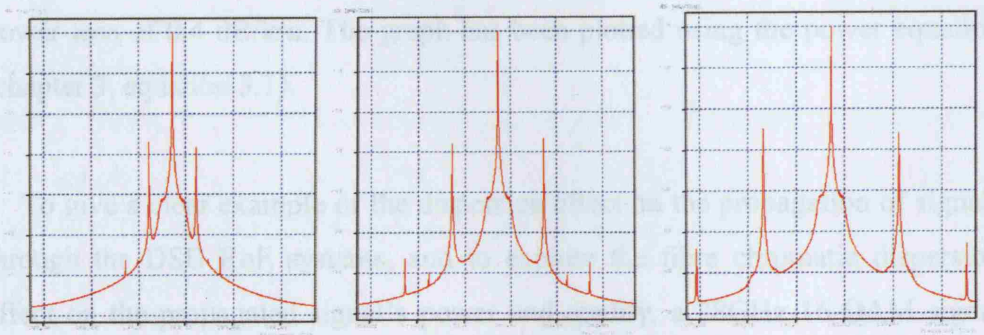

(a) (b) (c)

Figure 4.26: Optical spectra of DSB modulation of M-QAM with (a) 10 GHz RF signal, (b) 20 GHz RF signal, and (c) 28 GHz RF signal.

Additionally, as demonstrated in chapter 3 (section 3.1), fibre dispersion can effect the RoF links transmission length-frequency product over single mode fibre. Theoretical curves of dispersion limitation showing the nulls of the power penalty against fibre length have been produced in figure (4.27) for the three RF frequencies of interest.

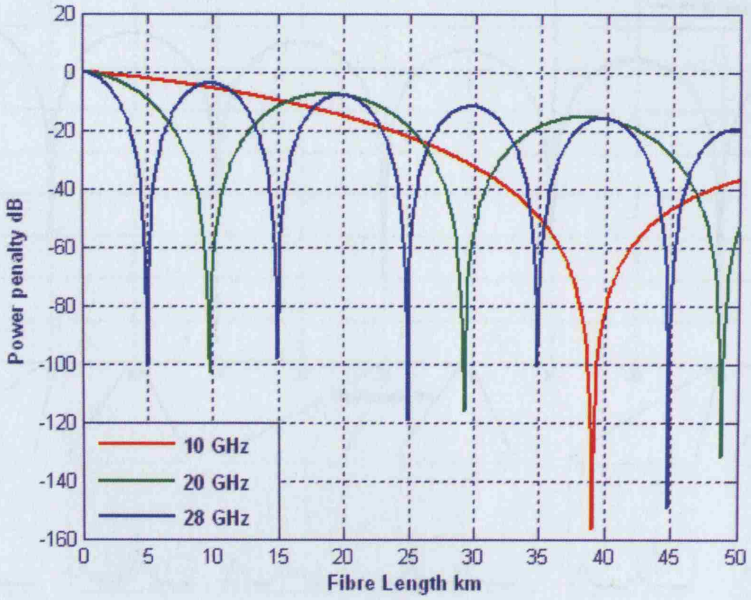

Figure 4.27: Power penalty against fibre length (theory) of RF signals with DSB modulation.

The figure shows theoretical power variation of an RF carrier at 10, 20, and 28 GHz transmitted on an optical carrier, and at wavelength of 1550nm over a standard single-mode fibre, with dispersion parameter *D* of 16 ps/nm.km and with considering fibre loss of 0.2 dB/km, which produce an output electrical power loss of 0.4 dB/km. The graph has been plotted using the power equation (chapter 3, equation 3.1).

To give a clear example of the dispersion effect on the propagation of signals through the DSB RoF systems, and to explore the fibre chromatic dispersion effect on the propagated signal's power and quality, a 28GHz 16-QAM signal has been propagated and monitored throughout the entire constructed RoF system model. Figure (4.28) is combines theoretical curves and simulation model results, of the power dispersion penalty versus fibre length of 28GHz signal at wavelength of 1550nm optical carrier, over a standard single-mode fibre with dispersion parameter *D* of 16 ps/nm.km and 0.2 dB/km fibre loss. The small graphs illustrate the received signal amplitude and electrical spectrum variations of the simulated RF electrical signal, for particular fibre lengths, at the output of conventional DSB IM-DD RoF system.

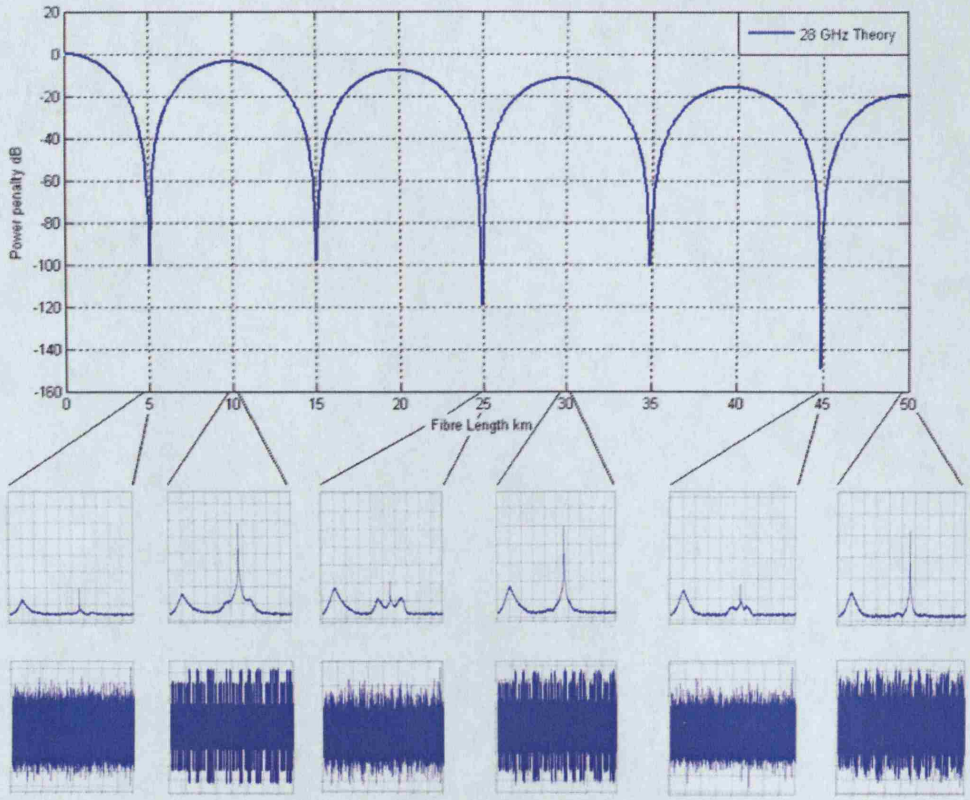

Figure 4.28: Power penalty versus fibre length with simulation resulted electrical spectrums and signals of 28 GHz 16-QAM using DSB modulation scheme.

The electrical spectrum and electrical signal scope plots of the recovered simulated signal confirm the power degradation at the null points proposed by theory. The spectra of the received signal shows a high power degradation at fibre lengths of 5, 25, and 45 km, while it show high signal to noise ratio at lengths of 10, 30, and 50 km, including a small power penalty introduced by the fibre attenuation of 0.2 dB/km.

Accordingly, the next step was to simulate the DSB RoF to produce the BER against Es/No for signals and frequencies of interest. Thus, signals have been transmitted through OptSim RoF simulation platform, then, sent back to Matlab transceiver system (figure 4.5) to compare the recovered signals with transmitted in order to produce the BER curves of the QAM RF signals after transmission and optical processing through the RoF systems.

The next few graphs show samples of simulations resulting BER vs. Es/No ratio curves of signals and frequencies of interest at different fibre lengths confirming the theoretical power penalty induced with DSB IM-DD RoF systems at certain fibre lengths due to fibre chromatic dispersion.

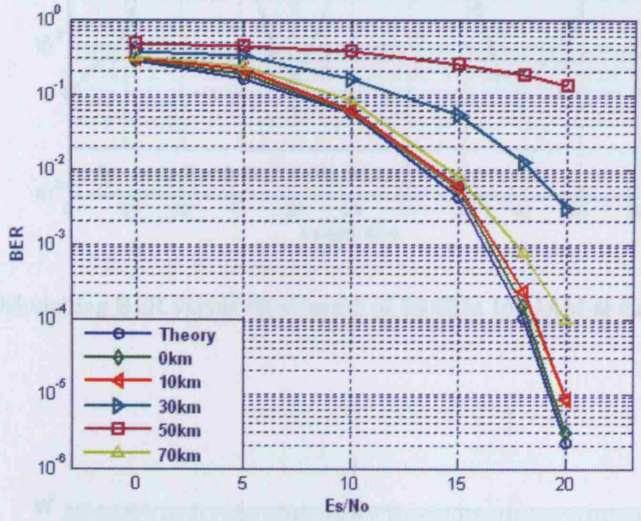

Figure 4.29: Modelling BER vs. Es/No of 10 GHz 16-QAM with using DSB modulation.

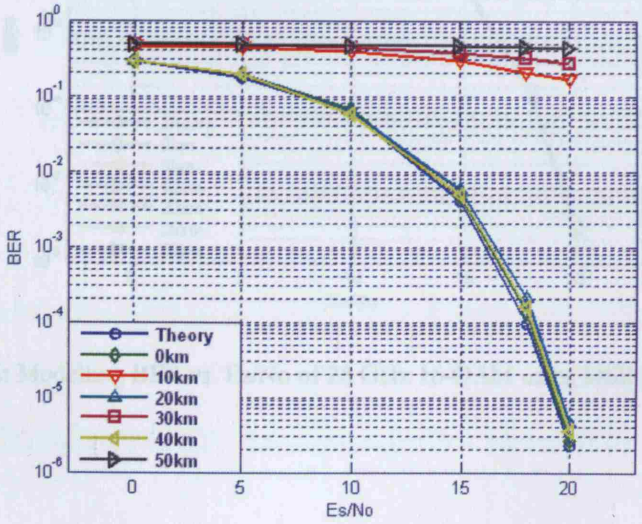

Figure 4.30: Modelling BER vs. Es/No of 20 GHz 16-QAM with using DSB modulation .

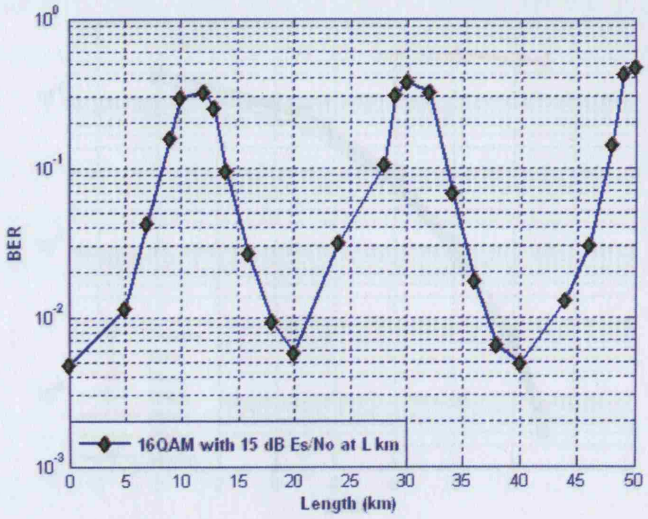

Figure 4.31: Modelling BER versus fibre length of 20 GHz 16-QAM at Es/No of 15dB.

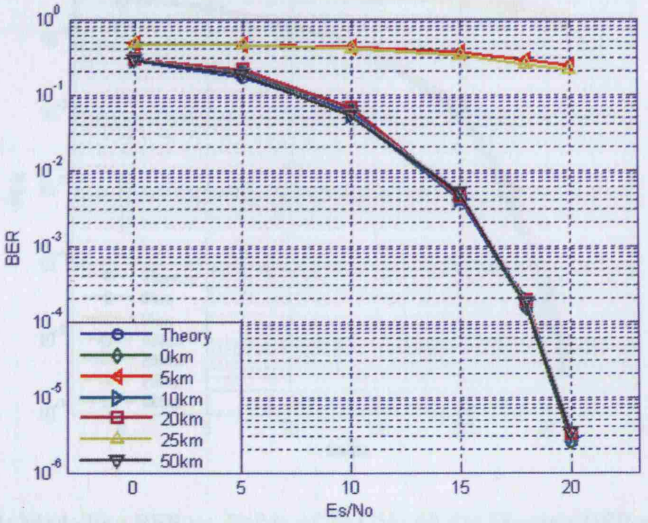

Figure 4.32: Modelling BER vs. Es/No of 28 GHz 16-QAM using DSB modulation.

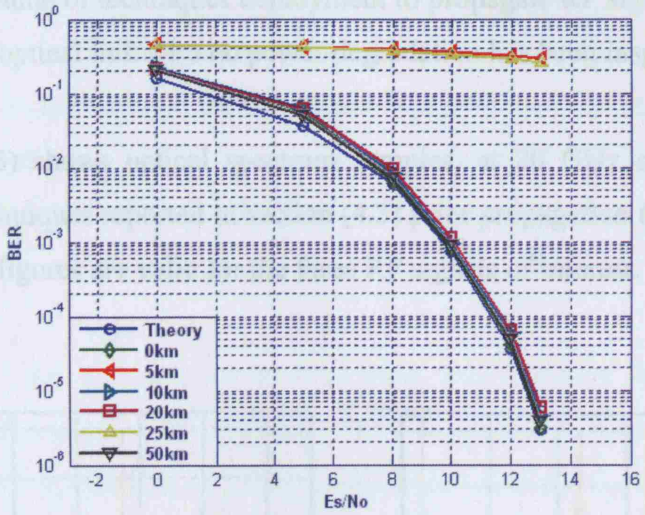

Figure 4.33: Modelling BER vs. Es/No of 28 GHz QPSK using DSB modulation.

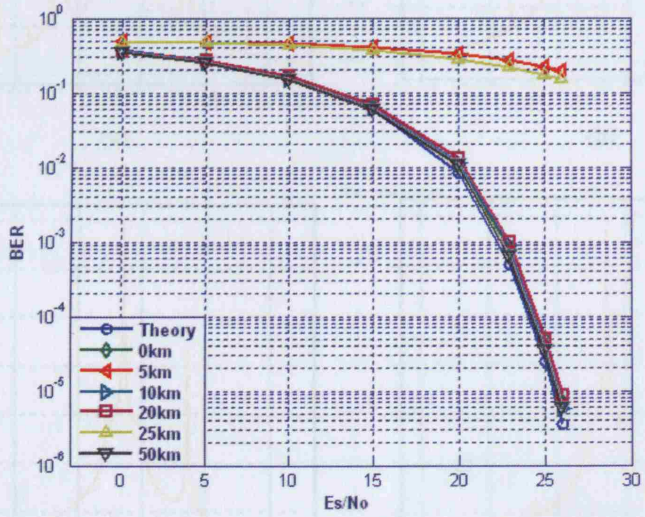

Figure 4.34: Modelling BER vs. Es/No of 28 GHz 64-QAM using DSB modulation.

4.6.2 Modulation Techniques Results

Since that theoretically calculated results have been confirmed with working on simulating the conventional Double Sideband (DSB) RoF system, and system's performance limitations of propagating the RF signals had been examined. Simulations were carried on investigating the ability of the reported modulation techniques to overcome fibre chromatic dispersion limitations.

Thereafter, aptitude of techniques deployment to propagate RF signals of interest over the entire optical link with no power degradation has been inspected.

Figure (4.35) shows optical spectrum samples, at 20 GHz carrier, for the modulation techniques reported in section (4.3) prior propagation through optical fibre link. The figures are valid for the three RF signals of interest.

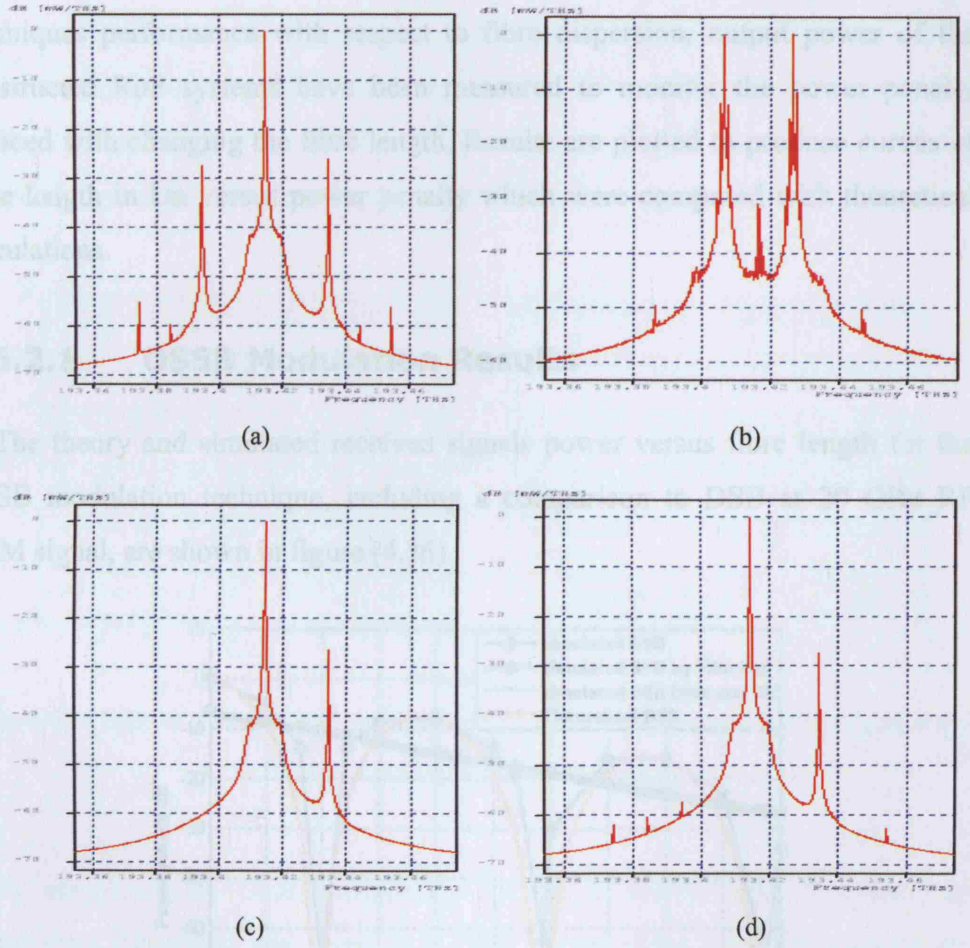

Figure 4.35: Optical spectra of 20 GHz signal with (a) DSB modulation, (b) DSB-SC modulation, (c) OSSB+C by filtering modulation, and (d) OSSB+C using dual arm MZM.

The optical spectrum of the conventional DSB modulation, figure (4.35 a), shows the optical carrier at 194 THz with the upper and lower sidebands of the modulation RF signal at 20 GHz spaced from the optical carrier. The optical modulation harmonics were present with relatively low power. Moreover, figure (4.35 b) shows the optical spectrum of the simulated DSB-SC modulation technique, where the optical carrier suppressed to more than 30 dB with respect

to the LO frequency which are located at ($f$opt ± fc/2). Parameters of the designed system are illustrated in (Appendix A). And finally figures (4.35 c) and (4.35 d) show the optical spectrum of the simulated OSSB+C modulation technique by filtering and dual arm MZM techniques respectively, both figures are very similar except that with filtering technique, the harmonic sidebands were totally removed.

To examine the accuracy of RoF systems and compare the modulation techniques performance with respect to fibre dispersion, output power of the constructed RoF systems have been measured to monitor the power penalty induced with changing the fibre length. Results are plotted to produce curves of fibre length in km versus power penalty which were compared with theoretical calculations.

4.6.2.1 OSSB Modulation Results

The theory and simulated received signals power versus fibre length for the OSSB modulation technique, including a comparison to DSB at 20 GHz RF QAM signal, are shown in figure (4.36).

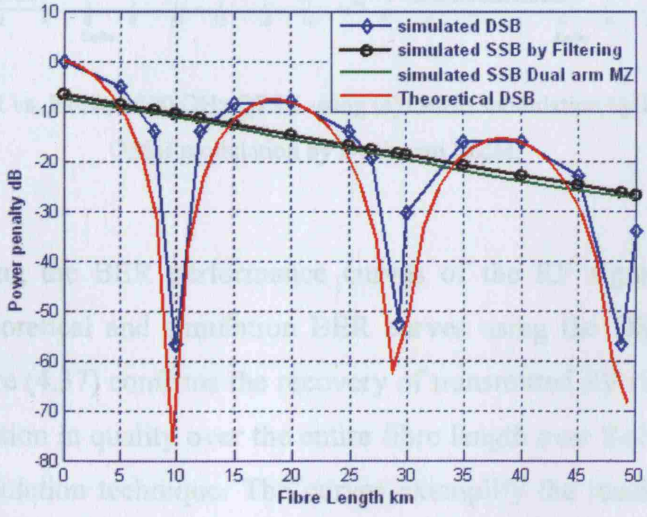

Figure 4.36: Power penalty versus fibre length of 20 GHz QAM using OSSB+C modulation.

The power is normalized to the received signal power at 0 km and considers fibre loss. Simulated OSSB systems lines illustrate that there is a very small power difference comparing the filtering and dual arms MZM systems, which

can be explained with taking into consideration the modulators arm's excess loss for each case, while the mismatch in theoretical and simulated curves was due to resolution variation between theory and simulation. In general, the graph shows a very good match between simulations and theory. Moreover, results demonstrated the systems capability of limiting destructive power penalty variation occurs with DSB modulation.

With using the OSSB modulation technique, the nulls were eliminated over the entire fibre length. Though, when one sideband is removed, half of the optical modulated sidebands power was removed (-3dB) which results in a (6dB) electrical loss relative to the maximum electrical signal power of a double sideband signal. This loss can be compensated with using electrical amplifiers.

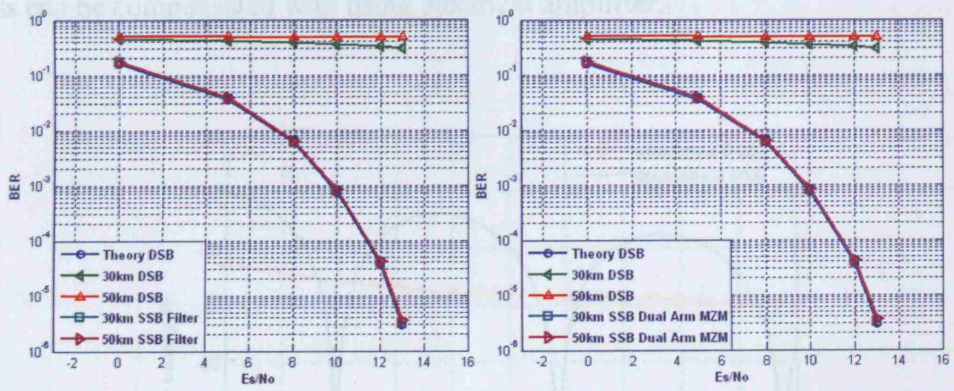

Figure 4.37: BER vs. Es/No of 20 GHz QPSK using (a) OSSB modulation by Filtering, and (b) OSSB modulation by Dual Arm MZM.

By comparing the BER performance curves of the RF signals at the null points with theoretical and simulation BER curves using the DSB modulation technique, figure (4.37) confirms the recovery of transmitted RF signals, without serious degradation in quality over the entire fibre length over RoF system using the OSSB modulation technique. The curves exemplify the results of a QPSK signal at 20 GHz using both filtering and dual arm MZM techniques to produce OSSB modulation. Results showed that it can be possible to recover the received signal without serious degradation in the signal performance. The results are valid for other frequencies of interest as well as for 16-QAM and 64-QAM signals at frequencies of interest.

4.6.2.2 DSB-SC Modulation Results

To investigate the performance of DSB-SC RoF system, a plot of simulated received signal power against fibre length of a DSB-SC QAM signal has been produced. Theoretical DSB and simulated received signal power against fibre length of a DSB-SC QAM signal at 20 GHz are shown in figure (4.38). The power was normalized to the DSB received signal power at 0 km and considers fibre loss. It can be seen from the results that this modulation technique can remove the signal power variation of the RF modulating frequency over the entire fibre length with no power variation in the electrical received power, while it offers a relatively low output power with respect to other modulation techniques which was due to directly modulated laser power limitation and optical carrier suppression. As the case with other techniques, this output power loss can be compensated with using electrical amplifier.

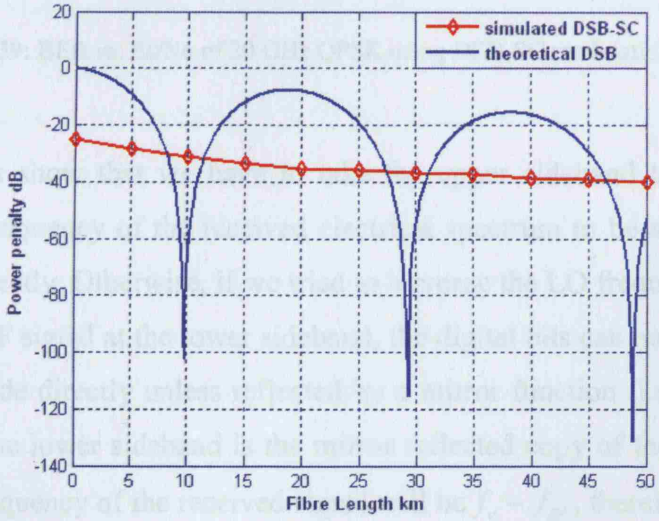

Figure 4.38: Power penalty versus fibre length of 20 GHz QAM using DSB-SC modulation.

The next step was to confirm the power penalty results by producing the BER curve of the signal. As a sample of the results, the DSB-SC RoF system with input signal of 50Mbps at IF frequency of 1 GHz QAM and 9.5 GHz RF LO frequency is simulated. The received electrical RF power is the carrier frequency at 19 GHz with lower and upper sidebands at 18 and 20 GHz respectively. To recover the required RF signal, the received electrical band has to go through

band pass filter to keep the upper sideband and remove all other frequency bands. Figure (4.39) is the BER curves of the received QPSK 20 GHz modulated signal at null points with conventional DSB and DSB-SC modulation techniques. The results were valid for the other frequencies and signals of interest.

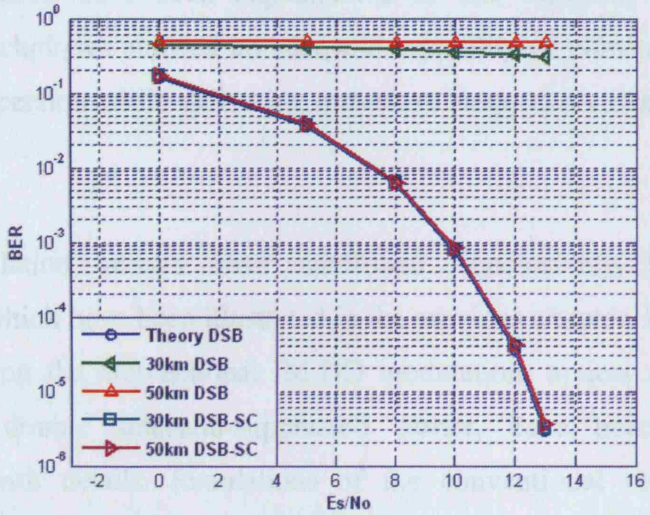

Figure 4.39: BER vs. Es/No of 20 GHz QPSK using DSB-SC modulation scheme.

Simulations show that we have to take the upper sideband to produce the required RF frequency of the received electrical spectrum to be able to recover the signal correctly. Otherwise, if we tried to increase the LO frequency to obtain the required RF signal at the lower sideband, the digital bits can not be recovered in the right code directly unless reflected by a mirror function (i.e. the received RF signal at the lower sideband is the mirror reflected copy of the generated IF code as the frequency of the received signal will be $f_c - f_{IF}$, therefore, the signal has to be reflected back to make it possible to recover the right bit code). Curves and results of this signal were valid for the rest of signals and frequencies of interest.

4.7 Conclusion

In this chapter we have carried out a series of simulations to demonstrate the performance evaluation of the investigated modulation techniques considering fibre chromatic dispersion. Digital signals including QPSK, 16-QAM and 64-QAM modulation have been implemented in this research. Inspected RoF modulation techniques showed an adequate capability of eliminating effects of chromatic dispersion while delivering mm-wave frequencies over optical single mode fibre.

The simulation results have confirmed conclusively the theoretical calculations which have been illustrated in the previous chapter. Fibre dispersion effects applying the conventional IM-DD modulation, optical single sideband and optical double sideband-suppressed carrier, have been demonstrated graphically with details. Simulations of the conventional modulation have authenticated the induced power penalty at the null points corresponding to the RF frequency applied when increasing the fibre length. Furthermore, models evaluation has been extended to identify the advantages and the negative aspects of the dispersion tolerant modulation techniques. It has been observed that the optical RoF systems applying OSSB+C modulation are advantaged of dispersion tolerant for the expense of constant power loss made by removing one of the optical sidebands. Moreover, applying DSB-SC modulation is advantaged of dispersion tolerant in addition to the system implementation simplicity, in spite of the expense of the received power loss made by suppressing the optical carrier which can be compensate.

Chapter 5

Performance of Modulation Techniques in Terms of Systems Nonlinearity (Theory and Simulation Results)

This chapter is investigates the Inter-Modulation-Free Dynamic Range (IM-FDR) of a class of systems that have good immunity to fibre dispersion, and explore their performance using experimentally justified simulation models. Following this opening paragraph, the optical systems of RoF links based on IM-DD modulation are discussed, with carrying out a comparison of modulation imposition techniques that are tolerant to dispersion. A Two tone test as an Inter-Modulation Distortion (IMD) measurement was discussed and described. Moreover, experimental justification of simulation models for the devices influencing the performance of modelled systems is established. After investigating the models performance of each individual technique, a performance analysis and a comparison of systems supported by detailed results are presented, followed by discussion of systems optimisation methods. Furthermore, the systems performance when adding optical fibre links is extensively investigated. Then after, a more advanced systems with multi-wavelength transmitting capability based on DSB-SC technique are discussed and illustrated. Final section was allocated for the conclusion and summarises the important results of this chapter.

5.1 Modulation Techniques of RoF Systems

In general, the principle of RoF technology is to simplify the remote antenna units and use the fibre as a propagating medium in the last-mile to centralize the signal processing tasks at the base stations [71;72]. As stated at previous chapters, Intensity-modulation direct-detection IM-DD is the simplest way to perform this task, but it suffers from limitations within the optical stage. When propagating an RF signal at high frequencies over relatively long distances of single mode fibre link, there are a number of issues. One of these issues is the fibre chromatic dispersion which we have discussed and explored at the previous chapter. Other issues, such as fibre nonlinearity [73;74], optical and electrical component nonlinearity results other system performance limitations of the RF signals [75-80].

Nonlinear effects may potentially have a significant impact on the performance of wavelength division multiplexing (WDM) optical communication systems. Therefore, nonlinearities may lead to attenuation, distortion, and cross-channel interference [81;82]. These effects place constraints on the spacing between adjacent wavelength channels, limiting the maximum power on channels, and may also limit the maximum bit rate. In the previous chapter, we have investigated the performance of modulation techniques of interest and explored the differences, advantages and disadvantages of RoF systems in terms of system's immunity to fibre chromatic dispersion. In this chapter we will investigate a class of systems that have good immunity to fibre dispersion and explore their performance with respect to the system Intermodulation-Free Dynamic Range (IM-FDR).

The main two categories for modulation techniques of interest are:

1. Optical Single Sideband + Carrier (SSB+C) modulation technique.

2. Optical Double Sideband-Suppressed Carrier (DSB-SC) modulation technique.

These two schemes are the main techniques discussed in this chapter, and each one may be implemented in a number of ways. In this chapter, we will list and explain the main techniques of interest to analyse and compare their performance with respect to optical devices nonlinearity.

1. Optical Single Sideband + Carrier (SSB+C):

This modulation technique could be applied by either filtering one of the modulated optical sidebands, prior to propagating through the fibre, or even at the far end of the fibre link using an optical filter [51;52]. Another method of implementing this technique uses a dual arm optical modulator to externally modulate the optical carrier by applying the RF signal to both arms of the modulator with a phase difference of 90 degree [55;56]. In this form, the optical spectrum consists of the optical carrier generated by the CW laser and one modulated sideband. The eliminated optical sideband can be made to be either the upper or lower sideband by changing the biasing points of the MZ dual arm external modulator.

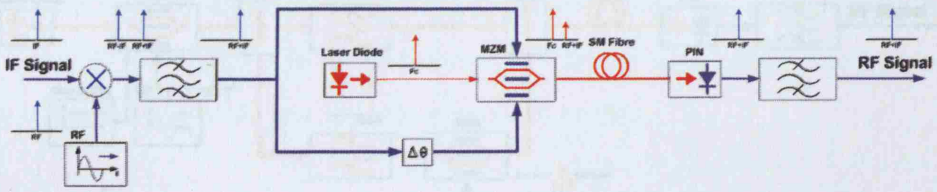

Figure 5.1: Schematic diagram of the optical SSB+C with Dual Arm MZ modulator.

2. Optical Double Sideband-Suppressed Carrier (DSB-SC):

The principle of this modulation technique is based on suppressing the optical carrier of the modulated optical spectrum. There is more than one way to achieve this, the first method is by directly modulating a laser diode with IF input signal and then modulating the laser output with an RF carrier at $f = f_C / 2$ using an external MZ modulator biased at the Minimum Transmission Biasing (MITB)

point (null point), as was discussed in chapter 3. The performance of this system has not been well studied previously.

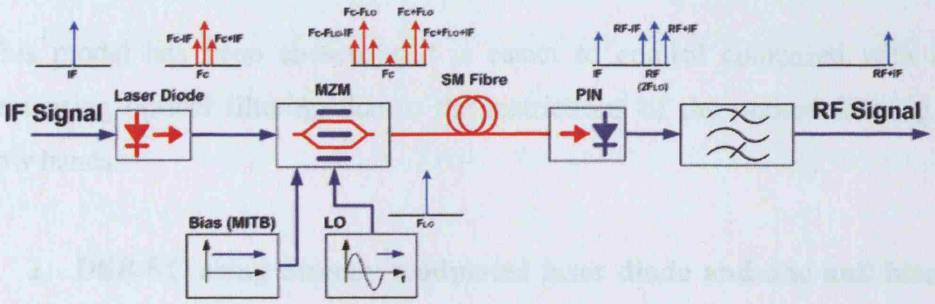

Figure 5.2: Schematic diagram of the DSB-SC using up-converted DM laser.

The second, more advanced, way of achieving this modulation scheme can be implemented by splitting the two RF modulated optical sidebands to externally modulate one of the sidebands with the IF signal and then recombine them to give one modulated sideband, one un-modulated sideband and suppressed carrier. Systems in details will be explained throughout this chapter.

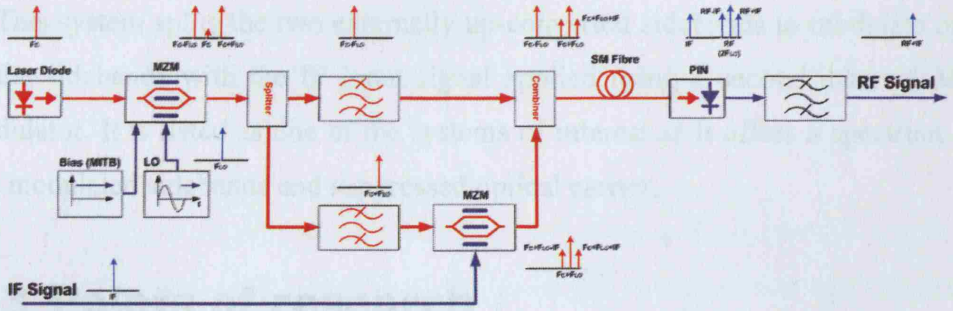

Figure 5.3: Schematic diagram of the optical DSB-SC modulation technique with two MZMs.

5.2 Comparison of Modulation Imposition Techniques

In this section, we will list the modulation techniques of interest, explaining the advantages and disadvantages of each technique, which will lead us to the aim of this chapter of comparing the performance of the considered techniques for delivering of modulated mm-wave signals.

5.2.1 Techniques to consider

1. **OSSB+C using dual armed External MZ modulator.**

This model has been chosen as it is easier to control compared with the system using optical filtering due to the restrictions of the optical filtering at narrow bands.

2. **DSB-SC using directly modulated laser diode and one null biased external MZ modulator.**

This system has been identified as both cost effective and simple to implement as it uses directly modulated laser and a single external modulator. Therefore, it will be the main system of interest to investigate in our work.

3. **DSB-SC using up converted CW laser and two MZ modulators.**

This system splits the two externally up-converted sidebands to modulate one of the sidebands with the IF input signal applied using a second external MZ modulator. It is listed as one of the systems of interest as it offers a spectrum of one modulated sidebands and suppressed optical carrier.

5.3 Points of research

The main points of interest of this work is to specify which of the three systems provide best linearity and therefore best performance as each system contain different nonlinear component combinations in the transmitter section. Afterwards, we will inspect the ways of optimising systems to enhance the overall system performance. Table (5.3.1) lists these techniques with the number of their nonlinear components at the transmitter. It can be seen that each system contains a minimum of two nonlinear devices.

Technique	Mixer	DM Laser	MZ modulator
1- OSSB+C	1	0	1
2- DSB-SC	0	1	1
3- DSB-SC 2	0	0	2

Table 5.3.1: The number of nonlinear components within each of the modulation techniques.

To perform a valuable performance evaluation study for the three considered systems with respect to nonlinearity, basic rules had to be set at the beginning of this work. These rules were:

1. The designed systems implemented to apply the three modulation techniques of interest will consist of the main elements without using any electrical or optical amplification to simplify and validate the evaluation points.

2. The receiver section of the three systems has to be simple and identical in all three systems to allow monitoring the output differences according to the same factors.

3. Varying the power of the input signal with constant steps, while fixing the power of other sources.

4. In order to validate the systems performance evaluation with respect to the input power variation, the electrical carrier power and the laser diode optical power will kept fixed whenever it is used at any of the three systems.

5.4 Work scenario

We have used OptSim as a modelling and simulation environment supporting the design and performance evaluation of the transmission level of optical communication systems. The optical simulation tools of OptSim do consider the noise and the nonlinear characteristics of the optical components, while the electrical simulation tools components had been modified when needed, using *OptSim Matlab interface* to consider the nonlinearity parameters. Simulated

components were experimentally compared to validate the simulations and to match simulation parameters with experimental components parameters.

5.5 The Two Tone Test

In order to investigate the system's performance in terms of nonlinearity, a two tone test is used to perform this task. A "two tone test" is a generic test signal composed of two different frequencies and used for Inter-Modulation Distortion (IMD) measurements. It involves the transmitting of two input signals with same amplitude, separated by small frequency difference Δf. In our systems, we have used a two test signals at frequencies of 1 GHz and 1.05 GHz (with Δf of 50 MHz).

By performing this test, it would be possible to produce the input-output power curves for the fundamental and the third-order Inter-Modulation Distortion (IMD), and therefore, to specify the Inter-Modulation-Free Dynamic Range of the systems. This represents a distortion measurement of system's nonlinearity defined as the IM3 intercept point and the maximum SNR with respect to the noise floor.

5.6 Simulation models Justification

In order to justify the simulation components and therefore the simulation models, each selected practical component has been experimentally examined to determine the operating characteristics and performance parameters. Accordingly, the simulation device models have to be specified to match the experimental component specifications. To do so, each component needed to construct the simulation RoF systems of interest has been investigated to perform in the same manor as the real experimental component. The experimentally examined components are detailed below:

1- **Directly Modulated Laser Diode:** The experimental reference device used was the HP LSC2500 (2.488 Gb/s DFB Laser Module with Integral Optical Isolator). Experimental measurements were performed to specify the actual practical characteristics of this device. Linear and logarithmic curves of the input bias current against the output optical power were produced for this device and the operating specifications were determined. For the simulation systems, a new laser model has been built using the OptSim *Best Fit Laser Toolkit* to setup the laser configurations matching this experimental device.

Parameter	Value	Units
Frequency	193.41449	THz
Wavelength	1550	nm
Threshold Current	16	mA
P-I Slope	0.0447	mW/mA
Linewidth	1	MHz
Start Frequency	0	GHz
Stop Frequency	2.488	GHz
Average RIN	-148	dB/Hz

Table 5.6.1: Properties of the directly modulated laser diode simulation model.

The figures below show the experimental and simulation characteristic curves of the directly modulated laser diode.

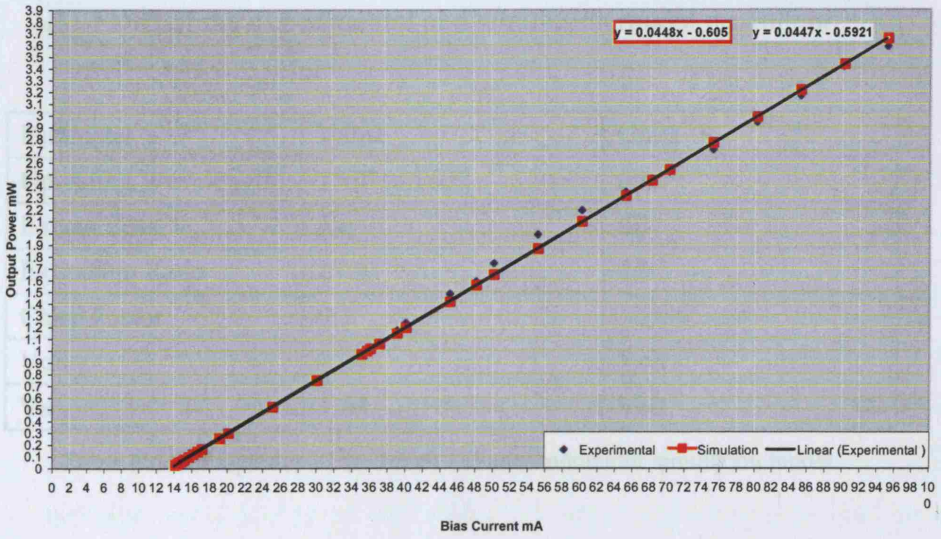

Figure 5.4: Input / output characteristic line of the directly modulated laser diode.

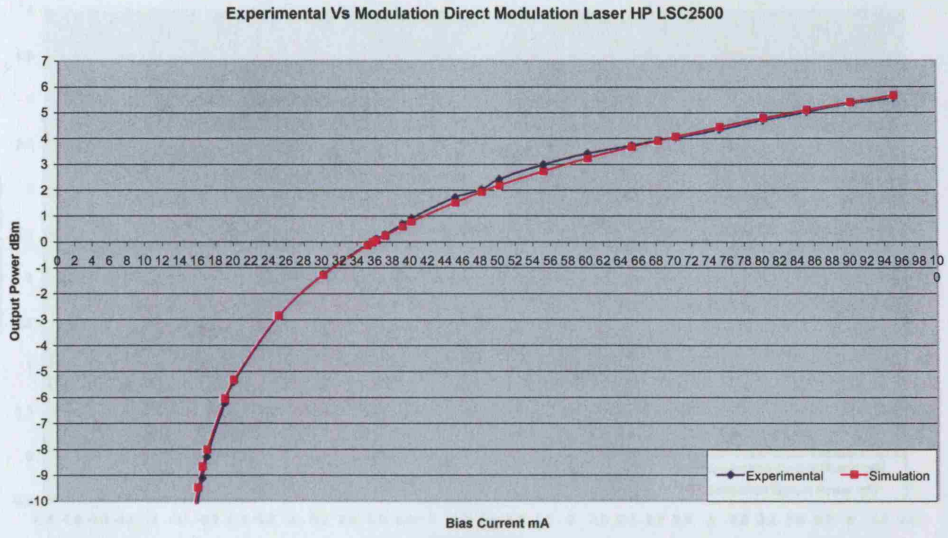

Figure 5.5: Input / output algorithmic curve of the directly modulated laser diode.

2- **Mach Zehnder Modulator:** The experimental device used for the systems was the JDS Uniphase (10Gb/s Integrated Amplitude Modulator with Attenuator 100-04003). The simulation model MZ modulator was specified to match the selected experimental device. The Trans-characteristic curve has been produced for both the device and the model, followed by a two tone test performed experimentally and in simulation to specify the device nonlinearity characteristics, and to justify the model nonlinearity performance used in simulation systems. Figures below show the Trans-characteristic and Inter-modulation-Free Dynamic Range (IM-FDR) of the experimental and simulation model modulator.

Parameter	Value	Units
Operating Wavelength	1530 to 1605	nm
Excess Loss	3.6	dB
Extinction Ratio	27.9	dB
Chirp Factor	0.2	
Von	3.24	Volt
Vπ	1.64	Volt

Table 5.6.2: Properties of the Mach Zehnder modulator simulation model.

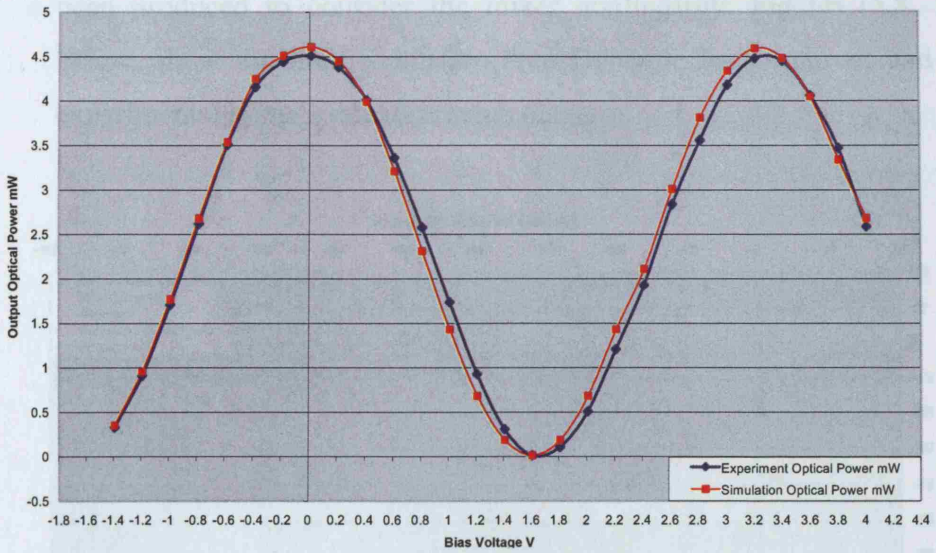

Figure 5.6: Trans-characteristic curves of the experimental and simulated MZ modulator.

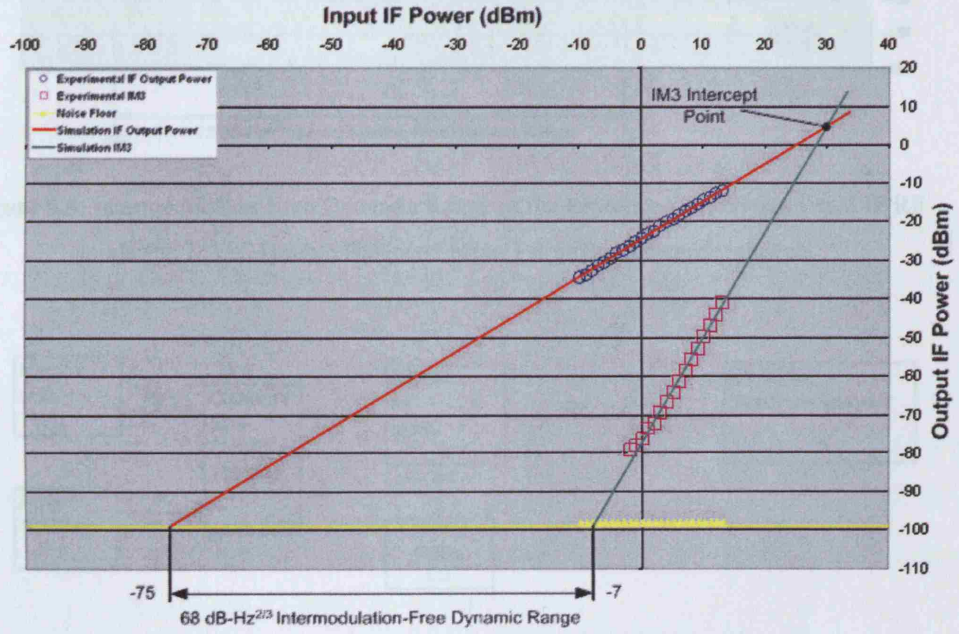

Figure 5.7: Intermodulation-Free Dynamic Range of the experimental and simulation MZM.

3- IF/RF Mixer: The mixer used experimentally was wj M86C Double-Balanced Mixer. A two tone test was performed experimentally to investigate the nonlinearity characteristics of the mixer. The I/O power curve was produced to specify the third order Intermodulation (IM3) intercept point (IIP3) of the mixer. To match the experimental mixer configurations in simulation, a modified model of the OptSim mixer have

been produced to consider the mixer nonlinearity. Figures (5.8, 5.9) below, show the Intermodulation-Free Dynamic Range curves and the experimental mixer evaluation setup diagram.

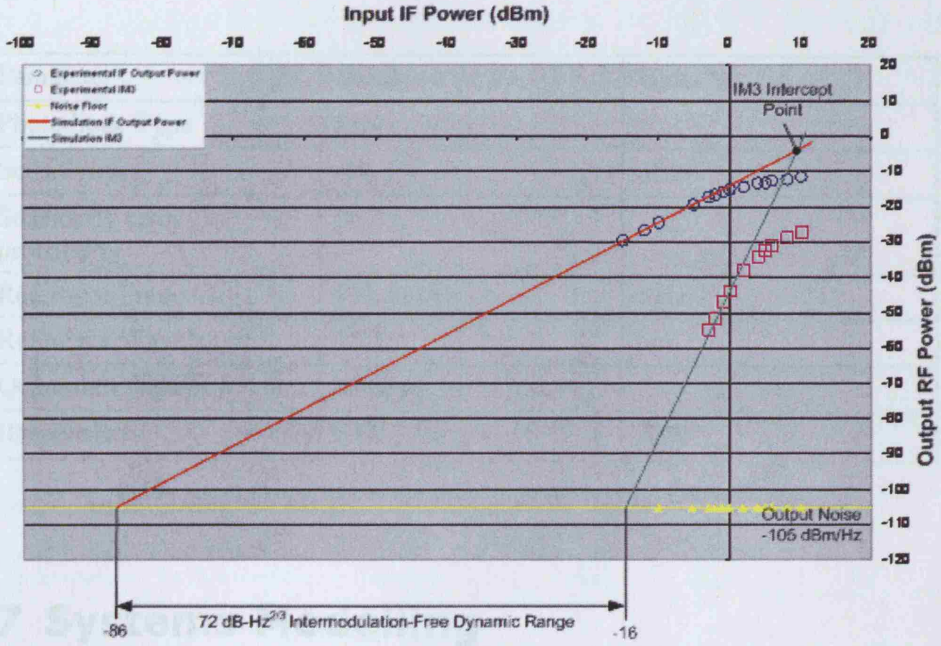

Figure 5.8: Intermodulation-Free Dynamic Range of the experimental and simulated IF/RF mixer (wj M86C Double Balanced Mixer) at 5dBm RF carrier power.

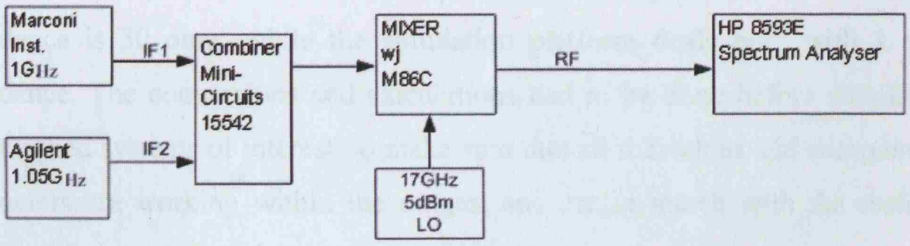

Figure 5.9: The Block diagram of the mixer experimental IM-FDR evaluation set up.

Parameter	Value	Units
LO Frequency	3.5 to 18	GHz
RF Frequency	6 to 18	GHz
Noise Figure	7	dB
IIP3	+10	dBm

Table 5.6.3: Properties of the RF mixer simulation model.

4- **Photo Diode:** The optical receiver used experimentally was a PIN photodiode (NORTEL Networks 10Gb/s PIN Preamp Receiver, PP10G C28J). Simulation model configurations were specified to match the experimental configurations with extended frequency operating range.

Parameter	Value	Units
Photodiode Type	PIN	
Sensitivity	-19	dBm
Sensitivity error probability	$1e^{-10}$	
Reference Frequency	193.41449	THz
Reference Wavelength	1550	nm
Quantum Efficiency	0.70392	
Responsivity	0.88	A/W

Table 5.6.4: Properties of the simulation model PIN Photo Diode.

5.7 Systems Modelling

After the determination of the experimental components values, these results had to be converted to the equivalent values within the simulation platform. It is important to consider that with experimental components, the matching impedance is 50 ohm, while the simulation platform deals only with 1 ohm impedance. The conversions and calculations had to be done before simulating the designed systems of interest, to make sure that all the values and components parameters are working within the ranges, and are in match with the realistic values of the experimental components parameters.

5.7.1 SSB + C using dual arm MZ modulator:

We have chosen this system as it represents an easy to implement modulation technique used for delivering modulated mm-wave signals over single mode fibre while still being chromatic dispersion tolerant. Figure (5.10) shows the simulation model of this system. It can be seen that it is constructed from a dual arm MZ modulator, an electrical RF carrier, a mixer, a CW laser, and a PIN photodiode receiver. To evaluate the IMD performance of this system, we have

applied the two tone test signal with various amplitudes to the input of the system. Figure (5.11) shows the Intermodulation-Free Dynamic Range of the simulated SSB+C RoF system using Dual Arm MZ modulator with varying the input IF power and applying 10 dBm electrical RF carrier power at the mixer input. It can be seen that this system can offer a 44 dB-Hz$^{2/3}$ IM-FDR with applying the used settings for the components. The system full settings are listed in appendix A.

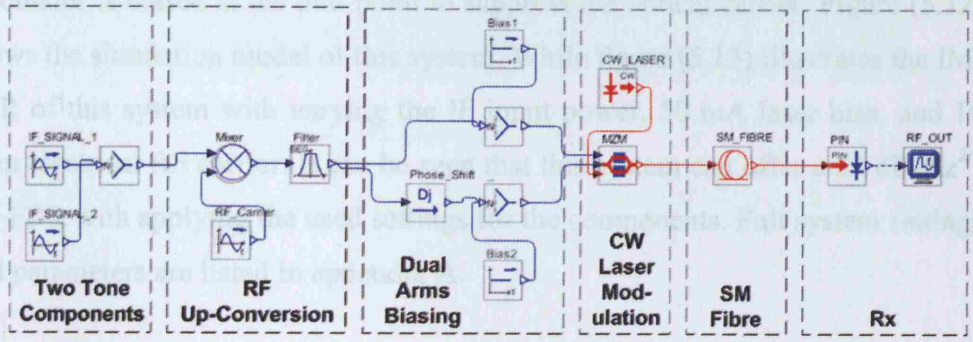

Figure 5.10: OptSim simulation model of the SSB+C modulation using Dual Arm MZM.

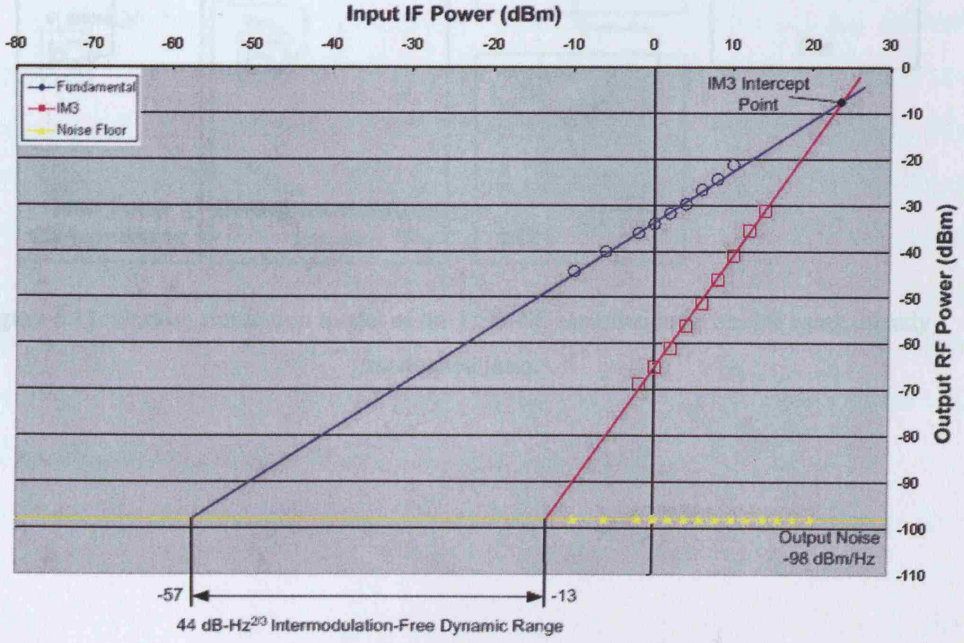

Figure 5.11: Intermodulation-Free Dynamic Range of the simulated OSSB+C RoF system using dual Arm MZ modulator.

5.7.2 DSB-SC using up-converted directly modulated (DM) laser:

This system has been chosen as the main system of interest. It represents a simple to implement, cost effective RoF modulation technique. This system is constructed from one directly modulated laser, a PIN photodiode receiver, and an MZ modulator to up convert the modulated optical signal using a local oscillator at a frequency of half of the required output electrical carrier frequency. The MZ modulator is biased at the null point to suppress the optical carrier. Figure (5.12) shows the simulation model of this system. While figure (5.13) illustrates the IM-FDR of this system with varying the IF input power, 50 mA laser bias, and 10 dBm electrical RF carrier. It can be seen that this system can offer a 35 dB-Hz$^{2/3}$ IM-FDR with applying the used settings for the components. Full system settings and parameters are listed in appendix A.

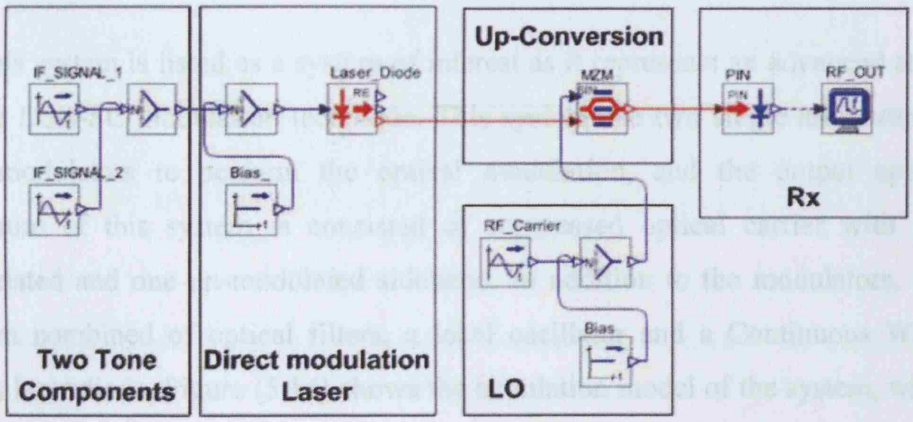

Figure 5.12: OptSim simulation model of the DSB-SC modulation technique using directly modulated laser.

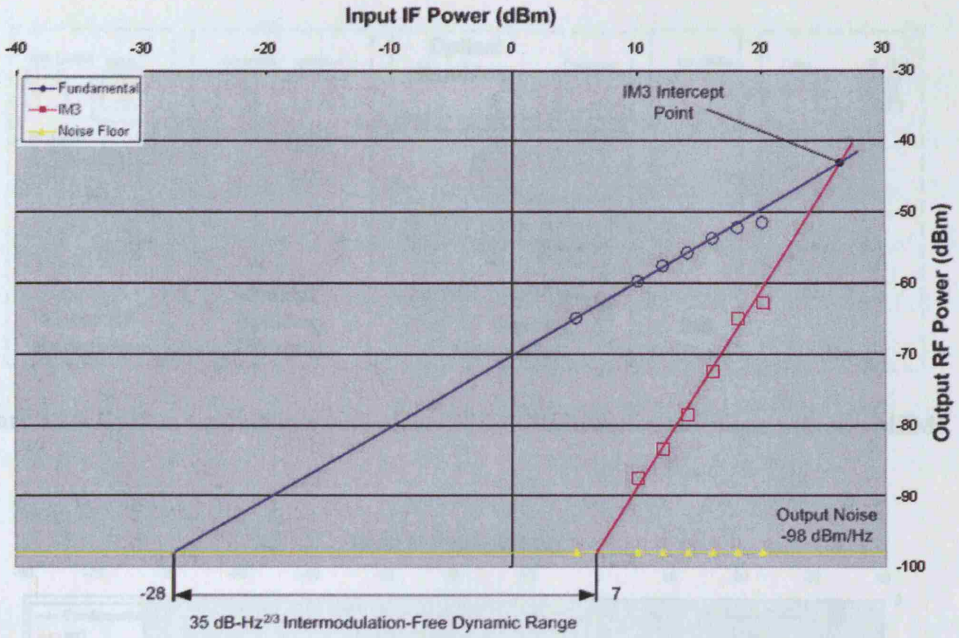

Figure 5.13: Intermodulation-Free Dynamic Range of the simulated ODSB-SC RoF system with directly modulated laser.

5.7.3 DSB-SC using two MZ Modulators:

This system is listed as a system of interest as it represents an advanced stage of the DSB-SC modulation technique. This system use two single arm external MZ modulators to perform the optical modulation, and the output optical spectrum of this system is consisted of suppressed optical carrier with one modulated and one un-modulated sideband. In addition to the modulators, this system combined of optical filters, a local oscillator and a Continuous Wave (CW) laser diode. Figure (5.14) shows the simulation model of the system, while figure (5.15) illustrate the IM-FDR of the system with varying the IF input power. It can be seen that this system can offer a 50 dB-$Hz^{2/3}$ IM-FDR with applying the used settings for the components. Full settings and parameters are listed in appendix A.

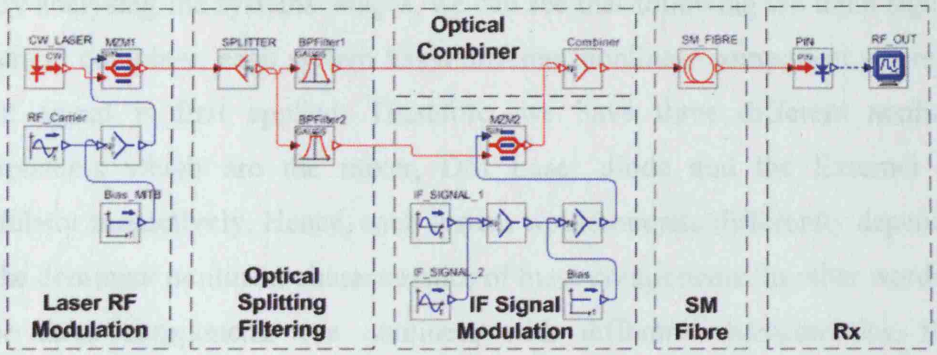

Figure 5.14: OptSim simulation model of the DSB-SC modulation technique with two MZMs.

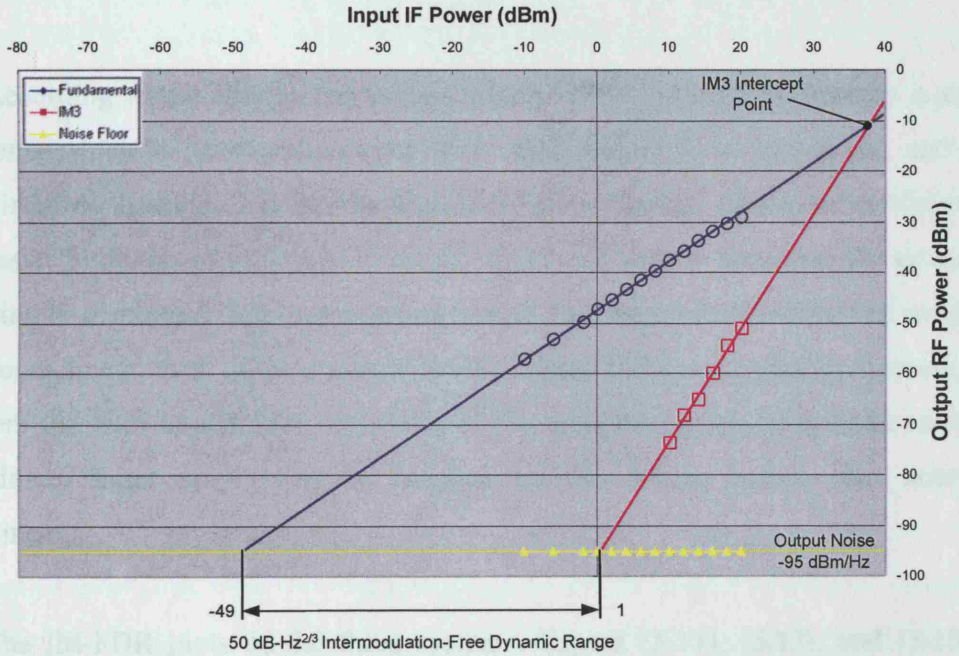

Figure 5.15: Intermodulation-Free Dynamic Range of the simulated ODSB-SC RoF system with using two MZ modulators.

5.8 Performance Analysis

To get a valuable comparison between the three systems and as each system has different component combinations it is necessary to fix the parameters of the common components in these systems. These common parameters were the local oscillator signal power, the CW laser output power, combiner loss, the settings of the modulators and the PIN receiver.

By analysing the systems' stages, we can see that following the input signal's electrical combiner, each system has a different nonlinear component where the input signal is first applied. Therefore, we have three different nonlinear components which are the mixer, DM Laser diode and the External MZ modulator respectively. Hence, each system would operate differently depending on the dominant nonlinear characteristics of these components. In other words, as these three components are nonlinear with different characteristics, these components will be the major factor required to characterize the IMD level of the systems which will perform more or less dependant on the performance of the first nonlinear component.

According to the results, the system which offers the highest linearity is the systems which it have components with small output loss, low noise, and a nonlinear components can handle high input power before becoming nonlinear. In easier form, we can use a nonlinearity-threshold term to state that the system starting or combined from components having high nonlinearity-threshold would be more linear than other systems having lower threshold point components. Where the term nonlinearity-threshold of the component can be defined as the maximum input power can be handled by the device before start acting nonlinear.

The IM-FDR plots of the three systems, figures (5.11), (5.13), and (5.15), show that the system where the IF is directly applied to the modulator has the highest dynamic range while the second system would be the SSB+C and the last system is the DSB-SC with the directly modulated laser diode. This would confirm that the MZ modulator can offers a high dynamic range with high intercept point.

5.9 System Optimisation

Though the three systems perform the same task, each one has its own advantages and disadvantages. In addition, each system delivers a different optical spectrum dependent on the modulation technique and the exact electrical and optical components which form the system. Therefore, in order to optimise

the performance of each system, the main system's nonlinear components would be the key elements to enhance the system linearity with respect to RF signal delivery.

5.9.1 Single Sideband + Carrier (SSB+C):

As previously shown, this system uses a dual arm external Mach-Zehnder modulator with a CW laser diode as the optical section and a mixer, LO, filter and a 90° phase shifter in the transmitter electrical section. The disadvantage of this system is that it has power loss at the output, which is due to removing one of the optical sidebands (-3dB) which would introduces a loss of 6dB in the electrical received output power. Moreover, this system needs filtering at the electrical transmitter side to remove the signal harmonics created by the mixer. Therefore, the most efficient method of optimizing this system is by optimising the electrical power of the local oscillator to reduce the mixer nonlinearity in addition to adding electrical amplifiers at either sides of the system, after the mixer or the receiver. The other optimization method is to use a mixer with high nonlinearity-threshold point which can allow a higher input signals power with no distortion.

Figure (5.16) show the RF output power of the simulated system versus the optical fibre length. It can be seen from the graph that the system offers a linear output power over the entire fibre length with using this modulation technique which eliminates the fibre dispersion penalty. Fibre loss of 0.2dB/km has been considered which would reduce the received electrical output RF signal power with increasing fibre length.

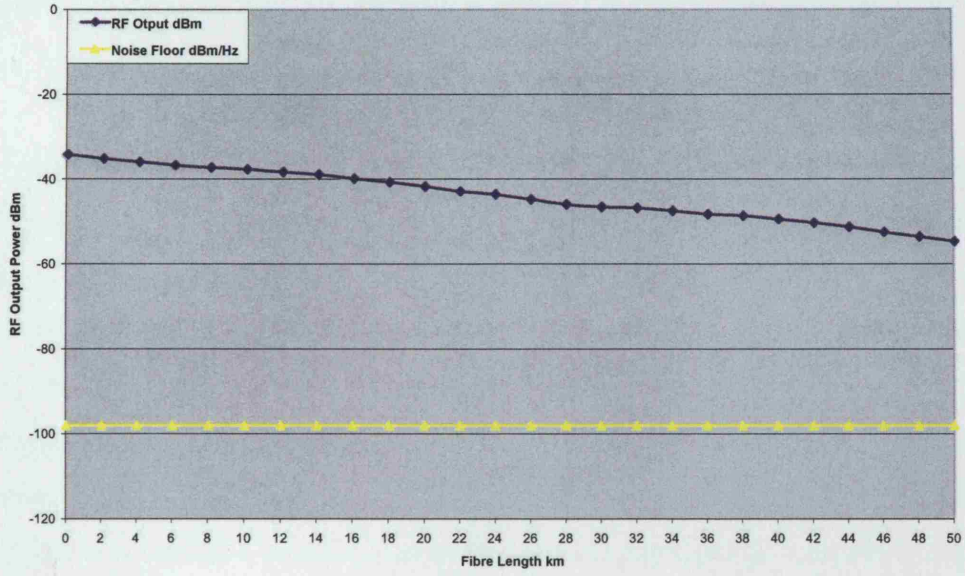

Figure 5.16: RF output power of the simulated SSB+C RoF system with respect to fibre length applying two tones 0dBm IF input, 10dBm RF carrier and 10dBm CW laser.

5.9.2 Double Sideband-Suppressed Carrier (DSB-SC) Using Two Modulators:

This system already offers a good dynamic range. The feature of this system, in terms of linearity dynamic range, is the combination of the nonlinear components used to construct the system, as it is constructed using only two MZ modulators, as nonlinear components, where each one can provide a good linearity level, therefore, a high dynamic range with signal processing. The weakness of this system is the need for optical filters (AWGs) to separate the RF modulated optical sidebands, in addition to the optical loss produced due to suppressing the optical carrier. These reasons classify the system as complicated and non cost effective systems. Moreover, as the case with systems using this modulation technique, the output electrical RF spectrum will need filtering to remove the undesired frequency components. The efficient way to enhance the performance of this system is by adding RF electrical amplification at the receiver end, following filtering stage to increase the output power level of the system.

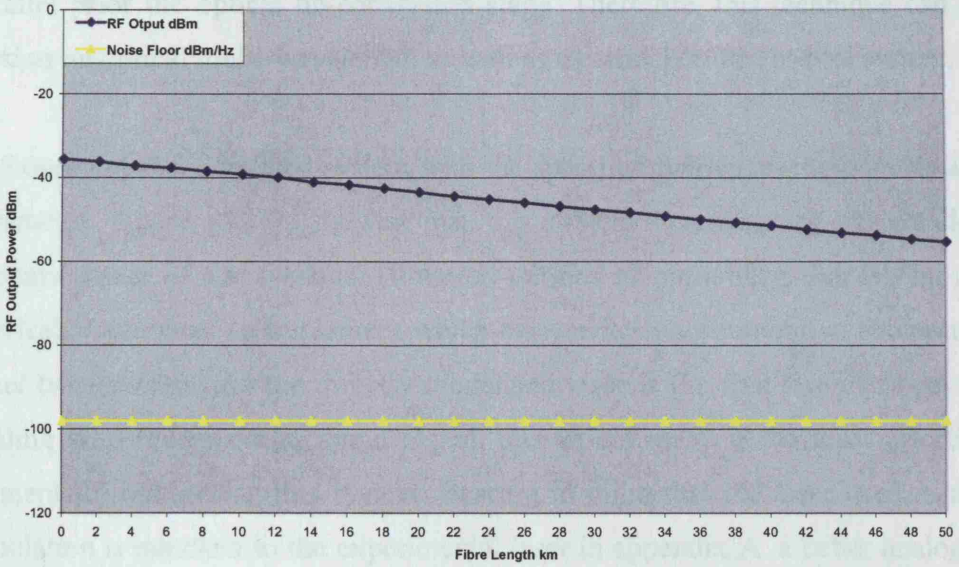

Figure 5.17: RF output power of the simulated DSB-SC RoF system using two MZ modulators with respect to fibre length applying two tones 10dBm IF input, 21.6dBm RF carrier and 10dBm CW laser.

Figure (5.17) shows the RF output power of the simulated system with fibre. The output RF line illustrates that the system offers a linear output power over the entire fibre length. By comparing the results of the last two figures, it can be seen that the SSB+C system can offer similar output signal levels while using lower input and carrier power signals when compare to the DSB-SC with two MZ modulators system. The IF input signal of the SSB+C system was 0 dBm, and the RF carrier was 10 dBm, while it was 10 dBm and 21.6 dBm respectively for the DSB-SC system using two MZ modulators.

5.9.3 Double Sideband-Suppressed Carrier (DSB-SC) using DM laser:

The advantages of this system are simplicity and cost effectiveness system, as were discussed in previous chapters. Moreover, this system has a unique advantage over the other two systems as it uses a directly modulated laser scheme, which offers the possibility of transmitting multi-wavelength optical signals simultaneously by using different wavelength directly modulated lasers in

parallel prior the optical up-conversion stage. Therefore, this technique can be used as an optical multi-wavelength as well as electrical multi-channel system.

Results of the simulated system with the specified particular components and parameter, figure (5.13), showed that this system demonstrates the smallest dynamic range of the systems. However, options of optimizing this system are applicable and easy to implement which may make it a competitive solution to other two systems. As the directly modulated laser is the first nonlinear device dealing with the incoming input signal, this would make it the most effective element for optimizing this system. Bearing in mind that the laser used in this simulation is matched to the experimental laser in appendix A. a better analogue DM laser with higher output power will certainly enhance the performance of this system. Moreover, adding an RF electrical amplifier after signal filtering of the PIN receiver output, would enhance the output power level and therefore improve the overall system performance.

It has been found that the DM laser diode characteristics play a very important role at the design of this system in terms of linearity of the output RF power. Therefore, the laser has to be selected with linear P-I slope and relatively small linewidth. The results we had, figure (5.13), was for the laser biasing current of 50 mA and an RF carrier power of 10 dB. The following results illustrate the improvement of the system performance by increasing only the laser bias current, and the electrical RF carrier power to 150 mA, and 21.6 dBm respectively, which would represent a maximum input values to give a good linear response. Figure (5.18) illustrating the improvement of system's dynamic range with applying the maximum feeding values, while figure (5.19) shows the power level of the desired output RF signal with applying the new feeding values.

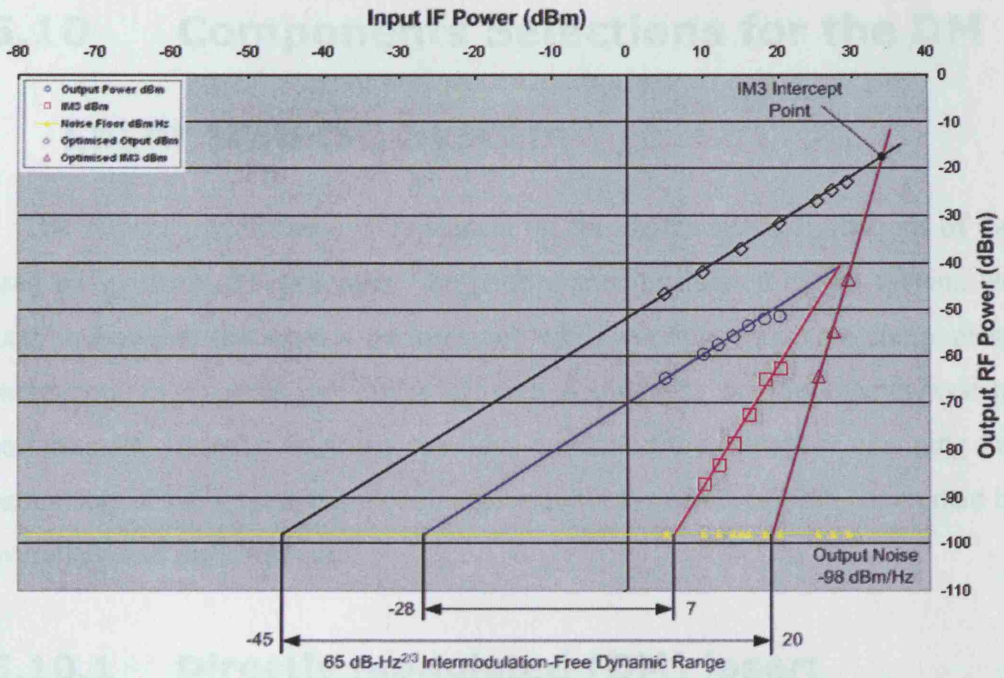

Figure 5.18: Intermodulation-Free Dynamic Range of the optimised simulated DSB-SC system.

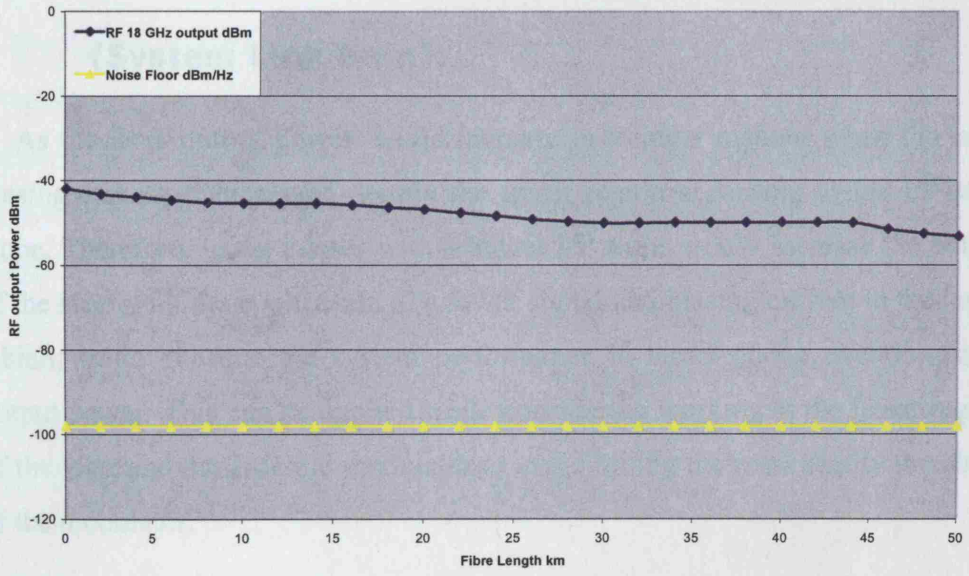

Figure 5.19: RF output power of the simulated DSB-SC RoF system with respect to fibre length applying two tones 10dBm IF input and 21.6dBm RF carrier.

It can be seen from figure (5.19), that the enhanced DSB-SC system's output is competitively close to the output power levels of the other two systems, keeping in mind that the output power of the directly modulated laser at this system is low, about 3.7 dBm, with compare to the optical output of the CW laser of 10 dBm used for the other two systems.

5.10 Components Selections for the DM Laser DSB-SC System

The system performance is dependent on the characteristic limitations of the used components. To generalize the performance evaluation of the system, we have to evaluate the system performance while varying the active components parameters to explore the effect of each component on the overall system performance. In order to do so, we have examined the effects of changing the parameters of the system components, to monitor the effect of each component to overall system performance.

5.10.1 Directly modulated (DM) laser:

5.10.1.1 Laser biasing current versus the output power (System Link Gain):

As the laser output power would increase in a linear manner when the laser biasing current is increased, within the linear region according to the I/P laser slope, Therefore, using a laser with a higher I/P slope would increase the output of the laser with the application of a lower signal and biasing current to the laser, which would enhance the system performance in terms of the overall system output power. This can be applied while considering working at the linear region of the laser and the external modulator to avoid hitting the nonlinearity threshold of the modulator.

To investigate the laser parameters effect on the overall system performance, we monitored the system output power in terms of output RF carrier, received RF output signal, and the third order interference IM3 versus laser biasing current.

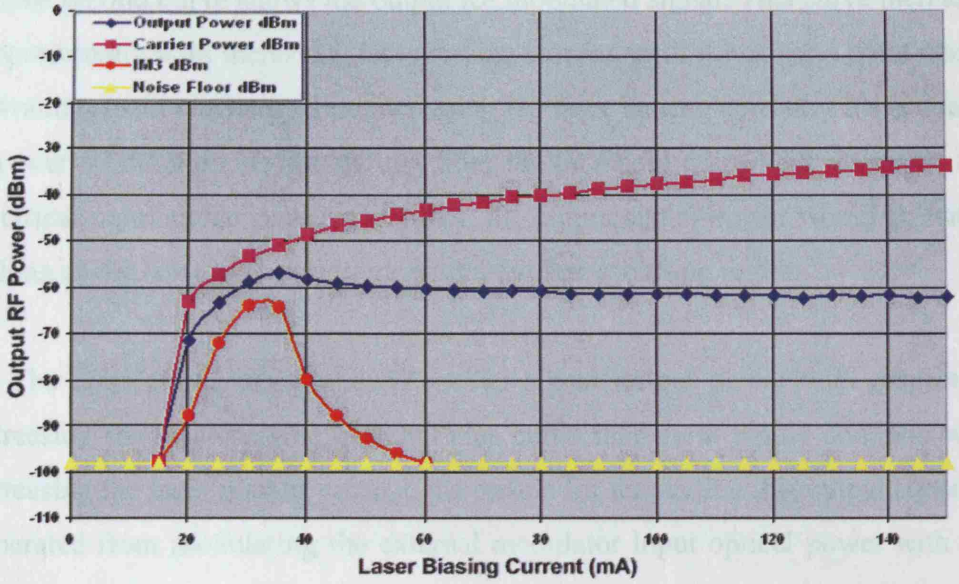

Figure 5.20: RF output power components of the simulated DSB-SC RoF system with respect to laser biasing current applying two tones 10dBm IF input and 10dBm RF carrier.

The graph above, figure (5.20), shows the output power frequency components of the DSB-SC against the laser biasing current, applying two tone signals at 10 dBm and electrical RF carrier power of 10 dBm. The graph shows that the optimum biasing area, in terms of minimum signal to carrier ratio, while fixing the input signal power, would be at the middle region (between 60 and 80 mA for the laser used). The results shows that the RF carrier signal power would keep increasing with increasing the laser biasing current, while the RF signal would have the maximum linear point at the middle biasing region, and will slightly decrease with increasing the biasing current.

To explain the graph, starting with the intermodulation distortion curve, it shows a reasonable response for the laser as a 10 dBm signal was applied to directly modulate the laser, thus, if low biasing current is applied, this would effect the performance of the laser as it would be over modulated with respect to the input IF signal power. The increment of the curve slope would start from the point of the laser threshold current up to the point where the laser biasing current allow the laser to work within the linear region with no over modulation.

The second curve shows the output RF modulated signal. This curve increases proportionally with increasing laser biasing current, until it reaches a point where it would remain constant while increasing the laser biasing current. This is due to the over modulation region starting from the threshold point with respect to the electrical input signal power, thereafter, the output signal power would be stable as long as the laser biased to work within the linear biasing region.

The third curve shows the RF carrier signal output power with respect to increasing the laser biasing current. This curve increment would continue with increasing the laser biasing current, the reason for that is that this output signal is generated from modulating the external modulator input optical power with the RF carrier. Therefore, the output power would be dependent on the optical input power of the external modulator, which would keep increasing with increasing the laser biasing current. Therefore, as this RF carrier signal have to filtered out to keep the modulated RF signal, smaller RF carrier power will give better results as the carrier signal need to be as small as possible to filter out efficiently. Therefore, it is advisable to bias the laser at the middle linear region in order to optimize the system performance in terms of signal to carrier ratio.

5.10.1.2 Output Signal to Carrier Ratio (SCR):

Figure (5.21) below shows the difference between the signal to carrier power ratio while increases the laser biasing current. It can be seen from the curve that the different between the carrier and the signal power is increases while increasing the biasing current. This increment in the carrier power would have a negative effect on the system performance as the signal need to be filtered to remove the boundary frequency components including the carrier signal, which would be effect the RF output as a noise signal. This would confirm the previous graph results, that the laser should be biased at the middle low biasing current values starting from the linear region to avoid the intermodulation interference at low values and the high carrier to signal ratios at the higher stage.

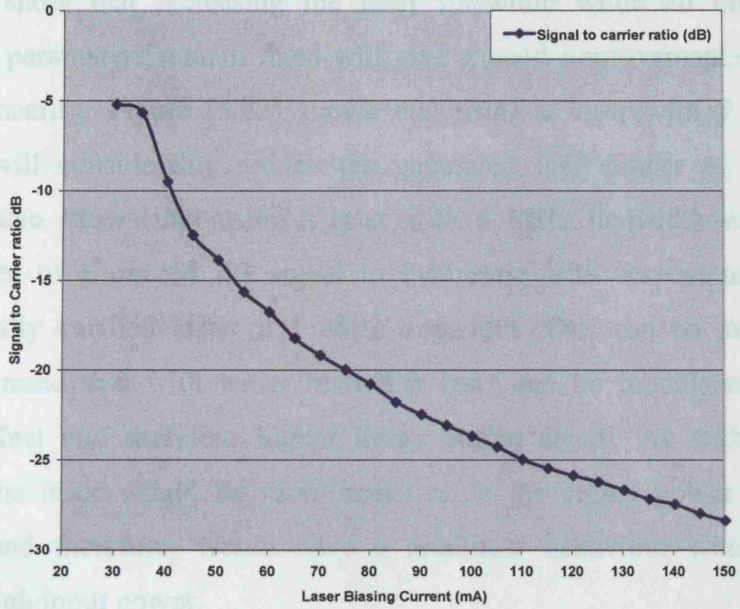

Figure 5.21: Output RF signal to carrier variation curve with respect to laser biasing current

5.10.1.3 The effect of the directly modulated laser Linewidth on the output signal:

To investigate the system output signal variation with respect to laser linewidth, lasers with different linewidth have been designed with OptSim *Best-Fit Laser toolkit*, and the other lasers parameters had been fixed. Changing the laser linewidth within the toolkit will, to some extent, affect the other parameters. Therefore, with fixing the other parameters and increasing the laser linewidth, we have designed ten different lasers starting with the experimentally verified at 1MHz linewidth.

Simulations have been run applying two tone IF input signals of 20 dBm while other system's parameters have been fixed to monitor the nonlinearity performance changes as the laser linewidth changes. The RF carrier power applied to the MZ modulator was 21.6 dBm, and the laser biasing current used was 80 mA to optimise the output signal power. The results are shown in figure (5.22). It shows that there is no effect on the output RF signal power or the RF carrier output power as the laser linewidth increases. A significant output power variation was noticed with the third order intermodulation interference (IM3) output power.

Results show that increasing the laser linewidth while all other system component parameters remain fixed will give a good improvement in terms of laser nonlinearity. Figure (5.22) shows that using a laser with 5 to 8 MHz linewidth will considerably reduce the generated IM3 power at the system output. It also shows that using a laser with 6 MHz linewidth will give an improvement of about 14 dB signal to IM3 ratio with respect to using the experimentally verified laser of 1 MHz linewidth. This can be explained by bearing in mind that with wider linewidth laser can be modulated with less chirping effect and therefore higher linear output signal. As with low laser linewidth the laser would be more sensitive to the signal power and signal variation, and therefore, would have a nonlinear behaviour when applying relatively high input power.

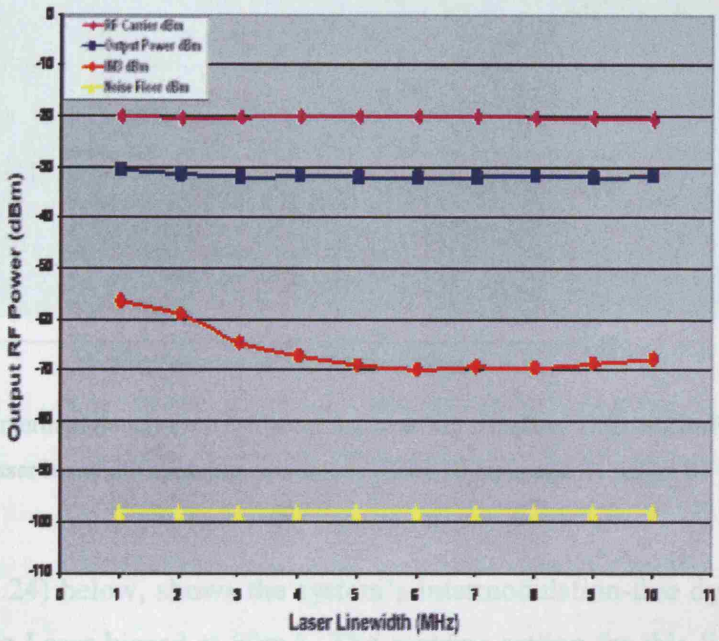

Figure 5.22: RF output power components of the simulated DSB-SC RoF system with respect to laser linewidth applying two tones 20dBm IF input and 21.6dBm RF carrier.

5.10.1.4 The Dynamic Range of the DSB-SC with higher linewidth laser:

To order to explore the changes to the system output in terms of linearity, the system's performance using wider linewidth laser has been investigated. Figure (5.23) below shows the intermodulation-free dynamic range of the simulated

DSB-SC system using a laser with 6MHz biased at 80mA. It can be seen that this system is offering 60 dB-$Hz^{2/3}$ IM-FDR with high RF signal output power and a lower RF carrier power output in comparison with the system using the 1 MHz laser and biased at the maximum biasing point. The output carrier power in this system was -20 dBm while its -13 dBm with the 1 MHz linewidth laser and 150 mA biasing current, which means that with this laser we are achieving a high dynamic range with improvement in the signal to carrier ratio.

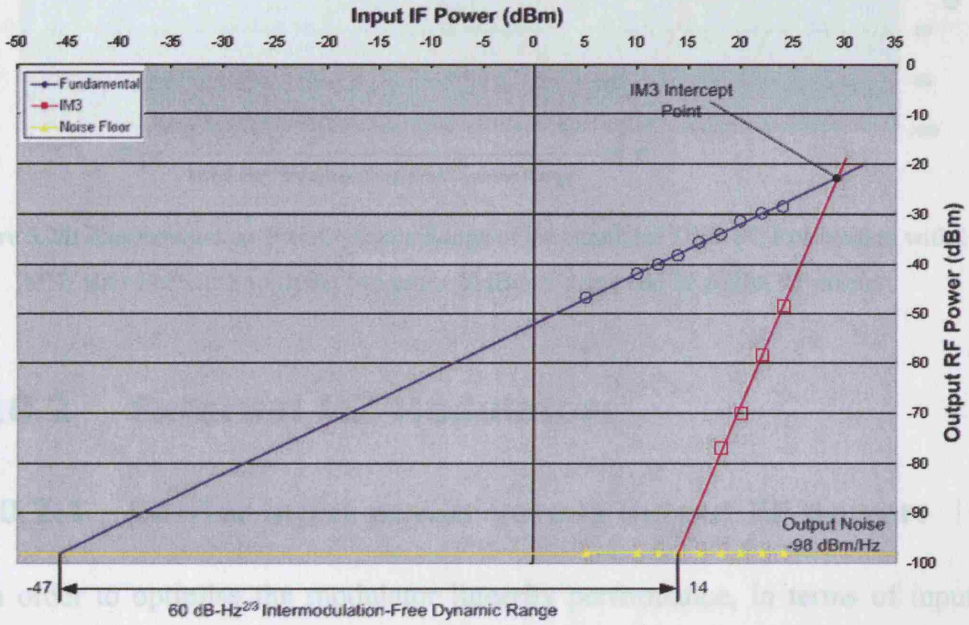

Figure 5.23: Intermodulation-Free Dynamic Range of the simulated DSB-SC RoF system with 6 MHz laser linewidth applying two tones 20dBm IF input and 21.6dBm RF carrier.

Figure (5.24) below, shows the system's intermodulation-free dynamic range using 1 MHz Laser biased at 80mA. The systems setting for this figure and the figure above are identical except the laser linewidth. It can be seen that the laser with 6 MHz linewidth is offers a dynamic range improvement of about 14 dB compared with the system applying laser with 1 MHz linewidth. These results confirm the results of figure (5.22) above that using the higher linewidth laser of 6 MHz will give improvement of the signal to IM3 ratio of about 14 dB.

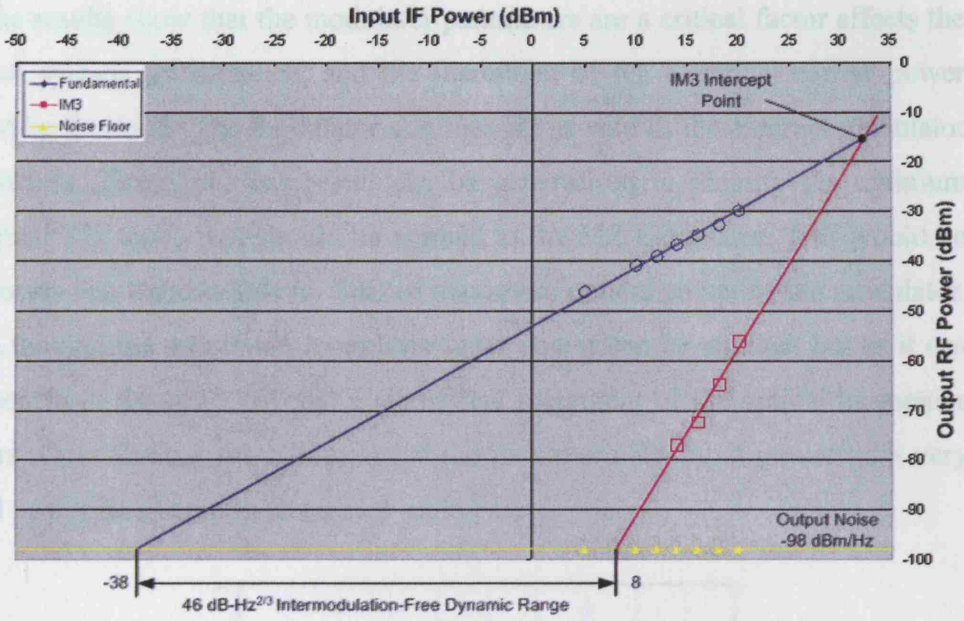

Figure 5.24: Intermodulation-Free Dynamic Range of the simulated DSB-SC RoF system with 1 MHz laser linewidth applying two tones 20dBm IF input and 21.6dBm RF carrier.

5.10.2 External MZ Modulator:

5.10.2.1 Carrier input power versus output RF power:

In order to optimise the modulator linearity performance, in terms of input electrical RF carrier power applied to the modulator, we have to identify the carrier input power corresponds to the maximum modulator's optical output power. For the particular modulator used, we have that the maximum optical output power is 4.86 dBm. Figure (5.25) shows the correlation between the input electrical RF carrier power of the nulled biased used MZ modulator and the optical output power of this modulator. Therefore, half power (-3dB) point for this MZ would be 2.43 dBm, which will correspond to carrier input power of 21.6 dBm. It has been seen that this point is the optimum feeding power can be applied to this modulator before optical output harmonics power grow to be significant, Figure (5.26). Hence, the maximum input power advised to be applied to this modulator is 21.6 dBm, to give an optical output power of 2.43 dBm (-3dB power of the modulator).

The results show that the modulator parameters are a critical factor effects the overall system performance, and the increment of RF electrical carrier power would be limited by the modulator nonlinearity as well as the external modulator parameters. Therefore, this result can be generalised to identify the optimum electrical RF signal that should be applied to the MZ modulator. This would be the power that corresponds to -3dB of maximum optical power of the modulator. Even though, the maximum modulator input power can be applied, but as it can be seen from figure (5.26) that a significant increment of the optical harmonics occurs while feeding the modulator at the maximum RF input power with very small power increment in frequency main bands.

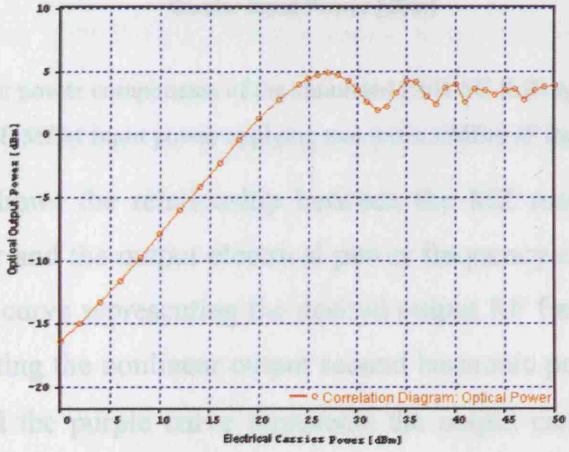

Figure 5.25: Correlation diagram of the input electrical carrier power against the output optical power of the null point biased MZ modulator.

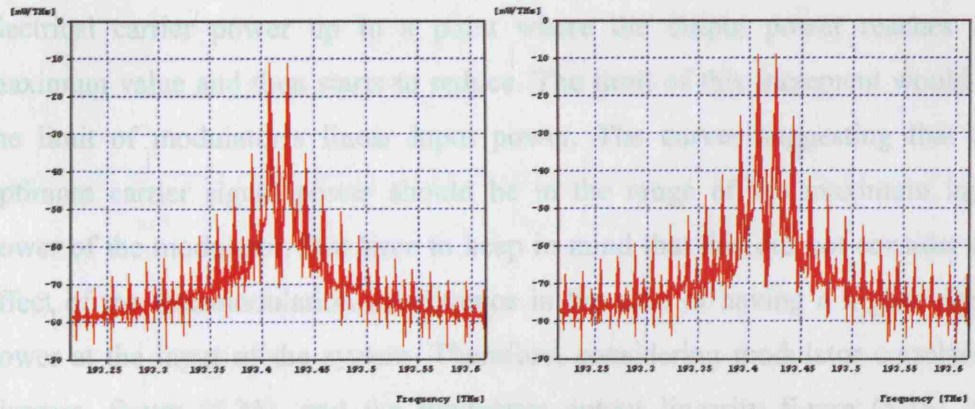

(a) (b)

Figure 5.26: MZ modulator optical spectrum for the simulated DSB-SC RoF system with respect to the RF carrier input power, (a) 21.6 dBm, (b) 26 dBm.

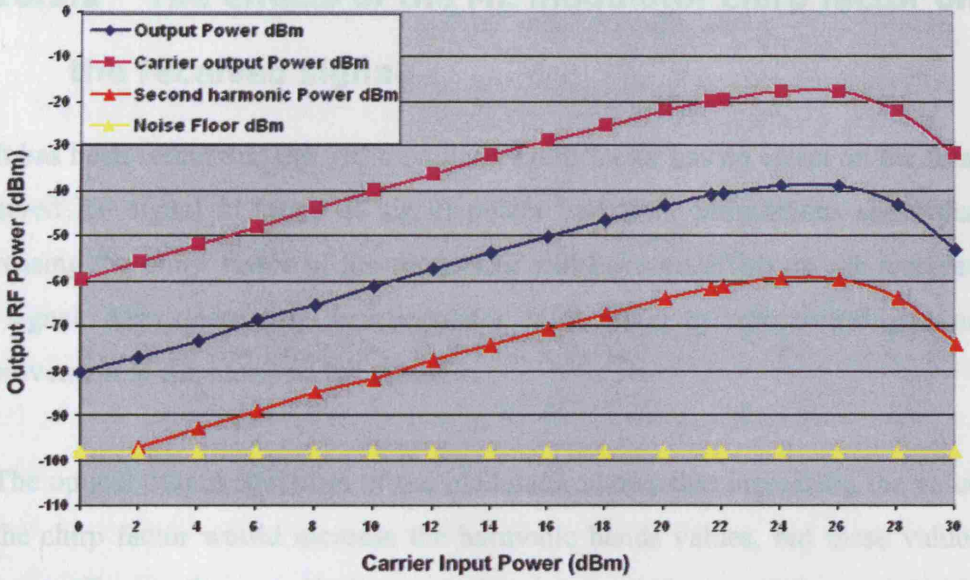

Figure 5.27: RF output power components of the simulated DSB-SC RoF system with respect to the RF MZM Input power applying two tones 10dBm IF input.

Figure (5.27) shows the relationship between the MZ modulator electrical carrier input power and the output electrical power frequency components at the receiver. The blue curve representing the desired output RF frequency while the red curve representing the nonlinear output second harmonic power at frequency of $f_{RF} + 2f_{IF}$, and the purple curve represents the output carrier power at RF frequency. The input signal was a two tone signal with 10 dBm power in each tone, and 80 mA laser biasing current.

The figure shows that the output powers increases linearly with increasing electrical carrier power up to a point where the output power reaches the maximum value and then starts to reduce. The limit of this increment would be the limit of modulator's linear input power. The curves suggesting that the optimum carrier signal power should be in the range of the maximum input power of the modulator. But have to keep in mind that this did not consider the effect of the intermodulation interference in the case of having a higher signal power at the input of the system. Therefore, considering modulator correlation diagram, figure (5.25), and the modulator output linearity figure (5.26), the advisable optimum carrier power would be at half the maximum power of the modulator to avoid modulator's nonlinearity.

5.10.2.2 The effects of the MZ modulator chirp factor on the received signal:

It has been found that the MZ modulator chirp factor has no effect on the final received RF signal in terms of signal power variation. Simulations show that increasing the chirp factor of the modulator will have no effect on the received RF signal. Also decreasing the modulator chirp factor to zero would give no improvement to the received RF signal.

The optical output spectrum of the modulator shows that increasing the value of the chirp factor would increase the harmonic bands values, but these values still not effecting the overall system performance as it is out of the modulation band, as well as the power of these harmonics is very low compared to the main modulation optical bands power. Figure (5.28) shows a two optical spectrum at the output of the MZ modulator with modulator chirp factors of 0 and 0.2 respectively.

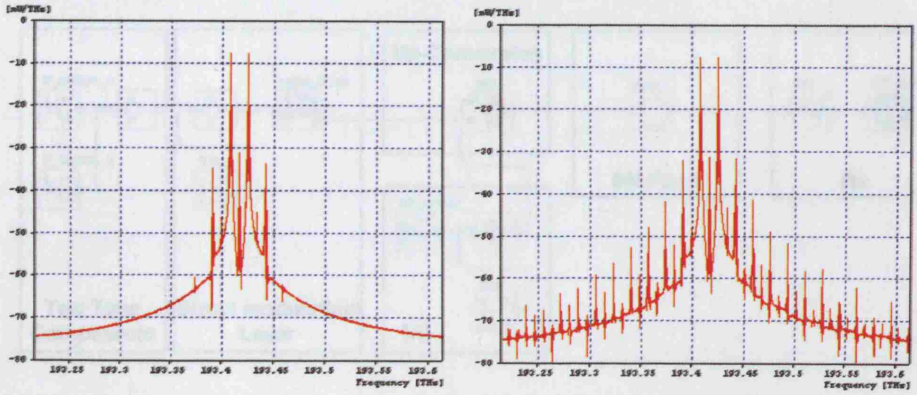

Figure 5.28: MZ modulator optical spectrum for the simulated DSB-SC RoF system with respect to modulator chirp factor, (a) chirp factor = 0, (b) chirp factor = 0.2.

5.11 DSB-SC Performance over Fibre With Respect to Nonlinearity

As the dispersion effect was limited in terms of length-frequency product when using this modulation technique, the system performance limitations will arise from the cumulative effects of noise and distortions from device nonlinearities. In the previous sections we have investigate and analysed the effect of each component of the system in terms of nonlinearity and we specified the dynamic range of the entire system with respect to the IMD effect within the system components and with no optical fibre. In this section we will investigate the effect of adding the SMF optical fibre link in terms of dynamic range limitations taking into account the fibre characteristics as a dispersive and nonlinear propagating medium. The system model used was with same components parameters of figure (5.12), with adding fibre link using the standard Single mode fibre SMF of 0.2 dB/km loss and dispersion parameter D of 16 ps/nm/km. Figure (5.29) shows the system model with adding the SMF link.

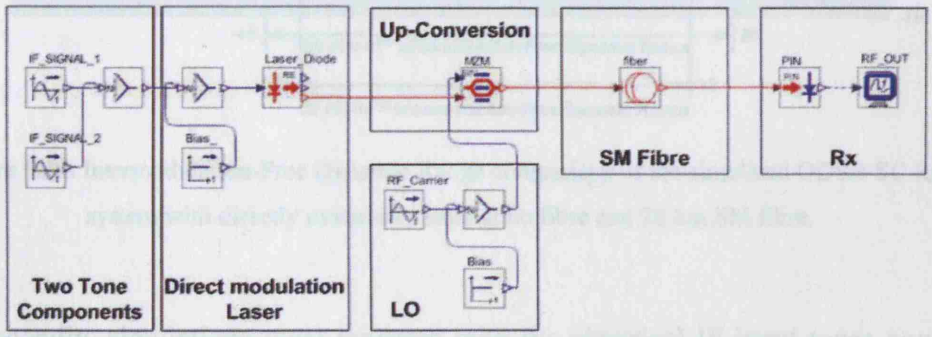

Figure 5.29: OptSim simulation model of the DSB-SC system with single mode fibre.

To investigate the effect of the fibre link to the performance of the system in terms of nonlinearity, a two tone test signal was fed into the system, once with varying input power and fixed fibre length to specify the system's dynamic range with the existence of fibre, and once with fixed input power and varying fibre length to examine the effect of increasing the fibre length in terms of system capability of transforming the two tone signals.

First, optical fibre link of 20 km have been added to the system to compare dynamic range variation when no fibre link existed. Figure (5.30) shows the SFDR of the two systems illustrating the effect of adding fibre to the system. We found that adding 20 km of fibre have reduced the dynamic range of the system with compare to the system have no fibre link. We can see that there is a loss of 13dB-Hz in the system SFDR after adding 20 km fibre, which demonstrates the limitation of fibre length when using narrow multi tones signals.

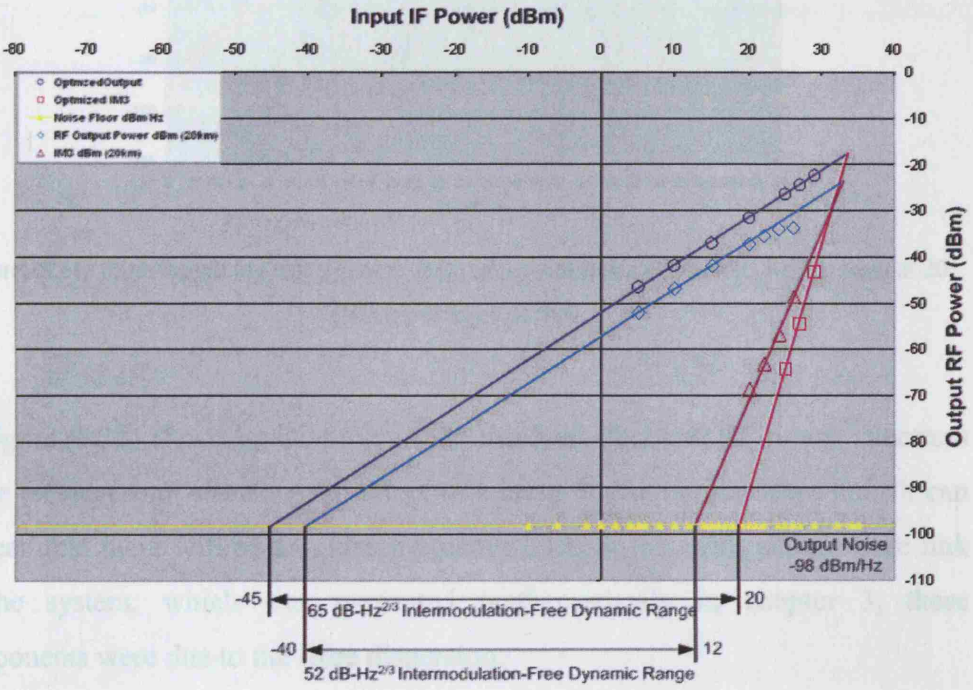

Figure 5.30: Intermodulation-Free Dynamic Range comparison of the simulated ODSB-SC RoF system with directly modulated laser at no fibre and 20 km SM fibre.

Secondly, simulations were repeated with the electrical IF input tones power fixed at +20 dBm to explore the characteristics of the system with increasing the fibre length. The results in figure (5.31) show that increasing the fibre length have a linear slope decreasing effect on the fundamental output tones, and increasing exponential effect on the IM3 with increasing fibre length. Therefore, each km of fibre will decrease the fundamental output power due to the fibre loss and increases the IM3 component power due to fibre dispersion.

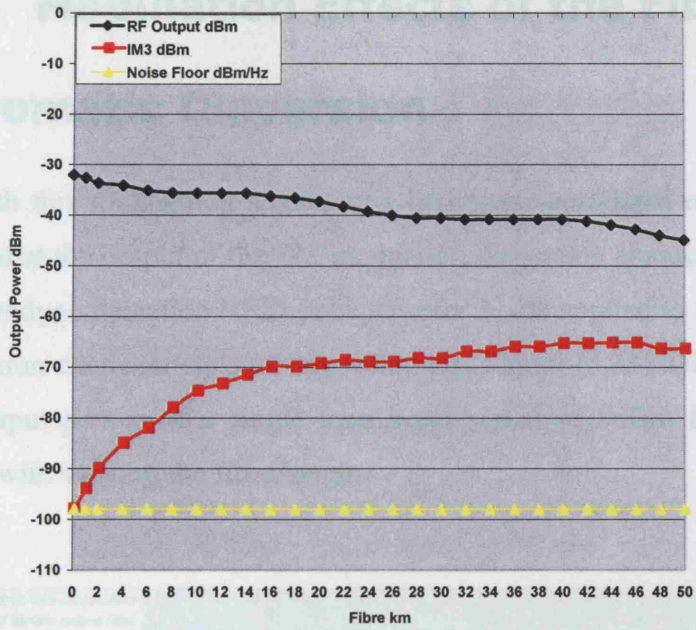

Figure 5.31: Fibre length against signal to IMD of the simulated ODSB-SC RoF system at 20 dBm input tones power.

Figure (5.32) shows an example of the received electrical RF power spectrum at the receiver end, showing the effect of adding 30 km optical fibre link. It can be seen that there will be an extra frequency components with adding fibre link to the system, which was presented mathematically in chapter 3, these components were due to the fibre dispersion.

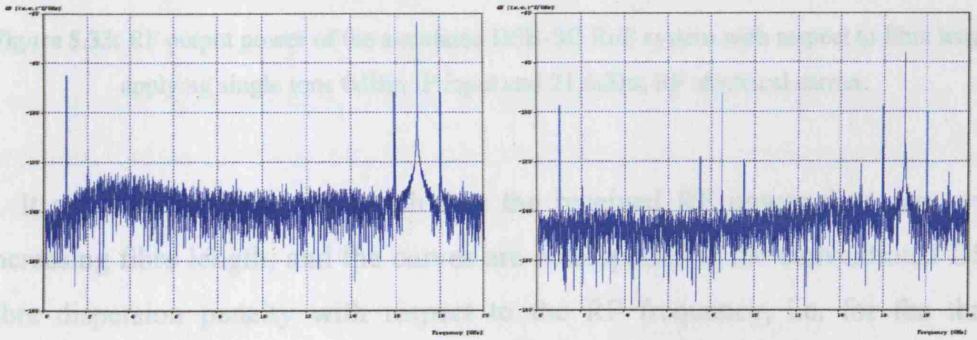

Figure 5.32: Received RF signal spectra with (a) no fibre, and (b) 30km single mode fibre.

5.12 Modulation Effects of the Fibre Chromatic Dispersion

Since with this modulation technique a two phase-correlated optical carriers are generated at the output of the MZ modulator, dispersion characteristics of the remote heterodyne detection RHD links, chapter 3, are applied to the fibre optic links dispersion characteristics of this technique. Figure (5.33) below shows the resulting output power of a single tone input signal of 0dBm for 3 different frequencies with varying the fibre length.

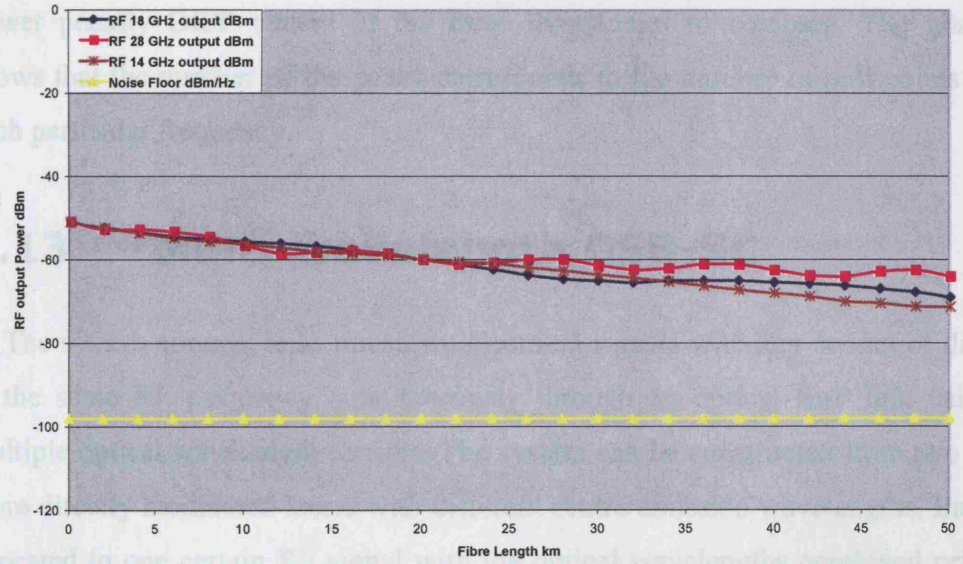

Figure 5.33: RF output power of the simulated DSB-SC RoF system with respect to fibre length applying single tone 0dBm IF input and 21.6dBm RF electrical carrier.

It can be seen from the graph that the received RF power decreases with increasing fibre length, and the curves are corresponds to the conventional DSB fibre dispersion penalty with respect to the RF frequency, i.e. for the three different frequencies, there are three different curve patterns with curve peaks reflecting the number of the power penalty nulls for that frequency of the conventional modulation.

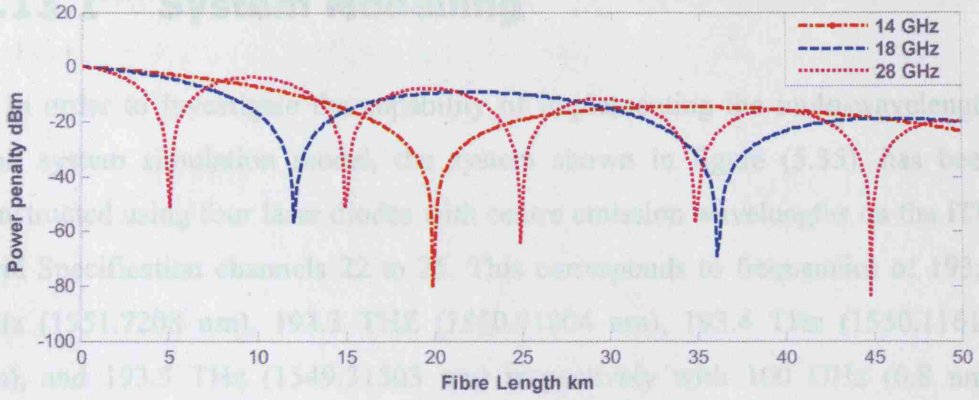

Figure 5.34: Conventional dispersion-induced power penalty DIPP curves.

Figure (5.34) illustrates the normalised conventional dispersion-induced power penalty DIPP curves of the three frequencies to compare. The graph shows that the number of the peaks corresponds to the number of null points of each particular frequency.

5.13 Multi-wavelength DSB-SC

The system concept is to transform electrical signals with any format or data at the same RF frequency simultaneously through an optical RoF link using multiple optical wavelength carriers. The system can be constructed from two or more directly modulated lasers with different centre emission wavelengths. Each allocated to one certain RF signal with the optical wavelengths combined prior the external modulator to be up-converted with one RF electrical carrier. At the receiver side, optical filters needed to separate the wavelengths prior the PIN receivers. Figure (5.35) shows the schematic diagram of multi-wavelength RoF system.

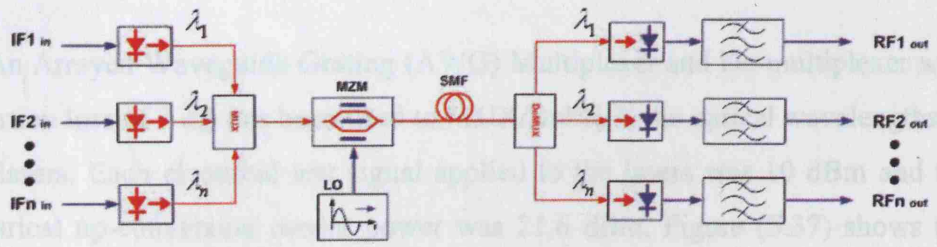

Figure 5.35: Schematic diagram of the multi-wavelength DSB-SC using up-converted DM laser.

5.13.1 System Modelling

In order to investigate the capability of implementing the multi-wavelength RoF system simulation model, the system shown in figure (5.35), has been constructed using four laser diodes with centre emission wavelengths on the ITU Grid Specification channels 22 to 25. This corresponds to frequencies of 193.2 THz (1551.7208 nm), 193.3 THZ (1550.91804 nm), 193.4 THz (1550.11612 nm), and 193.5 THz (1549.31503 nm) respectively with 100 GHz (0.8 nm) channel spacing. A two tone test was performed for the system with four symmetric signals with tones of 1 GHz and 1.05 GHz (50 MHz spacing) applied to the lasers biased with 150 mA. The up-conversion carrier power was 21.6 dBm at $f = 8.5\ GHz = f_{mm}/2$.

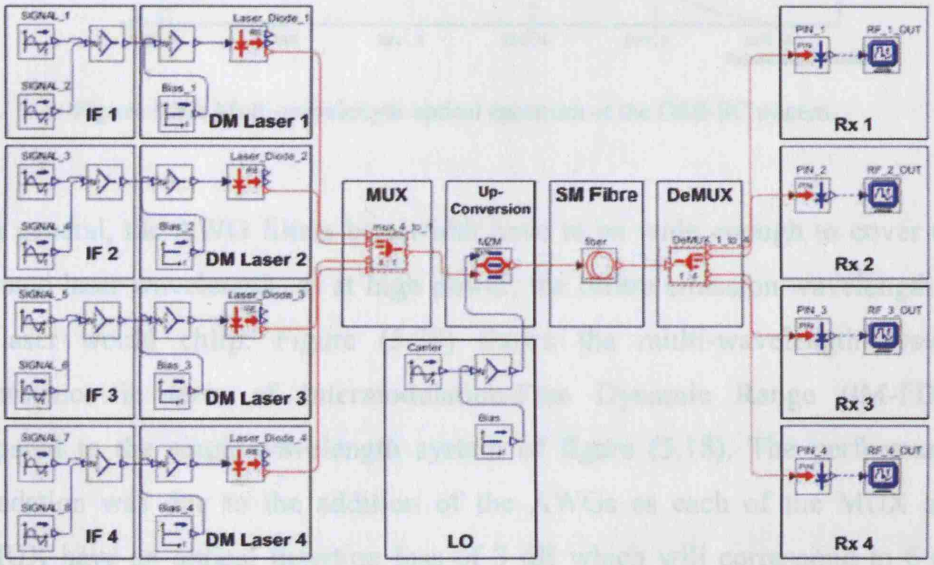

Figure 5.36: OptSim simulation model of the ITU Grid Specification channels multi-wavelength ODSB-SC using up-converted DM laser.

An Arrayed Waveguide Grating (AWG) Multiplexer and De-multiplexer with insertion loss of 3 dB has been used to MUX/DeMUX the optical wavelengths of the lasers. Each electrical test signal applied to the lasers was 10 dBm and the electrical up-conversion carrier power was 21.6 dBm. Figure (5.37) shows the multi-wavelength optical spectrum. The AWG comprises raised cosine filters

with a bandwidth of 100 GHz which were set up to optimise the AWG's performance in terms of the filters roll-off factor.

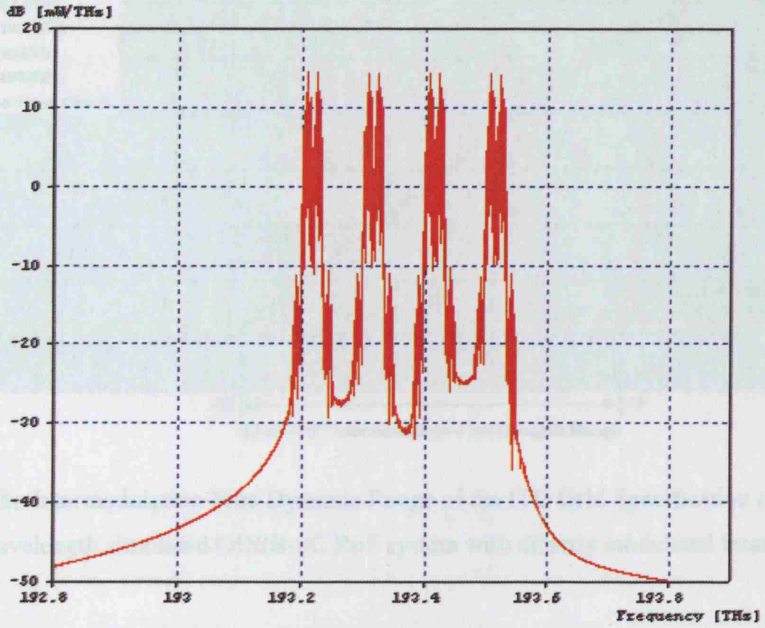

Figure 5.37: Multi-wavelength optical spectrum of the DSB-SC system.

In general, the AWG filters bandwidth have to be wide enough to cover the allocated laser wavelength, as at high power, the centre emission wavelength of the laser would chirp. Figure (5.38) shows the multi-wavelength system performance in term of Intermodulation-Free Dynamic Range (IM-FDR) compared to the single-wavelength system of figure (5.18). The performance degradation was due to the addition of the AWGs as each of the MUX and DeMUX have an optical insertion loss of 3 dB which will correspond to 6 dB electrical loss.

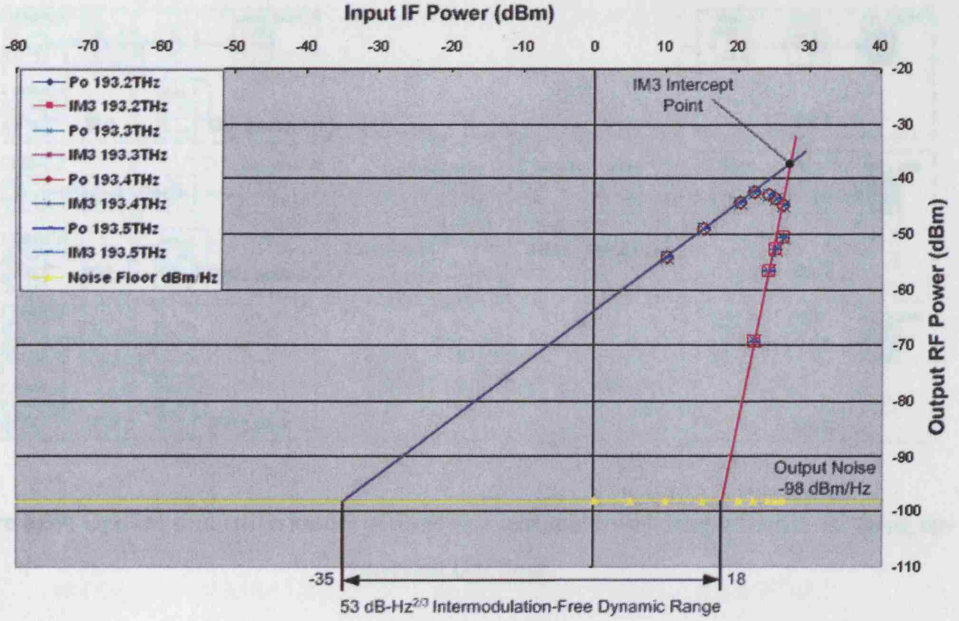

Figure 5.38: The Intermodulation-Free Dynamic Range of the ITU Grid Specification channels multi-wavelength simulated ODSB-SC RoF system with directly modulated laser.

Results shows, figure (5.38), that the multi-wavelength system channels have an Inter-modulation free dynamic range of 53dB-$Hz^{2/3}$ and third-order Inter-modulation intercept point IM3 of -37dBm. Therefore, this system is shown to perform as well as the single-wavelength system despite the optical power loss due to the AWG MUX/DeMUX.

5.13.2 Effect of MUX/DeMUX insertion loss:

A second multi-wavelength system has been constructed with three lasers at wavelengths of 1549 nm, 1550 nm, and 1551 nm with biasing current of 50 mA and electrical carrier power of 21.6 dBm, in order to verify the ability of the multi-wavelength system to match the performance of single-wavelength system, replacing the AWG's with an optical combiner at the modulator input side, and optical combiner with three optical filters at the receiver side. The losses of these components were ignored.

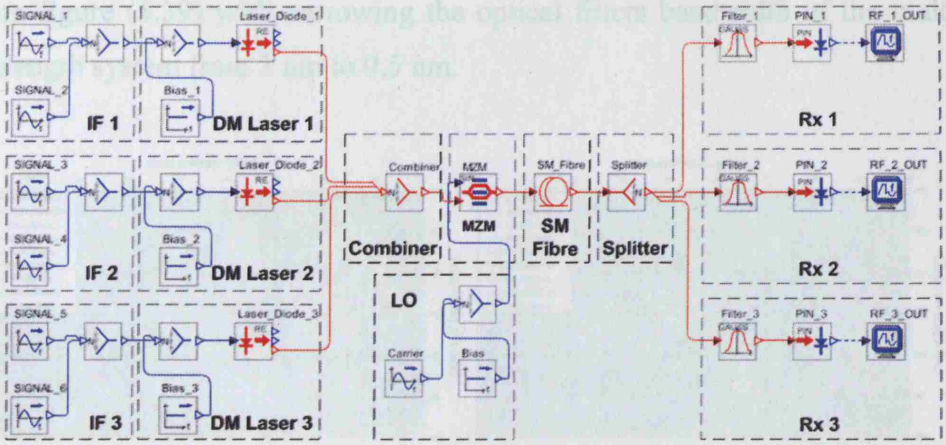

Figure 5.39: OptSim simulation model of three channels multi-wavelength ODSB-SC using up-converted DM laser.

Results of figure (5.40-a) shows that it is possible to achieve a very good matching in terms of linearity performance of a multi-wavelength system against the single wavelength system of similar characteristics using ideal combiner and splitter with no insertion loss. This figure illustrates the output power of the fundamental tones and the third order inter-modulation distortion of the single-wavelength system, alongside with each wavelength output power of the fundamental tones, and the third order inter-modulation distortion of the multi-wavelength system, using optical filters with bandwidth of 1 nm.

5.13.3 Filter bandwidth effect on system performance:

The centre light emission wavelength of the laser will chirp when input electrical power is applied to the laser, and especially when it reaches power values at the nonlinear region of the laser. Therefore, the system performance will be sensitive to the optical filtering process. If the filter bandwidth is too narrow to pass the required frequency band, it will degrade the system performance in terms of nonlinearity against the single tone system performance as the centre wavelength will goes out of the filter tune with increasing the power. Figure (5.40-b) shows a repeated system performance of the previous

system figure (5.39) with narrowing the optical filters bandwidth of the multi-wavelength system from 1 nm to 0.5 nm.

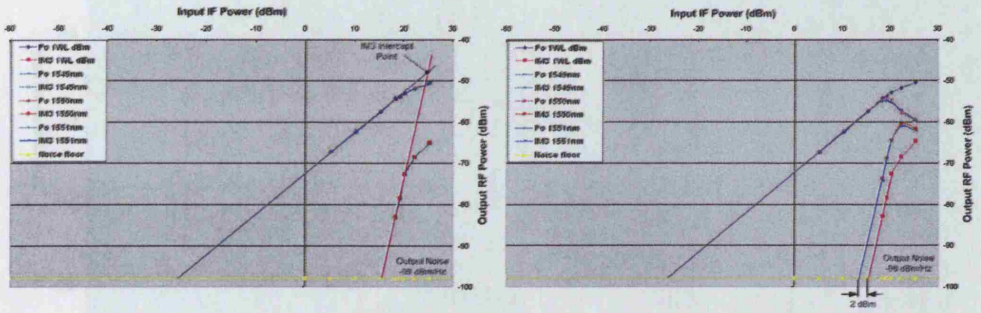

(a) (b)

Figure 5.40: Intermodulation-Free Dynamic Range comparison of the three channels multi-wavelength simulated ODSB-SC RoF system with directly modulated laser.

Figure (5.40-b) shows that the fundamental tones power was not changed while IM3 tones values have increased with respect to the same points when using 1 nm bandwidth filters causing 2 dBm degradation at the system dynamic range. Also the figure shows changes at the higher power performance readings occur as the light wavelength emission centre of the laser goes out of filters tune due to the chirping at higher power values.

5.14 Multi-wavelength DSB-SC with Fibre link

In order to investigate the performance of the multi-wavelength systems with the existence of the optic fibre link, the same system of figure (5.36), with four laser diodes at centre emission wavelengths of the ITU Grid Specification channels 22 to 25, corresponds to frequencies of 193.2, 193.3, 193.4, and 193.5 THz respectively with 100 GHz (0.8 nm) channel spacing, have been simulated with adding the standard single-mode fibre link. Single tones were applied to the system input with four symmetric signals of 1 GHz of 10dBm applied to the lasers biased with 150 mA, and electrical carrier power of 21.6 dBm with $f = 8.5\ GHz = f_c / 2$ has been applied.

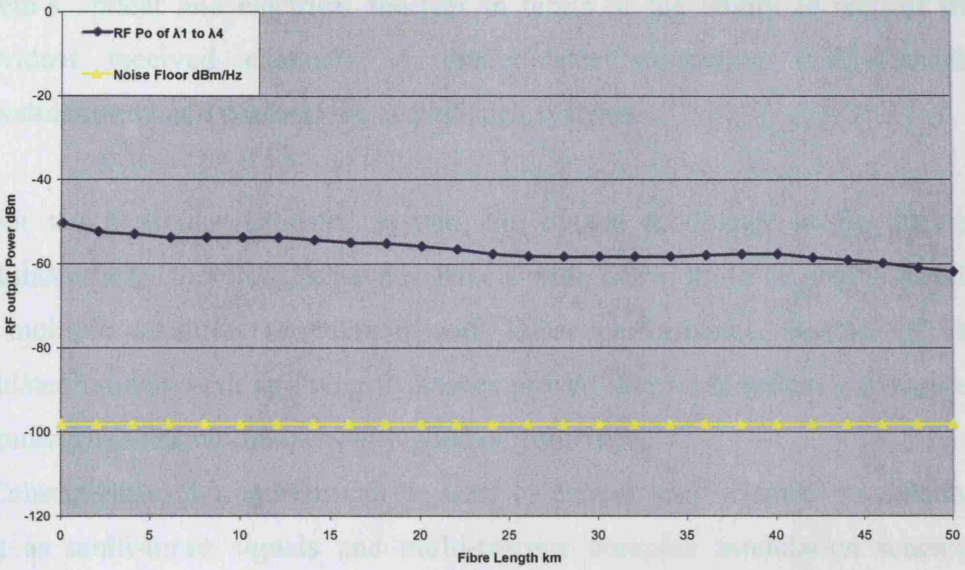

Figure 5.41: RF output power of the ITU Grid Specification channels multi-wavelength ODSB-SC With respect to fibre length applying 10dBm IF input and 21.6dBm RF carrier.

Figure (5.41) shows the RF output power curve of the system at 18 GHz at wavelengths of 1550.2, 1550.3, 1550.4, and 1550.5 nm. Result shows that the system output is very similar to the output curve of the single-wavelength system output, figure (5.19), except that there is an excess loss with this system due to the usage of the AWG MUX/DeMUX.

5.15 Multi-channel DSB-SC System

The generic principle of the multi-channel systems is to propagate two or more channels over the system link. The propagated channels have to be frequency separated to be possible to recover each single channel with no interference.

The case with the RoF, the optical fibre is used to deliver the electrical signals by optical means. As the fibre can offer a large bandwidth, there will not be a problem in terms of the bandwidth within the fibre link. Therefore, the system performance will be mainly dependant on the performance the electrical and optical modulation in terms of channel spacing and the optical modulator ability of accepting multi-channel input signals. At the other end, the performance of the

system's optical and electrical receiver in terms of the ability to recover the individual received channels. A demodulator supporting multi-channels demodulation would perform the task of such systems.

For the particular DSB-SC system, the optical modulator is the directly modulated laser, therefore, it have to have a wide linewidth to be able to handle the multiple channels modulation with linear performance. Results of the simulated models with applying two tones proved that such system can support the multi-channels modulation with good performance.

Consequently, this system can be used to deliver multi-channel modulation such as multi-tones signals and multi-carriers complex modulation schemes including OFDM signal.

5.16 Conclusion

In this chapter we have presented a comprehensive Inter-Modulation Distortion (IMD) study for RoF systems applying three different dispersion tolerant modulation techniques, and considering all the nonlinear contributions of both optical and electrical components. The Intermodulation-Free Dynamic Ranges of the systems were demonstrated to outline a performance measurement of systems linearity, verifying the range between the noise level at the specified bandwidths and the maximum input signals that produces no third-order intermodulation.

Compared to other modulation schemes, the IM-DD represents a simple technique to deliver RoF signals. Apart from the conventional DSB modulation, there are a number of modulation techniques that can be used for delivering the modulated mm-wave signals over the optical link of SMF with minimal dispersion frequency-length limitations. Although this dispersion effect has been mitigated, dispersion can still impact on the modulation.

As the effect of the fibre chromatic dispersion were limited using these modulation techniques, the system performance limitations will be arising from the cumulative effect of noise and distortions of devices nonlinearities. In this chapter we have investigated and analysed the effect of the IMD of RoF systems, applying dispersion tolerant modulation techniques of interest, to specify the systems limitations in terms of nonlinearity in such links.

System modelling with OptSim platform had been presented for this research supported by experimental set up to justify the devices modelling. It was found that the first nonlinear device facing the input signal would be having the dominant nonlinearity effect of the overall system performance, therefore, the system constructed from devices with low nonlinearity parameters, and the ability to handle high input power, will be having the higher dynamic range.

It has been shown that the DSB-SC system applying direct modulation laser can offer a dynamic range competitive to the other examined techniques, if the directly modulated laser and electrical carrier biasing are optimised. In addition, the direct modulation DSB-SC technique has a unique capability of transporting multi-wavelengths optical signals and multi-channels electrical signals, as well as it have the advantage of using oscillator frequency of one half the required RF carrier frequency. This lead can be a very useful parameter at particular cases when high carrier frequencies are required for delivering the RoF signals.

Chapter 6

RF QAM-OFDM over Fibre

This chapter is discussing the performance of RF modulated OFDM signal over optical systems. After this introduction section, the concept of Orthogonal Frequency Division Multiplexing (OFDM) is discussed with listing the advantages and disadvantages of this modulation, whereas later section is allocated to discuss the characteristics and the principle of operation of the OFDM signal. Moreover, a mathematical presentation of OFDM is carried out to identify the aspects of the modulation scheme. Then after, OFDM transmitter and receiver structure are discussed and demonstrated, followed by a detailed results of the RF OFDM signals generated by simulation models constructed using Matlab Simulink tool. The performance of the OFDM over optical links particularly over the DSB-SC optical system is then investigated and demonstrated extensively. The important results and conclusion are presented at the end of this chapter.

6.1 Orthogonal Frequency Division Multiplexing (OFDM)

OFDM is a digital multi-carrier modulation scheme, which uses a large number of closely-spaced, narrow bandwidth sub-carriers, simultaneously transmitted over the radio channel [83-85]. Each sub-carrier is modulated with a conventional modulation scheme (such as BPSK, QPSK, QAM modulation) at a low symbol rate, maintaining data rates similar to conventional single-carrier modulation schemes in the same bandwidth forming a block of spectrum. The frequency spacing and time synchronization of the sub-carriers is chosen to position sub-carriers orthogonally, which mean that sub-carriers do not cause interference to each other even when overlapping in the frequency domain.

OFDM is similar to Frequency Division Multiplexing (FDM), where multiple messages are transmitted over a single radio channel. However, OFDM is in much more controlled manner allowing spectral efficiency improvement due to sub-carriers orthogonality. With OFDM modulation, all sub-carriers need to be synchronised to each other, restricting the modulation to digital symbol based scheme which can be represented as a large number of low bit rate carriers transmitting in parallel. The 'sub-carriers' commonly refers to these low bit rate carriers forming a single transmission OFDM spectrum, while the term 'carrier' refers to describe the RF carrier mixing the OFDM signal to up-convert from base band.

The primary advantage of OFDM over single-carrier schemes is its ability to cope with severe channel conditions, for example, attenuation of high frequencies at a long copper wire, narrowband interference [86] and frequency-selective fading due to multipath without complex equalization filters [86;87]. Channel equalization is simplified because OFDM may be viewed as using many slowly-modulated narrowband signals rather than one rapidly-modulated wideband signal. Low symbol rate makes the use of a guard interval between symbols affordable, making it possible to handle time-spreading and eliminate inter-symbol interference (ISI).

OFDM scheme development originally started in the late 1950's [88] with the introduction of FDM for data communication to transmit information on multiple carriers. In 1966 Chang patented the structure of OFDM [89] and published the concept of using orthogonal overlapping multi-tone signals for data communications [90]. In 1971 Weinstein [91] introduced the idea of using a Discrete Fourier Transform (DTF) for the generation and reception of OFDM signals, eliminating the requirement for the high number of analogue sub-carrier oscillators. This simplifies OFDM implementation with the use of Fast Fourier Transforms (FFT) as an efficient implementation of the DFT, and it made OFDM deployment cost effective. Although the principles and some of the benefits have been known since the 1960s, OFDM is popular for wideband communications today by way of low-cost digital signal processing components that can efficiently calculate the FFT. Development of OFDM for commercial use was started in the late of 1980's with the introduction of Digital Audio Broadcasting (DAB) systems. In 1990's and early 2000's, OFDM has developed into a popular scheme for wideband digital communication systems. Examples of applications are:

- ADSL and VDSL broadband access via POTS copper wiring.
- Certain Wi-Fi (IEEE 802.11a/g) Wireless LANs.
- DAB systems EUREKA 147, Digital Radio Mondiale, HD Radio, T-DMB and ISDB-TSB.
- MediaFLO (Forward Link Only) Mobile TV/Broadband Multicast technology.
- DVB terrestrial digital TV systems DVB-T, DVB-H, T-DMB and ISDB-T.
- IEEE 802.16 or WiMAX Wireless MANs.
- IEEE 802.20 or Mobile Broadband Wireless Access (MBWA) systems.
- Flash-OFDM cellular systems.
- The WiMedia Alliance's Ultra wideband (UWB) implementation.
- Power line communication (PLC).
- MoCA home networking.

- Optical fibre communications and Radio over Fibre systems (RoF).
- Candidate for IEEE 802.15.3a standard for wireless PAN (MB-OFDM).
- Candidate for IEEE 802.11n standard for next generation wireless LAN
- Candidate for 3.75G mobile cellular standards (3GPP & 3GPP2 Long Term Evolution) named High Speed OFDM Packet Access (HSOPA)
- Candidate for 4G standards (CJK)

6.1.1 OFDM Advantages

- High data rate transmission due to parallel multi carriers data transmission
- Robust against Inter-Symbol Interference (ISI) with minimal SNR loss
- Robust against Inter-Carrier Interference (ICI) and fading caused by multipath propagation
- High spectral efficiency
- Efficient implementation using FFT
- Low sensitivity to time synchronization errors

6.1.2 OFDM Disadvantages

- Sensitive to Doppler shift.
- Sensitive to frequency synchronization problems.
- Inefficient transmitter power consumption, due to linear power amplifier requirement. (High peak-to-average-power ratio (PAPR)).

6.2 OFDM Characteristics and Principles of Operation

6.2.1 Orthogonality

In OFDM, the sub-carrier frequencies are chosen so that the sub-carriers are orthogonal to each other, meaning that inter-carrier guard bands are not required for transmitting sub-carriers over a common channel and detecting without cross-talk [84]. This greatly simplifies the design of both the transmitter and the receiver, unlike conventional FDM, where a separate filter for each sub-channel is required. Signals named to be orthogonal if they are equally independent to each other. The orthogonality also allows high spectral efficiency, sub-carriers in an OFDM signal are spaced as close as is theoretically possible, near the Nyquist rate, while maintain orthogonality between them, so almost the whole available frequency band can be utilised.

The orthogonality allows for efficient modulator and demodulator implementation using the FFT algorithm. OFDM achieves orthogonality in the frequency domain by allocating each of the separate information signals onto different sub-carrier. Therefore, OFDM signals are made up from a sum of sinusoids, each corresponding to a sub-carrier. The baseband frequency of each sub-carrier is chosen to be an integer multiple of the inverse of the symbol time, resulting in all sub-carriers having an integer number of cycles per symbol. As a consequence the sub-carriers are orthogonal to each other. Figure (6.1) illustrates a five sub-carriers OFDM signal structure.

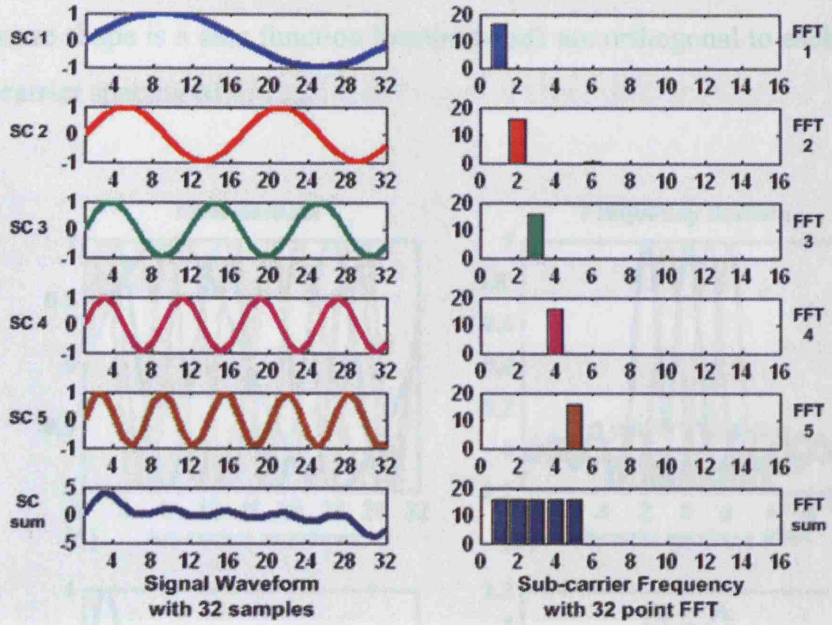

Figure 6.1: OFDM signal construction in time domain.

The first part of figure (6.1) shows the individual sub-carriers sine waveforms, with the last window showing the summation of the waveforms. The first sub-carrier has one cycle per symbol, next sub-carriers cycles each increase by one cycle per symbol. All sub-carriers have to be in phase, and each has to have an integer number of cycles per symbol to make it cyclic and to maintain orthogonality. The second part of figure (6.1) shows the FFT location of each individual time waveform respectively, with the last window showing the FFT summation of all signals. Two sub-carriers are said to be orthogonal to each other, equation (6.1), if their multiplication is integrated over a symbol period T, and gives a result of zero [92].

$$\int_0^T X_{k_1}(t)\, X_{k_2}(t)\, dt = \begin{cases} C & k_1 = k_2 \\ 0 & k_1 \neq k_2 \end{cases} \quad \ldots (6.1)$$

Figure (6.2) illustrates the time and frequency response of a five sub-carriers OFDM signal. The first part of figure (6.2) shows the five sub-carriers sinusoid waveforms in time domain with (6.2 c) showing their summation. The corresponding frequency domain representation of the baseband OFDM signal response is shown in the second part of this figure (6.2 b) with the spectrum of

individual sub-carriers and (6.2 d) showing their summation. Each sub-carrier response shape is a sinc function located which are orthogonal to each other with sub-carrier spacing of $1/T_{FFT}$.

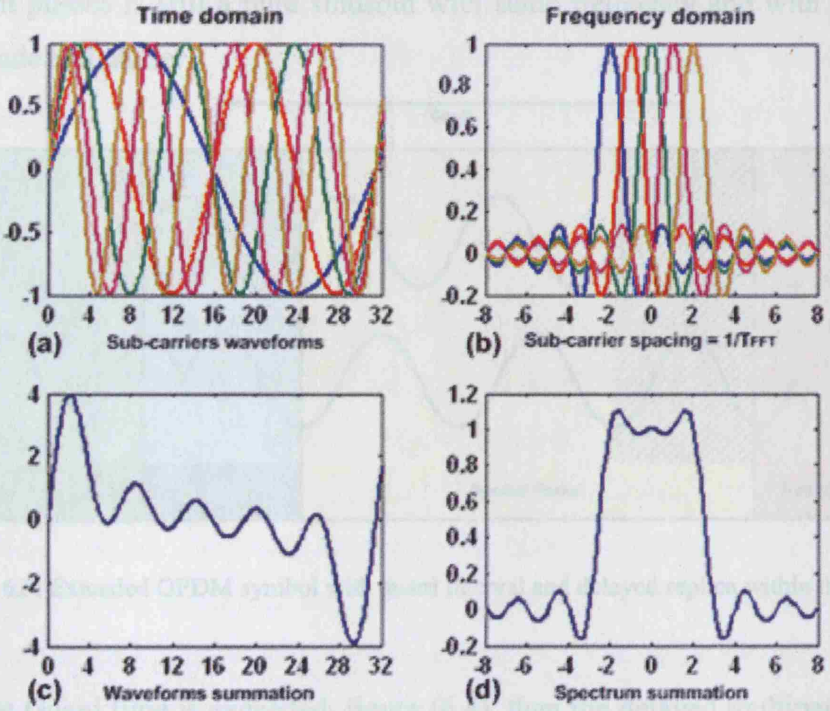

Figure 6.2: OFDM signal structure in time and frequency domain.

6.2.2 Guard interval and cyclic prefix

One advantage of OFDM signalling is that it is a combination of low symbol rate sub-carriers, which in turn provide a longer symbol period in comparison with high symbol rate, single carrier modulation. This makes OFDM more tolerant to multipath Inter-Symbol Interference (ISI) due to proportionally long symbol duration period. Moreover, since that the symbol duration is long, this makes it possible to insert a guard interval between the OFDM symbols in order to eliminate ISI [93]. The cyclic prefix, which is transmitted during the guard interval, is a repetition of the bits that form the end part of the symbol, used to avoid reception problems when receiving multi-path radio signal. The guard interval is transmitted followed by the OFDM symbol. Figure (6.3) shows an example of OFDM symbol with guard interval and a multipath delayed replica

located within the period of the guard interval time. In this case, a delayed multipath replica does not affect the orthogonality behaviour of the sub-carrier in frequency domain. There are still spectral nulls at other sub-carrier frequencies. This can explained by that the sum of two sinusoids with same frequency but in different phases is still a pure sinusoid with same frequency and with resultant magnitude and phase.

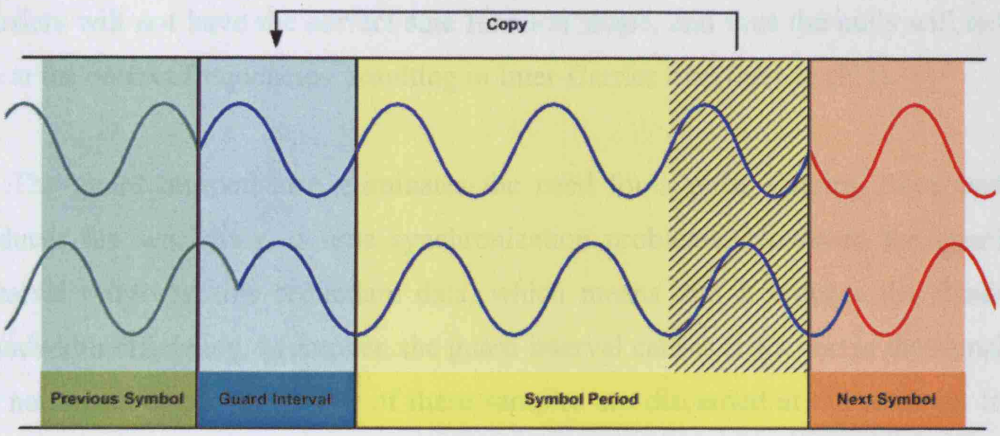

Figure 6.3: Extended OFDM symbol with guard interval and delayed replica within the period.

If the Guard time is exceeded, figure (6.4), then the delayed multipath replica will affect the orthogonality behaviour of the sub-carriers in frequency domain and resultants are no longer pure sinusoids. Therefore, there will be no more spectral nulls at other sub-carrier frequencies as the sum of signals is no longer a sinusoid. This will alter sub-carriers orthogonality and cause Inter-Carrier Interference (ICI).

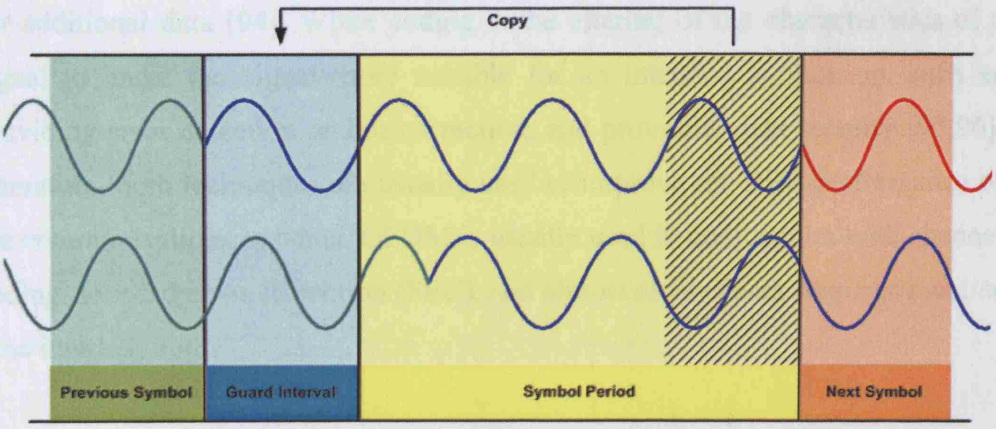

Figure 6.4: Extended OFDM symbol with guard interval and delayed replica exceeding the period.

The reason that the guard interval consists of a copy of the end of the OFDM symbol is so that the receiver will integrate over an integer number of sinusoid cycles, resulting in a smooth and continuous signal for each of the multipaths when performs OFDM demodulation with the FFT. Consequently, the amplitude and phase remain constant over the symbol period for each sub-carrier in order to maintain the sub-carriers orthogonality. Otherwise, the spectral shape of sub-carriers will not have the correct sinc function shape, and thus the nulls will not be at the correct frequencies, resulting in Inter-Carrier Interference (ICI).

The guard interval also eliminates the need for a pulse-shaping filter, and reduces the sensitivity to time synchronization problems. However, the guard interval only contains redundant data, which means that it reduces the signal bandwidth efficiency. Moreover, the guard interval causes reduction in the signal to noise ratio since the power of these samples are discarded at the receiver. In our model systems, we will not need to include the cyclic prefix bits in our generated OFDM signal, as we are working with a back to back systems and optical fibre links. Therefore, no multi-path interference would be existed.

6.2.3 Channel coding and interleaving

Forward Error Correction (FEC) is a system of error control for data transmission, whereby the sender adds *redundant data* to its message, which allows the receiver to detect and correct errors without the need to ask the sender for additional data [94], While coding is the altering of the characteristics of a signal to make the signal more suitable for an intended application, such as providing error detection and/or correction, and providing data security [95;96]. Therefore, both techniques are usually used to improve the BER performance of the communications systems. OFDM is usually used in conjunction with channel coding, forward error correction (FEC), and almost always uses frequency and/or time interleaving.

Frequency sub-carrier interleaving increases resistance to frequency-selective channel conditions such as fading. For example, when a part of the channel bandwidth is faded, frequency interleaving ensures that the bit errors that would

result from those sub-carriers in the faded part of the bandwidth are spread out in the bit stream rather than being concentrated. Similarly, time interleaving ensures that bits that are originally close together in the bit stream are transmitted far apart in time, thus mitigating against severe fading as would happen when transmitting at high speed.

The reason why interleaving is used on OFDM is to attempt to spread the errors out in the bit stream that is presented to the error correction decoder, because when such decoders are presented with a high concentration of errors the decoder is unable to correct all the bit errors, and a burst of uncorrected errors occurs [97]. A common type of error correction coding used with OFDM-based systems is convolutional coding, which is often concatenated with Reed-Solomon coding [98]. In our modelling systems and in order to use the generated OFDM signals as a reference in terms of BER, OFDM models will not include the FEC or any coding technique in our signals as the systems performance would be examined with respect to the reference BER of the systems with no optical links. The performance measurements in turn will reflect the effects of optical links with compare to reference BER signals performance.

6.2.4 Pilot sub-carriers

Pilot sub-carriers are usually a single frequency carriers transmitted over a communication system for supervising, control, equalization, continuity, and synchronisation [99], or for reference purposes [100;101]. The pilot carriers are redundant symbols with specific pattern arrangement and carry no useful data information. Pilot sub-carriers contain signal values that are known for the receiver in order to estimate the received OFDM signal frequency response. Thus, pilot signals are used in the receiver for correcting the magnitude and phase shift offsets of the received symbols. An example of pilot arrangement is the IEEE 802.11a/g standard. It consist 52 sub-carriers, 48 are data sub-carriers, 4 pilot sub-carriers, and a null at the centre carrier. Also the IEEE 802.16a WiMAX standard consists of 200 sub-carriers, 192 are data sub-carriers, and 8 pilot sub-carriers. With our systems models, synchronisation will be always controlled for the transmitted bits streams. Therefore, there will not be any

difference in system's performance if the OFDM ware included the pilots signal or transmitted with no pilots signal.

6.3 Mathematical Representation

In order to represent the OFDM signal analytically as a multi-carrier signal, assuming N sub-carriers are used to form the signal, and each sub-carrier is modulated using M alternative symbols, the OFDM symbol would consist of M^N combined symbols. The baseband OFDM signal can be expressed as [92]:

$$S(t) = \sum_{k=0}^{N-1} X_k e^{j2\pi\, k\, t/T} \quad , \quad 0 \le t < T \qquad \ldots (6.2)$$

where X_k are the data symbols, N is the number of sub-carriers, and T is the OFDM symbol time. The sub-carrier spacing of $1/T_{FFT}$ makes each sub-carrier orthogonal over each symbol period. This can be expressed as [92]:

$$\frac{1}{T}\int_0^T \left(e^{j2\pi\, k_1\, t/T}\right)^* \left(e^{j2\pi\, k_2\, t/T}\right) dt \qquad \ldots (6.3)$$

$$= \frac{1}{T}\int_0^T e^{j2\pi\,(k_2 - k_1)\, t/T}\, dt = \begin{cases} 1 \ , & k_1 = k_2 \\ 0 \ , & k_1 \neq k_2 \end{cases} \qquad \ldots (6.4)$$

where $(\cdot)^*$ denotes the complex conjugate operator. Equation (6.4) confirms the assumption of equation (6.1) of orthogonality. It can be seen that the sub-carriers would be orthogonal as long as this condition applied, otherwise, sub-carriers will interfered and Inter-Symbol Interference (ISI) would occur.

6.4 OFDM Transmitter

An OFDM signal can be defined as the sum of a number of orthogonal sub-carriers, modulated with baseband data on each sub-carrier using some type of digital modulation [102;103]. This composite baseband signal is normally used

to modulate a main RF carrier. OFDM signals are typically generated digitally due to the difficulty in creating large banks of phase lock oscillators and receivers in the analogue domain. Figure (6.5) illustrates the block diagram of a typical OFDM transmitter.

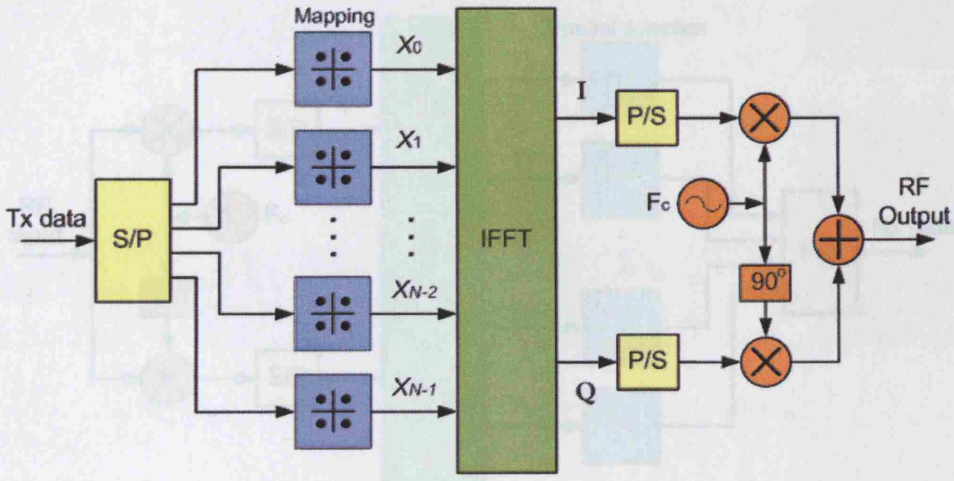

Figure 6.5: Typical OFDM transmitter block diagram.

The *Tx* data is a serial stream of binary bits. These bits are de-multiplexed into *N* parallel streams using a serial to parallel converter (S/P) to be mapped into symbol streams using a form of complex constellation modulation (e.g. QPSK, QAM). Then, an Inverse Fast Fourier Transform (IFFT) is computed on each set of symbols to give a set of complex samples in time domain. These samples are then multiplexed into serial sets of In-phase (I) and Quadreture-phase (Q) samples using a parallel to serial converters (P/S), which combine to give a baseband OFDM signal. Then these two signal sets are used to modulate cosine and sine waves respectively at the carrier frequency F_C, to give an output RF frequency OFDM signal. A transmitted RF signal is always a real signal as it is just a variation in field intensity.

6.5 OFDM Receiver

The OFDM receiver, figure (6.6), functions in reverse manner compared to the transmitter so as to recover the data signal [104-106]. It picks up the RF OFDM input signal, which is then multiplied with an in phase complex carrier to give a baseband OFDM signal, then the Fast Fourier Transform (FFT) is used to

compute the signal in frequency domain. The output symbol streams are then de-mapped to give N parallel binary digits streams. These digits are then multiplexed and recombined to form a serial stream of binary data Rx, which is an estimate of the transmitted original binary data stream.

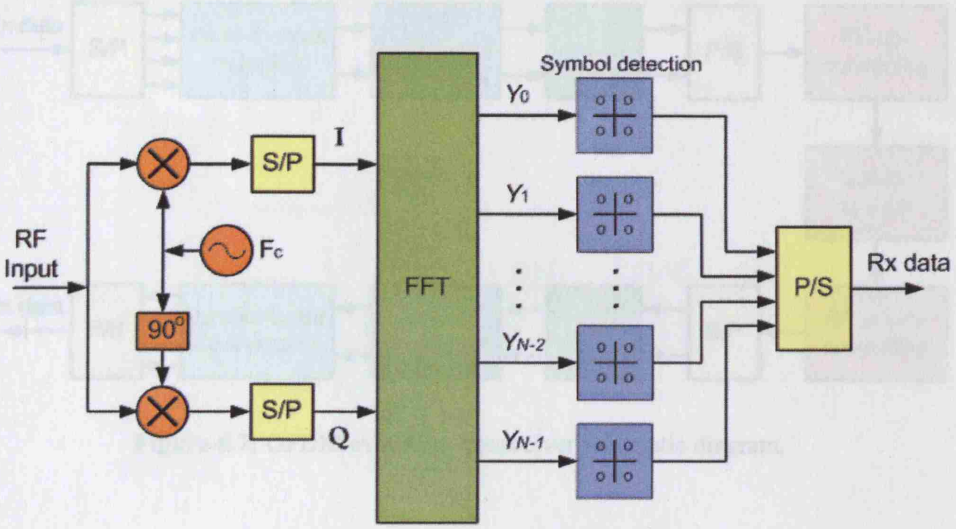

Figure 6.6: Typical OFDM receiver block diagram.

6.6 RF OFDM Signal Generation

In order to investigate the performance of the Orthogonal Frequency Division Multiplexing OFDM signal over optical system of interest, Matlab simulink has been used to build the transceiver systems with modifiable parameters of mapping, number of sub-carriers, signal bandwidth (bit rate), signal RF frequency and the IFFT size. OFDM signals have been generated with signal mappings of BPSK, QPSK, 16-QAM, and 64-QAM, and have been up-converted to RF frequencies. The optical system used directly modulated laser using DSB-SC technique constructed using the OptSim platform. In order to verify the systems accuracy and performance, BER curves have been produced for generated signals against the signal to noise ratio of different mapping and frequencies with various signal bandwidths.

Figure (6.7) illustrates the schematic structure of the designed RF over fibre OFDM models combining transmitter, optical system, and receiver, while figure

(6.8) shows the designed simulink systems with Matlab. Systems and settings were monitored to assure models performance for various signal parameters and frequencies.

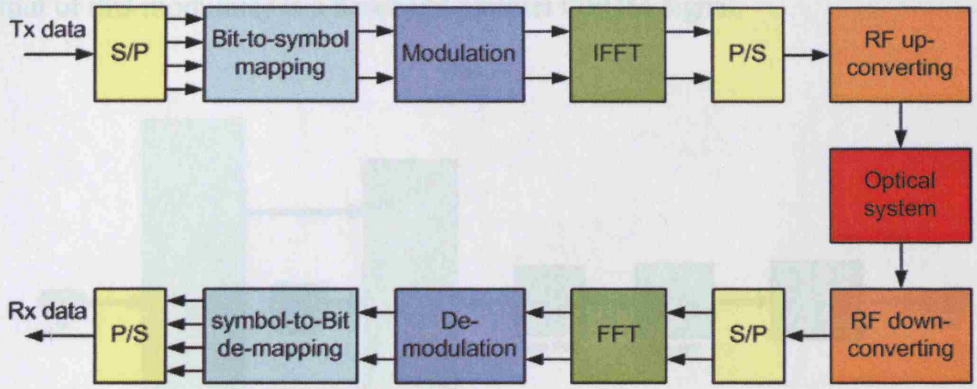

Figure 6.7: OFDM over fibre transceiver schematic diagram.

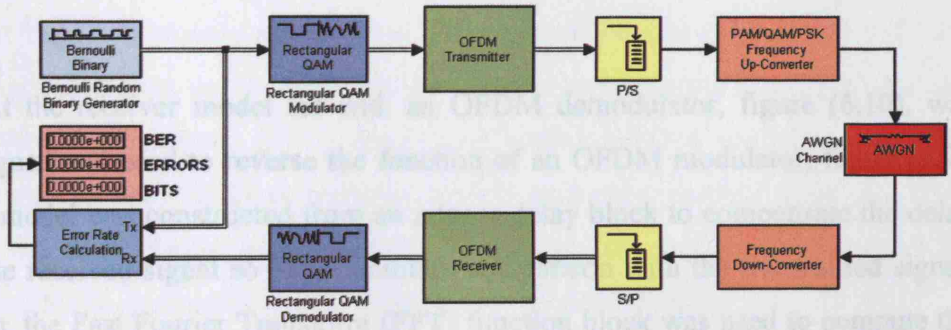

Figure 6.8: OFDM Matlab transceiver system model.

To explore the OFDM modulator in details, figures (6.9) and (6.10) illustrates the components of the constructed OFDM modulator and demodulator respectively. It can be seen from figure (6.9) that the Matlab OFDM modulator consists of a row selector block to divide the modulated input symbols into two similar sizes before adding the zero amplitude central carrier. Thereafter, a matrix concatenation block was added to recombine the modulated signal sequences equally on the sides of the central carrier.

As the OFDM signal were to be generated using the Inverse Fast Fourier Transform (IFFT), a zero padding block was used to add rows of zeros along

data carriers corresponding to IFFT input signal size. The selector block has been used to reorder input signal elements in order to centralise data rows among zero padding. Finally, an IFFT function block was used to compute the IFFT along the input signal vector dimension, which must have a power-of-2 length. The output of this modulator is a baseband parallel OFDM signal.

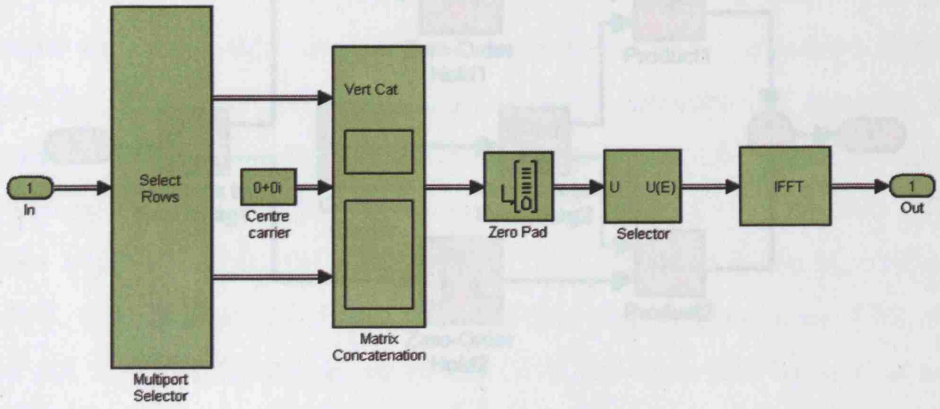

Figure 6.9: OFDM Matlab modulator model.

At the receiver model far end, an OFDM demodulator, figure (6.10), was designed and used to reverse the function of an OFDM modulator, figure (6.9). The model was constructed from an integer delay block to compensate the delay in the received signal so as to facilitate comparison with the transmitted signal. Then, the Fast Fourier Transform (FFT) function block was used to compute the FFT along the input signal vector dimension, which must have a power-of-2 length. FFT block output was fed to a frame converter to frame-based the output. Finally, a selector block had been used for removing the zero padding and to reorder the carriers.

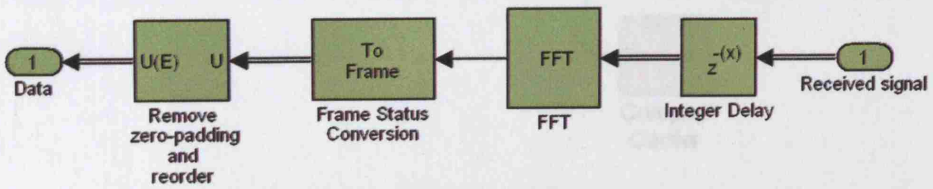

Figure 6.10: OFDM Matlab demodulator model.

After OFDM modulator, the output signal has to be converted to serial form so that it can be up-converted. A buffer block with an output size of one is used

to perform this task. RF up-conversion is carried out using an electrical up-converter model. Figure (6.11) shows the up-converter model. Blocks of complex to real, zero order holding, complex carrier, product, and summation were included to construct this model. Up-converter model output is an RF OFDM signal.

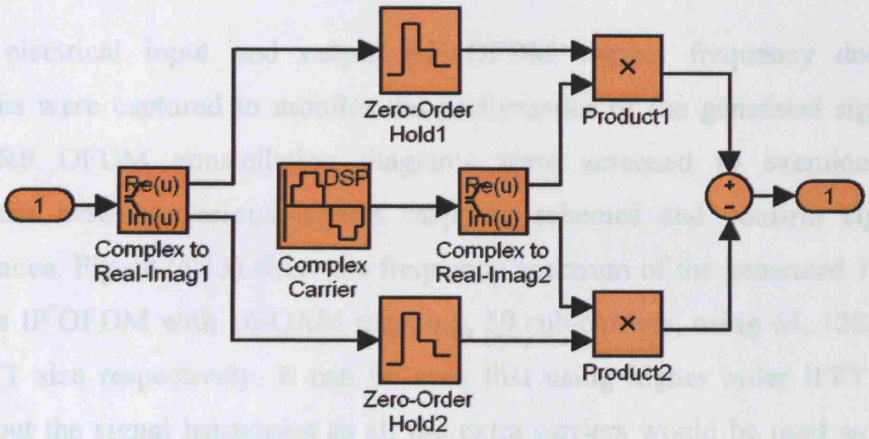

Figure 6.11: OFDM Matlab electrical RF up-converter model.

At the receiver side, an electrical frequency down converter model had been used to reverse the up-converter model function and generate an output baseband OFDM signal. Figure (6.12) shows the Matlab OFDM electrical RF down converter model. Blocks of complex carrier, conjugate, product averaging filter, and zero order holder were combined to construct the model. The output of RF down converter model is a serial form baseband OFDM signal.

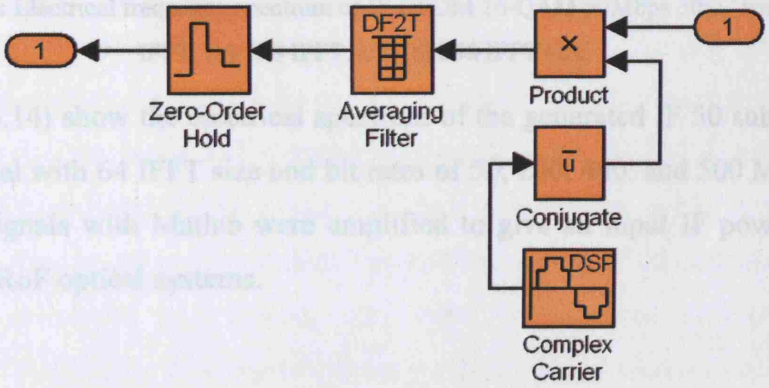

Figure 6.12: OFDM Matlab electrical RF down-converter model.

The OFDM down converter output has to be converted back to parallel form prior to feeding OFDM demodulator model. A buffer block with output size matching the FFT power-of-2 length is used to perform this task.

6.6.1 OFDM Spectrum and constellation

The electrical input and output RF OFDM signals frequency domain spectrums were captured to monitor the performance of the generated signals. While RF OFDM constellation diagrams were screened to examine the differences between various signals mapping schemes and confirm signals performance. Figure (6.13) show the frequency spectrum of the generated 1GHz 50 Mbps IF OFDM with 16-QAM mapping, 50 sub-carriers, using 64, 128, and 256 IFFT size respectively. It can be seen that using higher order IFFT will spaced out the signal harmonics as all the extra carriers would be used as zero padding but which in turn will decrease the signal data bit rate efficiency.

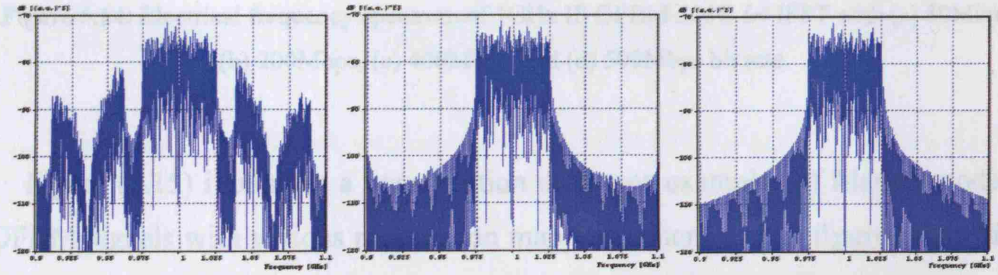

(a) (b) (c)

Figure 6.13: Electrical frequency spectrum of IF OFDM 16-QAM 50Mbps 50SC with (a) 64 IFFT, (b) 128 IFFT, and (c) 256 IFFT size.

Figure (6.14) show the electrical spectrum of the generated IF 50 sub-carriers OFDM signal with 64 IFFT size and bit rates of 50, 200, 400, and 500 Mbps. All generated signals with Matlab were amplified to give an input IF power of 10 dBm to the RoF optical systems.

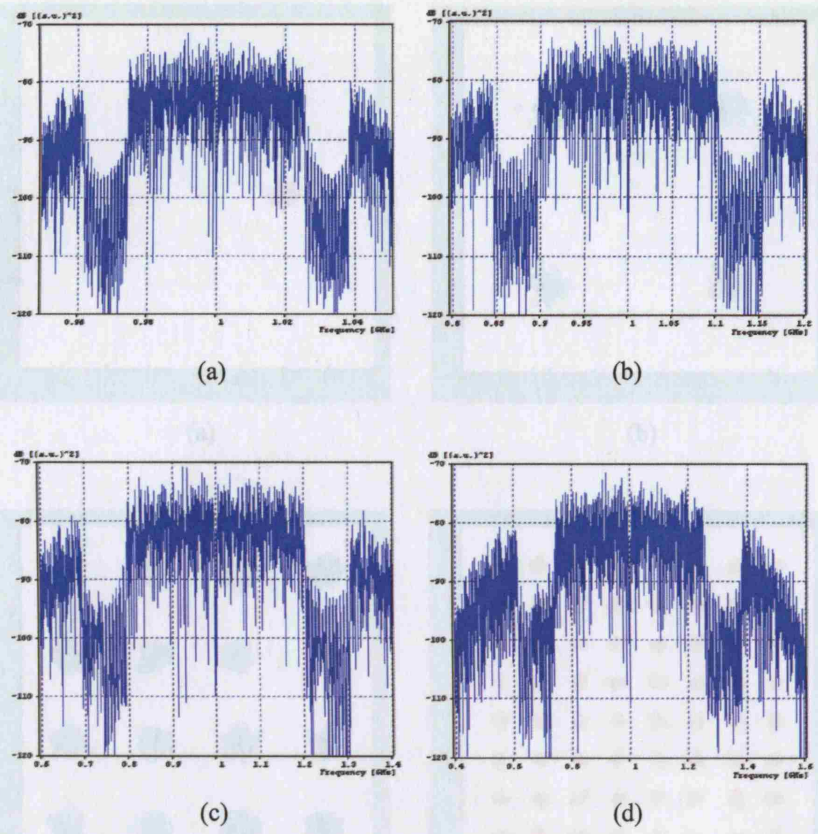

Figure 6.14: Electrical frequency spectrum of 1GHz IF OFDM 50SC 64 IFFT with (a) 50Mbps (b) 200Mbps, (c) 400Mbps, and (d) 500Mbps bit rate.

Figure (6.15) illustrates a constellation diagrams examples of Matlab models OFDM signals with various modulation mapping schemes. The figures show the constellation diagrams with mapping schemes of BPSK, QPSK, 16-QAM, and 64-QAM respectively. Signals were generated, recovered, and monitored within Matlab constructed models demonstrated in previous figures. An AWGN channel was added to system model in order to investigate the OFDM signal performance with respect to each individual mapping scheme. The RF OFDM signals neither had any pilot carriers, cyclic prefix nor coding as signal performance were investigated through an optical system link and have no wireless link where these parameters are used. In addition, the signal performance evaluation was compared to a reference transceiver system performance. The use of coding, pilot carrier, cyclic prefix, and zero padding were defined and explained in section (6.2).

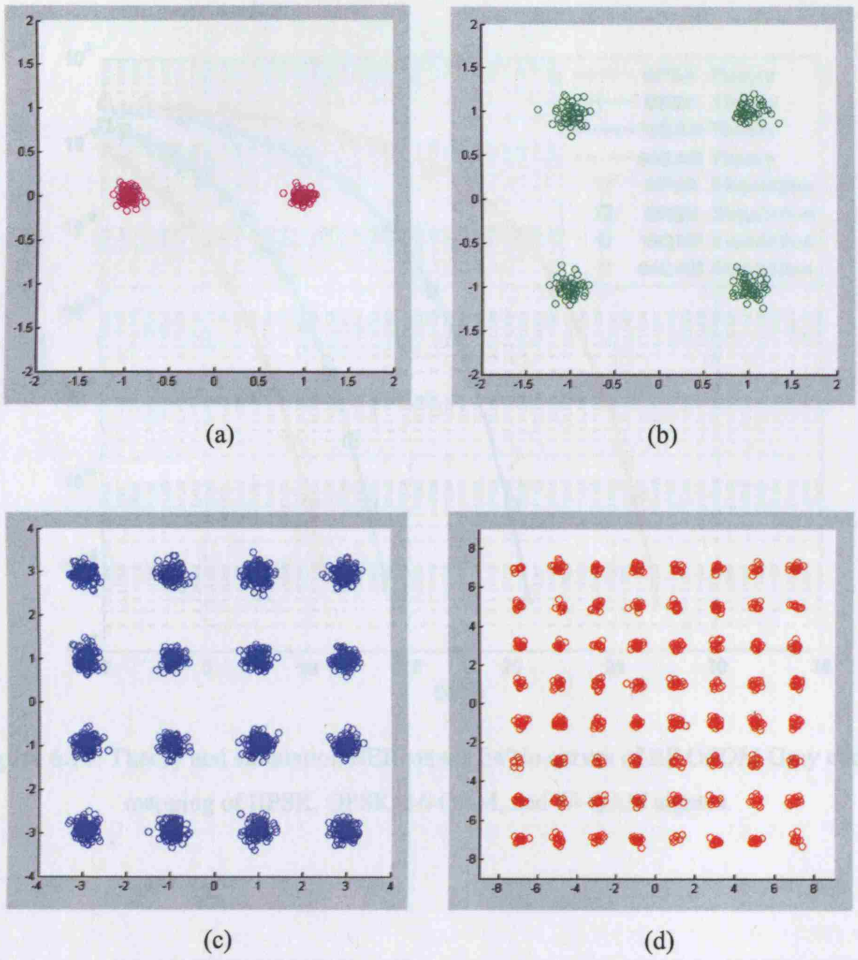

Figure 6.15: Constellation diagrams of Matlab models OFDM signals generated with (a) BPSK (b) QPSK, (c) 16-QAM, and (d) 64-QAM modulation mapping.

Figure (6.16) shows that the generated signals follow the reference theoretical signal performance curves of OFDM for each particular mapping. System simulation results show that as expected the BER curves are independent with respect to the RF carrier frequency and the signal bit rate within the electrical transceiver systems. Filter phase noise is one of the main parameters in signal recovering. Figure (6.17) illustrates improvement of recovered signal with optimizing receiver averaging filter numerator ratio (T_{out}/T_{in}). The filter optimum ratio is dependent on the signal bit rate, signal frequency, and signal bandwidth.

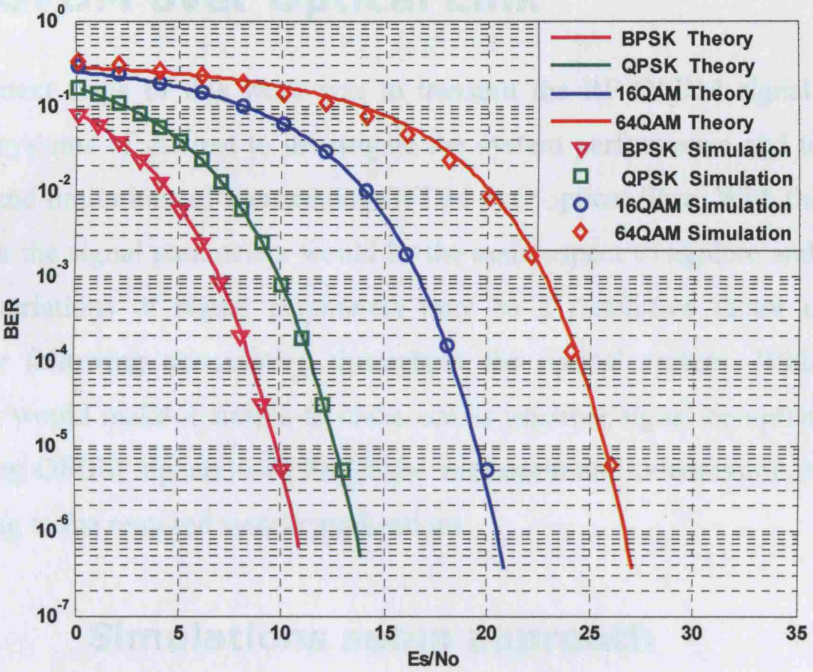

Figure 6.16: Theory and simulation BER versus Es/No curves of RF OFDM Gray coded mapping of BPSK, QPSK, 16-QAM, and 64-QAM signals.

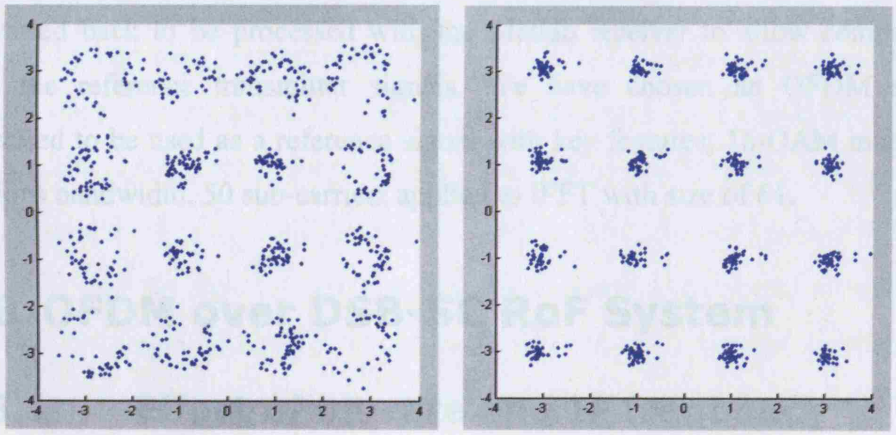

(a) (b)

Figure 6.17: Constellation diagrams of Matlab models OFDM recovered signal with different averaging filter numerator ratios. (a) Tout/Tin = 1, (b) Tout/Tin = 0.5

6.7 OFDM over Optical Link

The next stage of this work was to transmit the RF OFDM signal through optical systems of interest to investigate the system performance and to outline effects and limitations of transmitting OFDM over optical fibre. With this part of the work the signal parameters would be the main aspect to explore and inspect, where variations of signal parameters may be a restrictive factor of signal recovery following transmitting throughout the optical system. With such a study, it would make it simple to come across possible signal compromises for delivering OFDM signals over RoF links with optimum transmission capability according to the required system applications.

6.7.1 Simulations setup approach

In keeping with previous generated modulation schemes, the output OFDM signal has been recorded from the Matlab transmitter system and converted to a proper format to play back within the OptSim platform as an input to the optical system input signal. The output of the optical system can be recorded and converted back to be processed with the Matlab receiver to allow comparison with the reference transmitter signals. We have chosen an OFDM signal generated to be used as a reference signal with key features; 16-QAM mapping, 50Mbps bandwidth, 50 sub-carriers applied to IFFT with size of 64.

6.8 OFDM over DSB-SC RoF System

6.8.1 Effect of bit rate and IF frequency

The generated OFDM signal has been applied to the DSB-SC optical system in order to investigate the performance of the signal over this system. The system laser bias current set to be 100mA, the RF electrical carrier power was 10dBm at 5.5GHz and fibre length of 10 km as a trial length, while the generated input OFDM signal power was 10dBm with 1GHz frequency to give 12GHz output RF signal. Figure (6.18) shows BER curves of 16-QAM OFDM signal with bit rates of 50 Mbps, and 100 Mbps respectively. It can be seen that these two RF signals

with 50 sub-carriers can be recovered in good match with the reference signal performance in the existence of 10 km single mode fibre.

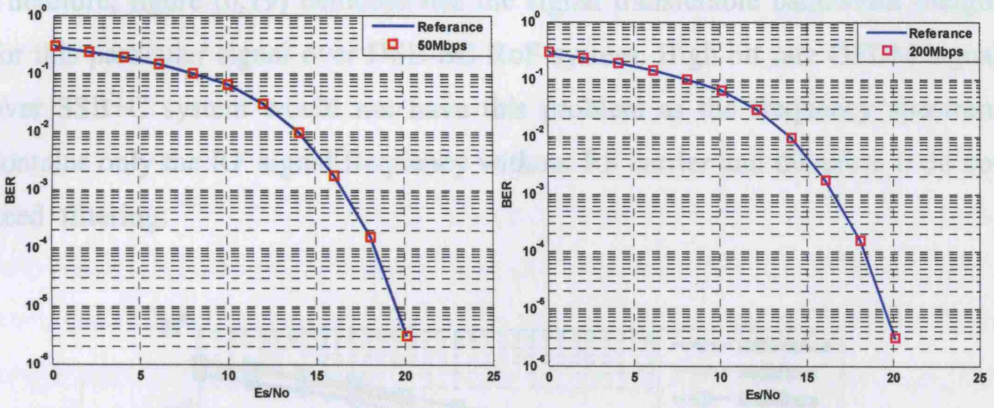

(a) (b)

Figure 6.18: Simulation BER versus Es/No curves of 16-QAM Gray coded mapping RF OFDM signal over DSB-SC RoF system with 10 km single mode fibre, (a) 50Mbps, (b) 100Mbps.

The next set of curves, figure (6.19), shows the BER performance of signals with higher bit rates. The figure illustrates that the recovery of 12 GHz OFDM signal with 50 sub-carriers and bit rates of 400Mbps and 500 Mbps, had been strongly limited after being through the DSB-SC RoF system. It has been found that the main limiting factor for the high bit rate signals over this system is the filtering. the output carrier frequency for this system was 11 GHz ($2\times f_{LO}$) and the IF signal frequency was 1 GHz (i.e. 1 GHz is the frequency spacing between the carrier and the signal), which means that increasing the signal bit rate and therefore the signal bandwidth would make the frequency spacing between the required output signal to filter and the carrier frequency very small and therefore hard to filter.

Figure (6.20) shows the electrical frequency spectrum of the received signals of 50 Mbps and 500 Mbps respectively. It can be seen that the signal frequency spacing is very small with the signal of 500 Mbps. Simulations have been done for signals with bit rates of 400 Mbps and 500 Mbps with IF frequency of 2 GHz and electrical carrier frequency of 5 GHz to give an output of 10 GHz RF carrier frequency and RF signal of 12 GHz. It has been found that it is possible to

recover the signal with such bit rates to match the theoretical curves by applying this higher IF signal frequency (2 GHz) as this will increase the frequency spacing between the carrier and the signal to allow signal filtering at the receiver. Therefore, figure (6.19) demonstrates the signal transferable bandwidth margin for this particular signal over DSB-SC RoF system. High bit rate OFDM signal over SSB+C system would not have this problem as the frequency spectrum contains only the RF signal frequency without RF carrier and therefore it do not need filtering.

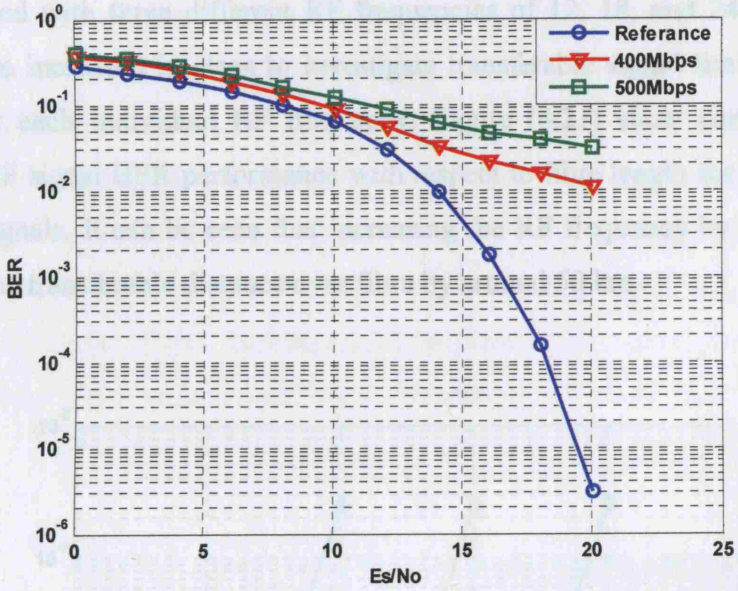

Figure 6.19: Simulation BER versus Es/No curves of 16-QAM gray coded mapping RF OFDM signal over DSB-SC RoF system with 10 km single mode fibre at 400Mbps, and 500Mbps.

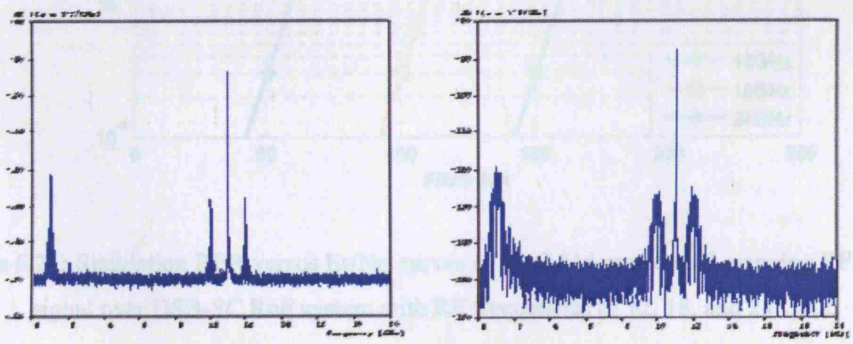

(a) (b)

Figure 6.20: Electrical frequency spectrum of received RF OFDM of 16-QAM 50 sub-carriers over DSB-SC RoF system with (a) 50Mbps, (b) 500 Mbps.

6.8.2 Effect of RF frequency

Signal frequency is one of the main parameters in the calculation of the dispersion penalty equation. Induced fibre dispersion found to be proportional to RF frequency transmitted over fibre, as well as other equation parameters (Chapter 3). To examine the signal frequency effect as one of OFDM parameters, and in order to take a broader view of signal transmitting limitations, we have applied an OFDM signal with fixed signal parameters at a set of RF carrier frequencies. OFDM of 50 Mbps, 16-QAM mapping, 50 sub-carriers 64 IFFT were applied with three different RF frequencies of 12, 18, and 24GHz. Fibre length were increased in steps to investigate transferable signal limit over RoF system for each individual RF frequency. Figure (6.21) show comparison of received RF signal BER performance with respect to fibre length for 12, 18, and 24 GHz signals. It can be seen that increasing the RF frequency by 6 GHz will decrease the transferable distance over fibre by around 50 km.

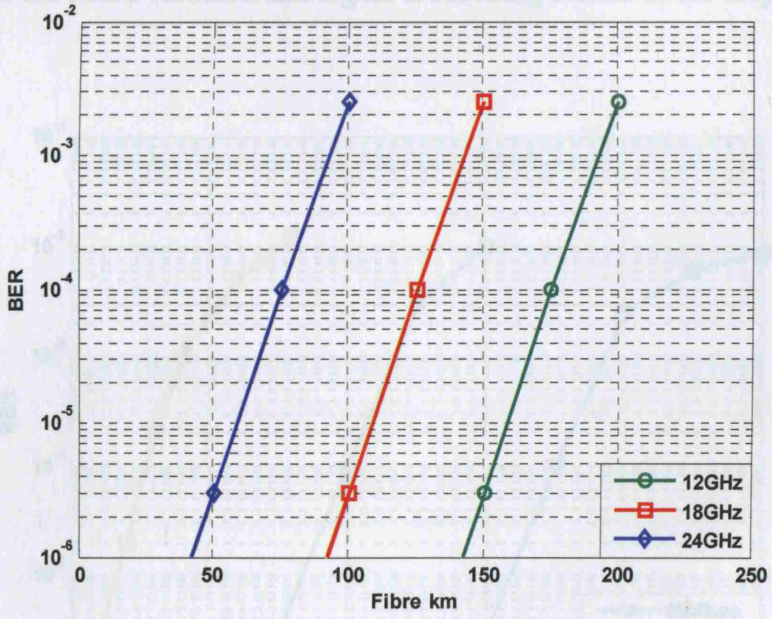

Figure 6.21: Simulation BER versus Es/No curves of 16-QAM gray coded mapping RF OFDM signal over DSB-SC RoF system with RF frequencies of 12, 18, and 24 GHz.

6.8.3 Fibre Dispersion

Further to work in the previous section, simulations were carried out to examine the effects of fibre dispersion on OFDM signals. Signals of 12 GHz with bit rates of 50, 100, and 200Mbps were generated and transmitted using the DSB-SC RoF system with varying fibre lengths (fibre loss ignored). Optical signals at the far end of the fibre were attenuated in order to acquire electrical received OFDM signals with signal to noise ratio of 20 dB as a reference point. Simulations show that OFDM over fibre performance is limited by dispersion to a value dependant on the signal bit rate. Figure (6.22) shows the 12 GHz 50 SC OFDM signal performance with 20dB signal to noise ratio with varying the bit rate of the signal. It shows the BER performance degradation with fixing the signal to noise ratio and eliminate the fibre loss. The resulted performance degradation was due to the fibre dispersion since that increasing the signal bit rate will decrease the signal's bit timing slot. Therefore, this will make the signal less tolerant to the fibre dispersion; consequently the signal will be more sensitive to the phase variation and signal broadening effects of the dispersion.

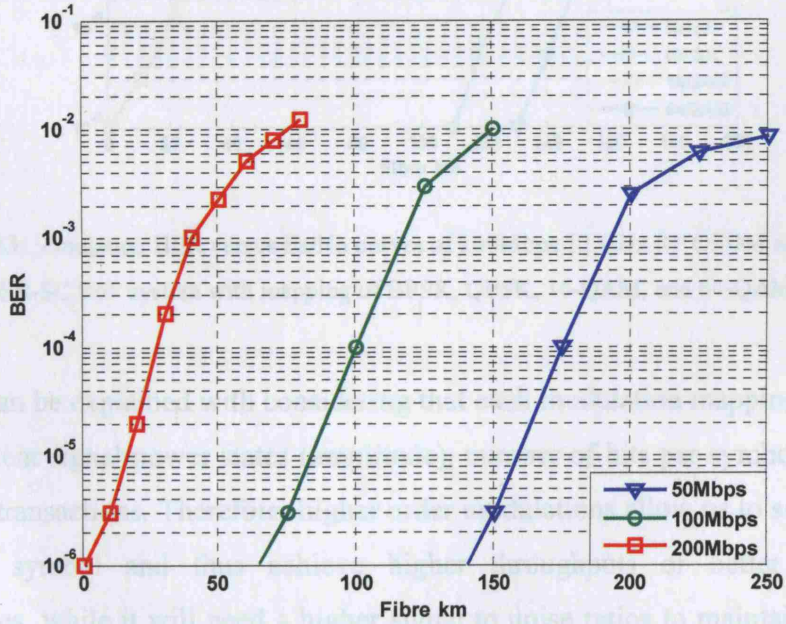

Figure 6.22: Simulation BER versus Es/No curves of 16-QAM Gray coded mapping RF OFDM signal over DSB-SC RoF system with bit rates of 50, 100, and 200 Mbps.

6.8.4 Effect of Mapping

We now evaluate performance when changing the signal mapping while fixing other signal parameters in order to determine mapping effect on signal over fibre performance. Figure (6.23) shows the BER performance of a 200Mbps OFDM signal using the DSB-SC with different signal mapping and zero fibre loss. The signal input power was 10 dBm, at 1 GHz and an RF carrier of 10 dBm at 5.5 GHz was used to give an RF output OFDM signal at a centre frequency of 12 GHz. Figure (6.23) demonstrates that the signal mapping of higher symbol rate has a shorter transmittable distance.

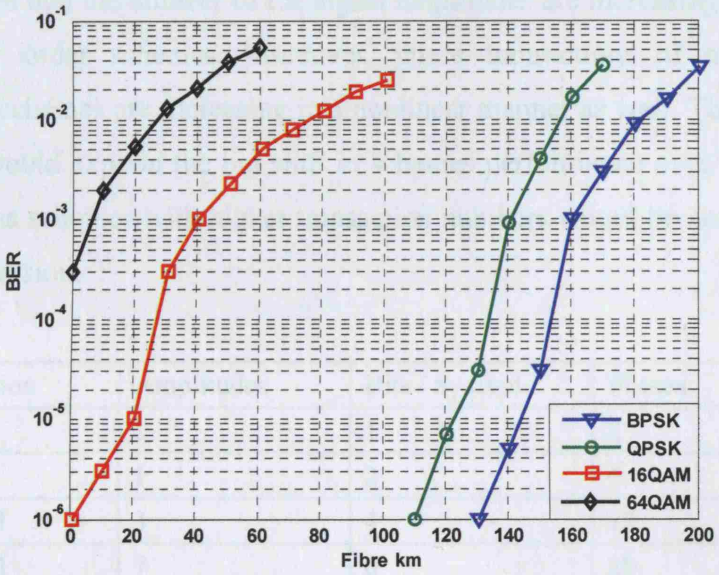

Figure 6.23: Simulation BER versus Es/No curves of 200Mbps 12 GHz RF OFDM signal over DSB-SC RoF system with mapping of BPSK, QPSK, 16-QAM, and 64-QAM.

This can be explained with considering that each modulation mapping scheme has different signal power states (amplitude), number of bits per symbol as well as phase transactions. Therefore, higher order modulations allow us to send more bits per symbol and thus achieve higher throughputs or better spectral efficiencies, while it will need a higher signal to noise ratios to maintain certain bit error ratios (BER). Adaptive modulation schemes can be used interchangeably in OFDM RoF systems to achieve the highest signal bit rate depending on the system channel conditions. This means that if the channel

condition can not support a high signal to noise ratio modulation schemes such as 64-QAM or 16-QAM, the system would switch the modulation scheme to a lower required signal to noise ratio scheme such as QPSK or even BPSK.

To understand the results, by comparing modulation schemes, BPSK modulation has single signal amplitude, one bit per symbol and two phases. QPSK has one amplitude two bits per symbol and four phases. 16-QAM modulation has three signal amplitudes four bits per symbol and twelve phases, while 64-QAM modulation has six bits per symbol seven signal amplitudes and twenty eight phases. Table (6.8.1) illustrates differences in modulation schemes used with OFDM signal. By linking the curves of figure (6.23) with table (6.8.1), it can be seen that the number of the signal amplitudes are increasing nonlinearly with higher order schemes. Moreover, phase transactions of higher order modulation schemes are increasing in a nonlinear manner as well. This nonlinear increment would explain the big shift in schemes performance over fibre due to dispersion, as schemes with higher transaction numbers would be more sensitive to fibre dispersion.

Modulation	Amplitudes	Bits / Symbol	Phases
BPSK	1	1	2
QPSK	1	2	4
16-QAM	3	4	12
64-QAM	7	6	28

Table 6.8.1: Modulation schemes differences applying BPSK, QPSK, 16-QAM, and 64-QAM.

6.8.5 The effect of fibre dispersion on OFDM signal with various mappings

In order to summaries the BER performance of OFDM over fibre with respect to all investigated parameters, curves of OFDM performance for each individual mapping and bit rate have been produced. Figure (6.24) gives a guide to the achievable transmission distances with various OFDM signal mappings while negates the fibre loss. It can be seen that the transmission distance is proportional

to signal mapping as well as signal bit rate. The curves illustrate signal performance of 50 sub-carriers input OFDM signal over DSB-SC system with bit rates from 50 Mbps to 400 Mbps, and signals mapping of BPSK, QPSK, 16-QAM and 64-QAM OFDM with BER of $\left(1e^{-6}\right)$ or better. This figure summarises the performance limitations of previous figures, and indicates a general dispersion limitation for the achievable transmission distances for each individual mapping and bit rate for this optical system.

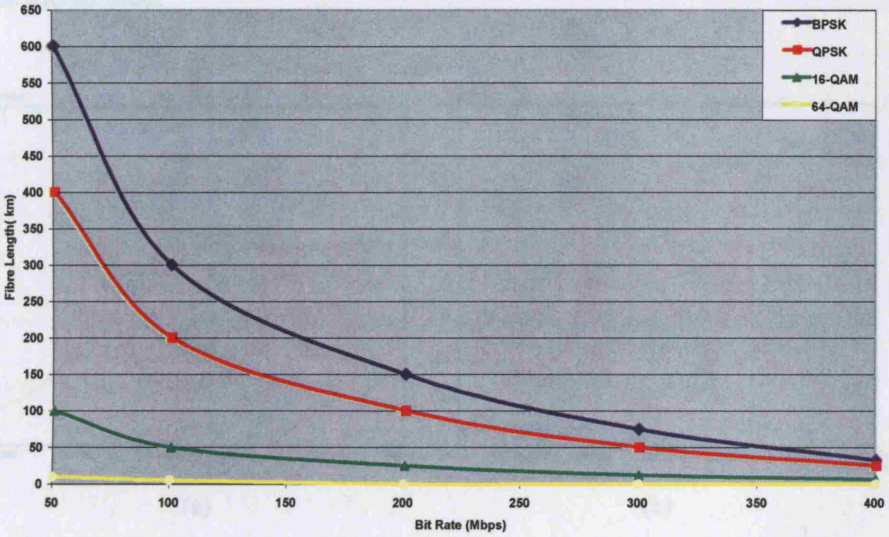

Figure 6.24: Bit rate versus fibre length curves of RF OFDM signal over DSB-SC RoF system with mapping of BPSK, QPSK, 16-QAM, and 64-QAM.

6.8.6 Influence of optical modulation technique

For the purpose of comparing directly modulated laser DSB-SC system of interest with DSB-SC using two optical modulators (Chapter 5), in terms of system linearity as each system deliver a different optical spectrum, OFDM signal has been transmitted over these two systems with increasing fibre lengths. As it have discussed in the previous chapter (chapter 5), the DSB-SC technique with directly modulated laser would generate an optical spectrum with two modulated sidebands and suppressed carrier, while the case with the system using two modulator would produce an optical spectrum with one modulated

sideband, one unmodulated sideband, and suppressed optical carrier. Figure (6.25) illustrates simulated optical frequency spectrum of both modulation techniques. Simulations show that directly modulated laser DSB-SC technique offers same transferable fibre lengths compared to the single modulated sideband technique. This can be explained as the two modulated sideband system would produce extra nonlinear components at the receiver but these components will not interfere with the RF frequency band of interest. Therefore, directly modulated laser technique performance would not be enhanced if one sideband were not modulated.

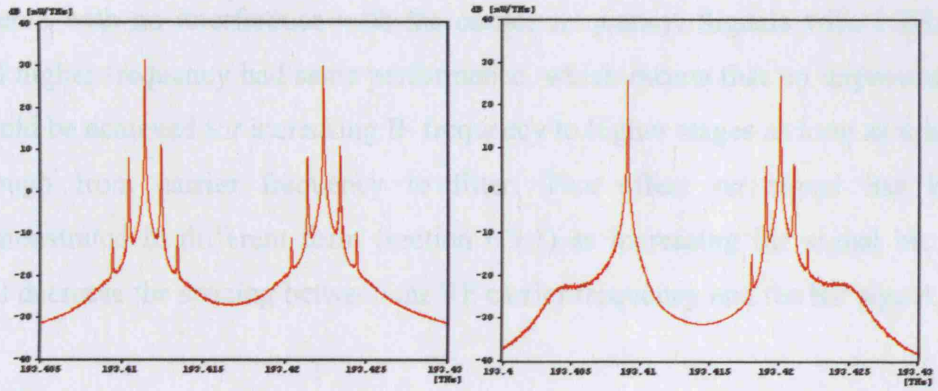

(a) (b)

Figure 6.25: Optical frequency spectrum of OFDM 50Mbps 50SC with (a) DML DSB-SC and (b) two modulators DSB-SC system.

6.8.7 IF frequency influence on the system performance

With the double sideband-suppressed carrier (DSB-SC) modulation, the electrical frequency spectrum would contain frequency components of IF signal frequency, RF carrier frequency, and modulated RF signal sidebands separated by $f = f_{IF}$ from the RF carrier. In order to recover the received RF frequency of interest, the signal has to be filtered to remove other frequency components. For this reason, RF frequency of interest needs to be far enough from carrier frequency to make it possible to filter. Therefore, IF signal frequency has to be high enough to make it feasible in order to filter out the carrier frequency at the

receiver. For our OFDM signal, IF signals have been generated with 50 Mbps, 50 sub-carriers and IF frequencies of 500 MHz, 1GHz, and 2 GHz to investigate possibility of recovering received RF OFDM signals, and compares performance for each individual case.

It has been found that it's not possible to recover the transmitted signal of 500 MHz without errors penalty due to the carrier power interference and filter limitations in recovering the signal very close to the RF carrier frequency. IF signal of 1 GHz and higher were received with no interference. For that reason, it can be say that it would be possible to recover the RF signals as long as it can be filtered with no interference with the carrier frequency. Signals with 1GHz IF and higher frequency had same performance, which means that no improvement would be achieved for increasing IF frequency to higher stages as long as it is far enough from carrier frequency to filter. This effect on signal has been demonstrated in different form (section 6.9.1) as increasing the signal bit rate will decrease the spacing between the RF carrier frequency and the RF signal.

6.9 Conclusion

In this chapter, a detailed study of the OFDM modulation performance over RoF systems applying DSB-SC has been presented. Up-converted OFDM modulation based on BPSK, QPSK, 16-QAM and 64-QAM Gray coded mapping have been applied. Electrical RF carrier of 12 GHz was selected as a reasonable frequency for evaluating the signal transporting limitations over fibre. The effects of OFDM modulation parameters on the attainable signal transmission over the RoF link were evaluated. The input signal IF frequency, RF carrier frequency, signals bit rate and mapping influence were investigated. Moreover, the concern of fibre dispersion as a limiting factor applying OFDM signal was also explored.

It has been shown that applying the DSB-SC modulation technique for transmitting OFDM signals of 50 sub-carriers, 50 Mbps and 1 GHz IF frequency will be limited to 200 Mbps. Therefore, applying signals with higher bit rates will need to be up-converted to higher IF frequencies in order to allow filtering

the received signal efficiently. Results illustrate that chromatic dispersion limiting the achievable BER performance when increasing fibre length. 16-QAM OFDM signal of 12 GHz can be transmitted over 150 km of fibre before observing effects of fibre dispersion, while it will be limited to 100 km when increasing signal frequency to 18 GHz, and to 50 km when 24 GHz OFDM signal is applied.

With changing the signals bit rate from 50 Mbps to 200 Mbps, it has been observed that the BER performance of the received OFDM signals is degrades with increasing the fibre length while fixing the signal to noise ratio and eliminating the fibre loss. It has been found that the resulted performance degradation is caused by the fibre dispersion, since that increasing the signal bit rate will decrease the signal's bit timing slot. Therefore, this will make the signal less tolerant to the fibre dispersion; consequently the signal will be more sensitive to the phase variation and signal broadening effects of dispersion. An inclusive plot of signal parameters effects has been developed in this chapter.

Simulation results demonstrate that the ODFM signal mapping represents a fundamental parameter of the achievable lengths over fibre. A 12 GHz OFDM signal based on BPSK modulation and 200 Mbps can travel over 130 km single mode fibre before noticing any performance degradation, while applying a higher bits per symbol mapping with fixing other signal parameters, will reduce the achievable fibre lengths. The assessed reduction gap between the applied mappings can be explained by that the numbers of phase transactions of higher order schemes, as well as the signal amplitude levels, are rising in a nonlinear approach which therefore increases their sensitivity to the fibre dispersion.

Chapter 7

Conclusions

The work in this thesis was concerned with evaluating the performance of Radio-over-Fibre (RoF) optical systems that have good immunity to fibre chromatic dispersion. The systems performance has been evaluated by applying RF multi-level digital modulation signals, and using the Monte Carlo techniques to calculate the Bit Error Rate (BER) of the recovered signals. At the first stage, QPSK, 16-QAM and 64-QAM are applied to systems based on modulation techniques of conventional Double Sideband (DSB) modulation, Optical Single Sideband (OSSB+C) modulation, and Double Sideband-Suppressed Carrier (DSB-SC) modulation. The modulation techniques of interest have been constructed, using the simulation models, and applying different approaches when applicable, in order to investigate the impact of the applied method on the system performance. Then after, this work has been extended to include Orthogonal Frequency division Multiplexing (OFDM) modulation.

7.1 Conclusions

In chapter 2 we have presented a review of optical communications Radio-over-Fibre (RoF) systems included a study of the benefits together with the applications and the ability of these systems to effectively transport mm-waves. Moreover, this chapter presented a review of the optical modulation techniques used for generating and distributing microwave and mm-wave signals. We have shown that optical communication systems can offers many advantages over electrical communication systems by working in the optical domain including high bandwidth and flexibility, while it suffers from restrictions created within the optical medium such as noise and distortion.

In Chapter 3 we have reviewed the Radio-over-Fibre optical systems based on the Intensity Modulation-Direct Detection (IM-DD), considering the conventional modulation technique and systems applying modulation techniques which are tolerant to fibre dispersion. It has been confirmed that the conventional modulation technique is limited by the fibre dispersion regardless the modulation of the input signal. With the conventional intensity modulation systems of a single mode fibre (SMF), fibre chromatic dispersion, especially at 1550 nm, can cause severe signal power penalties at certain distances and frequencies, which limits the frequency-length product. Moreover, it has been shown that the chromatic dispersion has a significant influence on the obtainable transmission distance over the SMF in intensity modulated direct detection IM-DD RoF links where the RF signal is above 10 GHz Range.

In order to eliminate, or shift up, the dispersion penalty to a useful frequencies and distances, several modulation techniques had been developed to limit the fibre dispersion penalties of the single-mode fibre links on RoF systems. These techniques are varying from simple to more complicated. These dispersion tolerant modulation techniques can be classified into two main categories, the first one is based on removing one of the optical modulated sidebands which is called the optical single sideband (OSSB) modulation, where it can be totally avoided the dispersion power penalty. This technique can be applied be either adding a filter to the conventional DSB system to remove one of the sidebands,

or it can be applied by using a two arm MZM to produce the single sideband modulation.

The second modulation technique is based on suppressing the optical carrier of the modulated optical signal, it is called the Double Sideband-Suppressed Carrier (DSB-SC) modulation, and it can shift the dispersion penalty points to a higher frequency or/and fibre lengths. This technique is based on a combination of two modulation techniques, which are directly modulating the laser, and the external modulation using MZM biased nonlinearly to up-convert the optical signal while suppressing the optical carrier. Each of these modulation techniques have an advantages over other techniques as well as drawbacks which were stated through the evaluation. The choice of considering a particular technique will be depending on the desired application of the RoF system.

In chapter 4, we have demonstrated the performance evaluation of the RoF modulation techniques reported in chapter 3, by modelling the systems using simulation platforms. We have considered the conventional technique as well as the dispersion tolerant modulation techniques. We have applied a complex digital modulation input signals of QPSK, 16-QAM and 64-QAM modulation which are up converted to RF frequencies of 10, 20, and 28 GHz as a candidate frequency bands to use for the Fixed Wireless Access (FWA) systems such as WiMAX.

The simulation results have confirmed the mathematical analysis of the systems investigated which were developed in chapter 3. The conventional DSB system model show a limited capability of transmitting the modulated RF signals over the single mode fibre link due to the chromatic dispersion. Moreover, simulations confirmed the theoretically expected power penalty nulls which were occurred in a cyclic behaviour while increasing fibre length or the RF frequency. On the other hand, the potential to eliminate the fibre dispersion penalty applying dispersion tolerant techniques had been proved using the models constructed. It has been found that each of the examined techniques has a unique advantages as well as weak points related to the performance or the system cost.

It has been shown that the Optical Single Sideband (OSSB+C) modulation can be constructed by two methods. The first technique is based on adding an optical filter to the conventional RoF system based on an external MZ modulator, while the second technique is based on using an external dual arm MZ modulator to modulate the CW laser. The main advantage of the OSSB+C technique is that it can eliminate the power variation over the entire range of the modulation frequency and fibre length, therefore, dispersion only adds a phase shift with no amplitude variation. However, the main drawback of this modulation technique is that it relies on using optical filtering or a dual arm modulator, which means that its deployment could lead to tuning limitations and complexity or equipment high cost.

Moreover, it has been demonstrated that the Double Sideband-Suppressed Carrier (DSB-SC) modulation can shift the dispersion effect to a higher frequency-length products. This technique is simple and potentially low-cost method for the remote delivery and generation of millimetre-waves by using directly modulated laser. It removes the need for complex circuitry to maintain the required frequency offset of the optical carriers as it only uses a single laser source. In addition, this technique uses an IF band input signal to modulate the laser rather than RF frequencies. This could be useful in RoF systems as it will be possible to generate a high frequency signals using devices with low frequency working range, this could be very useful and cost effective with regard to the applications and requirements of such systems.

In chapter 5, we have demonstrated, using experimentally verified modelling, the Inter-Modulation Distortion (IMD) measurement of the RoF systems and carrying out a comparison of modulation imposition techniques that are tolerant to dispersion. A two tone test as an Inter-Modulation Distortion (IMD) measurement was applied to perform this examination. The Intermodulation-Free Dynamic Range (IM-FDR) of a class of systems that have good immunity to fibre dispersion has been investigated, and a comparison of the performances of the investigated techniques was carried out resulting in the optimisation of the systems' performance.

The systems examined are: the Single Sideband (OSSB+C) modulation based on applying dual arm MZ modulator; The Double Sideband-Suppressed Carrier (DSB-SC) modulation based on directly modulated laser and second order optical up-conversion using nonlinear biased MZ modulator; and the Double Sideband-Suppressed Carrier (DSB-SC) modulation based on using two MZ modulators. The devices used in the simulated systems were experimentally verified to match the experimental reference devices.

Simulations showed that the DSB-SC system based on using two MZ modulators offers the highest IM-FDR among the three systems, followed by the SSB+C modulation system based on using the dual arm MZ modulator. It has been found that the DSB-SC based on directly modulated laser and nonlinear second order optical up conversion offers the smallest dynamic range among the three examined systems. It has been shown that by optimising the optical devices parameters of this system, the IMD performance of this system could be improved so that it is comparable with the other systems examined.

Moreover, the Double Sideband-Suppressed Carrier (DSB-SC) modulation, based on directly modulating the laser and applying the second order optical up conversion has a very unique advantage over the other modulation schemes. This technique has a capability of transmitting multi-wavelength optical carriers simultaneously and over a single fibre link, which means that this system can allow higher data rates as well as enabling a multi-function or multi-application system over a single fibre link. Moreover, this system can be used as a multi-signal system where the single optical wavelength can be modulated simultaneously with multi-signal inputs allocated at different frequencies. Modelling results have showed that the multi-wavelength DSB-SC system is attainable and can achieve performance comparable with the single-wavelength system.

Finally in chapter 6, we have explored, for the first time, the performance of the RF up-converted OFDM signal over the RoF optical links. OFDM modulation signals based on BPSK, QPSK, 16-QAM and 64-QAM Gray coded

mappings have been applied, and the effects of OFDM modulation parameters on the achievable signal transmission over the RoF link were assessed. It has been found that the input signal IF frequency, RF carrier frequency, the signals bit rate and the signal mapping are all an effective parameters on the signal performance and the attainable transmission distances.

We have applied the OFDM signal over the DSB-SC modulation technique as a system of interest. Simulation results illustrate that the chromatic dispersion is a limiting factor of the achievable BER performance when increasing fibre length. Moreover, in order to avoid fibre dispersion limitations, signal parameters have to be kept within the estimated limits of operation. In addition, for increasing the signal bandwidth or bit rate, the applied IF signal frequency has to increased in order to avoid the RF carrier interference at the receiver. Moreover, it has been found that higher order mapping signals are less robust to fibre dispersion. It has been found that this was due to the nonlinear increment in the number of the phase transactions and signal levels when applying higher order mappings.

7.2 Suggestions for Further Work

Further possible aspects to investigate are suggested as a result of the research performed in this thesis. This work can include the following:

- Extend the performance evaluation of modulation techniques and devices parameters to include a wider set of techniques and applications.
- Considering bidirectional transmission over the single mode fibre link to model the simultaneous up and down link of the RoF systems.
- Use the link models developed to study full optical network architectures such as looped and star networks.
- Extend to OFDMA which is being popularised by WiMAX and the MC-CDMA systems.
- Include signal coding and interleaving parameters to the applied modulation schemes to consider wireless fading and multi-path interference.

Appendix A

op_esgnw.m

```
function WriteOptSimdata(filename,data_vector,sample_period)
% OP_ESGNW Write electrical signal data to an ASCII file using OptSim
%    Playback format
%    OP_ESGNW('filename',DATA_VECTOR,SAMPLE_PERIOD) creates an OptSim
%    data file for the electrical signal specified with a vector samples.
%    This file can be used in OptSim with the electrical Playback block.
%
%    FILENAME must be a string variable representing the filename for
%    the OptSim datafile. The file extension must be .DAT.
%
%    DATA_VECTOR is an array containig the eletrical signal samples
%    corresponding to the SAMPLE_PERIOD sampling time.
%
%    SAMPLE_PERIOD is the sampling time expressed in ps.
%

if exist(filename) == 2
    error('The specified file already exists')
end

if ~strcmp(filename(length(filename)-3:length(filename)),'.DAT')
    error('The file extension must be .DAT')
end

if isempty(data_vector)
    error('The second argument must be a vector containing the signal
samples')
end

if sum(size(sample_period)) ~= 2
    error('The sample period must be a scalar')
end

data_vector = data_vector(:);

fid=fopen(filename,'w');

fprintf(fid,'%s\n',['OptSimESGN 1']);
fprintf(fid,'%s\n',['##']);

line=mat2str([sample_period,0,1]);
fprintf(fid,'%s\n',line(2:length(line)-1));

fprintf(fid,'%12.5E\n', data_vector);

status = fclose(fid);
```

op_esgnr.m

```
function
[data_vector,sample_period,time_vector]=ReadOptSimdata(filename)
% OP_ESGNR Read data from an OptSim electrical datafile
%    [DATA_VECTOR,SAMPLE_PERIOD,TIME_VECTOR] = OP_ESGNR('filename')
%    reads data from an ASCII file generated from OptSim using
%    the electrical Recorder block.
%    The function argument must be a string variable containing the
%    OptSim data filename.
%
%    DATA_VECTOR is a column vector containing the signal samples.
%
%    SAMPLE_PERIOD is the OptSim sampling period expressed in ps
%
%    TIME_VECTOR is a column vector (same dimension as DATA_VECTOR)
%    containing sampling instants expressed in ps
%

if ~exist(filename)
    error('The specified file does not exist')
end

fid = fopen (filename);
line = fgetl(fid);

if strcmp(line,'OptSimESGN 1') == 0
    error('The format of the specified file is not correct')
end

while ~strcmp(line,'##') & ~isempty(line),
    line = fgetl(fid);
end

if isempty(line)
    error('The specified file is not an OptSim data file')
end

data_vector = fscanf(fid,'%g',inf);

if data_vector(3) ~= 1,
    msg = 'The OptSim data format is not compatible with this Matlab
routine';
    error(msg);
end

sample_period = data_vector(1);
data_vector = data_vector(4:length(data_vector));
time_vector = [0:sample_period:sample_period*(length(data_vector)-1)]';

status = fclose(fid);
```

Project: OptSim conventional IM-DD DSB RoF system model.

Description: Valid for 10, 20 and 28 GHz Bands.

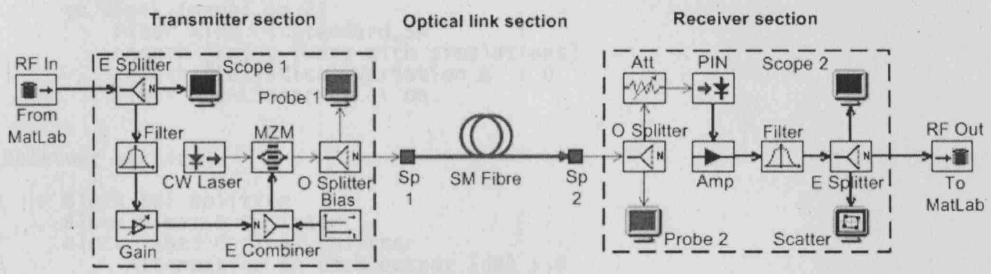

Figure 4.6: OptSim conventional IM-DD DSB RoF system model.

[Transmitter section]

Block Id: RF In
Block Name: From_Matlab
Block Type: Electrical Playback

Block Id: Splitter
Block Name: E Splitter
Block Type: Electrical Splitter
Attenuation on each output [dB] : 0
Attenuation on each output [lin] : 1

Block Id: Filter
Block Name: Filter
Block Type: Electrical Filter: Bessel
Type : Bandpass
Center Frequency [GHz] : 10, 20, 28
Number of Poles : 3
-3dB Bandwidth [GHz] : 2

Block Id: E Gain
Block Name: Gain
Block Type: Electrical Gain
Gain [db] : 4.34967888428

Block Id: Combiner
Block Name: E Combiner
Block Type: Electrical Combiner
Attenuation on each input [dB] : 0

Block Id: Bias
Block Name: Bias
Block Type: Bias wave generator
Level [AU] : 2.5

Block Id: CW_Lorentzian
Block Name: CW Laser
Block Type: Lorentzian Laser
Center emission frequency [THz] : 193.414489032
Center emission wavelength [nm] : 1550
CW Power [dBm] : 6.98970004336
CW Power [mW] : 5
FWHM Linewidth [MHz] : 10
Deterministic Initial Phase [rad] : 0
Noise Type : Realistic
Relaxation Oscillation peak Frequency [MHz] : 5
Relaxation Oscillation Peak Overshoot [dB] : 7
-20 dBm Linewidth [MHz] : 99.4987437107

Block Id: Sin2_MZ
Block Name: MZM
Block Type: Amplitude Modulator sin2
Excess loss [dB] : 3
Offset voltage corresponding to the phase retardation in the absence of any electric field [V] : 5
Extinction Ratio Type : Realistic
Extinction Ratio [dB] : 20
Chirp Factor : 0
V pi [V] : 5
Average power reduction due to modulation [dB] : 3

Block Id: Splitter
Block Name: O Splitter
Block Type: Optical Splitter
Attenuation on each output [dB] : 0

```
[Optical link section]

Model Fibers
      Fiber Id: SM Fiber
      from Block (name: Sp 1)
      to Block (name: Sp 2)
          Fiber kind  : Standard_SM
          Length [Km] : [Vary with simulations]
          Length Statistical Variation %  : 0
          Fiber Non-Linearity  : On


[Receiver section]

      Block Id: Splitter
      Block Name: O Splitter
      Block Type: Optical Splitter
           Attenuation on each output [dB] : 0

      Block Id: Attenuator
      Block Name: Att
      Block Type: Optical Attenuator
           Attenuation  [db] : [Vary with simulations]

      Block Id: PIN
      Block Name: PIN
      Block Type: PIN Photodiode
           Quantum Efficiency  : 0.7
           Responsivity (at reference frequency) [A/W] : 0.875104401174
           Quantum noise  : On
           Dark Current [nA] : 0.1
           Reference Frequency [THz] : 193.414489032
           Reference Wavelength [nm] : 1550

      Block Id: Amplifier
      Block Name: Amp
      Block Type: Electrical Amplifier: 50-Ohm
           DC Gain [dB] : 30
           Noise Figure F [dB] : 3
           Reference Temperature [K] : 300

      Block Id: Filter
      Block Name: Filter
      Block Type: Electrical Filter: Bessel
           Type  : Bandpass
           Center Frequency [GHz] : 10, 20, 28
           Number of Poles  : 3
           -3dB Bandwidth [GHz] : 2

     Block Id: RF Out
     Block Name: to_matlab
     Block Type: Electrical Signal Recorder
          Sampling Factor  : 3
```

Project: OptSim IM-DD OSSB (by filtering) RoF system model.

Description: Valid for 10, 20 and 28 GHz Bands.

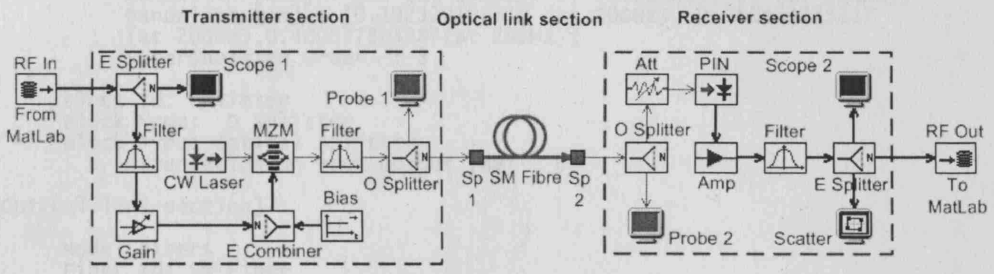

Figure 4.7: OptSim IM-DD OSSB (by filtering) RoF system model.

```
[Transmitter section]

      Block Id: RF In
      Block Name: From_Matlab
      Block Type: Electrical Playback

      Block Id: Splitter
      Block Name: E Splitter
      Block Type: Electrical Splitter
           Attenuation on each output [dB] : 0

      Block Id: Filter
      Block Name: Filter
      Block Type: Electrical Filter: Bessel
           Type  : Bandpass
           Center Frequency [GHz] : 10, 20, 28
           Number of Poles  : 3
           -3dB Bandwidth [GHz] : 2

      Block Id: E Gain
      Block Name: Gain
      Block Type: Electrical Gain

      Block Id: Combiner
      Block Name: E Combiner
      Block Type: Electrical Combiner
          Attenuation on each input [dB] : 0

      Block Id: Bias
      Block Name: Bias
      Block Type: Bias wave generator
           Level [AU] : 2.5

      Block Id: CW_Lorentzian
      Block Name: CW Laser
      Block Type: Lorentzian Laser
           Center emission frequency [THz] : 193.414489032
           Center emission wavelength [nm] : 1550
           CW Power [dBm] : 6.98970004336
           CW Power [mW] : 5
           FWHM Linewidth [MHz] : 10
           Initial Phase  : Deterministic
           Deterministic Initial Phase [rad] : 0
           Noise Type  : Realistic
           Relaxation Oscillation peak Frequency [MHz] : 5
           Relaxation Oscillation Peak Overshoot [dB] : 7
           -20 dBm Linewidth [MHz] : 99.4987437107

      Block Id: Sin2_MZ
      Block Name: MZM
      Block Type: Amplitude Modulator sin2
           Excess loss [dB] : 3
           Offset voltage corresponding to the phase retardation in the absence
           of any electric field [V] : 5
           Extinction Ratio Type  : Realistic
           Extinction Ratio [dB] : 20
           Chirp Factor  : 0
           V pi [V] : 5
           Average power reduction due to modulation [dB] : 3
           Average power reduction due to modulation [linear] : 0.707945784384

      Block Id: Optical Filter
      Block Name: Filter
      Block Type: Optical Filter Gaussian
           Notch Filter  : Bandpass
```

```
          Center Frequency [THz] : [193.421(at 10GHz), 193.422(at 20GHz),
          193.428(at 28GHz)]
          Center Wavelength [nm] : 1549.94782366(at 10GHz), 1549.93981036
          (at 20GHz), 1549.8917323(at 28GHz)
          Bandwidth [GHz] : [24 (at 10GHz), 35 (at20GHz), 50 (at 28GHz)]
          Bandwidth [nm] : [0.192320108819 (at 10GHz), 0.280463925317
          (at 20GHz),0.400637894287(at 28GHz)]
          SuperGaussian Order : 3

     Block Id: Splitter
     Block Name:  O Splitter
     Block Type: Optical Splitter
          Attenuation on each output [dB] : 0

[Optical link section]

     Model Fibers
     Fiber Id: SM Fiber
     from Block (name: Sp 1)
     to Block (name: Sp 2)
         Fiber kind  : Standard_SM
         Length [Km] : [Vary with simulations]
         Length Statistical Variation %  : 0
         Fiber Non-Linearity  : On

[Receiver section]

     Block Id: Splitter
     Block Name: O Splitter
     Block Type: Optical Splitter
          Attenuation on each output [dB] : 0

     Block Id: Attenuator
     Block Name: Att
     Block Type: Optical Attenuator
          Attenuation  [db] : [Vary with simulations]

     Block Id: PIN
     Block Name: PIN
     Block Type: PIN Photodiode
          Quantum Efficiency  : 0.7
          Responsivity (at reference frequency) [A/W] : 0.875104401174
          Quantum noise  : On
          Dark Current [nA] : 0.1
          Reference Frequency [THz] : 193.414489032
          Reference Wavelength [nm] : 1550

     Block Id: Amplifier
     Block Name: Amp
     Block Type: Electrical Amplifier: 50-Ohm
          DC Gain [dB] : 30
          Noise Figure F [dB] : 3
          Reference Temperature [K] : 300
     Block Id: Filter
     Block Name: Filter
     Block Type: Electrical Filter: Bessel
          Type  : Bandpass
          Center Frequency [GHz] : 10, 20, 28
          Number of Poles  : 3
          -3dB Bandwidth [GHz] : 2
     Block Id: Splitter
     Block Name: E Splitter
     Block Type: Electrical Splitter
          Attenuation on each output [dB] : 0
     Block Id: RF Out
     Block Name: to_matlab
     Block Type: Electrical Signal Recorder
          Sampling Factor  : 3
```

Project: OptSim IM-DD OSSB (by dual arm MZM) RoF system model.

Description: Valid for 10, 20 and 28 GHz Bands.

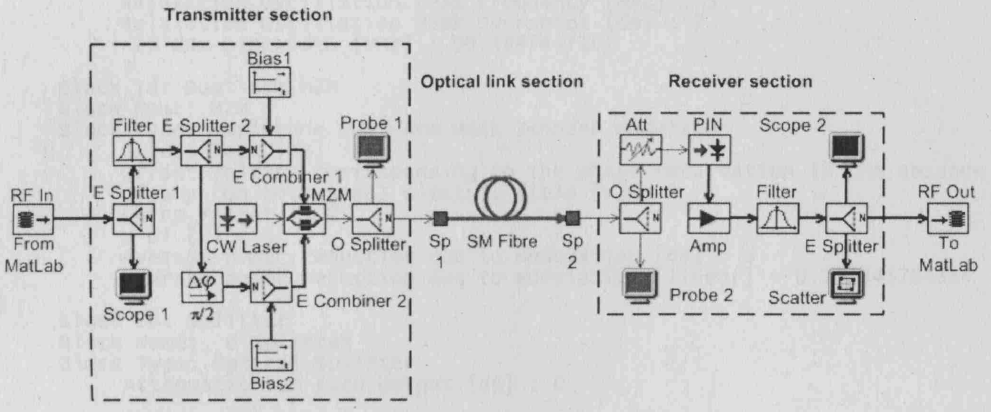

Figure 4.8: OptSim IM-DD OSSB (by dual arm MZM) RoF system model.

```
[Transmitter section]

    Block Id: RF In
    Block Name: From_Matlab
    Block Type: Electrical Playback

    Block Id: Splitter
    Block Name: E Splitter 1
    Block Type: Electrical Splitter
         Attenuation on each output [dB] : 0

    Block Id: Filter
    Block Name: Filter
    Block Type: Electrical Filter: Bessel
         Type  : Bandpass
         Center Frequency [GHz] : 10, 20, 28
         Number of Poles  : 3
         -3dB Bandwidth [GHz] : 2

    Block Id: Splitter
    Block Name: E Splitter 2
    Block Type: Electrical Splitter
         Attenuation on each output [dB] : 0

    Block Id: Phase shifter
    Block Name: π/2
    Block Type: PHASH2
         Fcentr [THz] : 0.01(10GHz), 0.02(20GHz), 0.28(28GHz)
         Theta [Rad] : 1.570796327

    Block Id: Combiner
    Block Name: E Combiner 1
    Block Type: Electrical Combiner
         Attenuation on each input [dB] : 0

    Block Id: Bias
    Block Name: Bias1
    Block Type: Bias wave generator
         Level [AU] : 2.5

    Block Id: Combiner
    Block Name: E Combiner 2
    Block Type: Electrical Combiner
         Attenuation on each input [dB] : 0

    Block Id: Bias
    Block Name: Bias2
    Block Type: Bias wave generator
         Level [AU] : -2.5

    Block Id: CW_Lorentzian
    Block Name: CW Laser
    Block Type: Lorentzian Laser
         Center emission frequency [THz] : 193.414489032
         Center emission wavelength [nm] : 1550
         CW Power [dBm] : 6.98970004336
```

```
            CW Power [mW] : 5
            FWHM Linewidth [MHz] : 10
            Initial Phase  : Deterministic
            Deterministic Initial Phase [rad] : 0
            Noise Type  : Realistic
            Relaxation Oscillation peak Frequency [MHz] : 5
            Relaxation Oscillation Peak Overshoot [dB] : 7
            -20 dBm Linewidth [MHz] : 99.4987437107

      Block Id: Dual arm MZM
      Block Name: MZM
      Block Type: Amplitude Dual-Arm Mach Zehnder Modulator
            Excess loss [dB] : 3
            Offset voltage corresponding to the phase retardation in the absence
            of any (on both arms) electric field [V] : 5
            Chirp Factor  : 0
            V pi [V] : 5
            Average power reduction due to modulation [dB] : 3
            Average power reduction due to modulation [linear] : 0.707945784384

      Block Id: Splitter
      Block Name:  O Splitter
      Block Type: Optical Splitter
            Attenuation on each output [dB] : 0

[Optical link section]

      Model Fibers
      Fiber Id: SM Fiber
      from Block (name: Sp 1)
      to Block (name: Sp 2)
          Fiber kind  : Standard_SM
          Length [Km] : [Vary with simulations]
          Length Statistical Variation %  : 0
          Fiber Non-Linearity  : On

[Receiver section]

      Block Id: Splitter
      Block Name: O Splitter
      Block Type: Optical Splitter
            Attenuation on each output [dB] : 0

      Block Id: Attenuator
      Block Name: Att
      Block Type: Optical Attenuator
            Attenuation  [db] : [Vary with simulations]

      Block Id: PIN
      Block Name: PIN
      Block Type: PIN Photodiode
            Quantum Efficiency  : 0.7
            Responsivity (at reference frequency) [A/W] : 0.875104401174
            Quantum noise  : On
            Dark Current [nA] : 0.1
            Reference Frequency [THz] : 193.414489032
            Reference Wavelength [nm] : 1550

      Block Id: Amplifier
      Block Name: Amp
      Block Type: Electrical Amplifier: 50-Ohm
            DC Gain [dB] : 30
            Noise Figure F [dB] : 3
            Reference Temperature [K] : 300

      Block Id: Filter
      Block Name: Filter
      Block Type: Electrical Filter: Bessel
            Type  : Bandpass
            Center Frequency [GHz] : 10, 20, 28
            Number of Poles  : 3
            -3dB Bandwidth [GHz] : 2

      Block Id: Splitter
      Block Name: E Splitter
      Block Type: Electrical Splitter
            Attenuation on each output [dB] : 0

      Block Id: RF Out
      Block Name: to_matlab
      Block Type: Electrical Signal Recorder
            Sampling Factor  : 3
```

Project: OptSim IM-DD DSB-SC RoF system model.

Description: Parameters are Valid for 10, 20 and 28 GHz Bands.

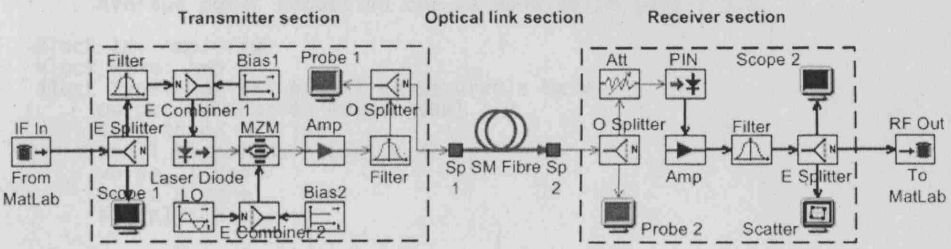

Figure 4.9: Optsim IM-DD DSB-SC RoF system model.

[Transmitter section]

Block Id: IF In
Block Name: From_Matlab
Block Type: Electrical Playback

Block Id: Splitter
Block Name: E Splitter
Block Type: Electrical Splitter
Attenuation on each output [dB] : 0

Block Id: Filter
Block Name: Filter
Block Type: Electrical Filter: Raised-Cosine
Shaping Function : Sinc
Raised Cosine function exponent : 1
Roll-off : 0.35
Bandwidth [GHz] : 2.3

Block Id: Combiner
Block Name: E Combiner 1
Block Type: Electrical Combiner
Attenuation on each input [dB] : 33.9794000867

Block Id: Bias
Block Name: Bias1
Block Type: Bias wave generator
Level [AU] : 4.2

Block Id: Laser
Block Name: Laser Diode
Block Type: Rate Equation Laser
Center emission wavelength [nm] : 1550
Type : yy_Lucent_D2525P_DFB_OC192
Threshold Current [mA] : 15.0
Linear Output Power [mW] : 10.0
P-I Slope [mW/mA] : 0.105263157889
Turn-On Delay [ns] : 0.295
Relaxation Oscillation Peak Frequency [GHz] : 10.0
Relaxation Oscillation Peak Overshoot [dB] : 35.49
Linewidth [MHz] : 2.0
Start Frequency [GHz] : 0.2
Stop Frequency [GHz] : 10
Average RIN [dB/Hz] : -135.36

Block Id: Combiner
Block Name: E Combiner 2
Block Type: Electrical Combiner
Attenuation on each input [dB] : 0

Block Id: Bias
Block Name: Bias2
Block Type: Bias wave generator
Level [AU] : -1.77

Block Id: Sinusoidal
Block Name: LO
Block Type: Sinusoidal Wave generator
Frequency [GHz] : 4.5(at 10GHz), 9.5(at 20GHz), 13.5(at 28GHz)
Amplitude [AU] : 1
Phase [rad] : 0

Block Id: Sin2_MZ
Block Name: MZM
Block Type: Amplitude Modulator sin2
Excess loss [dB] : 3
Offset voltage corresponding to the phase retardation in the absence

```
          of any electric field [V] : 3.53
          Extinction Ratio [dB] : 45
          Chirp Factor  : 0
          V pi [V] : 5.3
          Average power reduction due to modulation [dB] : 3.5

     Block Id: Amplifier
     Block Name: Amp
     Block Type: Optical Amplifier Saturable Gain
          Output Saturation Power [dBm] : 0
          Gain Shape  : Flat
          Small Signal Gain [dB] : 22
          Noise  : Yes
          Noise Figure  : Flat
          F [dB] : 6

     Block Id: Optical Filter
     Block Name: Filter
     Block Type: Optical Filter Gaussian
          Notch Filter  : Bandpass
          Center Wavelength [nm] : 1550
          Bandwidth [GHz] : 50
          Bandwidth [nm] : 0.4
          SuperGaussian Order  : 3

     Block Id: Splitter
     Block Name:  O Splitter
     Block Type: Optical Splitter
          Attenuation on each output [dB] : 0

[Optical link section]

     Model Fibers
     Fiber Id: SM Fiber
     from Block (name: Sp 1)
     to Block (name: Sp 2)
         Fiber kind  : Standard_SM
         Length [Km] : [Vary with simulations]
         Length Statistical Variation %  : 0
         Fiber Non-Linearity  : On

[Receiver section]

     Block Id: Splitter
     Block Name: O Splitter
     Block Type: Optical Splitter
          Attenuation on each output [dB] : 0

     Block Id: Attenuator
     Block Name: Att
     Block Type: Optical Attenuator
          Attenuation  [db] : [Vary with simulations]

     Block Id: PIN
     Block Name: PIN
     Block Type: PIN Photodiode
          Quantum Efficiency  : 0.7
          Responsivity (at reference frequency) [A/W] : 0.875104401174
          Quantum noise  : On
          Dark Current [nA] : 0.1
          Reference Wavelength [nm] : 1550

     Block Id: Amplifier
     Block Name: Amp
     Block Type: Electrical Amplifier: 50-Ohm
          DC Gain [dB] : 30
          Noise Figure F [dB] : 3
          Reference Temperature [K] : 300
     Block Id: Filter
     Block Name: Filter
     Block Type: Electrical Filter: Bessel
          Type  : Bandpass
          Center Frequency [GHz] : 10, 20, 28
          Number of Poles  : 3
          -3dB Bandwidth [GHz] : 0.3

     Block Id: Splitter
     Block Name: E Splitter
     Block Type: Electrical Splitter
          Attenuation on each output [dB] : 0

     Block Id: RF Out
     Block Name: to_matlab
     Block Type: Electrical Signal Recorder
          Sampling Factor  : 3
          Recording time-span  : Whole
```

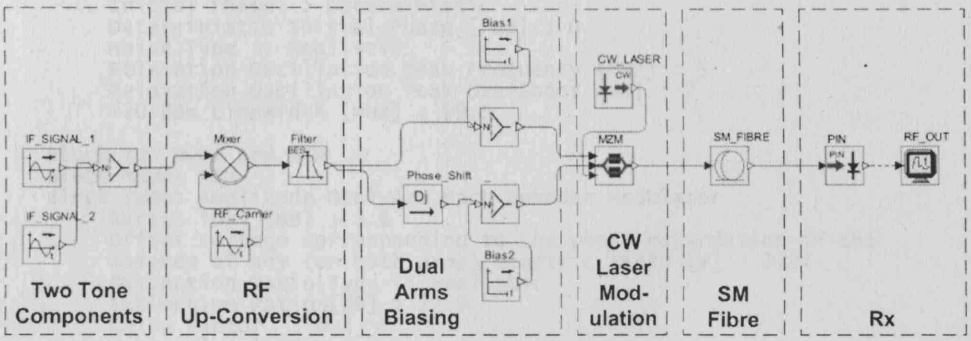

Figure 5.10: OptSim simulation model of the SSB+C modulation technique using Dual Arm MZ modulator.

Two Tone Components

```
Block Id: Signal Generator
Block Name: Signal 1
Block Type: Electrical Source
     Signal Frequency  [GHz] : 1.0
     Signal Phase  [rad] : 0.0

Block Id: Signal Generator
Block Name: Signal 2
Block Type: Electrical Source
     Signal Frequency  [GHz] : 1.05
     Signal Phase  [rad] : 0.0

Block Id: Combiner
Block Type: Electrical Combiner
     Attenuation on each input [dB] : 3.3
```

RF Up-Conversion

```
Block Id: Mixer
Block Name: Mixer
Block Type: Electrical Mixer
     IIP3 [dBm] : 10

Block Id: Filter
Block Name: Filter
Block Type: Electrical Filter: Bessel
     Type  : Bandpass
     Center Frequency [GHz] : 18
     Number of Poles  : 3
     -3dB Bandwidth [GHz] : 0.3
```

Dual Arms Biasing

```
Block Id: Phase shifter
Block Name: Phase Shift
Block Type: PHASH2
     Fcentr [THz] : 0.018
     Theta [Rad] : 1.570796327

Block Id: Bias
Block Name: Bias1
Block Type: Bias wave generator
     Level [V] : 4.06

Block Id: Bias
Block Name: Bias2
Block Type: Bias wave generator
     Level [V] : 2.42
```

CW Laser Modulation

```
Block Id: CW_Lorentzian
Block Name: CW Laser
Block Type: Lorentzian Laser
     Center emission frequency [THz] : 193.414489032
     Center emission wavelength [nm] : 1550
     Source Status  : 1
     CW Power [dBm] : 10.0
```

```
        CW Power [mW] : 10.0
        FWHM Linewidth [MHz] : 10
        Initial Phase  : Deterministic
        Deterministic Initial Phase [rad] : 0
        Noise Type  : Realistic
        Relaxation Oscillation peak Frequency [MHz] : 5
        Relaxation Oscillation Peak Overshoot [dB] : 7
        -20 dBm Linewidth [MHz] : 99.5

    Block Id: Dual arm MZM
    Block Name: MZM
    Block Type: Amplitude Dual-Arm Mach Zehnder Modulator
        Excess loss [dB] : 3.6
        Offset voltage corresponding to the phase retardation in the
        absence of any (on both arms) electric field [V] : 3.24
        Extinction Ratio Type  : Realistic
        Extinction Ratio [dB] : 27.9
        Chirp Factor  : 0.2
        V pi [V] : 1.64
```

SM Fibre

```
    Block Id: Fiber
    Block Name: SM Fiber
    Block Type: Standard_SM Fiber
        Loss [dB/Km] : 0.2
        Dispersion at the reference frequency [ps/nm/km] : 16
        Reference Frequency for Dispersion [THz] : 193.414489032
        Reference Wavelength for Dispersion [nm] : 1550
```

Rx

```
    Block Id: PIN
    Block Name: PIN
    Block Type: PIN Photodiode
        Quantum Efficiency  : 0.7
        Sensitivity [dBm]  : -19
        Responsivity (at reference frequency) [A/W] : 0.88
        Sensitivity Reference Error Probability : 1e-10
        Dark Current [nA] : 0.1
        Reference Frequency [THz] : 193.414489032
        Reference Wavelength [nm] : 1550

    Block Id: Scope
    Block Name: RF OUT
    Block Type: Electrical Scope
        Nominal Bit Rate [Gbit/s] : 0.05
        Time Resolution  : Automatic
```

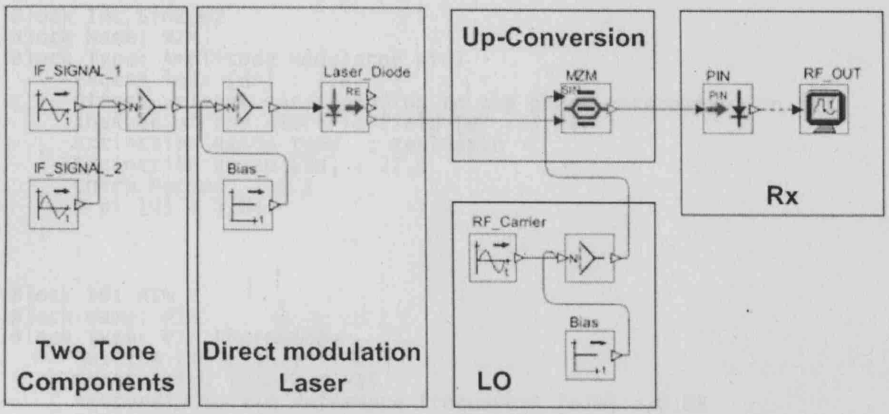

Figure 5.12: OptSim simulation model of the DSB-SC modulation technique using directly modulated laser.

Two Tone Components

```
Block Id: Signal Generator
Block Name: Signal 1
Block Type: Electrical Source
     Signal Frequency  [GHz] : 1.0
     Signal Phase  [rad] : 0.0

Block Id: Signal Generator
Block Name: Signal 2
Block Type: Electrical Source
     Signal Frequency  [GHz] : 1.05
     Signal Phase  [rad] : 0.0

Block Id: Combiner
Block Type: Electrical Combiner
     Attenuation on each input [dB] : 3.3
```

Direct Modulation Laser

```
Block Id: Bias
Block Name: Bias
Block Type: Bias wave generator
     Level [V] : 1.0

Block Id: Laser
Block Name: Laser Diode
Block Type: Rate Equation Laser
     Center emission frequency [THz] : 193.414489032
     Center emission wavelength [nm] : 1550
     Source Status  : 1
     Threshold Current [mA] : 16.0
     Linear Output Power [mW] : 6.0
     FWHM Linewidth [MHz] : 10
     P-I Slope [mW/mA] : 0.0447
     Turn On Delay [ns] : 0.683
     Start Frequency [GHz] : 0.0
     Stop Frequency [GHz] : 2.488
     Relaxation Oscillation peak Frequency [GHz] : 3.2
     Relaxation Oscillation Peak Overshoot [dB] : 3.85
     Linewidth [MHz] : 1.0
     Average RIN [dB/Hz] : -148.98
```

LO

```
Block Id: Bias
Block Name: Bias
Block Type: Bias wave generator
     Level [V] : 1.6
Block Id: Sinusoidal
Block Name: RF Carrier
Block Type: Sinusoidal Wave generator
     Frequency [GHz] : 8.5
     Phase [rad] : 0
```

UP-Conversion

```
Block Id: Sin2_MZ
Block Name: MZM
Block Type: Amplitude Modulator sin2
     Excess loss [dB] : 3.6
     Offset voltage corresponding to the phase retardation in the
     absence of any electric field [V] : 3.24
     Extinction Ratio Type  : Realistic
     Extinction Ratio [dB] : 27.9
     Chirp Factor  : 0.2
     V pi [V] : 1.64
```

Rx

```
Block Id: PIN
Block Name: PIN
Block Type: PIN Photodiode
     Quantum Efficiency  : 0.7
     Sensitivity [dBm]  : -19
     Responsivity (at reference frequency) [A/W] : 0.88
     Sensitivity Reference Error Probability : 1e-10
     Dark Current [nA] : 0.1
     Reference Frequency [THz] : 193.414489032
     Reference Wavelength [nm] : 1550

Block Id: Scope
Block Name: RF OUT
Block Type: Electrical Scope
     Nominal Bit Rate [Gbit/s] : 0.05
     Time Resolution  : Automatic
```

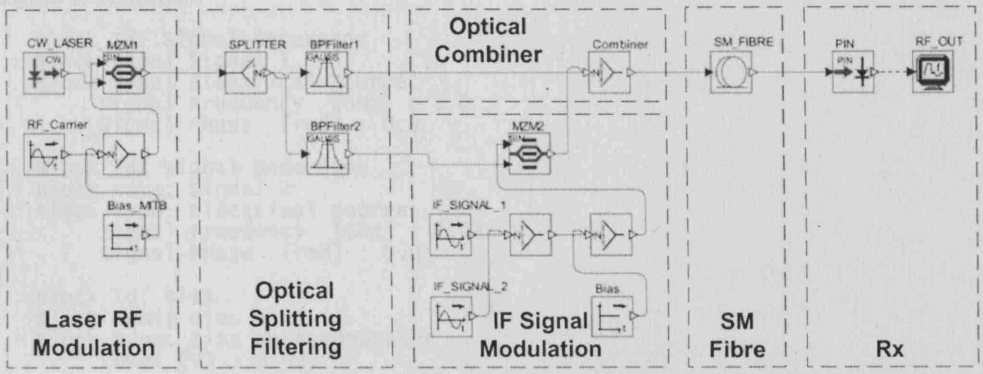

Figure 5.14: OptSim simulation model of the DSB-SC modulation technique with two MZ modulators.

Laser RF Modulation

```
Block Id: Sinusoidal
Block Name: RF Carrier
Block Type: Sinusoidal Wave generator
     Frequency [GHz] : 8.5
     Phase [rad] : 0

Block Id: Bias
Block Name: Bias MITB
Block Type: Bias wave generator
     Level [V] : 1.6

Block Id: CW_Lorentzian
Block Name: CW Laser
Block Type: Lorentzian Laser
     Center emission frequency [THz] : 193.414489032
     Center emission wavelength [nm] : 1550
     Source Status  : 1
     CW Power [dBm] : 10.0
     CW Power [mW] : 10.0
     FWHM Linewidth [MHz] : 10
     Initial Phase  : Deterministic
     Deterministic Initial Phase [rad] : 0
     Noise Type  : Realistic
     Relaxation Oscillation peak Frequency [MHz] : 5
     Relaxation Oscillation Peak Overshoot [dB] : 7
     -20 dBm Linewidth [MHz] : 99.5

Block Id: Sin2_MZ
Block Name: MZM1
Block Type: Amplitude Modulator sin2
     Excess loss [dB] : 3.6
     Offset voltage corresponding to the phase retardation in the
     absence of any electric field [V] : 3.24
     Extinction Ratio Type  : Realistic
     Extinction Ratio [dB] : 27.9
     Chirp Factor  : 0.2
     V pi [V] : 1.64
```

Optical Splitting Filtering

```
Block Id: Optical Filter
Block Name: BPFilter1
Block Type: Optical Filter Gaussian
     Notch Filter  : Bandpass
     Center Frequency [THz] : 193.405
     Center Wavelength [nm] : 1550.07605
     -3dB Two-Sided Bandwidth [GHz] : 10
     -3dB Two-Sided Bandwidth [nm] : 0.08015
     SuperGaussian Order  : 4

Block Id: Optical Filter
Block Name: BPFilter2
Block Type: Optical Filter Gaussian
     Notch Filter  : Bandpass
     Center Frequency [THz] : 193.424
     Center Wavelength [nm] : 1549.92378
     -3dB Two-Sided Bandwidth [GHz] : 10
     -3dB Two-Sided Bandwidth [nm] : 0.08015
     SuperGaussian Order  : 4
```

IF Signal Modulation

```
Block Id: Signal Generator
Block Name: Signal 1
Block Type: Electrical Source
     Signal Frequency  [GHz] : 1.0
     Signal Phase  [rad] : 0.0

Block Id: Signal Generator
Block Name: Signal 2
Block Type: Electrical Source
     Signal Frequency  [GHz] : 1.05
     Signal Phase  [rad] : 0.0

Block Id: Bias
Block Name: Bias
Block Type: Bias wave generator
     Level [V] : 2.42

Block Id: Combiner
Block Type: Electrical Combiner
     Attenuation on each input [dB] : 3.3

Block Id: Sin2_MZ
Block Name: MZM2
Block Type: Amplitude Modulator sin2
     Excess loss [dB] : 3.6
     Offset voltage corresponding to the phase retardation in the
     absence of any electric field [V] : 3.24
     Extinction Ratio Type  : Realistic
     Extinction Ratio [dB] : 27.9
     Chirp Factor  : 0.2
     V pi [V] : 1.64
```

SM Fibre

```
Block Id: Fiber
Block Name: SM Fiber
Block Type: Standard_SM Fiber
     Loss [dB/Km] : 0.2
     Dispersion at the reference frequency [ps/nm/km] : 16
     Reference Frequency for Dispersion [THz] : 193.414489032
     Reference Wavelength for Dispersion [nm] : 1550
```

Rx

```
Block Id: PIN
Block Name: PIN
Block Type: PIN Photodiode
     Quantum Efficiency  : 0.7
     Sensitivity [dBm]  : -19
     Responsivity (at reference frequency) [A/W] : 0.88
     Sensitivity Reference Error Probability : 1e-10
     Dark Current [nA] : 0.1
     Reference Frequency [THz] : 193.414489032
     Reference Wavelength [nm] : 1550

Block Id: Scope
Block Name: RF OUT
Block Type: Electrical Scope
     Nominal Bit Rate [Gbit/s] : 0.05
     Time Resolution  : Automatic
```

References

[1] H.Al-Raweshidy and S.Komaki, *Radio over Fiber Technologies for Mobile and Communications Networks* Artech House, Inc. March 1st, 2002.

[2] Carbon B., Girod V., and Maury G., "Optical Generation Of Microwave Functions," *Proceedings of the Workshop on Microwave Photonics for Emission and Detection of Broadband Communication Signals, Graduate School in Electronics and Communications (GSEC), Louvain-la-Nueve, Belgium,* Aprl 2001.

[3] Y. Le Guennec, B. Cabon, and G. Maury, "Conversions of the microwave subcarriers of digital signals in optical links,", 1 ed 2001, pp. 50-51.

[4] G. Maury, A. Hilt, T. Berceli, B. Cabon, and A. Vilcot, "Microwave-frequency conversion methods by optical interferometer and photodiode," *IEEE Transactions on Microwave Theory and Techniques*, vol. 45, no. 8, pp. 1481-1485, 1997.

[5] G. Maury, B. Cabon, A. Hilt, and J. F. Le Bigot, "Optical upconversion of 100 Mb/s BPSK microwave subcarrier signals using an unbalanced Mach-Zehnder interferometer," 2000, pp. 179-182.

[6] A. Hilt, T. Marozsak, G. Maury, T. Berceli, B. Cabon, and A. Vilcot, "Radio-node upconversion in millimeter-wave fiber-radio distribution systems," 1998, pp. 176-180.

[7] A.Powell, "Radio over Fiber Technology: Current Applications and Future Potential in Mobile Networks - Advantages and Challenges for a Powerful Technology," in *Radio over Fiber Technologies for Mobile Communications Networks*. H.Al-Raweshidy and S.Komaki, Eds. Artech House, Inc, 2002.

[8] "Supplement to IEEE standard for information technology telecommunications and information exchange between systems - local and metropolitan area networks - specific requirements. Part 11: wireless LAN Medium Access Control (MAC) and Physical Layer (PHY) specifications: high-speed physical layer in the 5 GHz band," *IEEE Std 802. 11a-1999*, 1999.

[9] "Supplement To IEEE Standard For Information Technology-Telecommunications And Information Exchange Between Systems-Local And Metropolitan Area Networks- Specific Requirements- Part 11: Wireless LAN Medium Access Control (MAC) And Physical Layer (PHY) Specifications: Higher-speed Physical Layer Extension In The 2.4 GHz Band," *IEEE Std 802. 11b-1999*, p. i-90, 2000.

[10] "IEEE Standard for Local and Metropolitan Area Networks Part 16: Air Interface for Fixed Broadband Wireless Access Systems," *IEEE Std 802. 16-2004 (Revision of IEEE Std 802. 16-2001)*, pp. 0-857, 2004.

[11] Worldwide Interoperability for Microwave Access Forum, "IEEE 802.16a Standard and WiMAX Igniting Broadband Wireless Access," *Worldwide Interoperability for Microwave Access Forum*, 2004.

[12] S. J. Vaughan-Nichols, "Achieving wireless broadband with WiMax," *Computer, Volume 37, Issue 6, June 2004 Page(s):10 - 13*, 2004.

[13] O'Reilly J.J., Lane P.M., and Capstick M.H., "Optical Generation and Delivery of Modulated mm-waves For Mobile Communications," in *Analogue Optical Fibre Communications*. Wilson B., Ghassemlooy Z., and Darwazeh I., Eds. The Institution of Electrical Engineers, London, 1995, pp229-256, 1995.

[14] Gliese U., Nielsen T.N., Norskov S., and Stubkjaer K.E., "Multifunction Fibre-Optic Microwave Links Based on Remote Heterodyne Detection," *IEEE Trans. On Microwave theory and Techniques, Vol. 46, No. 5, May 1998*, 1998.

[15] K. H. Yla-Jarkko and A. B. Grudinin, "Performance limitations of high-power DFB fiber lasers," *Photonics Technology Letters, IEEE*, vol. 15, no. 2, pp. 191-193, 2003.

[16] K. Sato, S. Kuwahara, and Y. Miyamoto, "Chirp characteristics of 40-gb/s directly Modulated distributed-feedback laser diodes," *Journal of Lightwave Technology*, vol. 23, no. 11, pp. 3790-3797, 2005.

[17] G.P.Agrawal, *Nonlinear Fiber Optics* Academic Pr, 1989.

[18] T. Yamanaka, "Ultrafast electroabsorption modulators with traveling-wave electrodes,", 3 ed 2001, pp. 328-331.

[19] D. Wake, C. R. Lima, and P. A. Davies, "Optical generation of millimeter-wave signals for fiber-radio systems using a dual-mode DFB semiconductor laser," *IEEE Transactions on Microwave Theory and Techniques*, vol. 43, no. 9, pp. 2270-2276, 1995.

[20] R. T. Ramos and A. J. Seeds, "Fast heterodyne optical phase-lock loop using double quantum well laser diodes," *Electronics Letters*, vol. 28, no. 1, pp. 82-83, 1992.

[21] J. J. O'Reilly, P. M. Lane, R. Heidemann, and R. Hofstetter, "Optical generation of very narrow linewidth millimetre wave signals," *Electronics Letters*, vol. 28, no. 25, pp. 2309-2311, 1992.

[22] R. P. Braun, G. Grosskopf, D. Rohde, and F. Schmidt, "Low-phase-noise millimeter-wave generation at 64 GHz and data transmission using optical sideband injection locking," *IEEE Photonics Technology Letters*, vol. 10, no. 5, pp. 728-730, 1998.

[23] L. A. Johansson and A. J. Seeds, "36-GHz 140-Mb/s radio-over-fiber transmission using an optical injection phase-lock loop source" *IEEE Photonics Technology Letters*, vol. 13, no. 8, pp. 893-895, 2001.

[24] R. Hofstetter, H. Schmuck, and R. Heidemann, "Dispersion effects in optical millimeter-wave systems using self-heterodyne method for transport and generation," *IEEE Transactions on Microwave Theory and Techniques*, vol. 43, no. 9, pp. 2263-2269, 1995.

[25] D. Wake, "Trends and prospects for radio over fibre picocells", pp. 21-24, 2002.

[26] W. Jiunn-Shyen, W. Jingshown, and T. Hen-Wai, "A radio-over-fiber network for microcellular system application," *IEEE Transactions on Vehicular Technology*, vol. 47, no. 1, pp. 84-94, 1998.

[27] Haroun I. and Gouin F., "WLANs Meet Fiber Optics - Evaluating 802.11a WLANs over Fiber Optics Links," *RF Design Magazine, pp. 39-44,April 2003*, 2003.

[28] A. Teixeira, R. Nogueira, J. Pinto, and J. Rocha, "Wavelength interleaved radio-over-fibre optimized scheme based on highly birefringent optical filters", 2 ed 2003, pp. 549-550.

[29] A.Nirmalathas, C.Lim, D.Novak, and R.B.Waterhouse, "Progress in millimeter-wave fiber-radio access networks" *Ann. Telecommun. , vol. 56, pp. 27-38, 2001*, 2001.

[30] K.Biesecker, "The promise of broad-band wireless" *Inf. Technol. Professional, vol. 2, pp. 31-39, 2000*, 2000.

[31] John M.Senior, *Optical fiber communications: principles and practice*, Second edition ed 1992.

[32] L.Kazovsky, S Benedetto, and A.Willner, *Optical Fiber Communication Systems* Artech House, 1996.

[33] M. S. Borella, J. P. Jue, D. Banerjee, B. Ramamurthy, and B. Mukherjee, "Optical components for WDM lightwave networks" *Proceedings of the IEEE*, vol. 85, no. 8, pp. 1274-1307, 1997.

[34] M. J. Adams, D. N. Payne, F. M. E. Sladen, and A. H. Hartog, "Optimum operating wavelength for chromatic equalisation in multimode optical fibres," *Electronics Letters*, vol. 14, no. 3, pp. 64-66, 1978.

[35] I.P Kaminow, D.Marcuse, and H.M.Presby, "Multimode fiber bandwidth: theory and practice" *Proc. IEEE, 68(10), pp. 1209-1213*, 1980.

[36] Olshansky R., "Propagation in glass optical waveguides," *Rev. Mod. Phys. , 51(2), pp. 341-367, 1979*, 1979.

[37] W.A.Gambling, A.H.Hartog, and C.M.Ragdale, "Optical fibre transmission lines" *Radio Electron. Eng. J. IERE, 51(7/8), pp. 313-325, 1981*, 1981.

[38] B. Ainslie and C. Day, "A review of single-mode fibers with modified dispersion characteristics," *Journal of Lightwave Technology*, vol. 4, no. 8, pp. 967-979, 1986.

[39] A.R.Chraplyvy, "Limits on lightwave communications imposed by optical-fiber nonlinearities" *IEEE/OSA J. Lightwave Technol. , vol. 8, pp. 1548-1557, Oct. 1990*, 1990.

[40] John E Mitchell, "Techniques for Radio over Fiber Networks," 2006, pp. 346-347.

[41] A. F. Elrefaie and R. E. Wagner, "Chromatic dispersion limitations for FSK and DPSK systems with direct detection receivers" *IEEE Photonics Technology Letters,* vol. 3, no. 1, pp. 71-73, 1991.

[42] Wim Van Etten and Jan Van Der Plaats, *Fundamentals of Optical Fiber Communications* Prentice Hall, International Series in Optoelectronics, 1991.

[43] H. Schmuck, "Comparison of optical millimetre-wave system concepts with regard to chromatic dispersion" *Electronics Letters*, vol. 31, no. 21, pp. 1848-1849, 1995.

[44] J. Park, A. F. Elrefaie, and K. Y. Lau, "Fiber chromatic dispersion effects on multichannel digital millimeter-wave transmission" *IEEE Photonics Technology Letters,* vol. 8, no. 12, pp. 1716-1718, 1996.

[45] J. Park, A. F. Elrefaie, and K. Y. Lau, "1550-nm transmission of digitally modulated 28-GHz subcarriers over 77 km of nondispersion shifted fiber" *IEEE Photonics Technology Letters*, vol. 9, no. 2, pp. 256-258, 1997.

[46] A. F. Elrefaie, R. E. Wagner, D. A. Atlas, and D. G. Daut, "Chromatic dispersion limitations in coherent lightwave transmission systems" *Journal of Lightwave Technology*, vol. 6, no. 5, pp. 704-709, 1988.

[47] U. Gliese, S. N. Nielsen, and T. N. Nielsen, "Limitations in distance and frequency due to chromatic dispersion in fibre-optic microwave and millimeter-wave links", 3 ed, pp.1547-1550, 1996.

[48] G. Meslener, "Chromatic dispersion induced distortion of modulated monochromatic light employing direct detection" *IEEE Journal of Quantum Electronics*, vol. 20, no. 10, pp. 1208-1216, 1984.

[49] D. Wake, "Trends and prospects for radio over fibre picocells", pp. 21-24, 2002.

[50] U. Gliese, S. Norskov, and T. N. Nielsen, "Chromatic dispersion in fiber-optic microwave and millimeter-wave links" *IEEE Transactions on Microwave Theory and Techniques*, vol. 44, no. 10, pp. 1716-1724, 1996.

[51] J. Park, W. V. Sorin, and K. Y. Lau, "Elimination of the fibre chromatic dispersion penalty on 1550 nm millimetre-wave optical transmission" *Electronics Letters*, vol. 33, no. 6, pp. 512-513, 1997.

[52] K. Yonenaga and N. Takachio, "A fiber chromatic dispersion compensation technique with an optical SSB transmission in optical homodyne detection systems" *IEEE Photonics Technology Letters*, vol. 5, no. 8, pp. 949-951, 1993.

[53] A. Loayssa, D. Benito, and M. J. Garde, "Single-sideband suppressed-carrier modulation using a single-electrode electrooptic modulator" *IEEE Photonics Technology Letters*, vol. 13, no. 8, pp. 869-871, 2001.

[54] R. Montgomery and R. DeSalvo, "A novel technique for double sideband suppressed carrier modulation of optical fields" *IEEE Photonics Technology Letters*, vol. 7, no. 4, pp. 434-436, 1995.

[55] G. H. Smith, D. Novak, and Z. Ahmed, "Novel technique for generation of optical SSB with carrier using a single MZM to overcome fiber chromatic dispersion", pp. 5-8, 1996.

[56] G. H. Smith, D. Novak, and Z. Ahmed, "Technique for optical SSB generation to overcome dispersion penalties in fibre-radio systems" *Electronics Letters*, vol. 33, no. 1, pp. 74-75, 1997.

[57] S. Yichun, Z. Xianmin, and C. Kangsheng, "Optical single sideband Modulation of 11-GHz RoF system using stimulated Brillouin scattering" *IEEE Photonics Technology Letters*, vol. 17, no. 6, pp. 1277-1279, 2005.

[58] A. Loayssa, C. Lim, A. Nirmalathas, and D. Benito, "Design and performance of the bidirectional optical single-sideband modulator" *Journal of Lightwave Technology*, vol. 21, no. 4, pp. 1071-1082, 2003.

[59] Y. Le Guennec, G. Maury, Y. Jianping, and B. Cabon, "New optical microwave up-conversion solution in radio-over-fiber networks for 60-GHz wireless applications" *Journal of Lightwave Technology*, vol. 24, no. 3, pp. 1277-1282, 2006.

[60] S. Kawanishi and M. Saruwatari, "A very wide-band frequency response measurement system using optical heterodyne detection" *IEEE Transactions on Instrumentation and Measurement*, vol. 38, no. 2, pp. 569-573, 1989.

[61] A. J. Seeds and A. A. A. De Salles, "Optical control of microwave semiconductor devices" *IEEE Transactions on Microwave Theory and Techniques*, vol. 38, no. 5, pp. 577-585, 1990.

[62] T. S. Tan, R. L. Jungerman, and S. S. Elliott, "Calibration of optical receivers and modulators using an optical heterodyne technique" pp. 1067-1070, 1988.

[63] J. M. Fuster, J. Marti, V. Polo, and J. L. Corral, "Fiber-optic microwave link employing optically amplified electrooptical upconverting receivers" *IEEE Photonics Technology Letters*, vol. 9, no. 8, pp. 1161-1163, 1997.

[64] J. M. Fuster, J. Marti, and J. L. Corral, "Chromatic dispersion effects in electro-optical upconverted millimetre-wave fibre optic links" *Electronics Letters*, vol. 33, no. 23, pp. 1969-1970, 1997.

[65] J. M. Fuster, J. Marti, and J. L. Corral, "Experimental reduction of chromatic dispersion effects in electro-optical up-converted millimeter-wave fiber-optic links", pp.199-200, 1998.

[66] J. L. Corral, J. Marti, and J. M. Fuster, "General expressions for IM/DD dispersive analog optical links with external modulation or optical up-conversion in a Mach-Zehnder electrooptical modulator," *Microwave IEEE Transactions on Theory and Techniques*, vol. 49, no. 10, pp. 1968-1976, 2001.

[67] J. M. Fuster, J. Marti, V. Polo, F. Ramos, and J. L. Corral, "Nonlinear biasing of MZ-EOM devices to experimentally reduce chromatic dispersion effects in antenna remoting up-converting fiber-optic links", pp. 99-102, 1998.

[68] J. M. Fuster, J. Marti, J. L. Corral, V. Polo, and F. Ramos, "Generalized study of dispersion-induced power penalty mitigation techniques in millimeter-wave fiber-optic links" *Journal of Lightwave Technology*, vol. 18, no. 7, pp. 933-940, 2000.

[69] "IEEE Standard for Information technology-Telecommunications and information exchange between systems-Local and metropolitan area networks-Specific requirements - Part 11: Wireless LAN Medium Access Control (MAC) and Physical Layer (PHY) Specifications" *IEEE Std 802. 11-2007 (Revision of IEEE Std 802. 11-1999)*, pp. C1-1184, 2007.

[70] M. Jeruchim, "Techniques for Estimating the Bit Error Rate in the Simulation of Digital Communication Systems" *IEEE Journal on Selected Areas in Communications*, vol. 2, no. 1, pp. 153-170, 1984.

[71] T. Kuri, H. Toda, and K. Kitayama, "Dense wavelength-division multiplexing millimeter-wave-band radio-on-fiber signal transmission with photonic downconversion" *Journal of Lightwave Technology*, vol. 21, no. 6, pp. 1510-1517, 2003.

[72] J. Yu, Z. Jia, T. Wang, and G. K. Chang, "A Novel Radio-Over-Fiber Configuration Using Optical Phase Modulator to Generate an Optical mm-Wave and Centralized Lightwave for Uplink Connection" *IEEE Photonics Technology Letters*, vol. 19, no. 3, pp. 140-142, 2007.

[73] B. Cai and A. J. Seeds, "Optical frequency modulation link for microwave signal transmission" pp. 163-166, 1994.

[74] Z. Wang, A. Li, C. J. Mahon, G. Jacobsen, and E. Bodtker, "Performance limitations imposed by stimulated Raman scattering in optical WDM SCM video distribution systems" *IEEE Photonics Technology Letters*, vol. 7, no. 12, pp. 1492-1494, 1995.

[75] W. Caiqin and Z. Xiupu, "Impact of nonlinear distortion in radio over fiber systems with single-sideband and tandem single-sideband subcarrier modulations" *Journal of Lightwave Technology*, vol. 24, no. 5, pp. 2076-2090, 2006.

[76] C. Fazi and P. G. Neudeck, "Wide dynamic range RF mixers using wide-bandgap semiconductors", 1 ed, pp. 49-51, 1997.

[77] P. Horvath and I. Frigyes, "Effects of the nonlinearity of a Mach-Zehnder modulator on OFDM radio-over-fiber transmission" *Communications Letters, IEEE*, vol. 9, no. 10, pp. 921-923, 2005.

[78] I. S. C. Lu, N. Weste, and S. Parameswaran, "The effect of receiver front-end non-linearity on DS-UWB systems operating in the 3 to 4 GHz band", 2 ed, pp.776-781, 2005.

[79] L. Sang-Hoon, K. Jeung-Mo, C. In-Hyuk, and H. Sang-Kook, "Linearization of DFB laser diode by external light-injected cross-gain modulation for radio-over-fiber link" *IEEE Photonics Technology Letters*, vol. 18, no. 14, pp. 1545-1547, 2006.

[80] S. Yaakob, W. R. W. Abdullah, M. N. Osman, A. K. Zamzuri, R. Mohamad, M. R. Yahya, A. F. A. Mat, M. R. Mokhtar, and H. A. A. Rashid, "Effect of Laser Bias Current to the Third Order Intermodulation in the Radio over Fibre System", pp. 444-447, 2006.

[81] A. R. Chraplyvy, "Limitations on lightwave communications imposed by optical-fiber nonlinearities" *Journal of Lightwave Technology*, vol. 8, no. 10, pp. 1548-1557, 1990.

[82] M. S. Borella, J. P. Jue, D. Banerjee, B. Ramamurthy, and B. Mukherjee, "Optical components for WDM lightwave networks" *Proceedings of the IEEE*, vol. 85, no. 8, pp. 1274-1307, 1997.

[83] Z. Cvetkovic, "Modulating waveforms for OFDM", 5 ed, pp. 2463-2466, 1999.

[84] M.Pugel and L.Litwin, "The principles of OFDM," *www. rfdesign. com*, 2001.

[85] A. Pandharipande, "Principles of OFDM," *IEEE Potentials*, vol. 21, no. 2, pp. 16-19, 2002.

[86] K. Sang-Woo, Y. Kee-Hoo, G. J. Rag, S. Jong-Won, and R. Heung-Gyoon, "Adaptive frequency diversity OFDM (AFD-OFDM) communication system in the narrow-band interference channel", 2 ed, pp. 834-838, 2004.

[87] Y. Tsai, G. Zhang, and J. L. Pan, "Orthogonal frequency division multiplexing with phase modulation and constant envelope design", pp. 2658-2664, 2005.

[88] R.R.Mosier and R.G.Clabaugh, "Kineplex, a bandwidth-efficient binary transmission system" *AIEE Transactions, Vol. 76, January 1958, pp. 723 - 728*, 1958.

[89] Chang R., "Orthogonal frequency division multiplexing" *US. Patent 3,488445,filed November 14, 1966, issued January 6*, 1970.

[90] Chang R., "Synthesis of Band-Limited Orthogonal Signals for Multichannel Data Transmission" *The Bell System Technical Journal, December 1966, pp. 1775 -1796*, 1966.

[91] S. Weinstein and P. Ebert, "Data Transmission by Frequency-Division Multiplexing Using the Discrete Fourier Transform" *Communications, IEEE Transactions on [legacy, pre - 1988]*, vol. 19, no. 5, pp. 628-634, 1971.

[92] A. R. S. S. B. R. E. M. Bahai, *Multi Carrier Digital Communications: Theory and Applications of OFDM* Springer, 2004.

[93] W. Henkel, G. Taubock, P. Odling, P. O. Borjesson, and N. Petersson, "The cyclic prefix of OFDM/DMT - an analysis", pp. 22-1, 2002.

[94] S. Sasaki, K. I. Takizawa, S. Muramatsu, and H. Kikuchi, "Separate FEC coding for parallel combinatorial spread spectrum communication systems", 2 ed, p. F-11, 2001.

[95] Y. Q. Shi, M. Z. Xi, N. Zhi-Cheng, and N. Ansari, "Interleaving for combating bursts of errors," *IEEE Circuits and Systems Magazine*, vol. 4, no. 1, pp. 29-42, 2004.

[96] J. K. Jun and K. K. Parhi, "Interleaved cyclic redundancy check (CRC) code", 2 ed, pp. 2137-2141, 2003.

[97] S. Liu, S. Liu, C. Zhao, C. Li, and Y. Xiao-Hu, "Joint interleaving and phase rotation approach to reduce PAR and using blind detection in OFDM systems Joint interleaving and phase rotation approach to reduce PAR and using blind detection in OFDM systems", 7 ed. C. Zhao, pp. 5082-5086, 2004.

[98] J. N. Laneman, J. N. Laneman, and C. E. W. Sundberg, "Reed-Solomon decoding algorithms for digital audio broadcasting in the AM band Reed-Solomon decoding algorithms for digital audio broadcasting in the AM band" *Broadcasting, IEEE Transactions on*, vol. 47, no. 2, pp. 115-122, 2001.

[99] Y. Mostofi and D. C. Cox, "Mathematical analysis of the impact of timing synchronization errors on the performance of an OFDM system" *IEEE Transactions on Communications*, vol. 54, no. 2, pp. 226-230, 2006.

[100] T. Raffaello, H. Matti, and I. Jari, "Channel Estimation Algorithms Comparison for Multiband-OFDM,", pp. 1-5, 2006.

[101] E. Saberinia, A. H. Tewfik, and R. Gupta, "Pilot assisted multi-user UWB communications", 3 ed, pp. 1885-1889, 2003.

[102] L. Yuan-Pei and P. See-May, "OFDM transmitters: analog representation and DFT-based implementation" *IEEE Transactions on Signal Processing, [see also Acoustics, Speech, and Signal Processing]*, vol. 51, no. 9, pp. 2450-2453, 2003.

[103] F. Kristensen, P. Nilsson, and A. Olsson, "A generic transmitter for wireless OFDM systems", 3 ed, pp. 2234-2238, 2003.

[104] W. Yan, T. Chi-Ying, R. S. Cheng, and H. M. Wai, "Performance study of OFDM receiver using FFT based on log number system", 3 ed, pp. 1257-1259, 2002.

[105] H. Chien-Fang, H. Yuan-Hao, and C. Tzi-Dar, "Design of an OFDM receiver for high-speed wireless LAN", 4 ed, pp. 558-561, 2001.

[106] M. R. D. Rodrigues and I. J. Wassell, "Optimum receivers for non-linearly distorted OFDM signals", 2 ed, pp. 1223-1227, 2004.